



Institut für Anorganische Chemie

Visible-Light-Driven Functionalisation of White Phosphorus

Dissertation

Zur Erlangung des Doktorgrades der Naturwissenschaften

Dr. rer. nat.

an der Fakultät Chemie und Pharmazie der Universität Regensburg

vorgelegt von:

Ulrich Lennert

aus Undorf

Regensburg 2020

Der experimentelle Teil der vorliegenden Arbeit wurde in der Zeit zwischen Oktober 2016 und Dezember 2019 unter Anleitung von Prof. Dr. Robert Wolf am Institut für Anorganische Chemie der Universität Regensburg angefertigt.

Die Arbeit wurde angeleitet von:		Prof. Dr. Robert Wolf
Promotionsgesuch eingereicht am:		22.06.2020
Tag der mündlichen Prüfung:		30.07.2020
Promotionsausschuss:	Vorsitz	Prof. Dr. Rainer Müller
	Erstgutachter	Prof. Dr. Robert Wolf
	Zweitgutachter	Prof. Dr. Ruth Gschwind
	Dritter Prüfer	Prof. Dr. Frank-Michael Matysik

Prologue

This thesis reports mainly on photocatalytic transformation of white phosphorus into tertiary phosphines and quaternary phosphonium salts. Chapter 1 reviews state-of-the-art processes to transform white phosphorus into monophosphorus compounds. Reactions of white phosphorus in basic media, with anionic carbon centered nucleophiles and with carbenes are discussed. In addition, electrochemical and radical mediated methods are presented. Chapter 2 shows the first successful example of a direct and photocatalytic transformation of white phosphorus into organophosphorus compounds. Using the iridium catalyst $[\text{Ir}(\text{dtbbpy})(\text{ppy})_2]\text{PF}_6$ (dtbbpy = 4,4'-bis-tertbutyl-2,2'-bipyridine, ppy = 2-(2-pyridyl)phenyl) and the sacrificial donor triethylamine, a variety of aryl phosphines and phosphonium salts are obtained. The substrate scope of this method and the results of mechanistic investigations are described. Chapter 3 investigates the use of an organocatalyst 3DPAFIPN as an alternative to the iridium catalyst used in the previous chapter. With this catalyst, direct catalytic P_4 functionalisation was likewise achieved. Moreover, the photocatalytic synthesis of unsymmetrical phosphines and phosphonium salts was achieved starting from the precursors phenylphosphine and diphenylphosphine. The results of this thesis are summarised in Chapter 4.

Prolog

Diese Dissertation beschreibt Untersuchungen zur photokatalytischen Synthese von tertiären Phosphanen und quaternären Phosphoniumsalzen aus weißem Phosphor. Kapitel 1 gibt zunächst einen Überblick über bereits bekannte Methoden zur Umsetzung von weißem Phosphor in Monophosphorverbindungen. Dabei wird auf Reaktionen des weißen Phosphors in basischen Lösungen, mit anionischen kohlenstoffzentrierten Nucleophilen und mit Carbenen eingegangen. Des Weiteren werden elektrochemische und radikalische Methoden diskutiert. Im zweiten Kapitel wird das erste Verfahren zur direkten und photokatalytischen Umsetzung von weißem Phosphor in Organophosphorverbindungen vorgestellt. Die Verwendung des Iridiumkatalysators $[\text{Ir}(\text{dtbbpy})(\text{ppy})_2]\text{PF}_6$ (dtbbpy = 4,4'-bis-tertbutyl-2,2'-bipyridine, ppy = 2-(2-pyridyl)phenyl) und von Triethylamin als Opfersubstrat ermöglicht hierbei die Synthese einer Reihe von Arylphosphanen und Arylphosphoniumsalzen. Die Substratbreite der Reaktion wird beschrieben und die Ergebnisse mechanistischer Untersuchungen werden ausführlich diskutiert. Kapitel 3 untersucht die Verwendung des Organokatalysators 3DPAFIPN als Alternative zu dem im vorherigen Kapitel beschriebenen Iridiumkatalysators. Mit diesem Katalysator konnte die katalytische, direkte P_4 Funktionalisierung auf ähnliche Weise

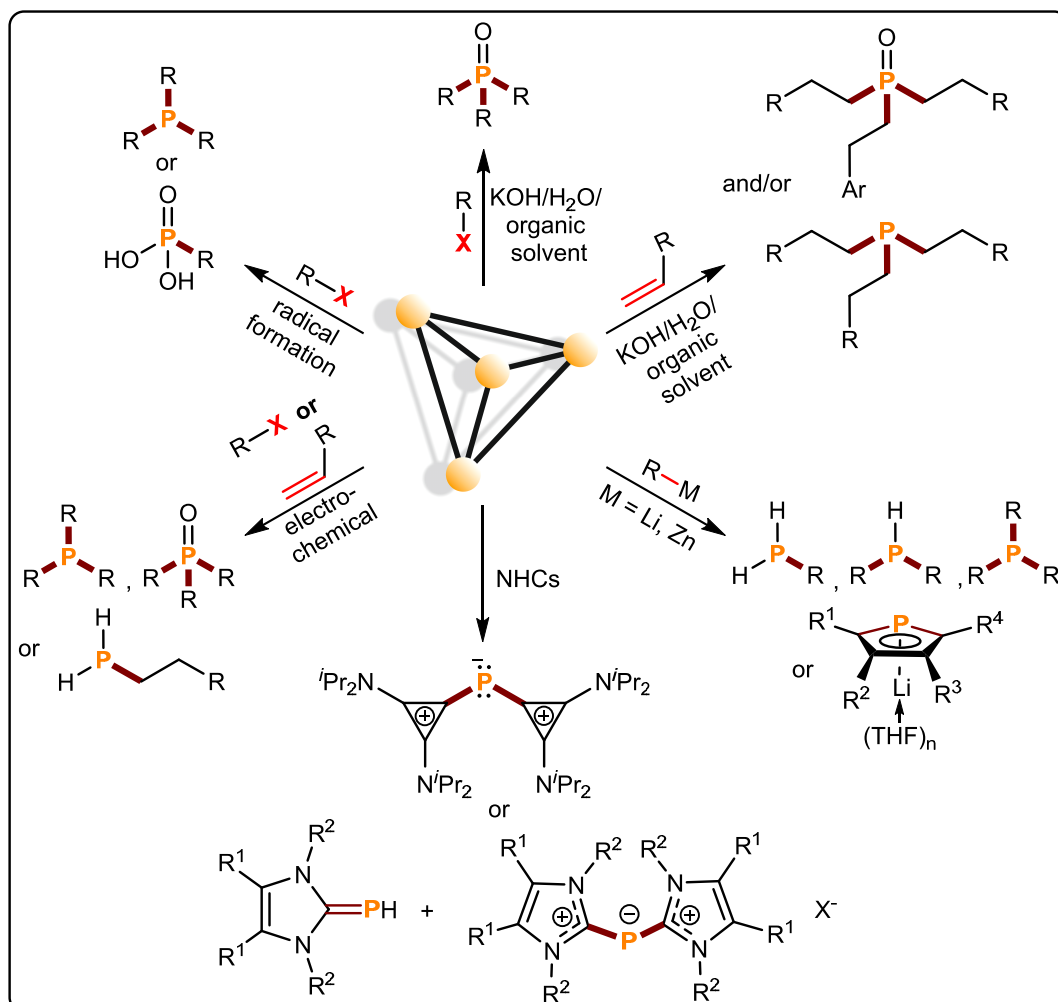
realisiert werden. Außerdem wird die Synthese von unsymmetrischen Phosphanen und Phosphoniumsalzen ausgehend von Phenylphosphan und Diphenylphosphan beschrieben. Die Ergebnisse dieser Arbeit werden in Kapitel 4 zusammengefasst.

Table of Contents

1	Direct Organofunctionalisation of White Phosphorus to Monophosphorus Compounds: State-of-the-Art and Perspectives	1
1.1	Introduction	2
1.2	P ₄ functionalisation in basic media	4
1.2.1	Reactions of white phosphorus with organyl halides, R–X	5
1.2.2	Reactions of white phosphorus with alkenes and alkynes	7
1.3	Reactions of P ₄ with anionic carbon centred nucleophiles	10
1.4	Reactions of white phosphorus with carbenes	13
1.5	Electrochemical functionalisation of white phosphorus	14
1.6	Reactions of white phosphorus with radicals	17
1.7	Summary	20
1.8	References	21
2	Direct Catalytic Transformation of White Phosphorus into Aryl Phosphines and Phosponium Salts	29
2.1	Introduction	31
2.2	Results and discussion	33
2.2.1	Reaction development.....	33
2.2.2	Reaction scope.....	36
2.2.3	Mechanistic Studies	38
2.3	Conclusions	41
2.4	References	42
2.5	Supporting information.....	45
2.5.1	General information.....	45
2.5.2	Supplementary Method 1. General procedure for photocatalytic functionalisation of P ₄ (0.1 mmol scale).....	47
2.5.3	Photocatalytic functionalisation of P ₄ on a 1 mmol scale	67
2.5.4	Supplementary Discussions	89
2.5.5	Supplementary References	106
3	Versatile Visible-Light-Driven Synthesis of Unsymmetrical Phosphines and Phosponium Salts	109
3.1	Introduction	111
3.2	Results and discussion	114
3.2.1	Arylation of diphenylphosphine mediated by [Ir(dtbbpy)(ppy) ₂] ⁺ PF ₆ ⁻	114
3.2.2	Arylation of diphenylphosphine mediated by 3DPAFIPN	116
3.2.3	Arylation of phenylphosphine mediated by 3DPAFIPN	118
3.2.4	Alkylation of phenylphosphine mediated by 3DPAFIPN.....	119
3.2.5	Alkylation of phenylphosphine mediated by 3DPAFIPN.....	121

3.2.6	Mechanistic investigations	123
3.2.7	Application to the synthesis of a PCP pincer ligand	124
3.2.8	Application of 3DPAFIPN in P ₄ functionalisation	125
3.3	Conclusion	127
3.4	References.....	128
3.5	Supporting Information.....	131
3.5.1	General Information	131
3.5.2	Experimental Procedures	132
3.5.3	General procedures for increased scale reactions	135
3.5.4	Table for optimisation reactions.....	138
3.5.5	Mechanistic studies	143
3.5.6	Reactions with tetraphenyl diphosphine with primary alkyl halides	147
3.5.7	Functionalisation of P ₄ with organic photocatalyst.....	148
3.5.8	Crude ³¹ P{ ¹ H} NMR spectra from optimisation of small scale reactions.....	150
3.5.9	Characterisation spectra and data of isolated compounds in 1 mmol scale.....	190
3.5.10	References.....	227
4	Summary.....	229
5	Acknowledgment.....	233
6	Curriculum Vitae.....	235
7	Eidesstattliche Erklärung.....	239

1 DIRECT ORGANOFUNCTIONALISATION OF WHITE PHOSPHORUS TO MONOPHOSPHORUS COMPOUNDS: STATE-OF-THE-ART AND PERSPECTIVES



This chapter reviews the state of the art in the synthesis of organophosphorus compounds directly from white phosphorus. The review focuses on the synthesis of compounds with one phosphorus atom which contain at least one P–C bond. These compounds are subsequently termed “P₁ compounds”. Six different approaches to form P₁ organophosphorus compounds from white phosphorus are critically discussed and the perspectives of this important area of organophosphorus chemistry are evaluated.

1.1 INTRODUCTION

The importance of phosphorus compounds in daily life cannot be overestimated. Alongside carbon, hydrogen, nitrogen, oxygen and sulphur, phosphorus is one of the six most important chemical elements for any living organism. Phosphates are part of nucleic acids and ATP, which are indispensable to all known forms of life. In particular, it is essential that food crops take up enough phosphates a phosphate fertiliser must be added to agricultural soils to fulfil the global food demand.

Industrially, phosphate fertilisers are produced from phosphate rock, which is an enriched product of the mineral apatite. 85% of the phosphate rock are converted to phosphate fertilisers (14.9 million tons per year) and 5% is used as livestock feed additives.¹ The remaining 10% (1.8 million tons per year) are used to produce other phosphorus compounds,¹ of which approximately 1 million tons of white phosphorus are formed.² This white phosphorus plays a crucial role as precursor for numerous organophosphorus compounds, which are important among many other applications as flame retardants,^{3,4} phase transfer catalyst,^{5,6} and ligands for transition metal catalysts.^{7,8} For example, one of the most prominent organophosphorus compounds is triphenylphosphine, which has great industrial importance as a ligand in homogeneous hydroformylation, hydrogenation, oligomerisation processes and as starting material for the preparation of Wittig reagents, especially for the synthesis of vitamin A and β -carotene.⁹ Phosphonium salts meanwhile are used as phase transfer catalysts in several processes, including the carbonylation of methanol, the production of stabilisers, isocyanurate esters and polysiloxanes.⁹ Moreover, phosphine oxides are used as solvent extraction media for metal ions, carboxylic acids, alcohol and phenol from aqueous solutions.⁹

Despite their numerous applications and significance in industry and academia, the current state-of-the-art synthesis of organophosphorus compounds are based on hazardous multistep protocols (Fig.1). In general, primary and secondary phosphines are synthesised via PH_3 . Industrially, PH_3 is produced either by reaction of P_4 with aqueous sodium hydroxide, yielding PH_3 and NaH_2PO_2 , or by an acid-catalysed disproportionation of P_4 . Primary and secondary phosphines are then prepared by radical- or acid-catalysed reaction of PH_3 with alkenes.

While only linear α -alkenes form tertiary phosphines by the PH_3 process, triarylphosphines are prepared via PCl_3 . In a first step, white phosphorus is oxidised with toxic chlorine gas to form PCl_3 . Organolithium or Grignard reagents are then used to replace the chloride anions by organic groups. Far better would be methods which circumvent the use of toxic chlorine gas or explosive PH_3

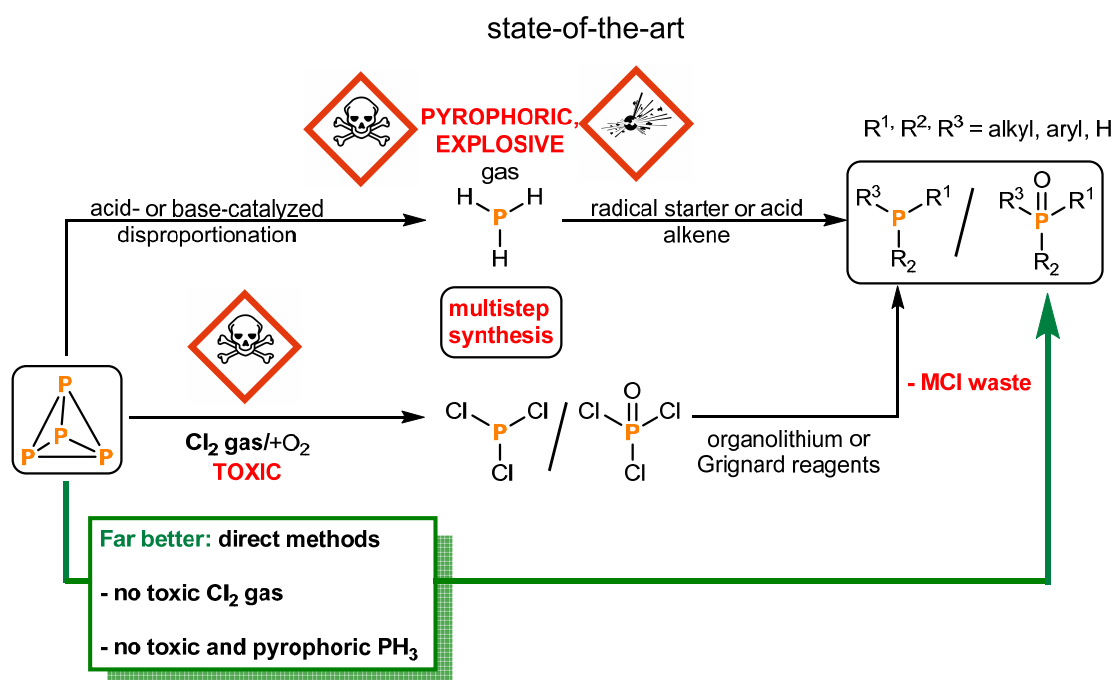


Fig. 1. Comparison of the state-of-the-art synthesis of phosphines and phosphine oxides and direct methods to functionalise white phosphorus to P_1 compounds.

and do not generate MCl waste. Several concepts have been investigated to activate and functionalise white phosphorus in a manner which furnishes organophosphorus compounds directly. In general, these approaches can be categorised into three major groups according to the way white phosphorus is activated: methods are based on the use of transition metal complexes,^{10–13} main group element compounds,^{14,15} and radical reagents.^{14,16} While the activation of white phosphorus and functionalisation to with two or more P atoms (P_n compounds with $n \geq 2$) has been reported in many publications, direct, one-pot methods to generate P_1 compounds from P_4 remain rare. These chapter will focus specifically on the single-step synthesis of P_1 organophosphorus compounds containing at least one P–C bond. Systems that employ particularly harsh conditions like liquid ammonia, Co-60- γ -rays irradiation, or extremely high pressure and/or high temperature methods are excluded from this report.^{17,18}

1.2 P₄ FUNCTIONALISATION IN BASIC MEDIA

The reaction of elemental phosphorus (red or white) or PH₃ in superbasic media (KOH/H₂O/organic solvent) with organic halides and alkenes was intensively studied and reviewed by Trofimov and co-workers.^{19,20} Several phosphines and phosphine oxides could be prepared by this method. Initial addition of OH⁻ opens the P₄ tetrahedron forming two species **A** and **B** in equilibrium.^{21,22} Addition of an alkene or organic halide to the phosphidic P atom of species **A** leads to the formation of tertiary phosphines, whereas attack on the phosphinite anion of species **B** leads preferentially to the formation of the corresponding phosphine oxides (Fig. 2).^{19,20,23,24} Interestingly, secondary and tertiary phosphine oxides are formed preferentially when white phosphorus reacts with organic halides. In contrast, addition of unsaturated organic compounds to white phosphorus in superbasic media leads to the formation of either tertiary phosphines, or tertiary phosphine oxides, or mixtures of both.

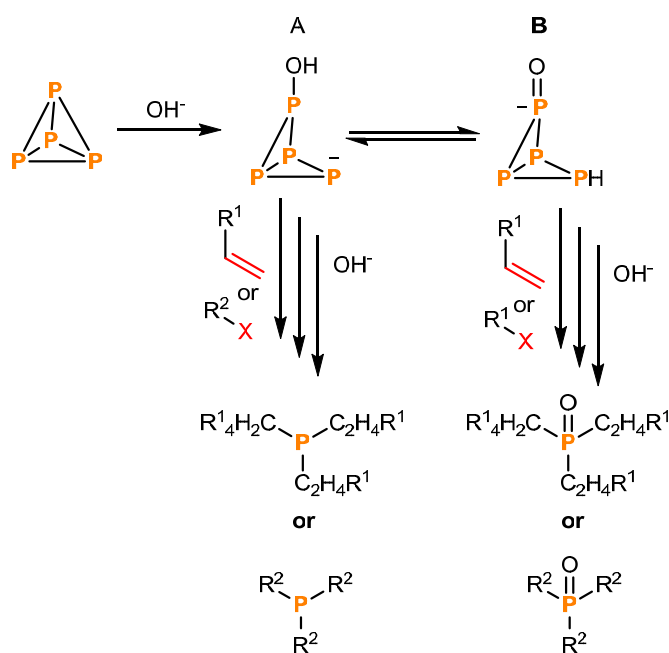


Fig. 2 Initial break-up of the P₄ tetrahedron in superbasic media KOH/H₂O/organic solvent.

1.2.1 Reactions of white phosphorus with organyl halides, R–X

The functionalisation of white phosphorus with an RX compound in a basic medium was reported as early as in 1904 by Auger. Reaction of white phosphorus and methyl iodide or iso-amyl iodide in NaOH/ethanol yielded the corresponding primary phosphine (**1**), sodium iodide and disodium hydrogen phosphite (Fig. 3).²⁵

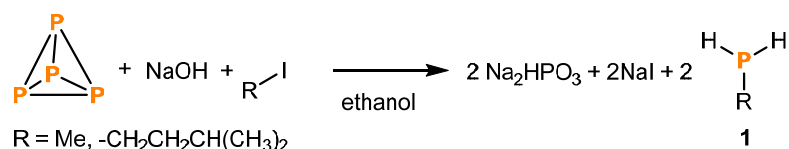


Fig. 3 White phosphorus functionalisation with methyl iodide and iso-amyl iodide.

Conceptually related methods were further investigated by the Trofimov group.²⁰ These P–C bond formation reactions were performed under phase transfer conditions. Employing Et₃BnN⁺Cl⁻ (Bn = CH₂Ph) as phase transfer catalyst (PTC) with a suspension of white phosphorus, KOH, organic solvent, water and organic chloride R–Cl yielded the corresponding secondary and tertiary phosphine oxides.^{20,23,26–30} 1-(chloromethyl)naphthalene yielded 45% secondary (**2a**) and 29% tertiary phosphine oxides (**2b**) in KOH/H₂O/benzene/Et₃BnN⁺Cl⁻ (Fig. 4a).²³ Meanwhile, white phosphorus reacted with 2-(chloromethyl)pyridine hydrochloride in the slightly different superbase system KOH/H₂O/toluene/Et₃BnN⁺Cl⁻ to form a mixture of the corresponding secondary (**3a**) tertiary phosphine oxide (**3b**) and potassium phosphinate (**3c**) in a total yield of 34% (Fig. 4b).²⁶ While a 56% yield of tris[(5-chloro-2-thienyl)methyl]phosphine oxide (**4**, Fig. 4c),²⁷ and 42% of tris(4-vinylbenzyl)phosphine oxide (**5**, Fig. 4b)²⁸ could be obtained in dioxane as solvent, a mixture of secondary (**6a**, **7a**) and tertiary phosphines (**6b**, **7b**) was formed with 4-methoxybenzyl chloride (Fig. 4c),³⁰ and benzyl chloride (Fig. 4d) as substrates.²⁹ Interestingly, in most above-mentioned cases, the potassium salts of the alkylphosponic and dialkylphosphinic acid were formed as side products and isolated as the corresponding acids after treatment of the reaction mixture with hydrochloric acid.^{23,28,29}

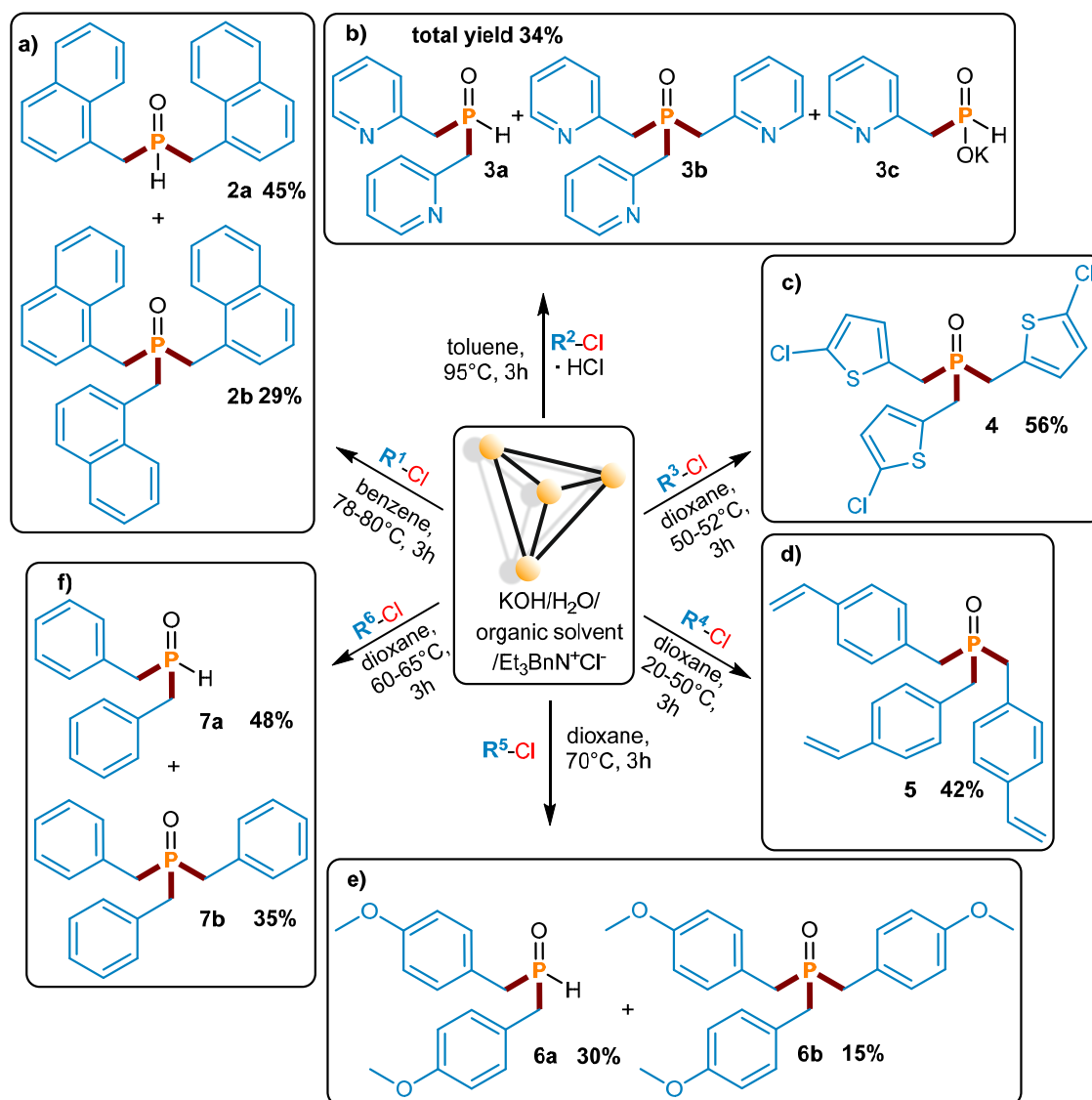


Fig. 4 White phosphorus functionalisation by alkyl chlorides. All reactions were performed in the superbasic media $KOH/H_2O/organic\ solvent/ Et_3BnN^+Cl^-$.^{23,26–30} NMR conversions based on the organic halide. c, d) Isolated yield. In case of a, d, and f the potassium salts of the alkylphosphonic and dialkylphosphinic acid were formed as side products and isolated as the corresponding acids after treatment of the reaction mixture with hydrochloric acid.^{23,28,29}

In some cases, the P–C bond formation with an R–X compound is more efficient with bromides than with chlorides. In 2002, Trofimov and co-workers reported the formation of 13% of (prop-2-enyl)phosphine by addition of allylchloride to a mixture of KOH and P_4 in water/dioxane mixture. A much higher efficiency was observed by replacement of allylchloride by allylbromide. A total yield of 96 % (based on the allyl halide) could be detected with triallylphosphine oxide (**8a**), (E)-diallyl(prop-1-en-1-yl)phosphine oxide (**8b**) and (Z)-diallyl(prop-1-en-1-yl)phosphine oxide (**8c**) detected as major products in the reaction mixture (Fig. 5a).³¹

Good yields were also obtained using white phosphorus, 2-bromopyridine in a similar reaction with P_4 using KOH/DMSO/ H_2O to give 50% tris(2-pyridyl)phosphine (**9**) and only small amounts of the corresponding phosphine oxide. (Fig 5b).²⁴

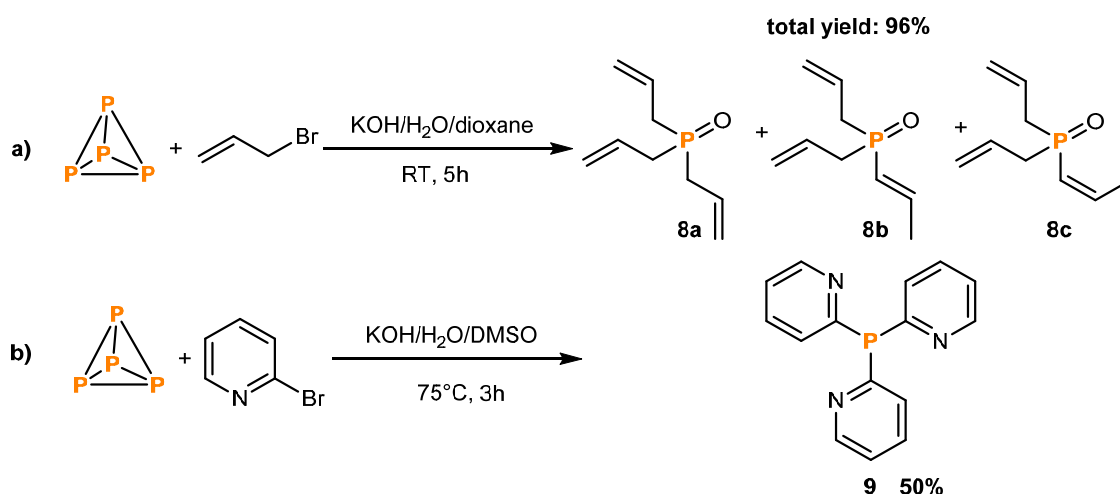


Fig. 5 White phosphorus functionalisation by alkyl and aryl bromides. a) NMR conversions based on the organic substrate. b) Isolated yield based on 2-bromopyridine.

It is also possible to replace halides with pseudohalides. The phase transfer system KOH/benzene/ $Et_3BnN^+Cl^-$ was used to form alkylphosphonic acids from white phosphorus and alkyl methanesulfonates. Butylphosphonic (**10a**), octylphosphonic (**10b**) and nonylphosphonic acid (**10c**) could be formed in yields up to 40% (Fig. 6).³²

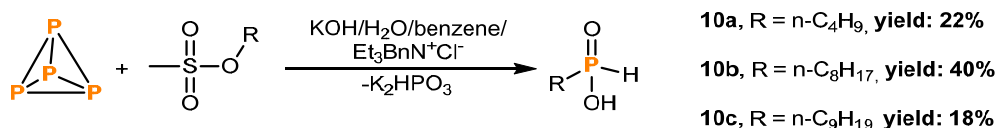


Fig. 6 White phosphorus functionalisation with methanesulfonates. All reactions were performed in the superbasic system KOH/ H_2O /benzene/ $Et_3BnN^+Cl^-$. Isolated yields based on the organic substrate after acidic work-up.

1.2.2 Reactions of white phosphorus with alkenes and alkynes

In 1962 Rauhut et al. reported a direct synthesis of tertiary phosphines from white phosphorus (Fig. 7).³³ Addition of aqueous KOH to a mixture containing white phosphorus and acrylonitrile in acetonitrile yielded 53% of tris(2-cyanoethyl)phosphine oxide (**11a**). Replacement of acrylonitrile by acrylamide led to the formation of side products; however, changing the solvent to ethanol instead of acetonitrile proved to be beneficial, and reaction of acrylonitrile and white phosphorus in a KOH/ H_2O /ethanol mixture yielded 74% of tris(2-carbamoyl)phosphine oxide (**11b**).

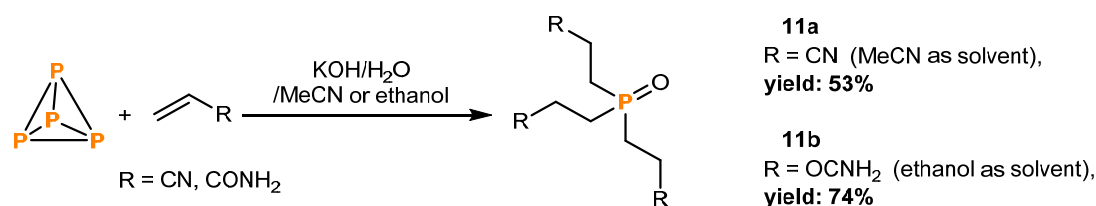


Fig. 7 White phosphorus functionalisation with acrylonitrile or acrylamide. The reaction of white phosphorus with acrylonitrile in KOH/H₂O/MeCN and the reaction with acrylamide in KOH/H₂O/ethanol. Isolated yields based on phosphorus.

Maier subsequently found in 1973 that white phosphorus reacts with *N,N*-dialkyl acrylamides in the presence of KOH in a water/ethanol mixture. Six tris(*N,N*-dialkyl-carbamoyl)ethyl)phosphine oxides (**12a-f**) could be prepared by this method in 30-87% yield (Fig. 8a). Interestingly, mono *N*-alkyl-acrylamides only reacted with white phosphorus when three times more KOH is used in ethanol or the reaction is carried out in MeCN or (Fig 8b, **13a,b**).³⁴

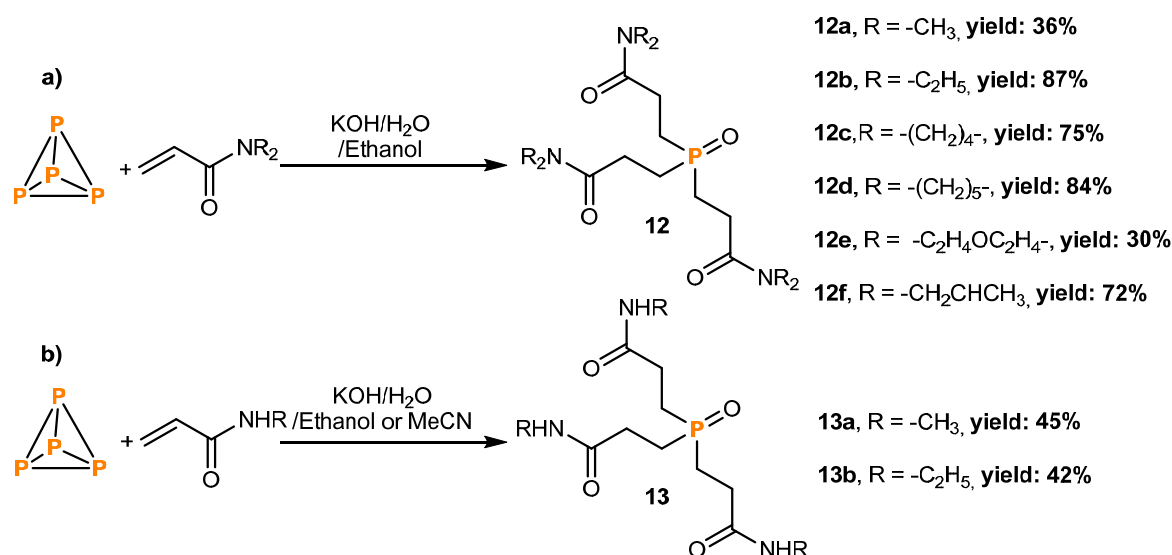


Fig. 8 White phosphorus functionalisation with *N,N*-dialkyl acrylamides, and *N*-alkyl acrylamides. a) Formation of tris(2-(*N,N*-dialkyl-carbamoyl)ethyl)phosphine oxides from white phosphorus. b) Formation of tris(2-(*N*-alkyl-carbamoyl)ethyl)phosphine oxides from white phosphorus. Isolated yield.

Further pioneering work was done by Trofimov and co-workers.^{19,20} In general, the functionalisation of alkenes was performed using a suspension of white phosphorus and KOH in DMSO (or HMPA) in the presence of the alkene (Fig. 9). Styrene (Fig. 9a) yielded a mixture of secondary (**14a**) and tertiary phosphine oxide (**14b**) in 59% total yield.²² 2-vinylnaphthalene (Fig. 9b) reacted with white phosphorus at 90-96 °C to yield the targeted tertiary phosphine (**15a**) and phosphine oxide (**15b**) in 11% and 52% yield, respectively.³⁵ The conversion of tris[2-(2-naphthyl)ethyl]phosphine (**15a**) could be increased to 58% by treatment of the reaction mixture with oxygen.

The analogous reactions of 2- and 4-vinylpyridines meanwhile gave tris[2-(2-pyridyl)ethyl]phosphine oxide (**16**) and tris[2-(4-pyridyl)ethyl]phosphine oxide (**17**), respectively in good conversions even at room temperature (Fig. 9c, d).³⁶

An unsaturated tertiary phosphine could also be synthesised by replacing the alkenes by phenyl acetylene. The corresponding triphenylethenylphosphine (**18a**) could be synthesised in total conversions up to 48%, with a further 10% of the related phosphine oxide (**18b**, Fig. 9e).³⁷

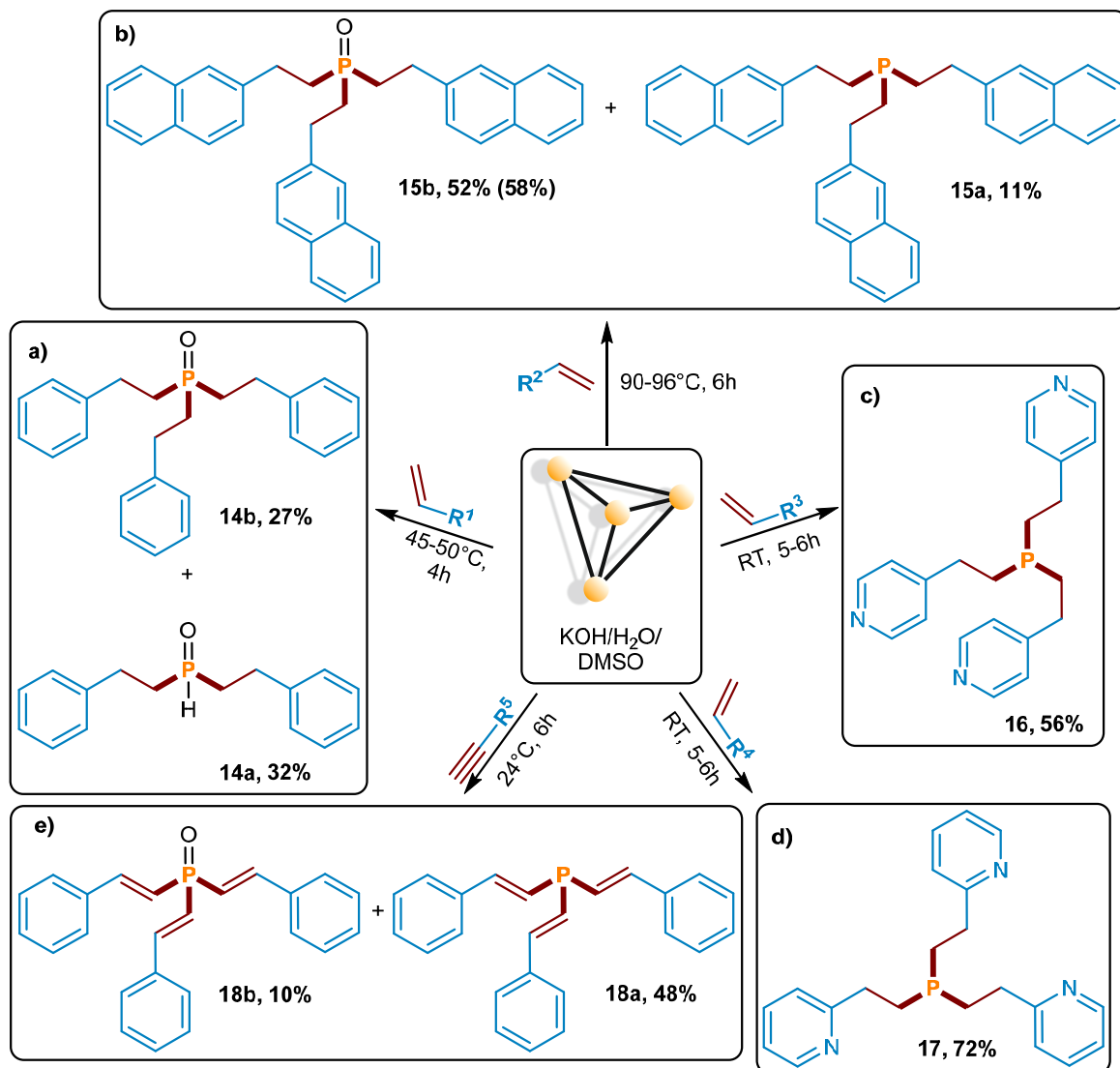


Fig. 9 White phosphorus functionalisation with styrene derivatives and phenylacetylene. The reactions were performed in the superbasic system KOH/H₂O/DMSO. Different substituted phosphines and phosphine oxides could be prepared in NMR conversions up to 72% (based on the organic substrate).

Finally, Trofimov and co-workers reported the hydrophosphorylation of vinyl sulfide.³⁸ Reaction of isobutyl vinyl sulphide with white phosphorus in a superbasic system at 75°C and subsequent workup with hydrochloric acid yielded 10 % of [2-(isobutylthio)ethyl]phosphinic acid (**19**, Fig. 10).

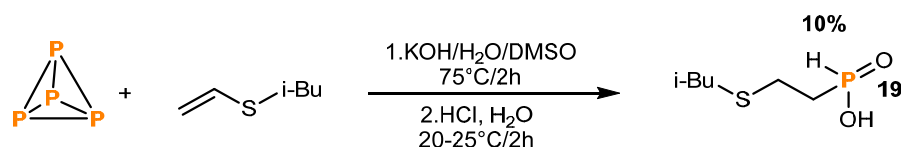


Fig. 10 White phosphorus functionalisation with isobutyl vinyl sulphide.

1.3 REACTIONS OF P₄ WITH ANIONIC CARBON CENTRED NUCLEOPHILES

White phosphorus is known to undergo reactions with nucleophilic compounds. Rauhut and Semsel used organic nucleophiles and reacted them with white phosphorus.³⁹ In their initial publication in 1963, they reported the formation of up to 40% of phenylphosphine (**20a**) by stirring white phosphorus and phenyllithium in refluxing ether followed by addition of excess LiAlH₄ (Fig. 11a).⁴⁰

The same authors also reported the formation of mixtures of dibutylphenylphosphine (**21a**), butyldiphenylphosphine (**21b**) and small amounts of butyldiphenylphosphine oxide by reacting white phosphorus with a combination of phenyllithium or phenylsodium and butyl halides and subsequent hydrolysis (Fig. 11b).³⁹ Analogous formation of phosphines (**22a,b**; **23a,b**) was achieved by replacing phenyllithium by related nucleophiles such as 4-methoxyphenyllithium and 3-trifluoromethylithium (Fig 11c,d). Interestingly, the related reaction of 1-naphtyllithium and butyl bromide with white phosphorus gave a noticeably different product distribution, with the formation of the secondary product butyl(1-naphtyl)phosphine (**24a**) detected alongside that of dibutyl(1-naphtyl)phosphine (**24b**, Fig 11e).

As well as aryl- and alkyl/aryl- substituted phosphines, purely alkyl-substituted phosphines can also be prepared in a similar manner by replacing aryllithium with alkylolithium reagents. Butyllithium and butylbromide reacted with white phosphorus to yield the tertiary (**25a**) and secondary butylphosphines (**25b**) in 39% and 10% conversions, respectively (Fig 11f).

Trofimov applied broadly the same method to synthesise α,β -acetylenic phosphines. But-1-nyllithium was added to a suspension of white phosphorus in HMPA and THF. But-1-nyldialkyl (**26a**, **27a**) and alkyldi(but-1-yl)phosphines (**26b**, **27b**) were formed after stirring for one hour and subsequent addition of ethyl bromide or propyl chloride. Total yields of up to 20% were achieved (Fig. 11g, h).⁴¹

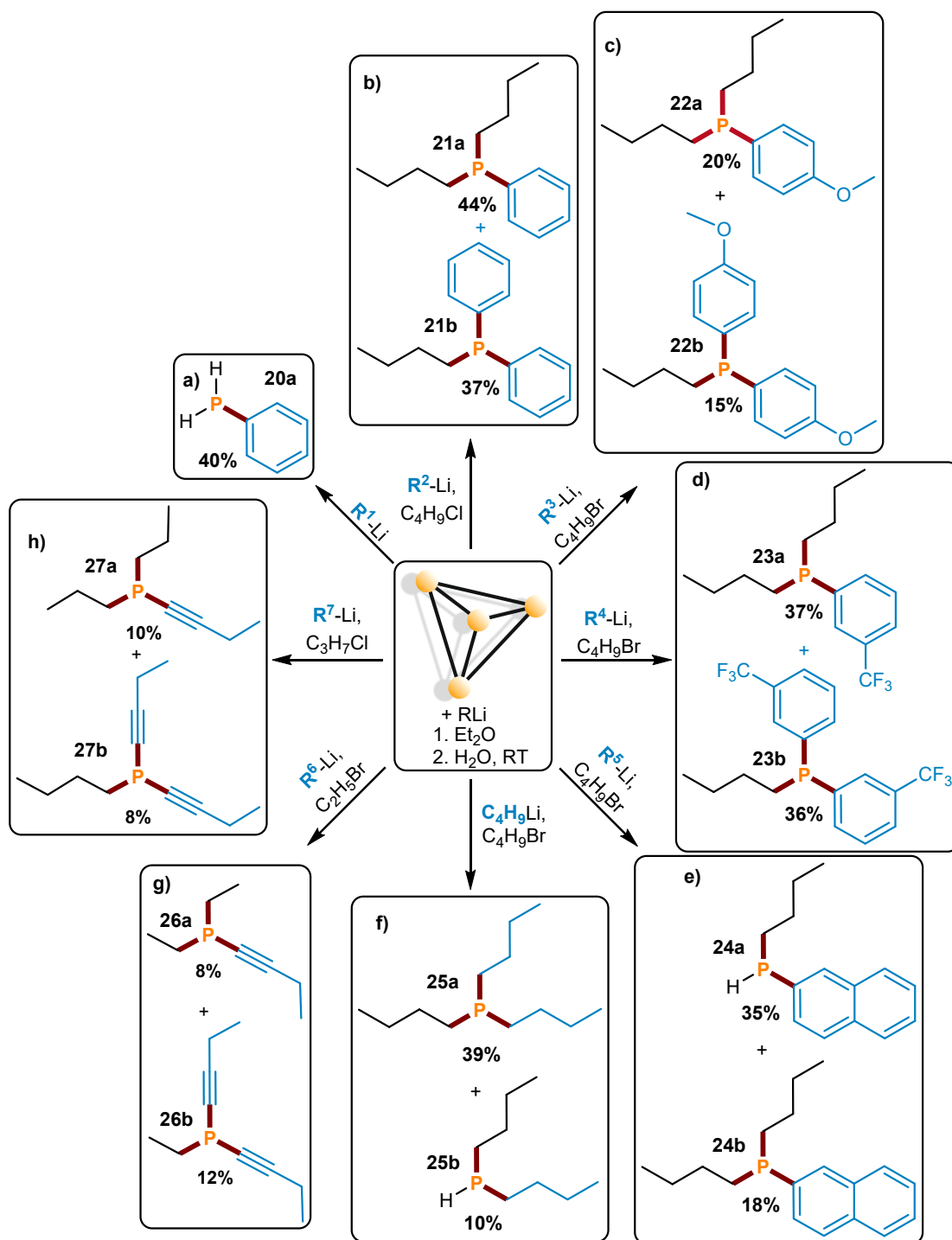


Fig. 11 White phosphorus functionalisation with organolithium compounds. Conversions based on phosphorus. In case of g and h a solvent mixture of hexane/HMPTA/THF was used instead of Et_2O .

Based on the above-mentioned work, Xu and co-workers developed an efficient one-pot reaction for the direct synthesis of phospholyl lithium compounds (**28a-d**; **29a,b**) from white phosphorus. Quantitative conversion to phospholyl lithium derivatives were obtained by stirring a THF solution containing a 1,4-dithio-1,3-butadiene derivative and white phosphorus in THF as solvent at RT for 12h. Six examples were isolated in almost quantitative fashion (Fig. 12).⁴²

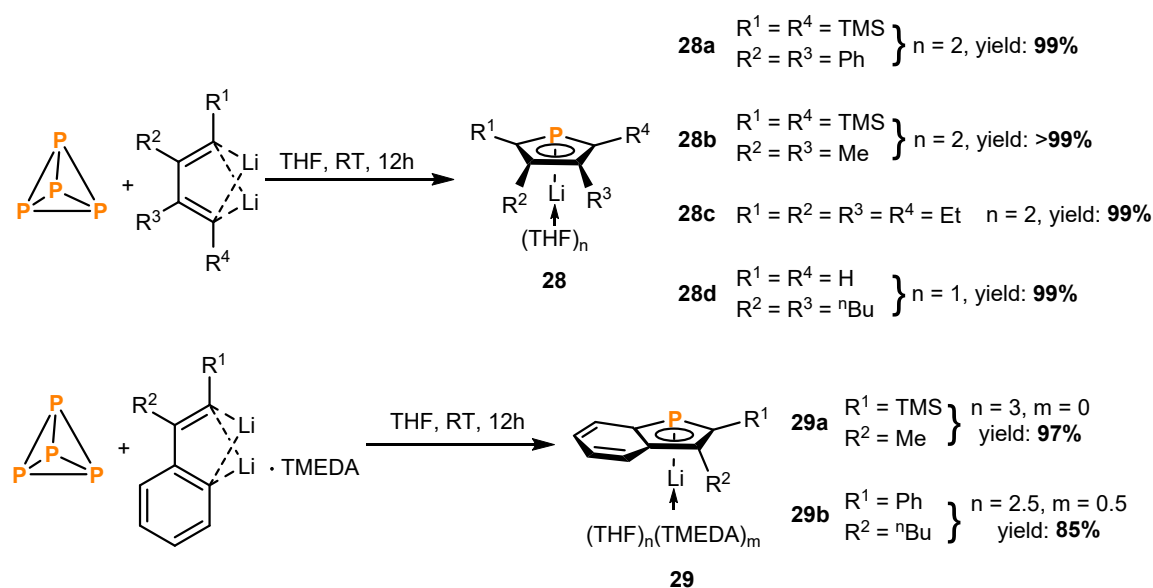


Fig. 12 White phosphorus functionalisation with 1,4-dilithio-1,3-butadienes. Isolated yields based on dilithium reagent.

The attack of nucleophiles to P₄ is not limited to organolithium compounds. Sinyashin and co-workers showed that organozinc reagents also react with white phosphorus to form the corresponding secondary and primary phosphines. Addition of solutions of the organozinc reagents Ph₂Zn and Mes₂Zn to solutions of white phosphorus in toluene and subsequent hydrolysis with a solution of HCl led to the formation of Ph₂PH (**20b**, 23%) and PhPH₂ (**20a**, 48%) or MesPH₂ (**30**, 36%), respectively (Fig. 13).⁴³

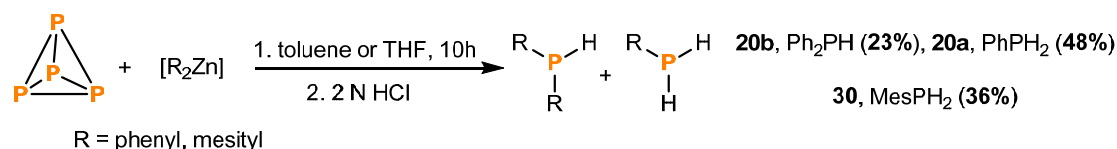


Fig. 13 White phosphorus functionalisation with organozinc compounds. Isolated yields based on phosphorus.

Cyanide anions can also be employed for the same approach as carbon-based inorganic nucleophiles. In 1985, Schmidpeter *et al.* reported the synthesis of dicyanophosphide (**31**) from elemental phosphorus and CN⁻ in excellent yields (Fig. 14).⁴⁴

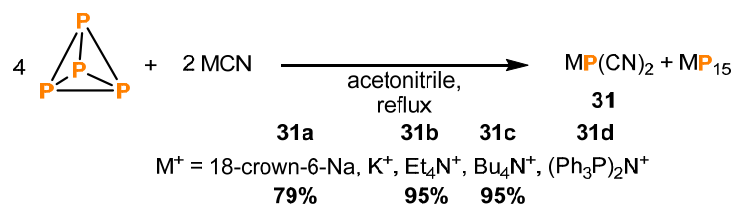


Fig. 14 White phosphorus functionalisation with CN⁻.

1.4 REACTIONS OF WHITE PHOSPHORUS WITH CARBENES

Activation of P₄ by nucleophiles is not limited to carbon-centered anionic species, also carbenes undergo reactions with P₄ to form P–C bonds. While sterically encumbered carbenes form polyphosphorus compounds, P₁ compounds are formed in the presence of sterically less hindered carbenes.¹⁶ In 2009, the group of Bertrand reported the formation of a bis(carbene) P₁ cation upon treatment of white phosphorus with 3 eq. of bis(diisopropylamino)cyclopropenylidene.⁴⁵ ³¹P NMR spectroscopy of the reaction mixture showed the formation of two main species. A singlet signal at -93.2 ppm, which could be ascribed to a doubly NHC-coordinated P₁ cation (**32**), and an ABX system which might be an allylic triphosphorus anion (Fig. 15).

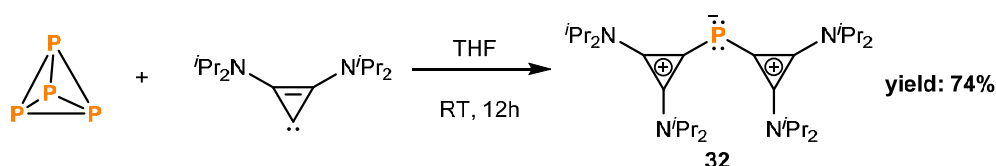


Fig. 15 White phosphorus functionalisation with bis(diisopropylamino)cyclopropenylidene.

Based on this work, the groups of Gudat and Grützmacher reported the synthesis of inversely polarised phosphalkenes (**33a-d**) and bis(carbene) stabilised P(I) cations (**34a,b**) by reacting NHCs and KOtBu with white phosphorus (Fig. 16).⁴⁶ The authors reported the formation of a red precipitate after 12-24h. For N-methylated derivatives, the supernatant solutions contained mainly phosphalkenes, minor amounts of cation **34** and polyphosphorus compounds. The reddish precipitate contained polyphosphorus compounds and **34**. N-arylated imidazolium salts did not form the bis(carbene) stabilised P(I) cation from P₄, but the formation of phosphalkenes and polyphosphorus compounds was observed. **33a-c** could be isolated in yields up to 26% (based on NHC), but **33d** was identified only by NMR spectroscopy.

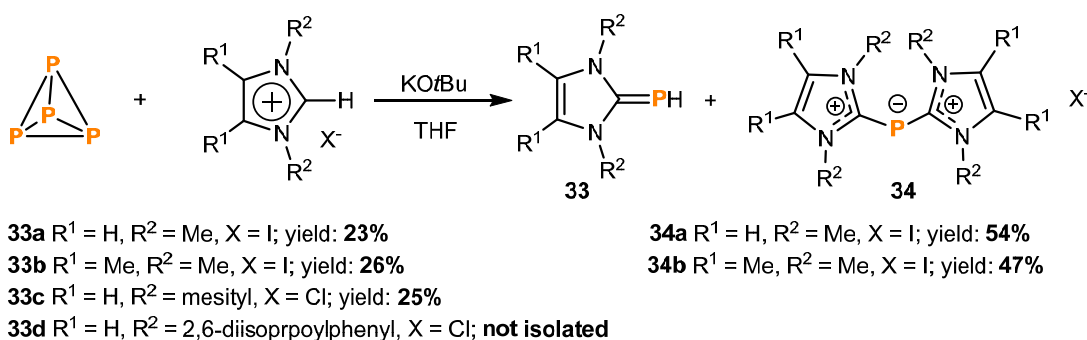


Fig. 16 White phosphorus functionalisation with imidazolium salts and KOtBu. Isolated yields based on the imidazolium salt.

1.5 ELECTROCHEMICAL FUNCTIONALISATION OF WHITE PHOSPHORUS

The group of Sinyashin was the first to explore an alternative concept for white phosphorus functionalisation, applying electrochemical methods to yield phosphates, phosphonium salts and phosphines.^{47–51} Electrogenated nickel(0) complexes were used as active compounds. Applying a defined potential to a solution containing $[\text{Ni}(\text{bpy})]\text{Br}_2$ (**35**), a halobenzene and P_4 resulted in the formation of phenyl-substituted phosphines and phosphine oxides (Fig. 17a). The proposed mechanism is based on initial two electron reduction of the nickel complex (**35**, Fig 17a, step *i*) and subsequent oxidative addition of the halobenzene (step *ii*). The resulting nickel(II) species (**36**) then reacts with white phosphorus to transfer a phenyl group and ultimately form the observed product (step *iii*). Interestingly, the anode material and the choice of the halide species had a huge impact on the product selectivity. While electrocatalytic P_4 functionalisation with bromobenzene as substrate and a Zn anode in DMF formed up to 80% of triphenylphosphine (**20c**), $(\text{PhP})_5$ (**37**) was formed in 60 % yield with a Mg anode in DMF, and an aluminium anode led to the selective formation of PPh_3O (**38**) in acetonitrile. Furthermore, triphenylphosphine (**20c**) was always the main product with iodobenzene as substrate, regardless of the anode material. This approach is not limited to arylphosphines: Tri(isopropyl)-, tributyl- and trihexylphosphine oxide could also be generated by this method in 73-78% yield.⁵¹

More recently, Budnikova and co-workers extended this method and reported the synthesis of fluoroalkylphosphines (Fig 17b). Tris(1H,1H,2H,2H-perfluorohexyl)- (**39**) and tris(perfluorohexyl)phosphine (**40**) could be detected by ^{31}P and ^{19}F NMR spectroscopy, and the corresponding oxides were isolated by treatment of the residue with hydrogen peroxide in 64% and 56% yield, respectively (Fig 17b, step *iv*).⁴⁹

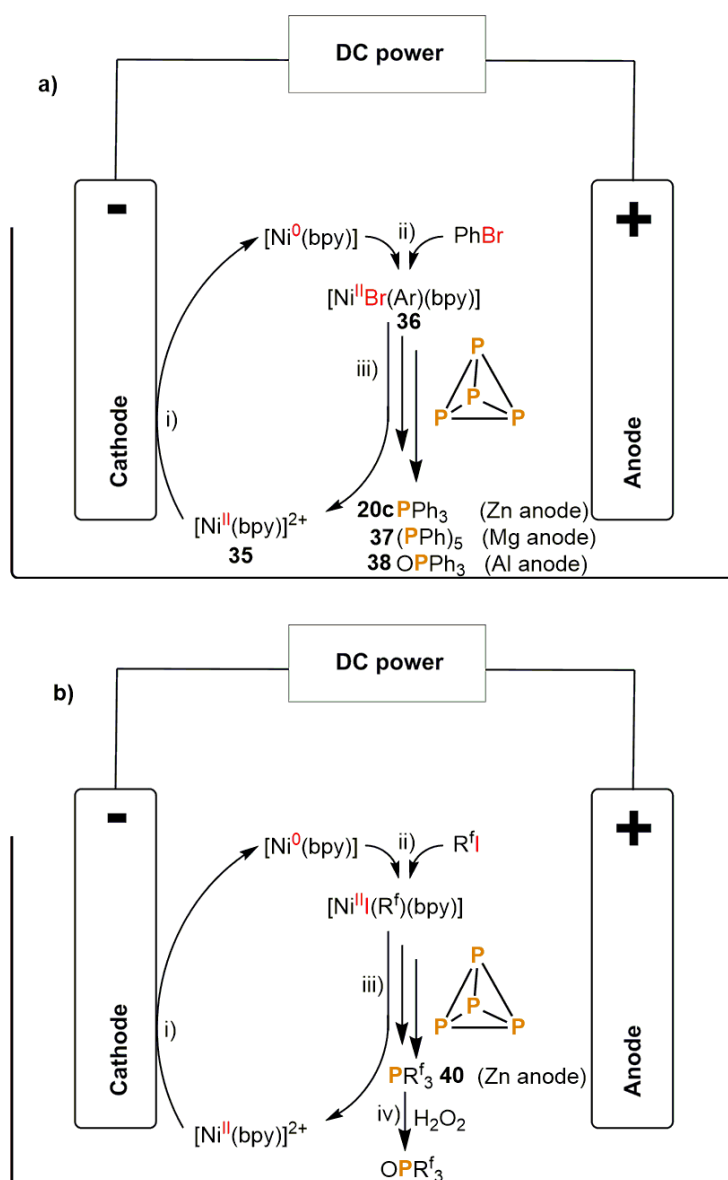


Fig. 17 Electrochemical functionalisation of white phosphorus catalysed by $[\text{Ni}(\text{bpy})]^{2+}$.

The same group also reported that triphenylphosphine (**20c**) can be directly synthesised from white phosphorus and iodo- or bromobenzene without a nickel catalyst, using DMF as solvent, a Pt cathode and a Zn anode in an undivided electrochemical cell. While $\text{Zn}(0)$ was formed by the cathode in the absence of halobenzene (Fig. 18, step *i, ii*), organozinc compounds are formed in the presence of halobenzene (step *iii*), which further react with white phosphorus to yield the corresponding tertiary phosphine (step *iv*) (c.f. Fig. 13 in section 1.3).

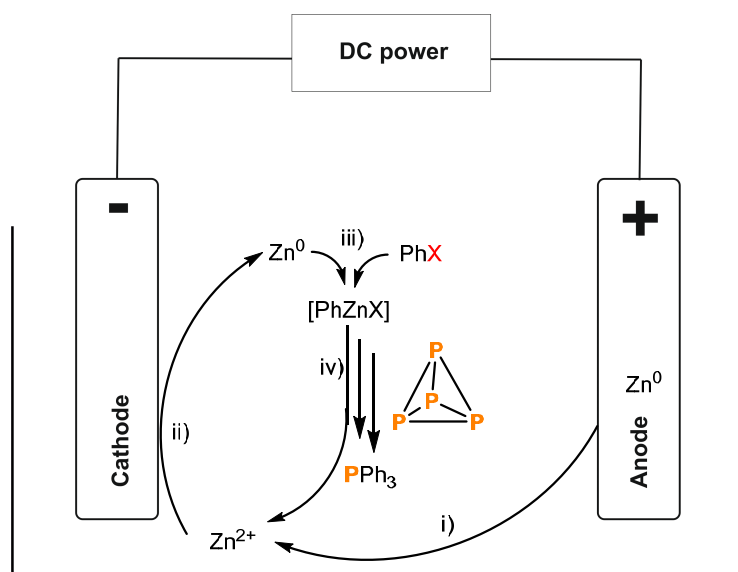


Fig. 18 Electrochemical functionalisation of white phosphorus with Zn^0 .

Electrochemical methods to functionalise white phosphorus can also be applied to alkenes (Fig. 19).⁵² This can be done in an indirect way, by electrochemical reductive production of PH_3 , which is then bubbled through a solution of alkene in superbasic media, or *in situ* in a buffer solution. For example, when white phosphorus and an alkene were added to potassium acetate buffer, heated up to 50 °C to melt the white phosphorus, and subjected to electrolysis conducted in separated anodic and cathodic compartments under galvanostatic conditions at 20 °C, the corresponding primary alkyl phosphines resulting from the hydrophosphination of styrene (**41a**), 2-methyl-2-phenylstyrene (**41b**), vinyl acetate (**41c**), and 1-hexene (**41d**) could be isolated in yields up to 46%. Alkenes with more positive reduction potentials than white phosphorus such as 2-vinyl pyridine, acrylamide, phenylacetylene and vinyl naphthalene did not form the product. Presumably, reduction of the alkene was favoured in these cases analogous over reduction of white phosphorus with the latter being necessary to achieve the desired reactivity.

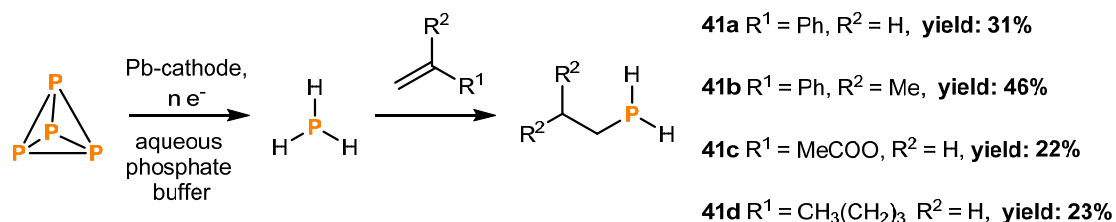


Fig. 19 Electrochemical functionalisation of white phosphorus with alkenes. Isolated yields based on phosphorus.

1.6 REACTIONS OF WHITE PHOSPHORUS WITH RADICALS

In 1992 Barton and Zhu reported a new route to phosphonic acids. Irradiation of a solution containing the so-called Barton PTOC ester (**42**) and white phosphorus in a $\text{CH}_2\text{Cl}_2/\text{CS}_2$ mixture with two tungsten lamps and subsequent oxidation with H_2O_2 afforded up to 87 % yield of the corresponding phosphonic acid (**43a-d**, Fig. 20, method 1).⁵³ Later, in 1998 Barton and Vonder Embse reported a modification of the initial method,⁵⁴ where the efficiency of the radical functionalisation was increased by replacement of the binary mixture $\text{CH}_2\text{Cl}_2/\text{CS}_2$ by THF. Addition of the Barton ester to P_4 in THF resulted in spontaneous evolution of CO_2 , and subsequent oxidation with H_2O_2 resulted in the formation of phenethyl- (**43a**), cyclohexyl- (**43c**), 1 adamantyl- (**43d**) and isopentylphosphonic acids (**43e**) in an almost quantitative fashion. Interestingly, these reactions performed in THF did not require any irradiation (Fig 20, method 2a). A slightly milder variant of the method could also be applied to modify natural carboxylic acids to the corresponding phosphonic acids (Fig. 20, method 2b).

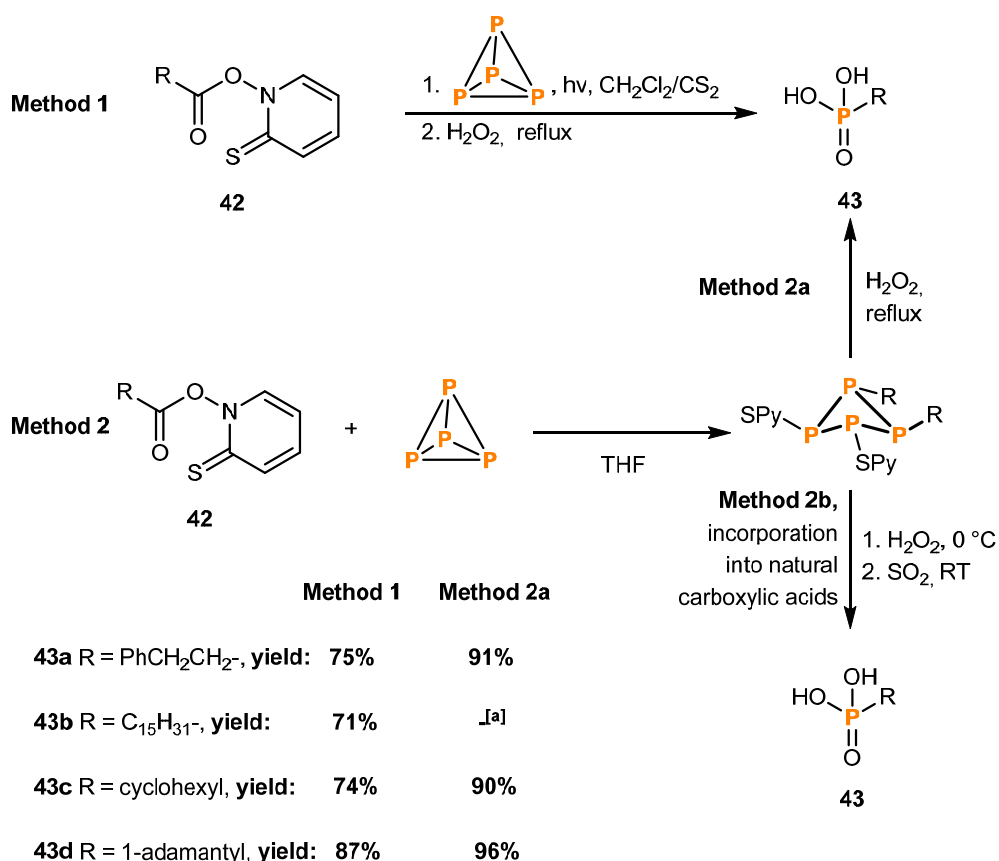


Fig. 20 White phosphorus functionalisation with an *in situ* generated carbon centered radical. Three different methods were reported by Barton and co-workers. For simplicity, not all reported products are shown in this figure. [a] not reported. Method 2b is used to form phosphonic acids from natural products. Isolated yields based on **42**.

While high concentrations of oxygen were detrimental and led to reduced yields of the targeted products, small amounts were in fact necessary to start the reactions. Based on this observation and further mechanistic studies, the authors proposed a mechanistic picture in which white phosphorus reacts with traces of oxygen to form $[P_4O_2]^\bullet$, which subsequently reacts with the Barton ester (**42**) to induce loss of CO_2 and formation of a carbon centered radical (**44**, Fig. 21, step *i*). The radical is trapped by white phosphorus forming RP_4^\bullet (**45**, step *ii*), which attacks more of the ester (**42**) yielding an RP_4SPy butterfly structure (**46**) and further R^\bullet (**44**, step *iii*). Subsequent further attack of the carbon centered radical (**44**, step *iv*) and the Barton ester (**42**) on the initially formed RP_4SPy (**46**) finally leads to the formation of the $R_2P_4(SPy)_2$ tetraphosphetane (**48**) and alongside yet another carbon centered radical (**44**), which re-enters the cycle (step *v*). Subsequent oxidation of $R_2P_4(SPy)_2$ (**48**) leads then to the targeted phosphonic acid (**43**, step *vi*).

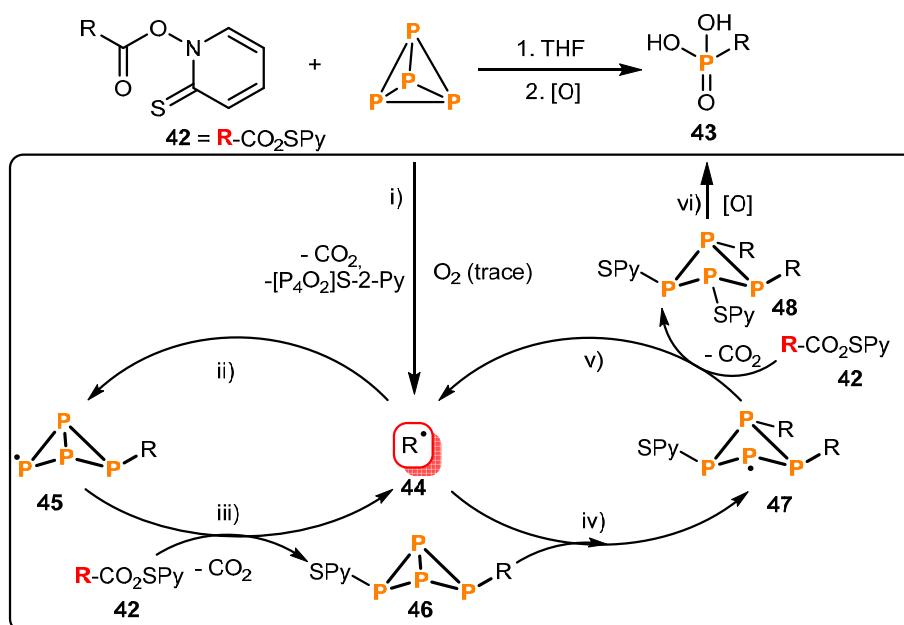


Fig. 21 Mechanistic details of the direct functionalisation of white phosphorus with the N-hydroxy-2-thiopyridone esters (PTOC).

Building on this pioneering work by Barton, Cummins and co-workers developed the radical-based synthesis of triaryl, trisilyl and trisannylphosphines from P_4 (Fig. 22).⁵⁵ For example, using 3 eq. of the titanium complex $Ti(N[{}^tBu]Ar)_3$ ($Ar = 3,5-C_6H_3Me_2$) as a stoichiometric halogen atom abstractor, the reaction of 3 eq. of bromobenzene and 0.25 eq. of P_4 yielded triphenylphosphine and tetraphenyldiphosphine. The latter is found to be a stable intermediate formed *en route* to PPh_3 and by using 5 eq. of bromobenzene the tertiary monophosphine was selectively formed. While the reaction proceeds in the same way with iodobenzene instead of bromobenzene, analogous functionalisation did not take place with chlorobenzene as a substrate.

Remarkably, the reaction was not limited to halobenzenes. Similar PR_3 compounds were also formed in excellent yields starting from bromocyclohexane, triphenyltin chloride and trimethylsilyl chloride.

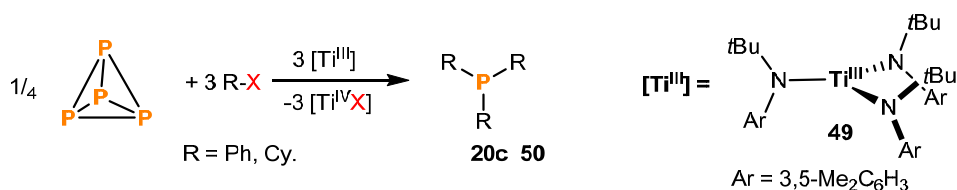


Fig. 22. Stoichiometric functionalisation of white phosphorus with $\text{Ti}(\text{N}[\text{tBu}]\text{Ar})_3$ ($\text{Ar} = 3,5\text{-C}_6\text{H}_3\text{Me}_2$). The titanium complex operates as halide abstractor and the formed carbon centered radical attacks white phosphorus to form tertiary phosphines.

Interestingly, while more typical one-electron reducing agents such as $\text{CoCl}(\text{PPh}_3)_3$, SmI_2 and Cp_2TiCl gave no reaction with bromobenzene and white phosphorus,⁵⁵ Ghosh, Cummins and Gladzy were able to use stronger reductants like SmX_2 ($\text{X} = \text{Br}, \text{Cl}$) in combination with P_4 and aryl iodides to form the corresponding tertiary arylphosphines in isolated yields ranging from 23–41% (**52**, **53a,b**).⁵⁶ These reactions are presumed to proceed in a similar manner as those mediated by $\text{Ti}(\text{N}[\text{tBu}]\text{Ar})_3$, with the aryl iodide being reduced to form an iodide anion and an aryl radical, which subsequently reacts with P_4 . Consistent with this interpretation, it was found that the formation of tertiary alkylphosphines (**51**) could be achieved using the milder SmI_2 for more easily reduced fluororous alkyl iodides (Fig. 23).

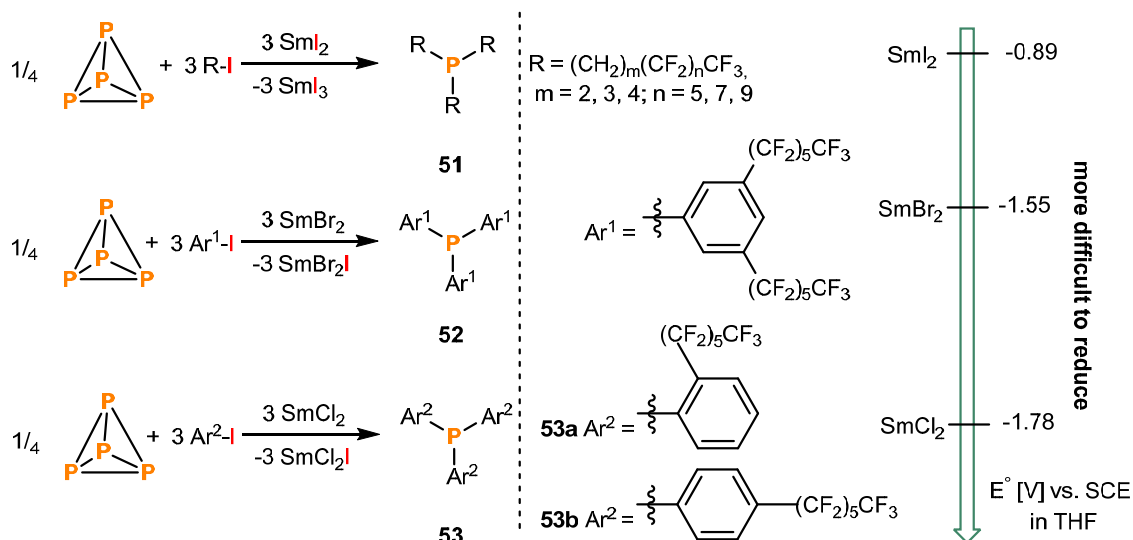


Fig. 23 Functionalisation of white phosphorus with samarium(II) halides. The two-electron reductant Sm^{2+} operates as halide abstractor for fluororous alkyl- and arylhalides. Redox potentials shown in this Figure are from reference 57. Isolated yields based on phosphorus.

1.7 SUMMARY

Current methods for the formation of P_1 compounds from P_4 have been reviewed. Such transformation can be performed with alkenes and organic halides in superbasic media, as well as with carbon centered nucleophiles, *via* electrochemical methods and with carbon centered radicals. Reactions in superbasic media or with anionic carbon centered nucleophiles yielded product mixtures and/or low yields. Reactions of NHCs with white phosphorus resulted in the selective formation of P_1 compounds, but more sterically demanding carbenes form P_n ($n \geq 2$) species. The electrochemical functionalisation of white phosphorus to tertiary phosphines is limited to alkylphosphines or triphenylphosphine. Other aryl substituted derivatives could not be accessed by this method. The pioneering work of Barton and co-workers in the field of radical mediated methods to functionalise white phosphorus is limited to the formation of phosphonic acids. Based on this work, Cummins showed that reductive dehalogenation of organo halides by a titanium complex is a versatile method to functionalise white phosphorus. Again, only triphenylphosphine was the only tertiary arylphosphine which could be formed by this method. The combination of samarium(II) halides, fluoruous aryl iodides and white phosphorus proved to be successful. A variety of triarylphosphines could be prepared by this method. Nevertheless, non-fluoruous aryl iodides could not be used and stoichiometric amounts of $Sm(II)X$ ($X = Br, Cl$) have to be added to the reaction mixture. In general, a direct and catalytic method to form tertiary triarylphosphines from white phosphorus, which replaces the industrial state-of-the-art method *via* PCl_3 is not known. This fact and the electrochemical and radical mediated work described in this chapter inspired us to seek a catalytic method to functionalise white phosphorus. This approach should catalytically generate radicals, which potentially are trapped by white phosphorus to yield P_1 organophosphorus compounds. The results are discussed in chapter 2 of this work.

1.8 REFERENCES

1. Cordell, D., Drangert, J.-O. & White, S. The story of phosphorus: Global food security and food for thought. *Global Environmental Change* **19**, 292–305 (2009).
2. Geeson, M. B. & Cummins, C. C. Phosphoric acid as a precursor to chemicals traditionally synthesized from white phosphorus. *Science* **359**, 1383–1385 (2018)
3. Weil, E. D. & Levchik, S. V. Phosphorus Flame Retardants. in *Kirk-Othmer Encyclopedia of Chemical Technology* 1–34 (American Cancer Society, 2017).
4. Van der Veen, I. & de Boer, J. Phosphorus flame retardants: Properties, production, environmental occurrence, toxicity and analysis. *Chemosphere* **88**, 1119–1153 (2012).
5. He, R., Wang, X., Hashimoto, T. & Maruoka, K. Binaphthyl-Modified Quaternary Phosphonium Salts as Chiral Phase-Transfer Catalysts: Asymmetric Amination of β -Keto Esters. *Angewandte Chemie International Edition* **47**, 9466–9468 (2008).
6. Ponmuthu, K. V., Kumaraguru, D., Arockiam, J.B., Velu, S., Sepperumal, M., Ayyanar, S. New quaternary phosphonium salt as multi-site phase-transfer catalyst for various alkylation reactions. *Res. Chem. Intermed.* **42**, 8345–8358 (2016).
7. Hayashi, T. Chiral Monodentate Phosphine Ligand MOP for Transition-Metal-Catalyzed Asymmetric Reactions. *Acc. Chem. Res.* **33**, 354–362 (2000).
8. Pignolet, L. M. *Homogeneous Catalysis with Metal Phosphine Complexes*. (Springer Science & Business Media, 2013).
9. Wiley-VCH. *Ullmann's Fine Chemicals*. (John Wiley & Sons, 2014).
10. Scalambra, F., Peruzzini, M. & Romerosa, A. Chapter Four - Recent advances in transition metal-mediated transformations of white phosphorus. in *Advances in Organometallic Chemistry* (ed. Pérez, P. J.) vol. 72 173–222 (Academic Press, 2019).
11. Peruzzini, M., Gonsalvi, L. & Romerosa, A. Coordination chemistry and functionalization of white phosphorus via transition metal complexes. *Chem. Soc. Rev.* **34**, 1038–1047 (2005).

12. Cossairt, B. M., Piro, N. A. & Cummins, C. C. Early-Transition-Metal-Mediated Activation and Transformation of White Phosphorus. *Chem. Rev.* **110**, 4164–4177 (2010).
13. Caporale, M., Gonsalvi, L., Rossin, A., Peruzzini, M., P₄ Activation by Late-Transition Metal Complexes. *Chem. Rev.* **110**, 4178–4235 (2010).
14. Giffin, N. A. & Masuda, J. D. Reactivity of white phosphorus with compounds of the p-block. *Coordination Chemistry Reviews* **255**, 1342–1359 (2011).
15. Scheer, M., Balázs, G. & Seitz, A. P₄ Activation by Main Group Elements and Compounds. *Chem. Rev.* **110**, 4236–4256 (2010).
16. Borger, J. E., Ehlers, A. W., Slootweg, J. C. & Lammertsma, K. Functionalization of P₄ through direct P–C Bond Formation. *Chem. Eur. J.* **23**, 11738–11746 (2017).
17. Maier, L. Synthesis of organic phosphorus compounds from elemental phosphorus. in *The Chemistry of Organophosphorus Compounds I* 1–59 (Springer, 1971).
18. Serrano-Ruiz, M., Romerosa, A. & Lorenzo-Luis, P. Elemental Phosphorus and Electromagnetic Radiation. *European Journal of Inorganic Chemistry* **2014**, 1587–1598 (2014).
19. Gusarova, N., Arbuzova, S. & Trofimov, B. Novel general halogen-free methodology for the synthesis of organophosphorus compounds., *Pure Appl. Chem.* **84**, 439–459 (2012).
20. Trofimov, B. A. & Gusarova, N. K. Elemental phosphorus in strongly basic media as phosphorylating reagent: a dawn of halogen-free ‘green’ organophosphorus chemistry. *Mendeleev Commun.* **19**, 295–302 (2009).
21. Kuimov, V. A., Gusarova, N. K., Malysheva, S. F., Sukhov, B. G., Smetannikov, Y. V., Tarasova, N. P., Gusarov, A. V. & Trofimov, B.A. Reactions of elemental phosphorus and phosphine with electrophiles in superbasic systems: XVIII. Phosphorylation of 1-(chloromethyl)naphthalene with the elemental phosphorus. *Russ. J. Gen. Chem.* **76**, 708–713 (2006).

22. Trofimov, B. A., Gusarova, N. K., Malysheva, S. F., Kuimov, V. A., Sukhov, B. G., Shaikhudinova, S. I., Tarasova, N. P., Smetannikov, Y. V., Sinyashin, O. G., Budnikova, Y. G., Kazantseva, T. I. & Smirnov, V. I. Reactions of Elemental Phosphorus with Electrophiles in Super Basic Systems: XVII. Phosphorylation of Arylalkenes with Active Modifications of Elemental Phosphorus. *Russ. J. Gen. Chem.* **75**, 1367–1372 (2005).
23. Kuimov, V. A. *et al.* Reactions of elemental phosphorus and phosphine with electrophiles in superbasic systems: XVIII. Phosphorylation of 1-(chloromethyl)naphthalene with the elemental phosphorus. *Russ J Gen Chem* **76**, 708–713 (2006).
24. Trofimov, B. A., Artem'ev, A. V., Malysheva, S. V., Gusarova N. K., Belogorlova, N. A., Korocheva, A. O., Gatilov, Y. V., Mamatyuk V. I. Expedient one-pot organometallics-free synthesis of tris(2-pyridyl)phosphine from 2-bromopyridine and elemental phosphorus. *Tetrahedron Lett.* **53**, 2424–2427 (2012).
25. Auger, V. CHIMIE ORGANIQUE. — Nouvelle méthode de préparation de dérivés organiques. *Compt. Rend.* **139**, 639-641 (1904)
26. Malysheva, S. F., Belogorlova, N. A., Kuimov, V. A., Litvintsev, Y. I., Sterkhova, I.V., Albanov, A. I., Gusarova, N.K., Trofimov, B. A. PCl_3 - and organometallic-free synthesis of tris(2-picoly)phosphine oxide from elemental phosphorus and 2-(chloromethyl)pyridine hydrochloride. *Tetrahedron Lett.* **59**, 723–726 (2018).
27. Gusarova, N. K., Arbuzova S. N., Shaikjudinova, S. I., Kazantseva, T. I., Reutskaya A. M., Ivanova, N. I., Papernaya, L., Trofimov, B. A. Tris[(5-Chloro-2-Thienyl)methyl] Phosphine Oxide from Elemental Phosphorus and 2-Chloro-5-(chloromethyl) Thiophene. *Phosphorus Sulfur Silicon Relat. Elem.* **175**, 163–167 (2001).
28. Malysheva, S. F., Kuimov, V. A., Gusarova, N. K., Sukhov, B. G., Smetannikov, Y. V., Tarasova, N. P. & Trofimov, B. A. Reactions of elemental phosphorus and phosphine with electrophiles in superbasic systems: XX. Phosphorylation of 4-

- vinylbenzyl chloride with elemental phosphorus. *Russ. J. Gen. Chem.* **77**, 1880–1886 (2007).
29. Trofimov, B. A., Gusarova, N. K., Malysheva, S. F., Shaikhudinova, S. I., Belogorlova, N. A., Kazantseva, T. I., Sukhov, B. G. & Plotnikova, G. V. Reactions of Elemental Phosphorus and Phosphine with Electrophiles in Superbasic Systems: XVI. Phosphorylation of Benzyl Chloride with Elemental Phosphorus and Phosphine. *Russ. J. Gen. Chem.* **75**, 684–688 (2005).
30. Shaikhudinova, S. I., Kazantseva, T. I., Gusarova, N. K., Dmitriev, V. I. & Trofimov, B. A. Reactions of Elemental Phosphorus and Phosphine with Electrophiles in Superbasic Media: XI.1 Phosphorylation of 4-Methoxybenzyl Chloride with Elemental Phosphorus and Phosphine. *Russ. J. Gen. Chem.* **71**, 58–60 (2001).
31. Malysheva, S. F., Sukhov, B. G., Gusarova, N. K., Afonin, A. V., Shaikhudinova, S. I., Kazantseva, T. I., Belogorlova, N. A., Kuimov, V. A., Plotnikova, G. V. & Trofimov, B. A. Reactions of Elemental Phosphorus and Phosphine with Electrophiles in Superbasic Systems: XV. Phosphorylation of Allyl Halides with Elemental Phosphorus. *Russ. J. Gen. Chem.* **74**, 1091–1096 (2004).
32. Verkhoturova, S. I., Arbuzova, S. N., Kazantseva, T. I., Gusarova, N. K. & Trofimov, B. A. Phosphorylation of alkyl methanesulfonates with elemental phosphorus in a strongly basic medium: Synthesis of alkylphosphinic acids. *Russ. J. Gen. Chem.* **87**, 1876–1878 (2017).
33. Rauhut, M. M., Bernheimer, R., Semsel, A. M. The Synthesis of Tertiary Phosphine Oxides from Elemental Phosphorus. *J. Org. Chem.* **28**, 478–481 (1963).
34. Maier, L. Organic Phosphorus Compounds 60. The direct synthesis of tris(N-substituted carbamoylethyl) phosphine oxides. *Helv. Chim. Acta* **56**, 1252–1257 (1973).
35. Gusarova, N. K., Shaikhudinova, S. I., Kazantseva, T. I., Malysheva, S. F., Sukhov, B. G., Belogorlova, N. A., V. I. Dmitriev, V. I. & Trofimov B. A. Reactions of Elemental Phosphorus and Phosphine with Electrophiles in Superbasic

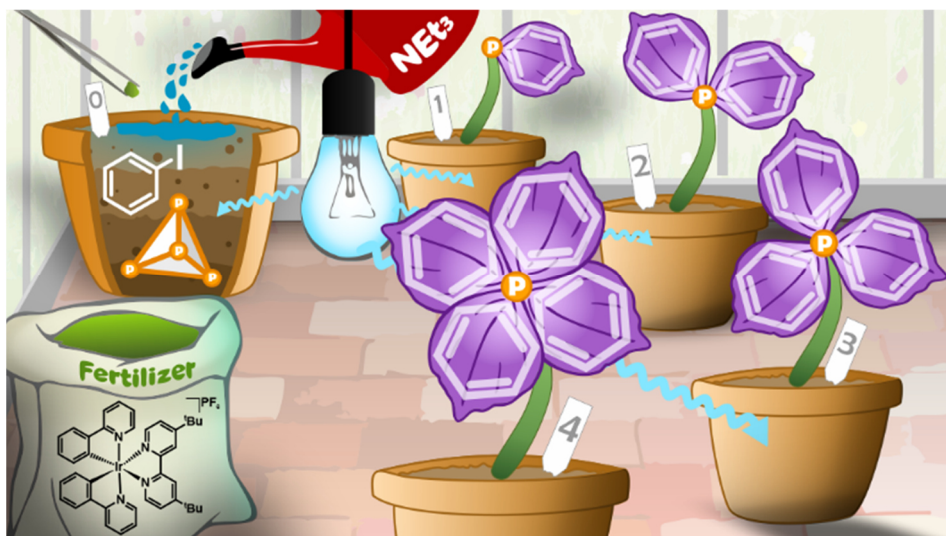
- Systems: XIV.1 Phosphorylation of 2-Vinylnaphthalene with Elemental Phosphorus and Phosphines in the KOH-DMSO System. *Russ. J. Gen. Chem.* **87**, 1876–1878 (2017).
36. Gusarova, N. K., Shaikhudinova, S. I., Kazantseva, T. I., Sukhov, B. G., Dmitriev, V. I., Sinegovskaya, L. M., Smetannikov, Y. V., Tarasova, N. P. & Trofimov, B. A. Reaction of Vinylpyridines with Active Modifications of Elemental Phosphorus in KOH/DMSO. *Chem. Heterocycl. Com.* **37**, 576–580 (2001).
37. Gusarova, N. K., Sukhov, B. G., Malysheva, S. F., Kazantseva, T. I., Smetannikov, Y. V., Tarasova, N. P. & Trofimov, B. A. Reactions of Elemental Phosphorus and Phosphines with Electrophiles in Superbasic Systems: XIII. Phosphorylation of Phenylacetylene with Active Modifications of Elemental Phosphorus. *Russ. J. Gen. Chem.* **71**, 721–723 (2001).
38. Trofimov, B. A., Artem'ev, A. V., Gusarova, N. K., Sutyryna, A. O. Malysheva, S. F. & Oparina, L. A. Hydrophosphorylation of vinyl sulfides with elemental phosphorus in the KOH/DMSO(H₂O) system: synthesis of 2-alkyl(aryl)thioethylphosphinic acids. *J. Sulfur Chem.* **39**, 112–118 (2017).
39. Rauhut, M. M. & Semsel, A. M. Reactions of Elemental Phosphorus with Organometallic Compounds and Alkyl Halides. The Direct Synthesis of Tertiary Phosphines and Cyclotetraphosphines. *J. Org. Chem.* **28**, 473–477 (1963).
40. Rauhut, M. M. & Semsel, A. M. Reactions of Elemental Phosphorus with Organometallic Compounds. *J. Org. Chem.* **28**, 471–473 (1963).
41. Trofimov, B. A., Brandsma, L., Arbusova, S. N. & Gusarova, N. K. A new method for the synthesis of α,β -acetylenic phosphines. *Russ Chem Bull* **46**, 849–850 (1997).
42. Xu, L., Chi, Y., Du, S., Zhang, W.-X. & Xi, Z. Direct Synthesis of Phospholyl Lithium from White Phosphorus. *Angew. Chem. Int. Ed.* **55**, 9187–9190 (2016).

43. Yakhvarov, D., Ganushevich, Y. & Sinyashin, O. Direct formation of P–C and P–H bonds by reactions of organozinc reagents with white phosphorus. *Mendeleev Commun.* **17**, 197–198 (2007).
44. Schmidpeter, A., Burget, G., Zwaschka, F. & Sheldrick, W. S. Cyanphosphorverbindungen. IX. Cyanidabbau von weißem Phosphor zu Dicyanphosphiden und die Dicyanphosphid-Struktur. *Z. Anorg. Allg. Chem.* **527**, 17–32 (1985).
45. Back, O., Kuchenbeiser, G., Donnadiou, B. & Bertrand, G. Nonmetal-Mediated Fragmentation of P₄: Isolation of P₁ and P₂ Bis(carbene) Adducts. *Angew. Chem. Int. Ed.* **48**, 5530–5533 (2009).
46. Cicač-Hudi, M., Bender, J., Schlindwein, S. H., Bispinghoff, M., Nieger, M., Grützmacher, H. & Gudat, D. Direct Access to Inversely Polarized Phosphaalkenes from Elemental Phosphorus or Polyphosphides. *Eur. J. Inorg. Chem.* **2016**, 649–658 (2016).
47. Budnikova, Y. H., Yakhvarov, D. G. & Sinyashin, O. G. Electrocatalytic eco-efficient functionalization of white phosphorus. *J. Organomet. Chem.* **690**, 2416–2425 (2005).
48. Yakhvarov, D. G., Gorbachuk, E. V. & Sinyashin, O. G. Electrode Reactions of Elemental (White) Phosphorus and Phosphane PH₃. *Eur. J. Inorg.* **2013**, 4709–4726 (2013).
49. Mikhaylov, D. Y., Gryaznova, T. V., Dudkina, Y. B., Polyancev, F. M., Latypov, S. K., Sinyashin, O. G., & Budnikova, Y. H. Novel electrochemical pathway to fluoroalkyl phosphines and phosphine oxides. *J. Fluor. Chem.* **153**, 178–182 (2013).
50. Kargin, Yu. M., Budnikova, Yu. H., Martynov, B. I., Turygin, V. V. & Tomilov, A. P. Electrochemical synthesis of organophosphorus compounds with P–O, P–N and P–C bonds from white phosphorus. *J. Electroanal. Chem.* **507**, 157–169 (2001).

51. Budnikova, Y. G., Yakhvarov, D. G. & Kargin, Y. M. Arylation and alkylation of white phosphorus in the presence of electrochemically generated nickel(0) complexes. *Mendeleev Commun.* **7**, 67–68 (1997).
52. Budnikova, Y., Krasnov, S. & Sinyashin, O. Electrochemical phosphorylation of unsaturated hydrocarbons. *Russian J. Electrochem.* **43**, 1175–1182 (2007).
53. Barton, D. H. R. & Zhu, J. Elemental white phosphorus as a radical trap: a new and general route to phosphonic acids. *J. Am. Chem. Soc.* **115**, 2071–2072 (1993).
54. Barton, D. H. R. & Vonder Embse, R. A. The invention of radical reactions. Part 39. The reaction of white phosphorus with carbon-centered radicals. An improved procedure for the synthesis of phosphonic acids and further mechanistic insights. *Tetrahedron* **54**, 12475–12496 (1998).
55. M. Cossairt, B. & C. Cummins, C. Radical synthesis of trialkyl, triaryl, trisilyl and tristannyl phosphines from P₄. *New. J. Chem.* **34**, 1533–1536 (2010).
56. Ghosh, S. K., Cummins, C. C. & Gladysz, J. A. A direct route from white phosphorus and fluoros alkyl and aryl iodides to the corresponding trialkyl- and triarylphosphines. *Org. Chem. Front.* **5**, 3421–3429 (2018).
57. Szostak, M., Spain, M. & Procter, D. J. Determination of the Effective Redox Potentials of SmI₂, SmBr₂, SmCl₂, and their Complexes with Water by Reduction of Aromatic Hydrocarbons. Reduction of Anthracene and Stilbene by Samarium(II) Iodide–Water Complex. *J. Org. Chem.* **79**, 2522–2537 (2014).

2 DIRECT CATALYTIC TRANSFORMATION OF WHITE PHOSPHORUS INTO ARYL PHOSPHINES AND PHOSPHONIUM SALTS

Ulrich Lennert, Percia Beatrice Arockiam, Verena Streitferdt, Daniel J. Scott, Christian Rödl, Ruth M. Gschwind and Robert Wolf



The synthesis of organophosphorus compounds from elemental phosphorus is an inefficient process, using multiple steps, stoichiometric metal complexes and/or hazardous reagents such as chlorine gas. Here, a direct photocatalytic route to convert white phosphorus (P_4) into phosphines and phosphonium salts is reported.

[I] Adapted from: Lennert, U., Arockiam, P. B. Streitferdt, V., Scott, D. J., Rödl, C., Gschwind, R. M. & Wolf, R. Direct catalytic transformation of white phosphorus into arylphosphines and phosphonium salts. *Nat. Catal.* **2**, 1101-1106 (2019).

[II] U.L. developed the initial catalytic procedure. U.L. and P.B.A. performed further optimisation; U.L., P.B.A. and D.J.S. investigated the substrate scope; U.L. and D.J.S. performed mechanistic investigations. V.S. and R.M.G. performed in situ NMR studies. C.R. performed (spectro)electrochemical experiments. R.W. oversaw and directed the project. U.L. and D.J.S. prepared the manuscript, with input from all authors.

2.1 INTRODUCTION

Phosphorus compounds are ubiquitous in the chemical sciences, finding applications throughout industry and academia. Of particular interest to synthetic chemists are organophosphorus compounds, which contain P—C bonds. However, state-of-the-art processes for the synthesis of these important materials rely on an inefficient, stepwise methodology involving initial oxidation of white phosphorus (P_4) with hazardous chlorine gas and the subsequent displacement of chloride ions. Catalytic P_4 organofunctionalisation reactions have remained elusive, as they require multiple P—P bond breaking and P—C bond formation events to break down the P_4 core, all of which must occur in a controlled manner. Herein, we describe an efficient transition metal-catalysed process capable of forming P—C bonds from P_4 . Using blue light photocatalysis, this method directly affords valuable triarylphosphines and tetraarylphosphonium salts in a single reaction step.

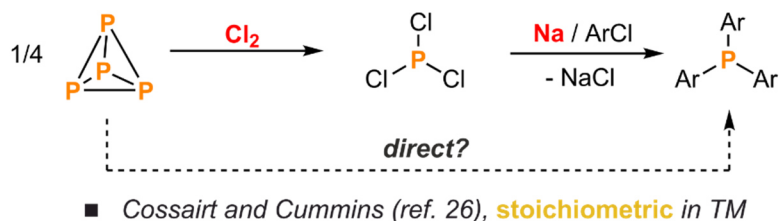
The academic, industrial and societal importance of phosphorus chemistry is difficult to overstate. Phosphorus is one of the six essential ‘biogenic elements’ required in large quantities by every living organism, and synthetic phosphorus compounds find myriad industrial and commercial applications due to their diverse array of useful chemical, physical and biological properties.¹ This importance is reflected in the fact that white phosphorus (P_4) is currently produced on an estimated scale of >1 Mt / year.² P_4 is by far the most reactive and industrially-relevant form of elemental phosphorus, and acts as the common precursor from which effectively all synthetic phosphorus-containing species are ultimately prepared.³ Notable families of industrially-relevant organophosphorus species prepared from P_4 include triarylphosphines (Ar_3P) and salts of the related quaternary phosphonium cations (Ar_4P^+). The former are widely used both in organic chemistry (notably in the classic Wittig reaction)^{4,5} and as ligands for homogeneous metal complexes,^{6–11} including the catalysts for numerous landmark chemical reactions (e.g. industrial-scale hydroformylation).¹² The latter meanwhile find uses as ion-pair extractants,¹³ phase-transfer catalysts,^{14–16} aryl-transfer reagents,^{17,18} and additives in Heck reactions.¹⁹ Like most organophosphorus species, these compounds are currently prepared using hazardous and wasteful multi-step procedures involving initial oxidation of P_4 to give phosphorus chlorides (PCl_3 , PCl_5), followed by displacement of chloride with suitable organometallic nucleophiles (Fig. 1a).¹ Far superior would be efficient catalytic methods to form the desired P—C bonds directly from P_4 ; however such reactions are all but unknown.²⁰ Notably, P_4 activation through binding to reactive low-valent transition metal complexes²¹ or unsaturated main group species²² such as carbenes^{3,23} has become well established in recent years (albeit with results that are often challenging to predict). However, selective subsequent functionalisation and,

in particular, release of the resulting organophosphorus compounds remains highly problematic (the new P_n moieties typically act as strong many-electron donors, with correspondingly low lability).^{21,22} Similarly, while direct reactions of P_4 with organic or organometallic nucleophiles are known, these typically proceed with poor yields and selectivities, or only lead to partial breakup of the P_4 tetrahedron.³

a) *state-of-the-art: industrial synthesis of triarylphosphines*

white phosphorus:

- reactive
- produced on >1 Mt scale
- direct functionalisation challenging



b) *this work: single-step synthesis of tetraarylphosphonium salts and triarylphosphines*

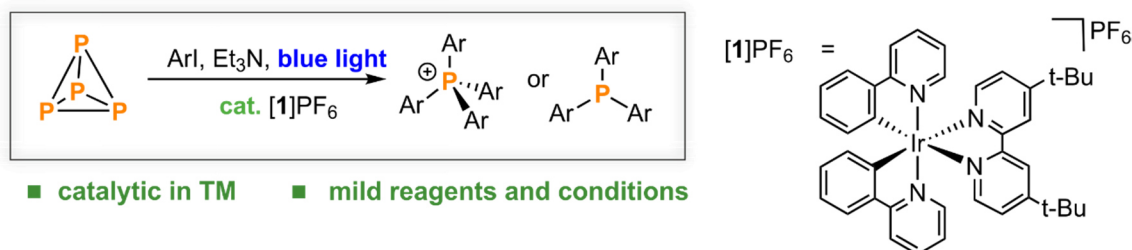


Fig. 1 White phosphorus functionalisation a) State-of-the-art methods for the industrial synthesis of triarylphosphines. b) Direct, catalytic functionalisation of P_4 to give triarylphosphines and tetraarylphosphonium salts, as described in this work. TM = transition metal complex

As a result, even stoichiometric functionalisation reactions that can efficiently convert P_4 into valuable monophosphorus species remain rare. In this context, Barton and coworkers have previously shown that P_4 can act as an excellent trap for carbon centered radicals and have applied this methodology to the synthesis of phosphonic acids;^{24,25} however, this method is inefficient with respect to P atom economy. Based on this work, Cossairt and Cummins were also able to develop a direct, stoichiometric method for P_4 activation: in the presence of equimolar amounts of a titanium(III) complex (or, in more recent work, samarium(II) halides)^{26,27} halogenated organic compounds undergo halide atom abstraction to yield reactive organoradicals, and subsequent addition to P_4 yielded the corresponding tertiary monophosphines.

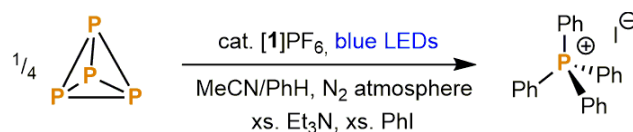
Herein, we describe a catalytic method for the preparation of valuable triarylphosphines and tetraarylphosphonium salts directly from P_4 using visible light. These useful organophosphorus compounds are obtained from P_4 and aryl iodides using an iridium photocatalyst and blue light irradiation in the presence of triethylamine. We present the

scope of this catalytic system and we propose an outline mechanism based on NMR monitoring and other spectroscopic observations.

2.2 RESULTS AND DISCUSSION

2.2.1 Reaction development

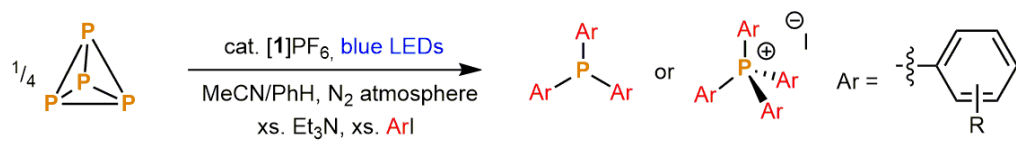
We reasoned that an efficient method for the catalytic transformation of P_4 directly into useful organophosphorus compounds could be developed if carboradicals were catalytically generated from a suitable precursor in the presence of P_4 ; fortunately, recent years have seen dramatic progress in this area through the use of photoredox methods driven by visible or UV light for the addition of carboradicals to unsaturated organic substrates,^{28–31} and we anticipated that photocatalytic functionalisation of white phosphorus could plausibly proceed *via* similar mechanisms. Notably, these methods do not require the use of powerful stoichiometric reagents that might be vulnerable to unproductive, direct reactions with P_4 . Thus, as a model system the reduction of halobenzenes was chosen for initial investigation. After screening several established visible-light-driven photoredox catalysts (see Supplementary Table 1 for further details), we were delighted to observe that the catalytic conversion of P_4 into tetraphenylphosphonium iodide is viable using the known photocatalyst $[Ir(dtbbpy)(ppy)_2]PF_6$ (**[1]** PF_6 ; dtbbpy = 4,4'-bis-tertbutyl-2,2'-bipyridine, ppy = 2-(2-pyridyl)phenyl; structure shown in Fig. 1b). Employing **[1]** PF_6 , blue light irradiation (455 nm) of a solution of P_4 , PhI (as a simple model substrate) and Et_3N (as a reductive quencher of the excited state photocatalyst; *vide infra*) in a 3:1 MeCN/PhH (v/v) mixture (chosen to ensure solubility of all components) for 18 h yielded with excellent selectivity the phosphonium salt $[Ph_4P]I$: 76 % conversion to $[Ph_4P]I$ was observed by quantitative ^{31}P NMR spectroscopy (Table 1, entry 1). Following oxidation the Et_3N reductant is presumed to undergo formal H atom loss to give the iminium salt $[Et_2NC(H)Me]I$, whose formation also accounts for the fate of the PhI-derived iodide, but this has not been confirmed experimentally. On a preparative scale, the clean salt could be isolated from the reaction mixture by simple crystallisation from H_2O on the open bench, followed by recrystallisation from EtOH (Table 2, entry 1 and Supplementary Method 2).


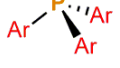

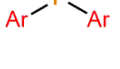
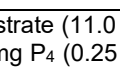
Table 1. Photocatalytic functionalisation of P₄ to [Ph₄P]⁺I⁻: screening of radical sources and control experiments.

Entry	Conditions	Conv. to [Ph ₄ P] ⁺ / % ^[b]	Full conv. of P ₄
1	standard ^[a]	76	✓
2	PhBr instead of PhI	<1 ^[c]	✓
3	PhCl instead of PhI	0 ^[c]	✓
4	no PhI	0	✓
5	no [1]PF ₆	0	✗
6	no light	0	✗
7	no Et ₃ N	0	✗

[a] All reactions were performed with iodobenzene (11 equiv. based on phosphorus atom), 200 μL Et₃N (14.4 equiv. based on phosphorus atom), 3.1 mg P₄ (0.025 mmol, 1 equiv.), and 2.0 mg [1]PF₆ (2.2 mol% based on phosphorus atom) in 2 mL MeCN/PhH (3:1, v/v) as solvent. The samples were prepared under N₂-atmosphere in a sealed tube and placed in a water-cooled block during irradiation (18 h) with blue LED light (455 nm). [b] Conversions determined by quantitative ³¹P NMR experiments with Ph₃PO as internal standard. [c] A complex mixture of P-containing species was observed by ³¹P NMR spectroscopy.

This represents an effective example both of catalytic P₄ transformation directly into an organophosphorus species, and of successful catalytic functionalisation of P₄ using a transition metal complex.²⁰ Switching from PhI to less reactive PhBr or PhCl was found to be severely detrimental (Table 1, entries 2 and 3); further variations in solvent, oxidant, catalyst loading, and reaction time (Supplementary Tables 2 and 3) indicate that the reaction parameters given in Table 1 are optimal. Meanwhile, control experiments confirmed that all reaction components (PhI, Et₃N, [1]PF₆ and blue light) are necessary in order to observe formation of the product (Table 1, entries 4-7). Interestingly, full conversion of white phosphorus was still observed in the absence of PhI (Table 1, entry 4), which suggests the possibility that it can be directly reduced under these reaction conditions (in this case, formation of small amounts of PH₃ was observed by ³¹P NMR spectroscopy, suggesting possible H atom transfer to P₄ from the oxidised sacrificial donor, [Et₃N]⁺).

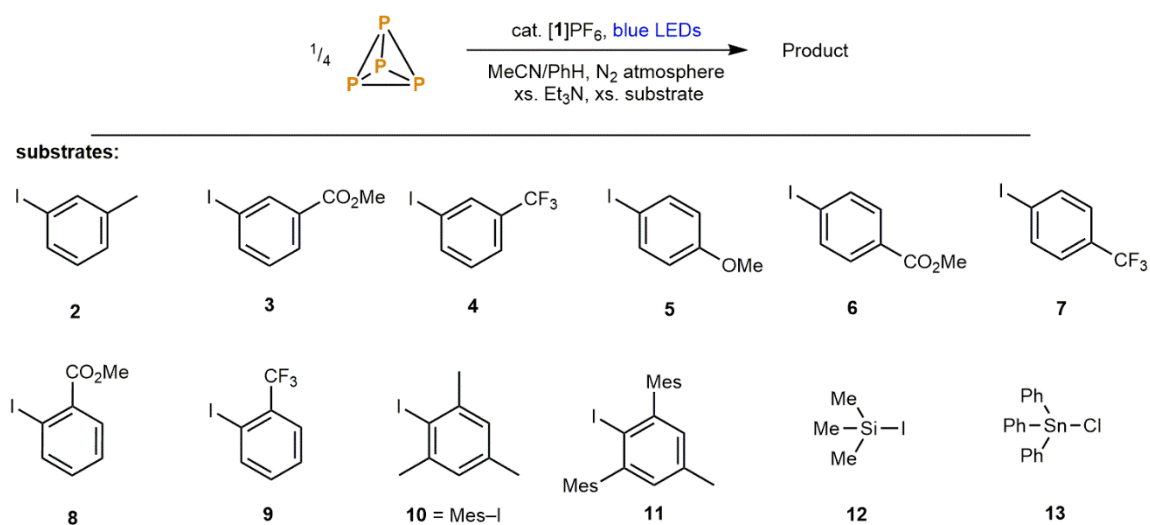
Table 2. Substrate scope for photocatalytic P₄ functionalisation.


Entry	R	Time / h	Product	Yield / % ^[a,b]
1	H	18		34 (76)
2	<i>p</i> -Me	30		41 (54)
3	<i>m</i> -OMe	24	-----	60 (63, 3 ^[c])
4	<i>o</i> -Me	18		71 (79)
5	<i>o</i> -OMe	30		37 (54)
6	<i>o</i> -SMe	18		19 (21)

[a] Isolated yields. Reactions were performed with substrate (11.0 equiv. based on phosphorus atom), 2.0 mL Et₃N (14.4 equiv. based on phosphorus atom), 31 mg P₄ (0.25 mmol, 1 equiv.), and 20 mg [1]PF₆ (2.2 mol% based on phosphorus atom) in 20 mL MeCN/PhH (3:1, v/v) as solvent. (Supplementary Methods 2–7). The samples were prepared under N₂-atmosphere in a sealed tube and placed in a water-cooled block during irradiation with blue light (455 nm). [b] Values in parentheses are conversions determined by quantitative ³¹P NMR experiments with subsequently-added Ph₃PO as internal standard, for equivalent reactions at 0.1 mmol scale (Supplementary Method 1). [c] Conversion to corresponding triarylphosphine.

2.2.2 Reaction scope

Having established an optimum procedure for the model substrate PhI, attention was shifted to investigating the scope of this new reaction. Gratifyingly, under identical conditions, a variety of substituted iodobenzene coupling partners could successfully be employed (Tables 2 and 3), including substrates bearing both electron-donating (Me, OMe) and electron-withdrawing (COOMe, CF₃) groups. Interestingly – and in contrast to the model substrate PhI – in many cases the expected [PAr₄]I salt was accompanied by significant quantities of the tertiary phosphine PAr₃ in the product mixture, often with high selectivity for the latter. In particular, the reaction of (*o*-tol)I (*o*-tol = 2-methylphenyl) was found to give exclusively the tertiary phosphine (*o*-tol)₃P (Table 2, entry 4), which has found extensive use as a bulky ligand in transition metal coordination chemistry and related catalysis,^{6–11} and could be cleanly isolated from a scaled up reaction mixture by simple sublimation (71% isolated yield, 216 mg; Supplementary Method 5). Other substituted derivatives of [Ph₄P]I and (*o*-tol)₃P could also be isolated using similar procedures (Table 2, entries 2, 3, 5, 6, Supplementary Methods 3, 4, 6, 7), although in practice this was limited to examples that proceeded with good conversion and high selectivity. The difference in reaction outcome between PhI and (*o*-tol)I is most likely steric in nature, with the additional bulk of the *o*-Me groups limiting the maximum coordination number at P. Indeed, when even bulkier substrates were employed the reaction was observed to stall earlier still: at the secondary (MesI; Mes = mesityl, 2,4,6-trimethylphenyl; Table 3, entry 9) or even primary phosphines (DmpI; Dmp = 2,6-dimesitylphenyl; Table 3, entry 10). In addition, electron-withdrawing groups also seemingly disfavour the quaternary phosphonium salt (for example, compare entry 4 to entries 5 and 6 in Table 3), plausibly due to destabilisation of the requisite positive charge. Finally, a pair of heteroatomic substrates were investigated (Table 3, entries 11 and 12). While the silicon-centered substrate Me₃SiI yielded no P—Si bonded products, reaction with Ph₃SnCl was found to selectively yield the potentially useful “P³⁻” synthon (Ph₃Sn)₃P with excellent conversion. The observed reactivity is qualitatively consistent with the known ready accessibility of Sn-based radicals, and the much lower stability of Si-centered analogues.³²

Table 3. Further substrate scope for photocatalytic P₄ functionalisation.^[a]

Entry	Time / h	Substrate	Product	Conv. / % ^[b]
1	18	2		63 (5 ^[c])
2	24	3		48 (8 ^[c])
3	24	4		25 (20 ^[c])
4	18	5		37 (5 ^[e])
5	18	6		39
6	24	7		30
7	24	8		11
8	24	9		-
9	18	10		24 (3 ^[d])
10 ^[e]	18	11		12
11	18	12	No P—Si bond formation	-
12	18	13		77, 14 ^[f]

[a] Refer to Table 1 and Supplementary Method 1 for standard conditions. [b] Conversions determined by quantitative ³¹P NMR experiments with subsequently added Ph₃PO as internal standard. [c] Conversion to corresponding triarylphosphine. [d] Conversion to corresponding monoarylphosphine. [e] The reaction was performed with 88.1 mg **11** (2.0 equiv. based on phosphorus atom), 200 μL Et₃N (14.4 equiv. based on phosphorus atom), 3.1 mg P₄ (0.025 mmol, 1 equiv.), and 2.0 mg [1]PF₆ (2.2 mol%) in 2 mL MeCN/PhH (1:3, v/v) as solvent. The sample was prepared under N₂-atmosphere in a sealed tube and placed in a water-cooled block during irradiation with blue light (455 nm). [f] Second value is isolated yield for equivalent reaction at 1 mmol scale (see Supplementary Method 8).

2.2.3 Mechanistic Studies

Mechanistic investigations strongly suggest that the functionalisation of P_4 proceeds *via* the mechanism summarised in Fig. 2. Radical generation proceeds through a reductive quenching cycle in which the catalyst first oxidises Et_3N in its excited state (steps i and ii), before then (as the reduced complex [1]) reducing PhI to $Ph\cdot$ (step iii). The aryl radicals thus generated then sequentially functionalise P_4 (step iv), producing in sequence $PhPH_2$, Ph_2PH , Ph_3P and finally Ph_4P^+ (steps v-viii). Other $P_xPh_yH_z$ species must presumably be formed *en route* to $PhPH_2$; however, attempts to observe these early intermediates have thus far been unsuccessful and we are therefore unable to propose a specific mechanism for initial break-up of the tetrahedral P_4 core. Nevertheless, we note that previous reports (for example, see ref. 26) have demonstrated the formation of stable P_4Ar_2 , P_3Ar_3 , and P_4Ar_4 compounds through direct reaction of P_4 with C-centred radicals. At this point the complexity of this reaction must be acknowledged, however. For each P_4 molecule functionalised six P—P and at least 16 C—I bonds are broken; 16 C—P bonds are formed; and at least 16 Et_3N are oxidized. As such the possibility that other elementary reaction steps may be mechanistically significant cannot be excluded. For example, UV/VIS observations (*vide supra*) and additional *in situ* NMR experiments (see Supplementary Discussions) both suggest that direct activation of P_4 by the reduced photocatalyst [1] is a plausible side-reaction (either productive or unproductive).

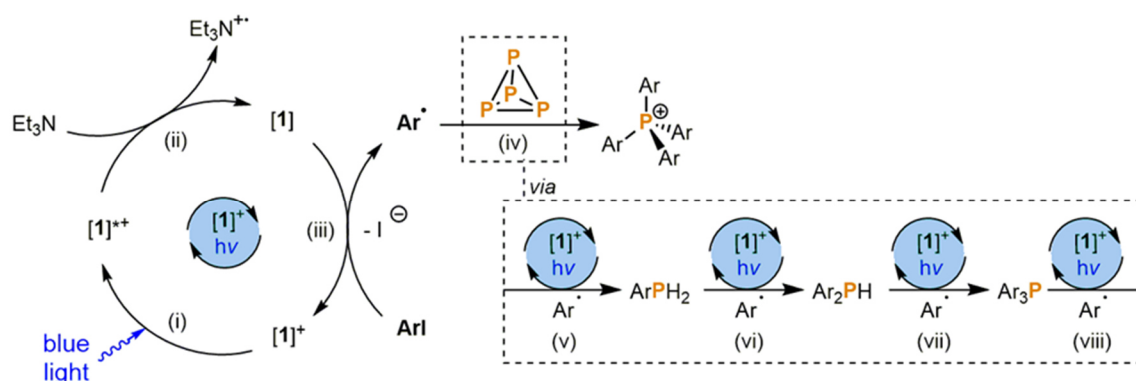


Fig. 2. Catalytic cycle. Proposed mechanism for the photocatalytic functionalisation of white phosphorus to triarylphosphines and tetraarylphosphonium salts with $[1]^+$ in the presence of aryl halides.

The proposed mechanism is nevertheless in line with both spectroscopic and electrochemical investigations. Measured redox potentials (Supplementary Figs. 42–44) support the plausibility a reductive quenching mechanism, in which the photocatalyst excited state is reduced by Et_3N to produce the neutral complex [1] (Fig. 2, steps i and ii). Further, conclusive evidence for this proposal was provided by emission quenching experiments, which showed that out of all the reaction components (including

intermediate phosphines PhPH_2 , Ph_2PH , Ph_3P), only Et_3N effectively quenches the excited state of the $[\mathbf{1}]^+$ catalyst in MeCN/PhH (Supplementary Figs. 45–52). Furthermore, photo-CIDNP effects were detected during *in situ* NMR experiments (*vide infra*), indicative of direct reaction of Et_3N with the $[\mathbf{1}]^+$ photoexcited state (Supplementary Fig. 62). An alternative oxidative quenching mechanism, in which the photoexcited state reacts directly with the aryl iodide, is thus highly improbable (Supplementary Fig. 53).

Following reduction by Et_3N , complex $[\mathbf{1}]$ can in turn effect reduction of the PhI substrate (Fig. 2, step iii), thereby forming phenyl radicals $\text{Ph}\cdot$. This was corroborated by UV/VIS spectroscopy (Supplementary Fig. 54). While a solution containing Et_3N and $[\mathbf{1}]\text{PF}_6$ in MeCN/PhH showed only a broad absorption band up to 500 nm, two new bands ($\lambda_{\text{max}} = 501 \text{ nm}$, 537 nm) were formed after irradiation with 455 nm blue light (a new orange/red coloration was also noticeable by eye), which was taken to indicate the formation of the reduced neutral catalyst $[\mathbf{1}]$ as discussed above (despite its significance to many reported photocatalytic cycles, to our knowledge neutral $[\mathbf{1}]$ has not previously been characterised in detail; as such, chemical and electrochemical reduction experiments have been performed to support this assignment, as described in detail in the Supplementary Information (see Supplementary Figs. 55 and 56)). The initial spectrum was quickly regenerated upon addition of excess PhI (within seconds), confirming the ability of the substrate to effect oxidation of $[\mathbf{1}]$ back to the catalyst resting state $[\mathbf{1}]^+$ (similar recovery was also observed upon addition of P_4 as a solution in PhH). In the absence of PhI and P_4 the $[\mathbf{1}]\text{PF}_6$ signal recovered far more slowly (over the course of ca. 20 minutes in the absence of blue light irradiation, presumably due to re-oxidation by the previously-generated $[\text{Et}_3\text{N}]^+$ cation or decomposition products thereof).

Having established a feasible mechanism for aryl radical generation, *in situ* NMR monitoring was used to investigate subsequent P_4 functionalisation. A slightly altered 1:1 MeCN:PhH solvent mixture was used to ensure homogeneity throughout. This change was not found to significantly alter the final reaction outcome. (see Supplementary Method 9). Time-resolved $^{31}\text{P}\{^1\text{H}\}$ NMR spectra showed rapid consumption of the P_4 starting material (completely consumed within five hours under *in situ* NMR conditions) with the primary, secondary and tertiary monophosphines (PhPH_2 , Ph_2PH , Ph_3P) all visible as sequential reaction intermediates (Fig. 3). While practical limitations preclude a quantitative analysis, it is qualitatively clear that the concentrations of these species in the initial stages of the reaction are too low to fully account for the consumption of P_4 . This suggests the presence of other as-yet-unidentified P-containing intermediates. Traces of the diphosphine Ph_4P_2 were observed by ^{31}P NMR. The H atoms in the primary and secondary products most likely derive from the Et_3N reductant (experiments using deuterated solvents showed no deuterium incorporation), either by deprotonation or H

atom abstraction from its oxidation products. The subsequent loss of these hydrogen atoms (as required for conversion to Ph_4P^+) presumably involves similar steps; for example, ^1H NMR shows formation of PhH during the course of the reaction, plausibly through H atom abstraction by a phenyl radical. ^1H NMR spectroscopy also suggests formation of Et_2NH as a minor side-product, which is also observed in many other photochemical reactions that use Et_3N as a reductant.³³

Given the observation of PhPH_2 , Ph_2PH and Ph_3P as successive reaction intermediates, control experiments were performed using these phosphines as individual starting materials in place of P_4 . In all cases conversion to Ph_4P^+ was observed *via* the respective downstream intermediates, with similar or superior conversion to the analogous reaction using P_4 , consistent with the above *in situ* observations. Notably, each individual arylation step appears to be photochemically-mediated, with comparable conversions never observed in the absence of light, $[\mathbf{1}]\text{PF}_6$ or Et_3N . Low, but non-zero conversions were observed for these substrates in the absence of $[\mathbf{1}]\text{PF}_6$ or Et_3N , suggesting some, much slower background photochemical reaction (see Supplementary Tables 4-6 and Supplementary Figs. 58, 59).

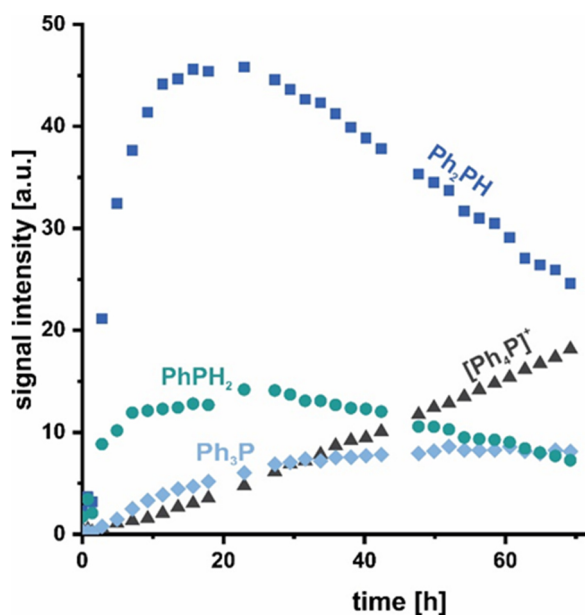


Fig .3. Time-resolved $^{31}\text{P}\{^1\text{H}\}$ NMR study. *In situ* ^{31}P NMR monitoring of the formation of primary, secondary, and tertiary phosphines and quaternary phosphonium salt during photocatalytic P_4 functionalisation using PhI as substrate (see Supplementary Method 9 for full reaction details). The relatively long reaction time is probably attributed to the reduced irradiation power of the *in situ* light source and non-stirring conditions in the NMR tube.

2.3 CONCLUSIONS

In summary, we have described a direct catalytic formation of P–C bonds from P₄. Synthetically useful triarylphosphines and tetraarylphosphonium salts were formed in up to *ca.* 80% yield. This Cl₂-free process represents an important step towards direct and catalytic approaches for the production of organophosphorus compounds and highlights the ability of modern photoredox techniques to solve pressing challenges in inorganic as well as organic chemistry. Furthermore, the successful catalytic functionalization of P₄ illustrates the promising potential of radical methods for the activation and functionalisation of white phosphorus, and their increasing significance in organophosphorus chemistry. Ongoing research efforts in our groups are focused on further clarifying the mechanism of this highly elaborate transformation, as well as expanding the range of viable organic radical precursors

2.4 REFERENCES

1. Corbridge, D. E. C. Phosphorus 2000. Chemistry, Biochemistry and Technology (Elsevier: Amsterdam. 2000).
2. Schipper, W. Phosphorus: Too Big to Fail. *Eur. J. Inorg. Chem.* 1567–1571 (2014).
3. Borger, J. E., Ehlers, A. W., Slootweg, J. C. & Lammertsma, K. Functionalization of P₄ through Direct P–C Bond Formation. *Chem. Eur. J.* **23**, 11738–11746 (2017).
4. Wittig, G. & Schöllkopf, U. Über Triphenyl-phosphin-methylene als olefinbildende Reagenzien (I. Mitteil.) *Chem. Ber.* **87**, 1318–1330 (1954).
5. Wittig, G. & Haag, W. Über Triphenyl-phosphinmethylene als olefinbildende Reagenzien (II. Mitteil.1). *Chem. Ber.* **88**, 1654–1666 (1955).
6. Guo, Y., Fu, H., Chen, H. & Li, X. Synthesis of new triarylphosphine ligand and their application in styrene hydroformylation. *Catal. Commun.* **9**, 1842–1845 (2008).
7. Kamer, P. C. J., van Leeuwen, P. W. N. M. & Reek, J. N. H. Wide Bite Angle Diphosphines: Xantphos Ligands in Transition Metal Complexes and Catalysis. *Acc. Chem. Res.* **34**, 895–904 (2001).
8. Martin, R. & Buchwald, S. L. Palladium-Catalyzed Suzuki–Miyaura Cross-Coupling Reactions Employing Dialkylbiaryl Phosphine Ligands. *Acc. Chem. Res.* **41**, 1461–1473 (2008).
9. Pignolet, L. M. *Homogeneous Catalysis with Metal Phosphine Complexes*. (Springer US, 1983).
10. Surry, D. S. & Buchwald, S. L. Biaryl Phosphane Ligands in Palladium-Catalyzed Amination. *Angew. Chem. Int. Ed.* **47**, 6338–6361 (2008).
11. Fujihara, T., Yoshida, S., Terao, J. & Tsuji, Y. A Triarylphosphine Ligand Bearing Dodeca(ethylene glycol) Chains: Enhanced Efficiency in the Palladium-Catalyzed Suzuki–Miyaura Coupling Reaction. *Org. Lett.* **11**, 2121–2124 (2009).
12. Börner, A. Franke, R. Organic Ligands. in *Hydroformylation* 73–266 (John Wiley & Sons, Ltd, 2016).
13. El-Shahawi, M. S., Hassan, S. S. M., Othman, A. M., Zyada, M. A. & El-Sonbati, M. A. Chemical speciation of chromium(III,VI) employing extractive spectrophotometry and tetraphenylarsonium chloride or tetraphenylphosphonium bromide as ion-pair reagent. *Anal. Chim. Acta* **534**, 319–326 (2005).

14. Starks, C. M. & Halper, M. *Phase-Transfer Catalysis: Fundamentals, Applications, and Industrial Perspectives*. (Springer Netherlands, 1994).
15. Kondo, S., Mori, T., Kunisada, H. & Yuki, Y. Synthesis of polymer-supported tetraphenylphosphonium bromides as effective phase-transfer catalysts at alkaline conditions. *Makromol. Chem. Rapid Commun.* **11**, 309–313 (1990).
16. Manabe, K. Asymmetric phase-transfer alkylation catalyzed by a chiral quaternary phosphonium salt with a multiple hydrogen-bonding site. *Tetrahedron Lett.* **39**, 5807–5810 (1998).
17. Ramanjaneyulu, B. T., Pareek, M., Reddy, V. & Vijaya Anand, R. Direct Esterification of Aromatic Aldehydes with Tetraphenylphosphonium Bromide under Oxidative N-Heterocyclic Carbene Catalysis. *Helv. Chim. Acta* **97**, 431–437 (2014).
18. Deng, Z., Lin, J.-H. & Xiao, J.-C. Nucleophilic arylation with tetraarylphosphonium salts. *Nat. Commun.* **7**, 10337 (2016).
19. Reetz, M. T., Lohmer, G. & Schwickardi, R. A New Catalyst System for the Heck Reaction of Unreactive Aryl Halides. *Angew. Chem. Int. Ed.* **37**, 481–483 (1998).
20. Budnikova and coworkers have also investigated conceptually-related electrochemical methods for the reductive reaction of P₄ with aryl halides. For an overview, see: Budnikova, Y. H., Gryaznova, T. V., Grinenko, V. V., Dudkina, Y. B., Khrizanforov, M. N. Eco-efficient electrocatalytic C-P bond formation *Pure Appl. Chem.* **89**, 311-330 (2017).
21. Caporali, M., Gonsalvi, L., Rossin, A. & Peruzzini, M. P₄ Activation by Late-Transition Metal Complexes. *Chem. Rev.* **110**, 4178–4235 (2010).
22. Scheer, M., Balázs, G. & Seitz, A. P₄ Activation by Main Group Elements and Compounds. *Chem. Rev.* **110**, 4236–4256 (2010).
23. Khan, S., Sen, S. S. & Roesky, H. W. Activation of phosphorus by group 14 elements in low oxidation states. *Chem. Commun.* **48**, 2169–2179 (2012).
24. Barton, D. H. R. & Zhu, J. Elemental white phosphorus as a radical trap: a new and general route to phosphonic acids. *J. Am. Chem. Soc.* **115**, 2071–2072 (1993).
25. Barton, D. H. R. & Vonder Embse, R. A. The invention of radical reactions. Part 39. The reaction of white phosphorus with carbon-centered radicals. An improved procedure for the synthesis of phosphonic acids and further mechanistic insights. *Tetrahedron* **54**, 12475–12496 (1998).

26. Cossairt, M. B. & Cummins, C.C. Radical synthesis of trialkyl, triaryl, trisilyl and tristannyl phosphines from P₄. *New J. Chem.* **34**, 1533–1536 (2010).
27. Ghosh, S. K., Cummins, C. C. & Gladysz, J. A. A direct route from white phosphorus and fluororous alkyl and aryl iodides to the corresponding trialkyl- and triarylphosphines. *Org. Chem. Front.* **5**, 3421-3429 (2018).
28. König, B. *Chemical Photocatalysis*. (Walter de Gruyter GmbH & Co.KG, 2013).
29. Romero, N. A. & Nicewicz, D. A. Organic Photoredox Catalysis. *Chem. Rev.* **117**, 10075-10166 (2016)
30. Marzo, L., Pagire, S. K., Reiser, O. & König, B. Visible-Light Photocatalysis: Does It Make a Difference in Organic Synthesis? *Angew. Chem. Int. Ed.* **57**, 10034–10072 (2018).
31. Twilton, J., Chi L. Zhang, P., Shaw, H. S., Evans, W. E., MacMillan D. W. C. The merger of transition metal and photocatalysis. *Nat. Rev. Chem.* **1**, 0052 (2017).
32. Davies, A. G. Radical chemistry of tin. in *Chemistry of Tin* 265–289 (Springer Netherlands, 1998).
33. Vyas, S. V., Lau, V. W. & Lotsch, B. V. Soft Photocatalysis: Organic Polymers for Solar Fuel Production. *Chem. Mater.* **28**, 5191–5204 (2016).

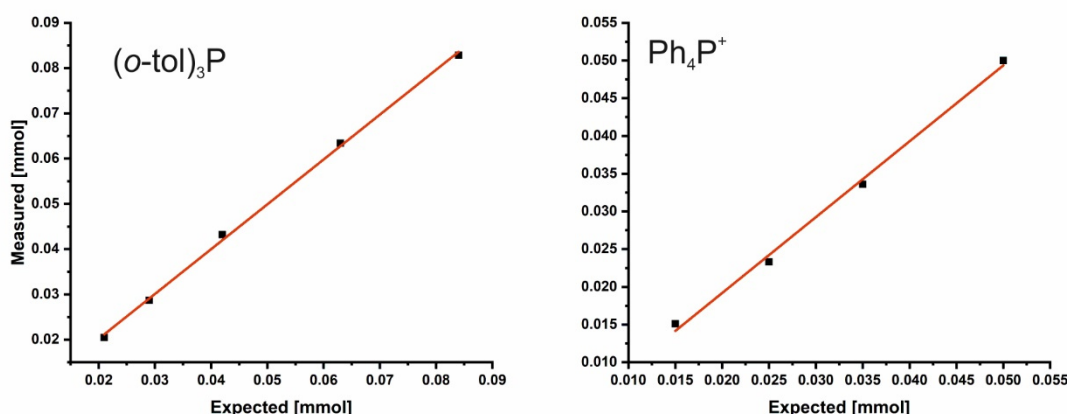
2.5 SUPPORTING INFORMATION

2.5.1 General information

All reactions and manipulations were performed under an N₂ atmosphere (< 0.1 ppm O₂, H₂O) through use of an MBraun Unilab glovebox. All glassware was oven-dried (160 °C) overnight prior to use. Benzene was dried over Na and stored over molecular sieves (3 Å). Acetonitrile, dimethylsulfoxide and dimethylformamide were distilled from CaH₂ and stored over molecular sieves (3 Å). THF was purified using an MBraun SPS-800 system and stored over molecular sieves (3 Å). C₆D₆ was distilled from K and stored over molecular sieves (3 Å). CD₃CN was stored over molecular sieves (3 Å). KC₈ was prepared in accordance with the literature.^{S1} All other chemicals were purchased from major suppliers (Aldrich, ABCR) liquids were purified by Kugelrohr distillation and freeze-pump-thaw degassed three times prior use; P₄, Ph₃P and Ph₃PO were purified by sublimation; all others were used as received.

GC-MS spectra were recorded using a mass detector model Agilent-5977B coupled with a GC oven 7820A and a Restek 5 Sil MS column with H₂ as carrier gas, using a 30 m × 0.25 mm × 0.25 μm column. Injection parameters: temperature of injection = 250 °C, split ratio = 25/1, volume injected = 1 μL, flow rate = 1.2 mL/ min. Oven parameters: starting temperature = 50 °C, rate = 15 °C/ min, end temperature = 300 °C, held for 5 min. Mass parameters: Temp source = 230 °C, Quad temperature = 150 °C, start mass = 50.00, end mass = 550.00.

With the exception of in situ experiments (for details of which, see Supplementary Discussions), qualitative NMR spectra were recorded at room temperature on Bruker Avance 400 (400 MHz) spectrometers and were processed using Topspin 3.2. Chemical shifts, δ, are reported in parts per million (ppm); ¹H NMR and ¹³C NMR shifts are reported relative to SiMe₄ and were referenced internally to residual solvent peaks, while ³¹P NMR shifts were referenced externally to 85 % H₃PO₄ (aq.). NMR samples were prepared in the glovebox using NMR tubes fitted with screw caps. Optimization reactions (see Supplementary Table 1-3) and photocatalytic phenylation reactions of Ph₃P, Ph₂PH and PhPH₂ (see Supplementary Table 4-6) were analysed by ³¹P{¹H} spectra using only a single scan (DS = 0, D1 = 2 s). The accuracy of this method was confirmed by preparing solutions of (o-tolyl)₃P or Ph₄PCl and 0.05 mmol Ph₃PO in MeCN/benzene (1.5 mL, 0.5 mL, respectively), and comparing the measured and expected relative integrations (Supplementary Figure 1).



Supplementary Figure 1. Plots showing the consistency between measured (by integration against 0.05 mmol Ph_3PO using a $^{31}\text{P}\{^1\text{H}\}$ experiment (zgpg) with a single scan) and expected (based on mass added) molar quantities of (*o*-tolyl) $_3\text{P}$ (left) or Ph_4P^+ (right) in MeCN/benzene (3:1) solutions.

Quantitative ^{31}P NMR measurements for the substrate screening were conducted on a Bruker Avance III HD 600 MHz spectrometer with a fluorine selective TBIF probe and on a Bruker Avance NEO 600 MHz spectrometer with a double resonance broad band probe (BBO H&F). Yields were determined by 1D ^{31}P NMR spectroscopy. In order to meet quantitative conditions special attention was paid to the following aspects:

- Pulse lengths were calibrated. The O1P of the spectrum was set close to the frequencies of interest to enable maximum excitation. In cases where the distance between signals of interest was greater than 21000 Hz, one spectrum was recorded for each signal of interest, having its O1P close to the respective frequency.
- T_1 relaxation times were determined for all peaks of interest and a D1 of $\geq 5 \times T_1$ was used to ensure full relaxation between scans.
- The NS was adjusted so that the S/N-ratio (signal to noise ratio) was higher than 100/1. In order to reduce measurement time and to increase the S/N-ratio compared to a standard 1D experiment using only a 90° pulse (zg experiment), the zgig pulse program (inverse gated decoupled) was used, applying proton decoupling during the acquisition time. Since the zgig pulse program uses decoupling, it had to be ensured that any signal enhancement due to NOE (nuclear Overhauser effect) is negligible. Therefore, zg and zgig experiments were conducted and the integrals of the signals of interest were compared. For all reaction mixtures investigated (except those for the product DmpPH_2), the integrals corresponding to both the internal standard (Ph_3PO) and the product remained constant. In the case of DmpPH_2 , in the zgig experiment a higher integral for the signal of the product was obtained compared to the zg experiment (probably due to greater impact of the NOE since two protons are bound to the

phosphorus atom). Hence, the zg pulse program was used to determine the yield of DmpPH₂.

- After acquisition, the spectra were processed and integrated and the yields were determined by referencing the integral of the product to that of the standard Ph₃PO. In cases where two spectra with different O1P had to be recorded (see above) these spectra were scaled to each other with the command intser.
- The qualitative spectra of the substrate screening are shown in Supplementary Figures 3-18 for reasons of clarity and comprehensibility.

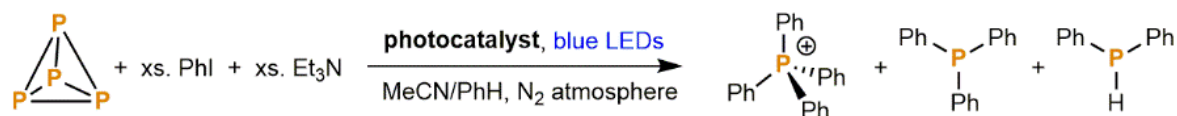
2.5.2 Supplementary Method 1. General procedure for photocatalytic functionalisation of P₄ (0.1 mmol scale)

In a 10 mL stoppered tube equipped with a stirring bar, the appropriate iodobenzene derivative (1.1 mmol, 11 equiv. based on the phosphorus atom), electron donor (1.44 mmol, 14.4 equiv.), catalyst (2.2 μmol, 2.2 mol%), and P₄ (0.025 mmol, 1 equiv.) were added to 1.5 mL acetonitrile and 0.5 mL benzene in an N₂ filled glove box. The tube was sealed, placed in a water-cooled block to maintain near-ambient temperature (Supplementary Figure 2), and irradiated with blue light (455 nm (±15 nm), 3.2 V, 700 mA, Osram OSOLON SSL 80) for 18 h (unless stated otherwise, refer to Table 2 and 3). A solution of Ph₃PO (13.9 mg, 0.05 mmol) in approximately 0.5 mL of benzene was subsequently added to act as an internal standard. The resulting mixture was subjected to GC-MS and NMR analysis.



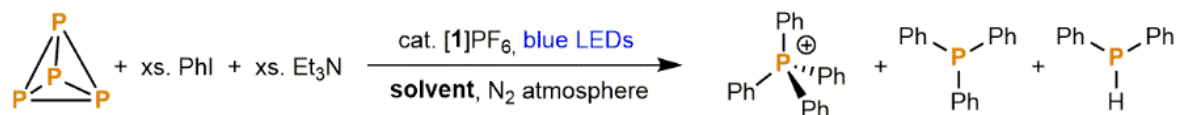
Supplementary Figure 2. Illustration of the equipment setup used for photocatalytic reactions at 0.1 mmol scale.

Tables for the optimization of reaction conditions

Supplementary Table 1. Photocatalytic functionalisation of P₄ to [Ph₄P]⁺: screening of photocatalysts^[a]

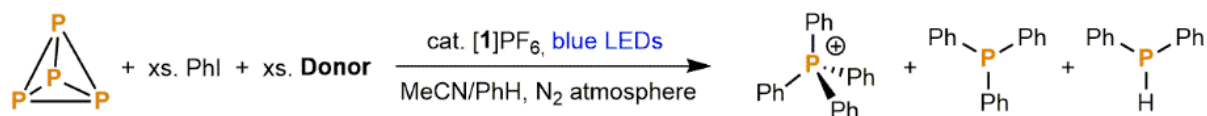
Entry	Photocatalyst	Full conv. of P ₄ ?	Conv. to [Ph ₄ P] ⁺ / %	Conv. to Ph ₃ P / %	Conv. to Ph ₂ PH / %
1	[1]PF ₆	✓	76	0	0
2	Ir(ppy) ₃	✓	0	0	0
3	RuCl ₂ (bpy) ₃ · 6H ₂ O	✗	0	0	0
4	EOSIN Y	✗	0	0	0
5 ^[b]	EOSIN Y	✗	0	0	0
6 ^[b]	Rhodamine 6G	✗	0	0	0
7	(Ir[dF{CF ₃ }ppy] ₂ [dtbpy])PF ₆	✓	25	22	8

[a] For the general procedure, see Supplementary Method 1. [b] Irradiated with green LEDs (528 nm). [1]PF₆ = Ir(dtbbpy)(ppy)₂PF₆.

Supplementary Table 2. Photocatalytic functionalisation of P₄ to [Ph₄P]⁺: screening of solvents^[a]

Entry	Solvent	Full conv. of P ₄ ?	Conv. to [Ph ₄ P] ⁺ / %	Conv. to Ph ₃ P / %	Conv. to Ph ₂ PH / %
1	DMF / benzene (3:1)	✓	7	11	5
2	DMF / benzene (3:1)	✓	25	13	1
3	DMSO	✓	28	11	3
4	DMF	✓	5	13	5

[a] The general procedure (Supplementary Method 1) was modified to use the solvent system indicated (identical solvent volume). [1]PF₆ = Ir(dtbbpy)(ppy)₂PF₆, DMF = Dimethylformamide, DMSO = Dimethylsulfoxide.

Supplementary Table 3. Photocatalytic functionalisation of P₄ to [Ph₄P]⁺: screening of sacrificial electron donors^[a]

Entry	Electron donor	Full conv. of P ₄ ?	Conv. to [Ph ₄ P] ⁺ / %	Conv. to Ph ₃ P / %	Conv. to Ph ₂ PH / %
1	EtN(<i>i</i> Pr) ₂	X	2	7	11
2	EDTA	✓	0	0	0
3	DBU	X	0	0	0
4	DABCO	X	0	0	0
5	2,6-lutidine	✓	0	0	0
6	<i>p</i> -anisidine	✓	0	0	0
7	(HOCH ₂ CH ₂) ₃ N	X	0	0	0
8	Ph ₃ N	✓	0	0	0
9	<i>n</i> Bu ₃ N	X	31	12	0

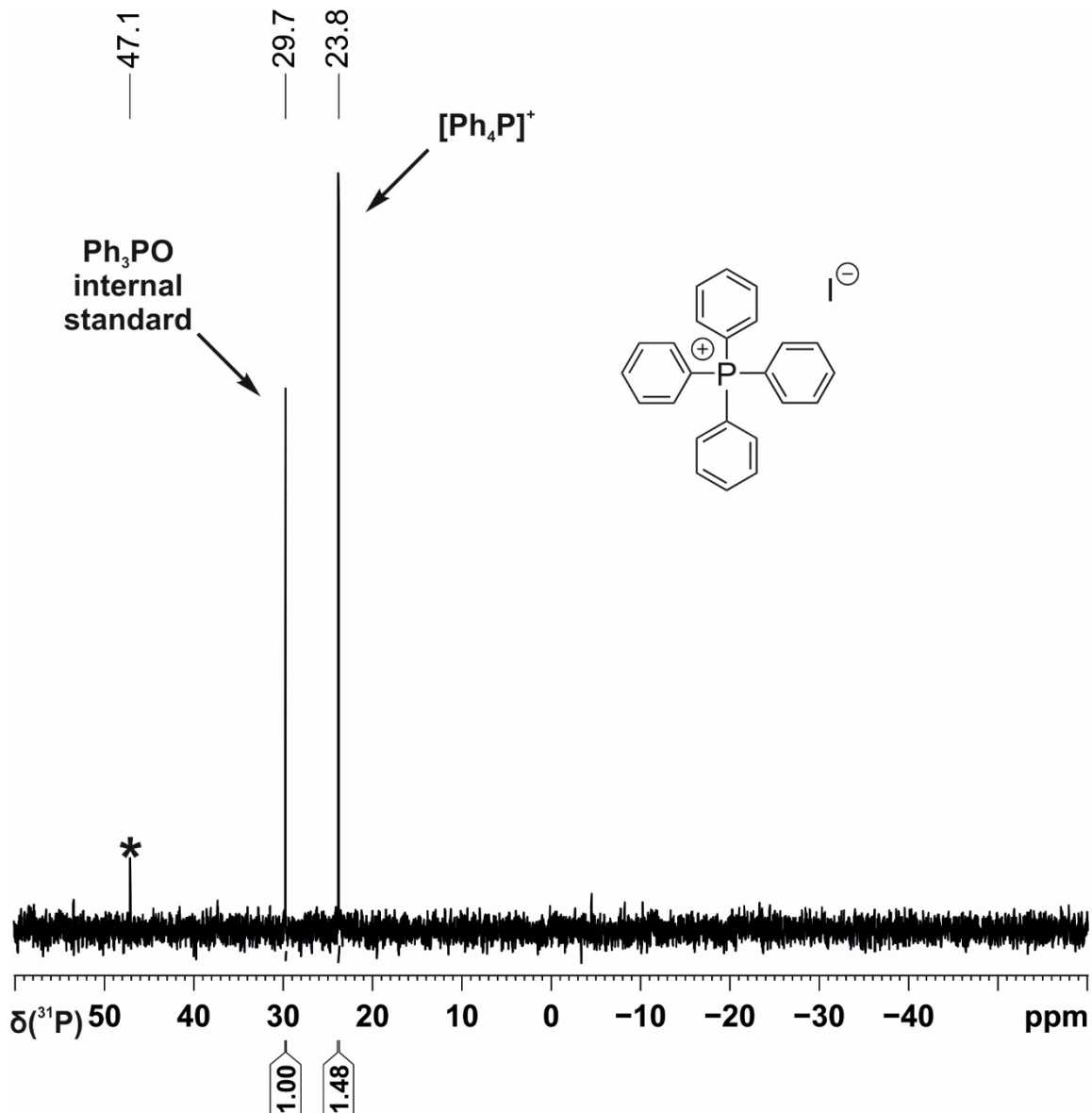
[a] For the general procedure, see Supplementary Method 1. [1]PF₆ = Ir(dtbbpy)(ppy)₂PF₆, EDTA = Ethylenediamine tetraacetic acid, DBU = 1,8-Diazabicyclo[5.4.0]undec-7-ene, DABCO = 1,4-diazabicyclo[2.2.2]octane.

Characterization of optimized 0.1 mmol scale reactions

The substrate screening was performed for each substrate at least twice to ensure reproducibility. The spectra of the qualitative single scan $^{31}\text{P}\{^1\text{H}\}$ (zgpg) NMR experiments are shown for every substrate to give an overview of the phosphorus species formed. The conversions were determined by quantitative ^{31}P NMR (zg and zgig) experiments as mentioned in the text (see Supplementary Methods for further information).

Tetraphenylphosphonium iodide (Table 2, Entry 1)

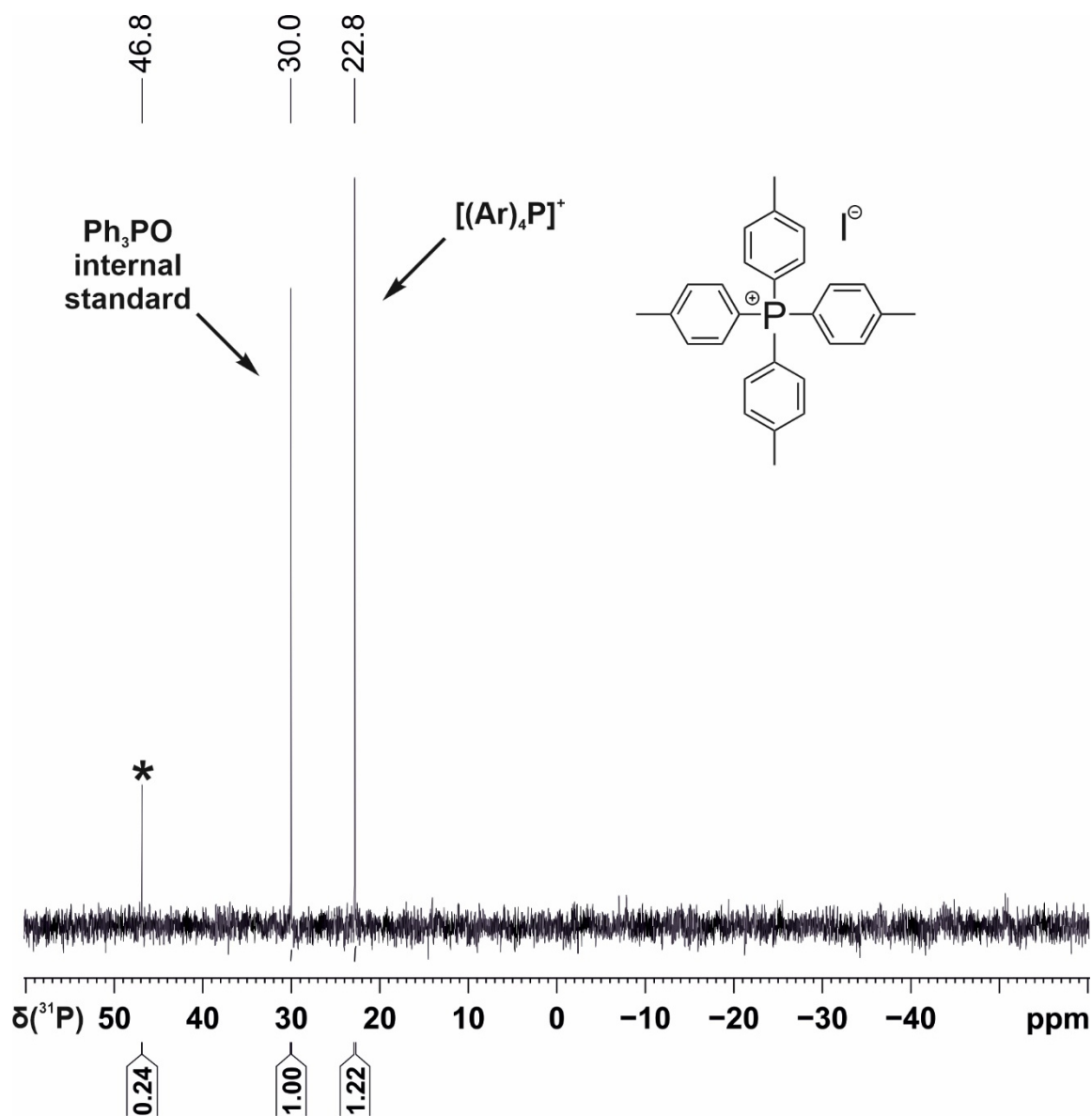
The general procedure was followed using iodobenzene (130 μ L, 1.1 mmol), which resulted in 76% conversion to tetraphenylphosphonium iodide as judged by quantitative $^{31}\text{P}\{^1\text{H}\}$ (zgpg) NMR spectroscopy (ESI-MS: expected = 339 m/z; observed = 339 m/z).



Supplementary Figure 3. Qualitative single scan $^{31}\text{P}\{^1\text{H}\}$ (zgpg) NMR spectrum for the photocatalytic functionalisation of P_4 using iodobenzene. * marks the signal of an unknown by-product.

Tetra(*p*-tolyl)phosphonium iodide (Table 2, Entry 2)

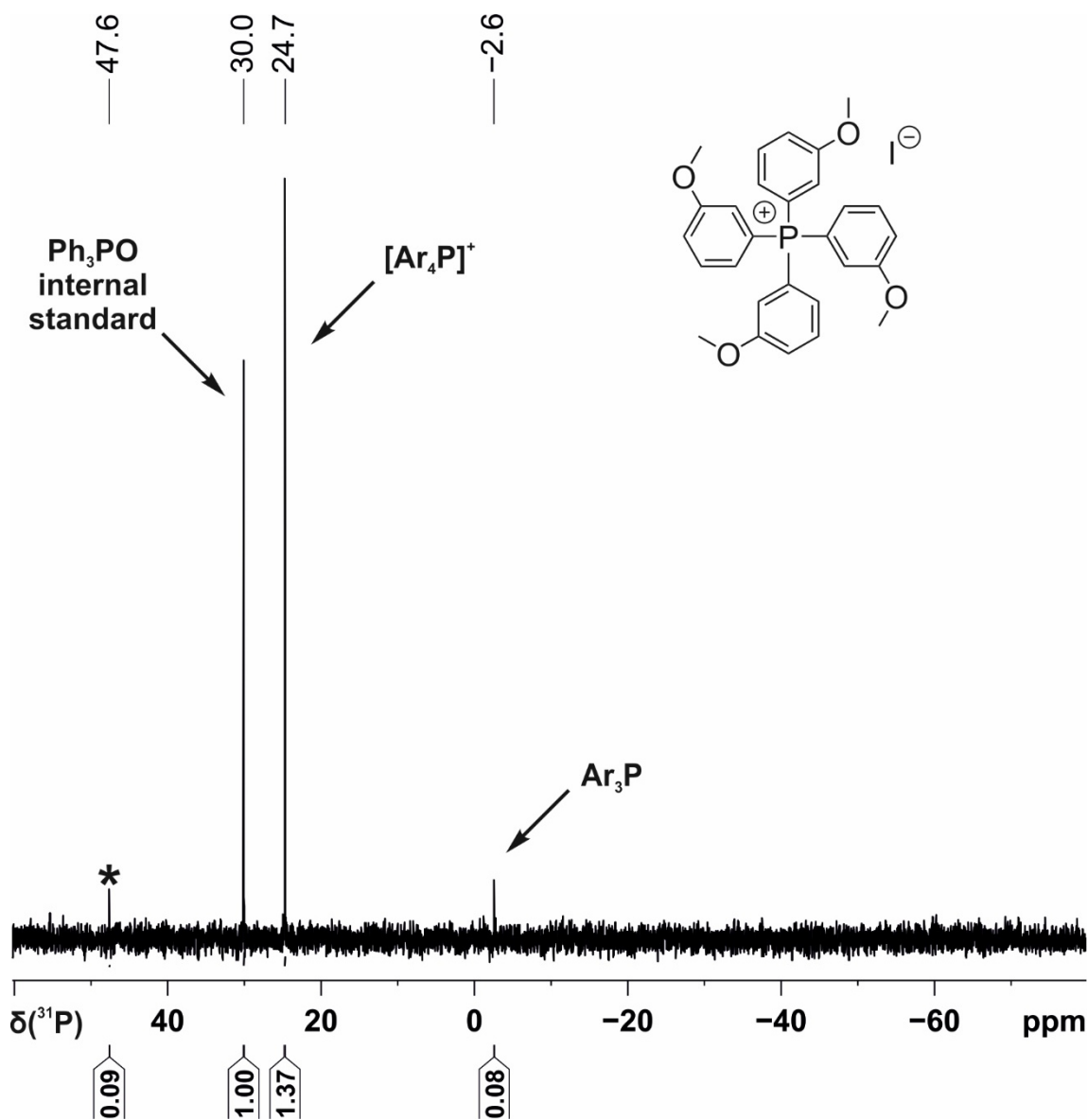
The general procedure was followed using 4-iodotoluene (239.8 mg, 1.1 mmol), which resulted in 54% conversion to tetra(*p*-tolyl)phosphonium iodide as judged by quantitative $^{31}\text{P}\{^1\text{H}\}$ (zgpg) NMR spectroscopy.



Supplementary Figure 4. Qualitative single scan $^{31}\text{P}\{^1\text{H}\}$ (zgpg) NMR spectrum for the photocatalytic functionalisation of P_4 using 4-iodotoluene. Ar = *p*-tolyl. * marks the signal of an unknown by-product.

Tetrakis(3-methoxyphenyl)phosphonium iodide (Table 2, Entry 3)

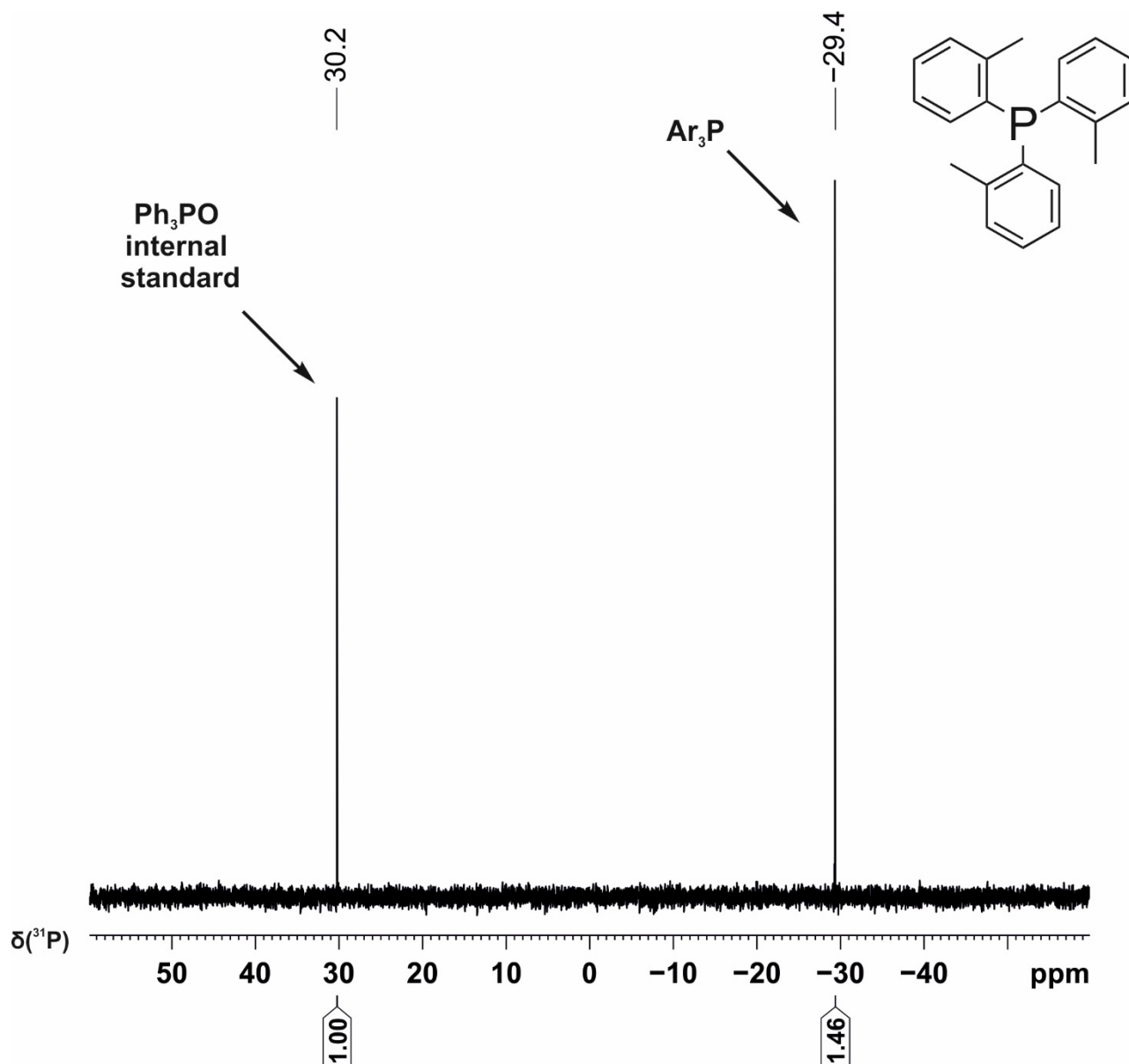
The general procedure was followed using 3-iodoanisole (131 μL , 1.1 mmol), which resulted in 63% conversion to tetrakis(3-methoxyphenyl)phosphonium iodide and 3% conversion to tris(3-methoxyphenyl)phosphine as judged by quantitative $^{31}\text{P}\{^1\text{H}\}$ (zgpg) NMR spectroscopy.



Supplementary Figure 5. Qualitative single scan $^{31}\text{P}\{^1\text{H}\}$ (zgpg) NMR spectrum for the photocatalytic functionalisation of P_4 using 3-iodoanisole. Ar = 3-methoxyphenyl. * marks the signal of an unknown by-product.

Tri(*o*-tolyl)phosphine (Table 2, Entry 4)

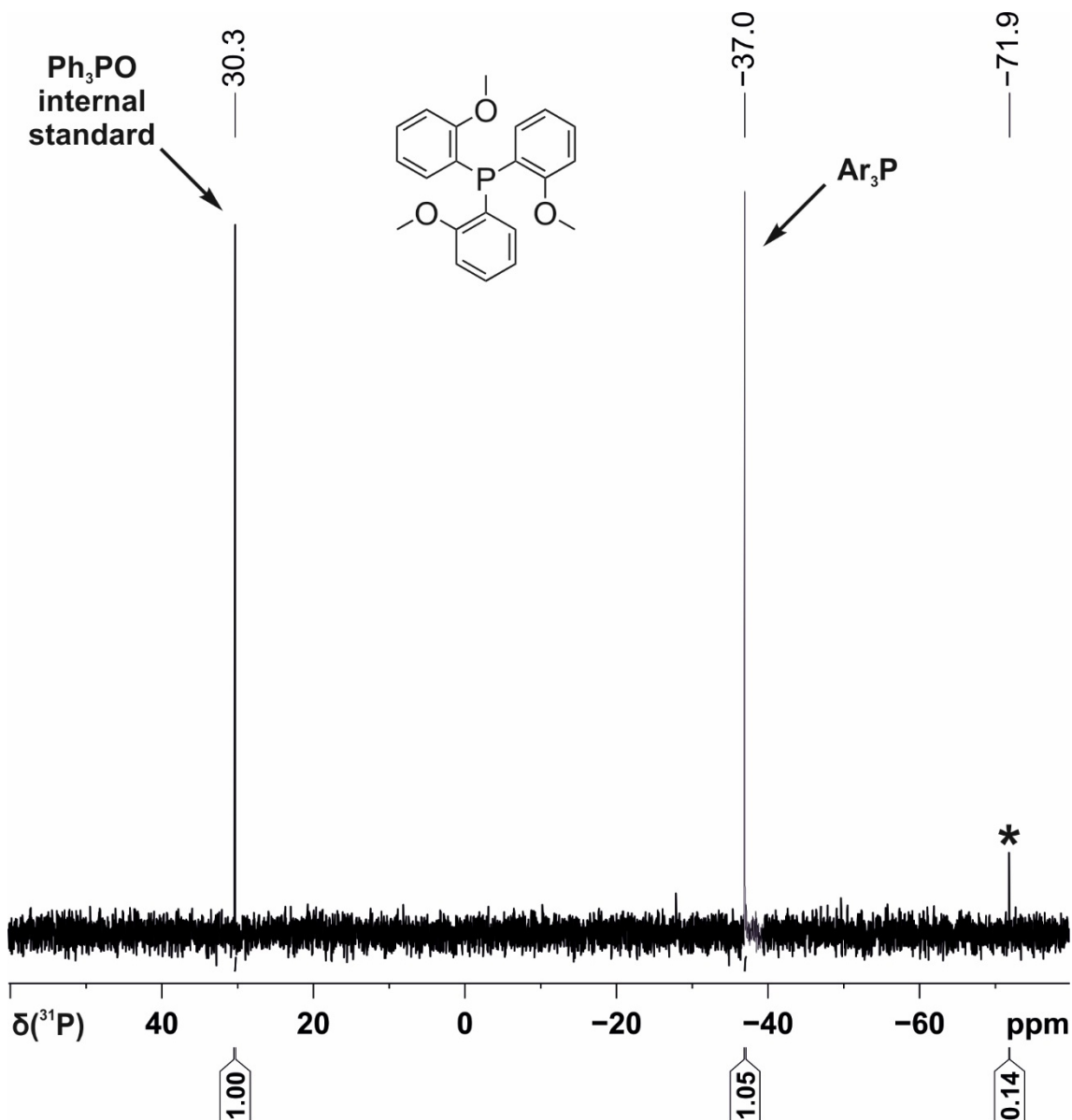
The general procedure was followed using 2-iodotoluene (140 μ L, 1.1 mmol), which resulted in 79% conversion to tri(*o*-tolyl) phosphine as judged by quantitative $^{31}\text{P}\{^1\text{H}\}$ (zgpg) NMR spectroscopy (GC-MS: expected = 304 m/z; observed = 304 m/z).



Supplementary Figure 6. Qualitative single scan $^{31}\text{P}\{^1\text{H}\}$ (zgpg) NMR spectrum for the photocatalytic functionalisation of P_4 using 2-iodotoluene. Ar = *o*-tolyl.

Tris(2-methoxyphenyl)phosphine (Table 2, Entry 5)

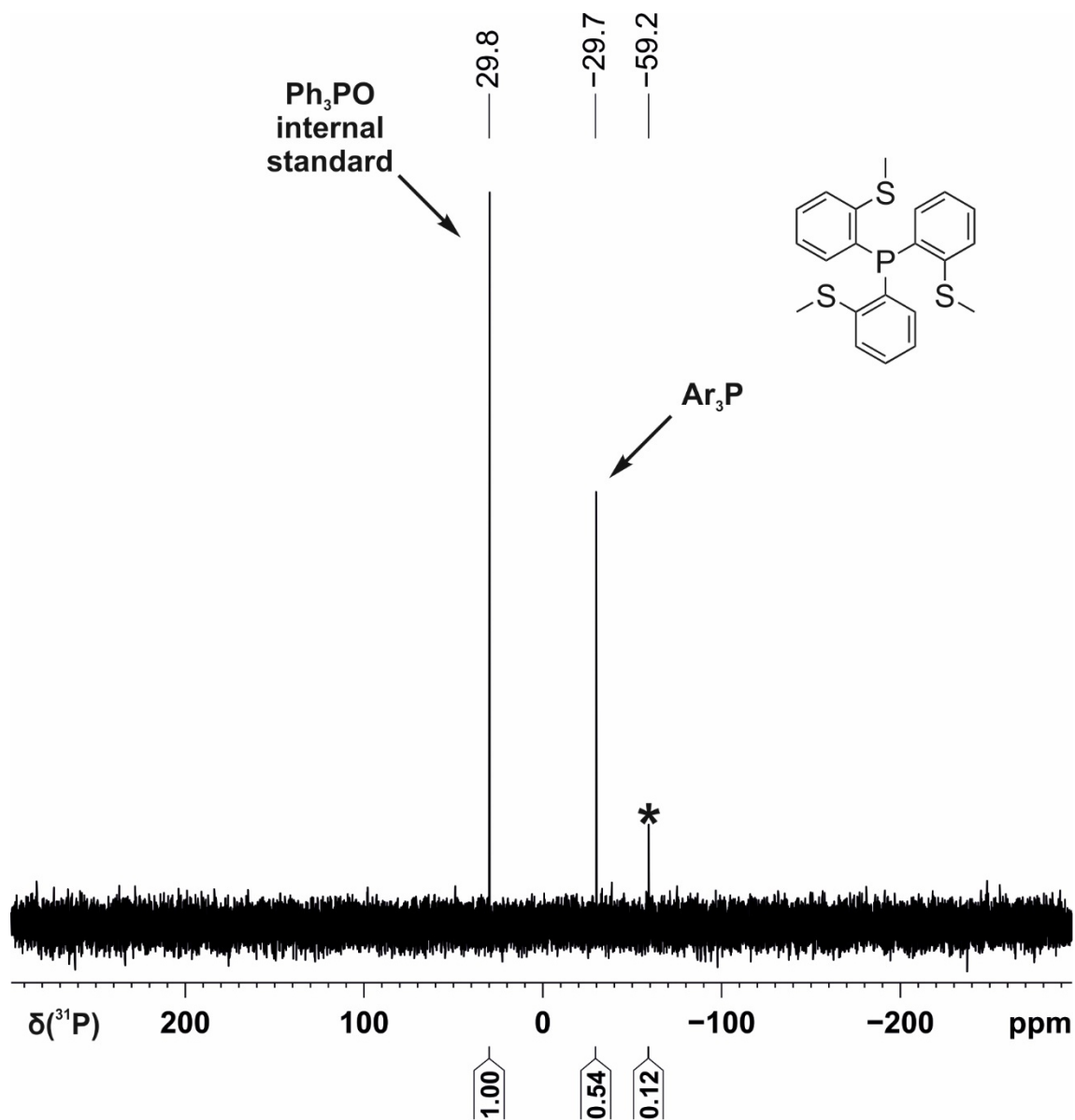
The general procedure was followed using 2-iodoanisole (143 μL , 1.1 mmol), which resulted in 54% conversion to tris(2-methoxyphenyl)phosphine as judged by quantitative $^{31}\text{P}\{^1\text{H}\}$ (zgpg) NMR spectroscopy (GC-MS: expected = 352 m/z; observed = 352 m/z).



Supplementary Figure 7. Qualitative single scan $^{31}\text{P}\{^1\text{H}\}$ (zgpg) NMR spectrum for the photocatalytic functionalisation of P₄ using 2-iodoanisole. Ar = 2-methoxyphenyl. * marks the signal of an unknown by-product.

Tris-2-(methylthio)phenylphosphine (Table 2, Entry 6)

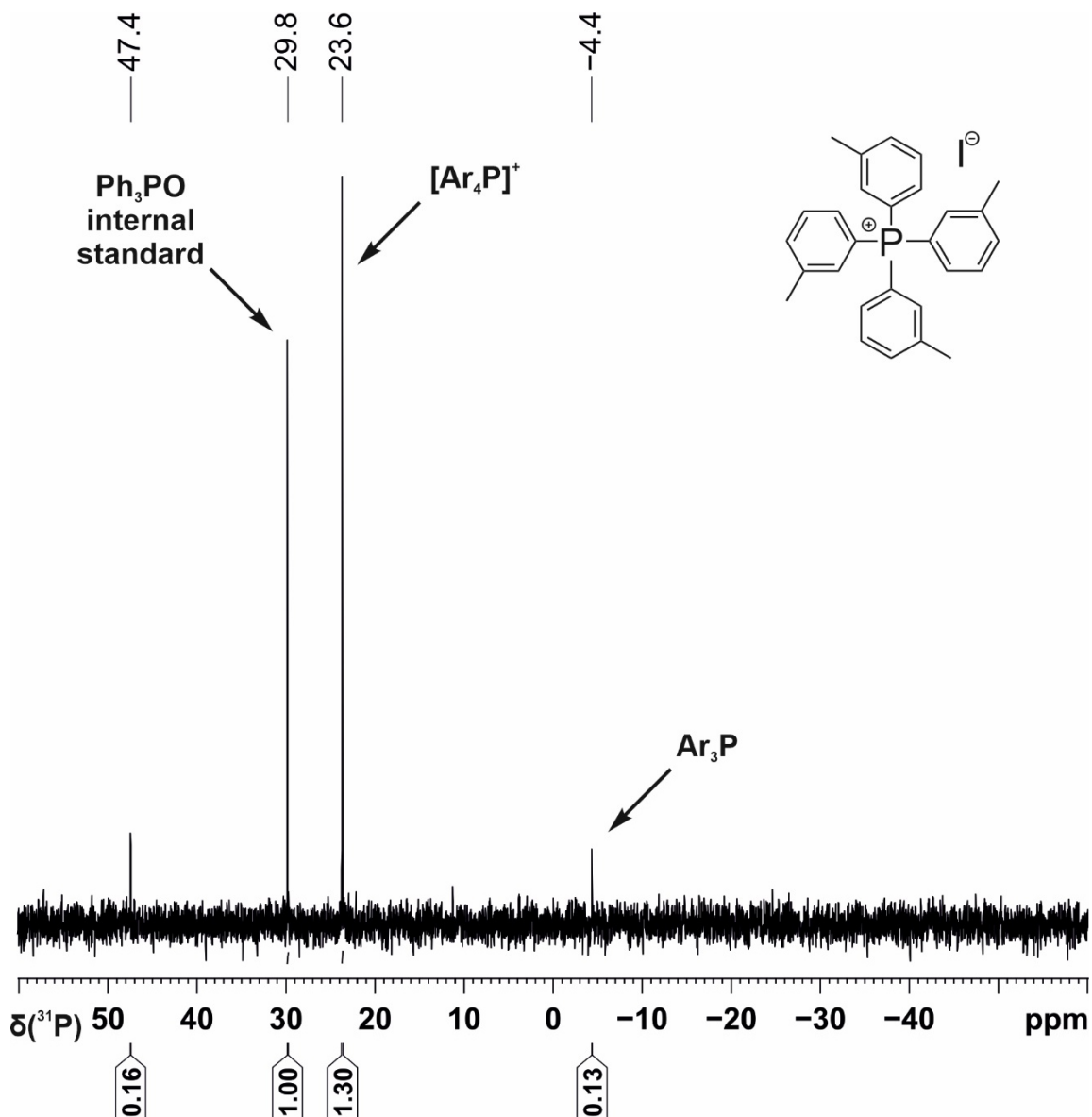
The general procedure was followed using 2-iodothioanisole (160 μL , 1.1 mmol), which resulted in 21% conversion to tris(2-(methylthio)phenyl)phosphine as judged by quantitative $^{31}\text{P}\{^1\text{H}\}$ (zgig) NMR spectroscopy (GC-MS: expected = 401 m/z; observed = 400 m/z).



Supplementary Figure 8. Qualitative single scan $^{31}\text{P}\{^1\text{H}\}$ (zgpg) NMR spectrum for the photocatalytic functionalisation of P₄ using 2-iodothioanisole. Ar = 2-methylthiophenyl. * marks the signal of an unknown by-product.

Tetra(*m*-tolyl)phosphonium iodide (Table 3, Entry 1)

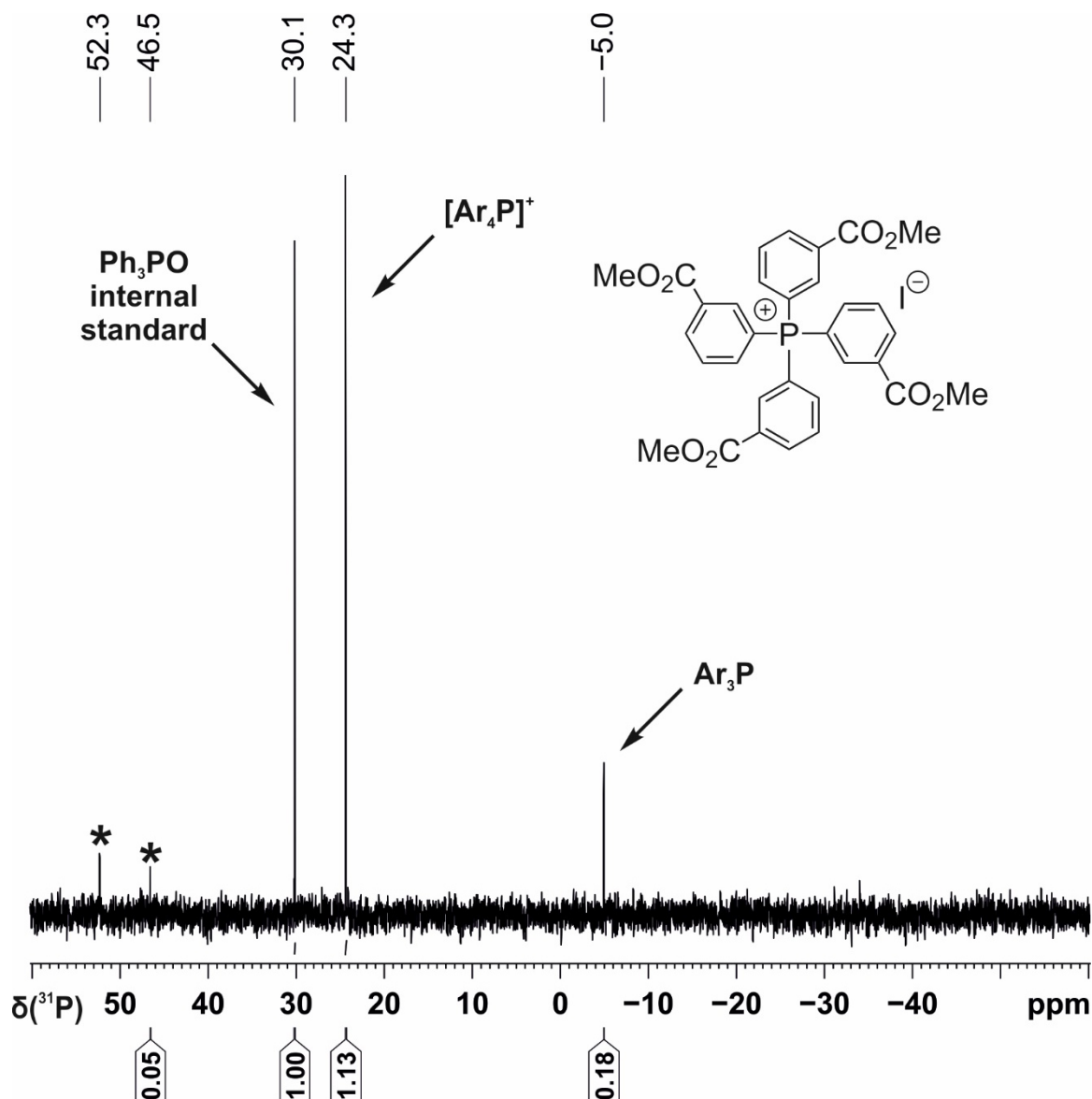
The general procedure was followed using 3-iodotoluene (140 μ L, 1.1 mmol), which resulted in 63% conversion to tetra(*m*-tolyl)phosphonium iodide and 5% conversion to tri(*m*-tolyl) phosphine as judged by quantitative $^{31}\text{P}\{^1\text{H}\}$ (zgpg) NMR spectroscopy.



Supplementary Figure 9. Qualitative single scan $^{31}\text{P}\{^1\text{H}\}$ (zgpg) NMR spectrum for the photocatalytic functionalisation of P₄ using 3-iodotoluene. Ar = *m*-tolyl. * marks the signal of an unknown by-product.

Tetrakis-3-(methylbenzoate)phosphonium iodide (Table 3, Entry 2)

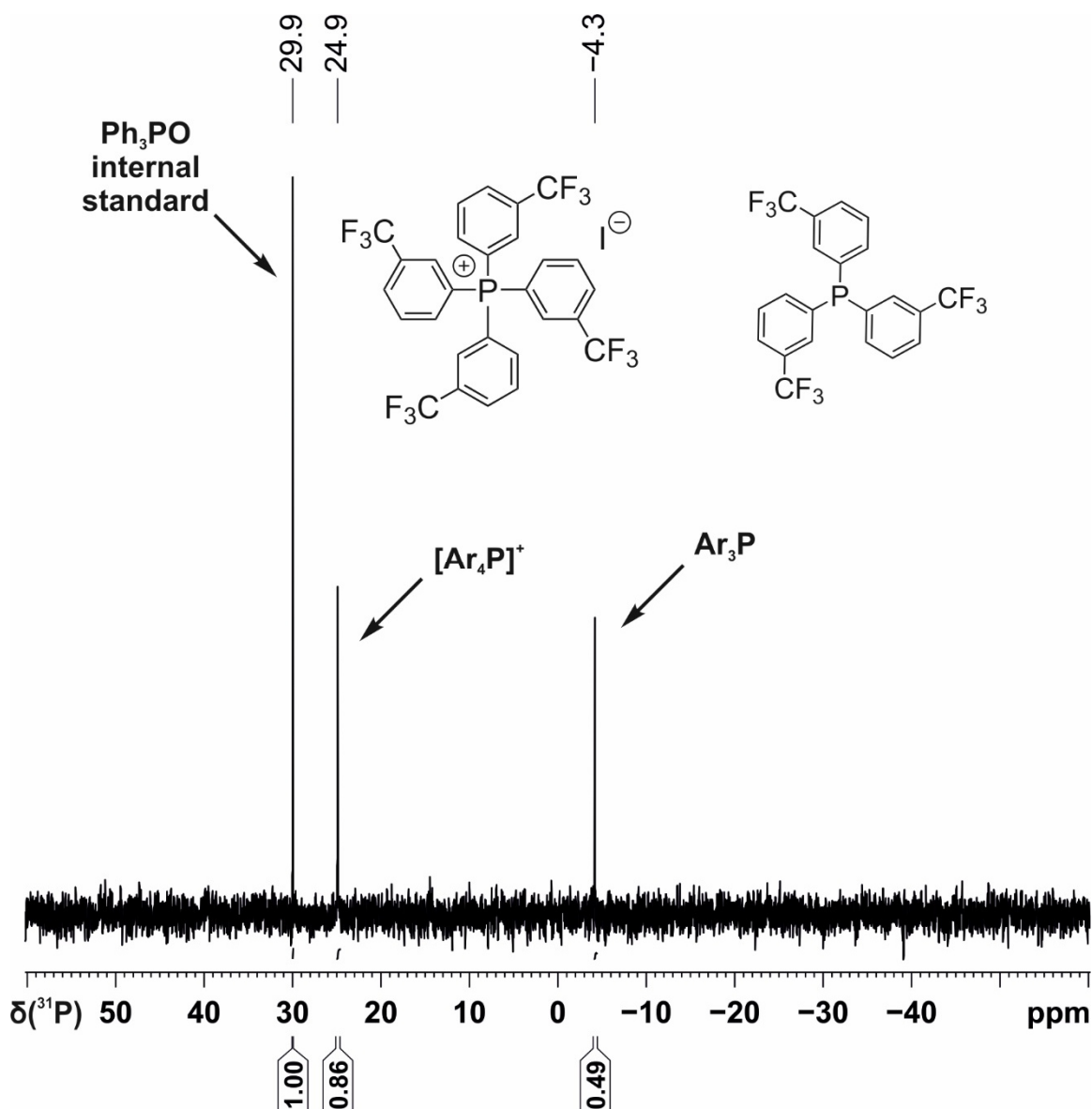
The general procedure was followed using methyl 3-iodobenzoate (288 mg, 1.1 mmol), which resulted in 48% conversion to tetrakis(3-(methyl benzoate))phosphonium iodide and 8% conversion to tris(3-(methyl benzoate))phosphine as judged by quantitative $^{31}\text{P}\{^1\text{H}\}$ (zgig) NMR spectroscopy.



Supplementary Figure 10. Qualitative single scan $^{31}\text{P}\{^1\text{H}\}$ (zgpg) NMR spectrum for the photocatalytic functionalisation of P_4 using methyl 3-iodobenzoate. Ar = 3-methylbenzoate. * marks the signals of unknown by-products.

Tetrakis-3-(trifluoromethyl)phenylphosphonium iodide (Table 3, Entry 3)

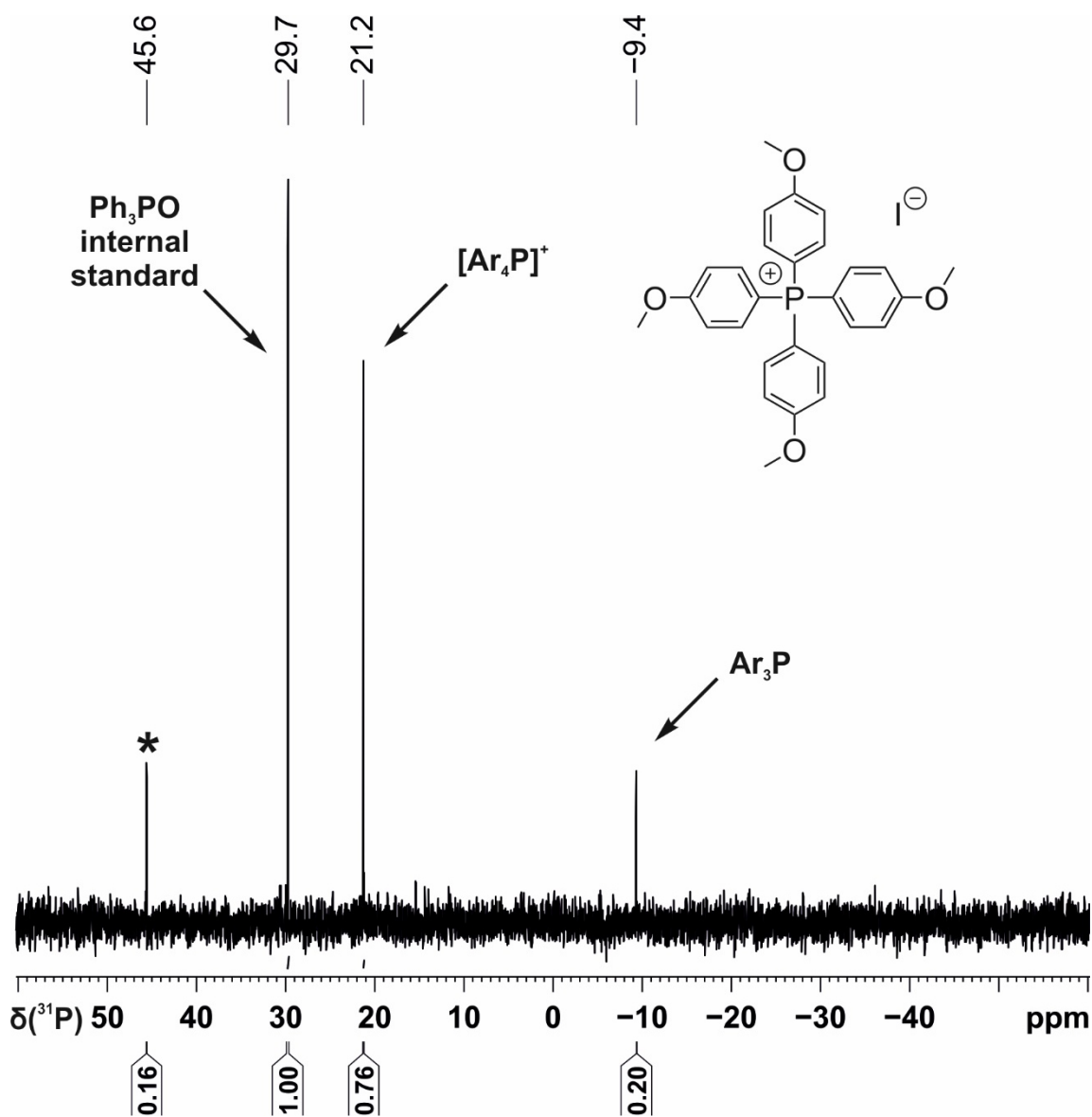
The general procedure was followed using 3-iodobenzotrifluoride (159 μL , 1.1 mmol), which resulted in 25% conversion to tetrakis(3-(trifluoromethyl)phenyl)phosphonium iodide and 20% conversion to tris(3-(trifluoromethyl)phenyl)phosphine as judged by quantitative $^{31}\text{P}\{^1\text{H}\}$ (zgig) NMR spectroscopy.



Supplementary Figure 11. Qualitative single scan $^{31}\text{P}\{^1\text{H}\}$ (zgpg) NMR spectrum for the photocatalytic functionalisation of P_4 using 3-iodobenzotrifluoride. Ar = 3-(trifluoromethyl)phenyl.

Tetrakis(4-methoxyphenyl)phosphonium iodide (Table 3, Entry 4)

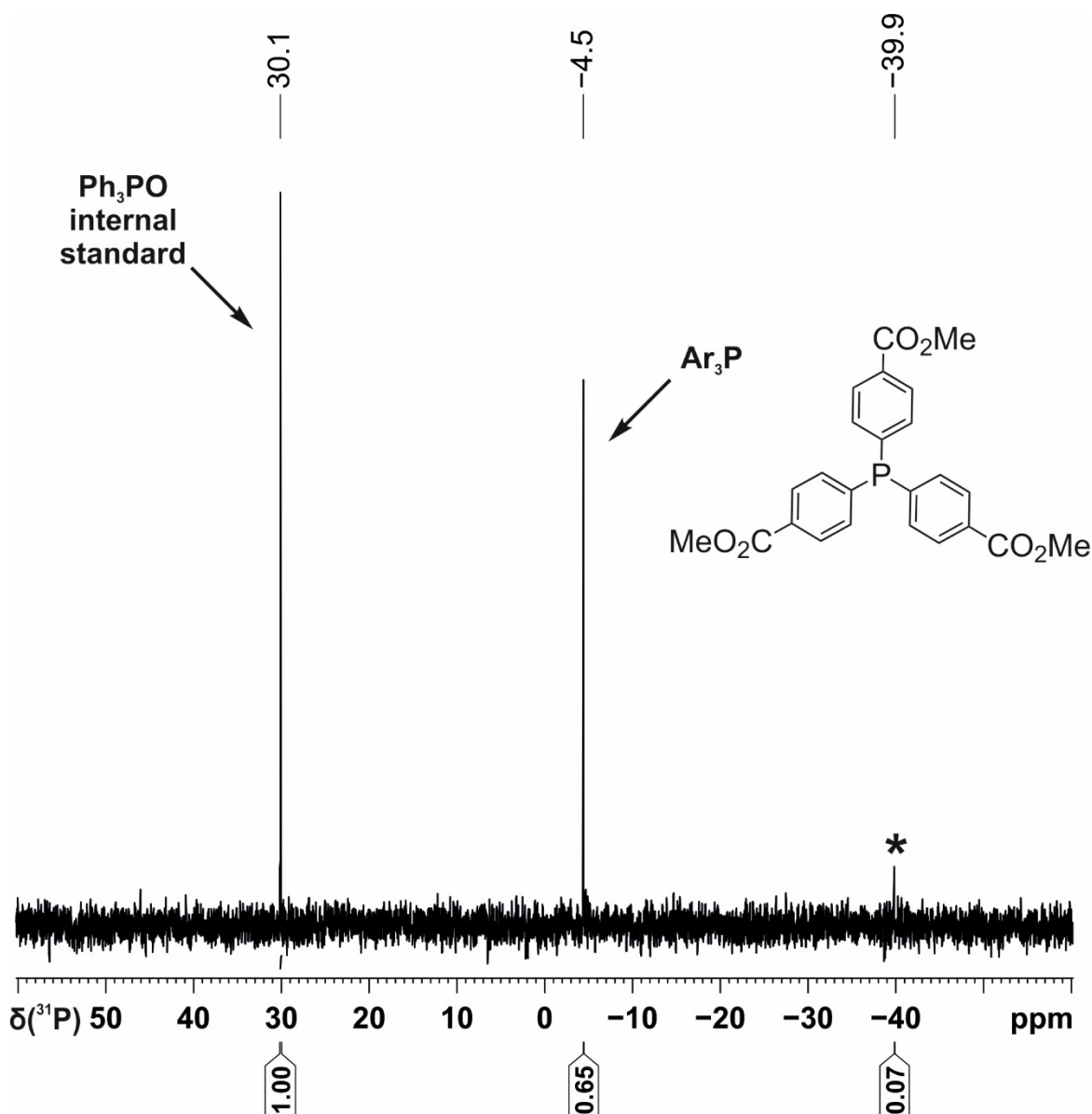
The general procedure was followed using 4-iodoanisole (257 mg, 1.1 mmol), which resulted in 37% conversion to tetrakis(4-methoxyphenyl)phosphonium iodide and 5% conversion to tris(4-methoxyphenyl)phosphine as judged by quantitative $^{31}\text{P}\{^1\text{H}\}$ (zgpg) NMR spectroscopy.



Supplementary Figure 12. Qualitative single scan $^{31}\text{P}\{^1\text{H}\}$ (zgpg) NMR spectrum for the photocatalytic functionalisation of P_4 using 4-iodoanisole. Ar = 4-methoxyphenyl. * marks the signal of an unknown by-product.

Tris[4-(methylbenzoate)]phosphine (Table 3, Entry 5)

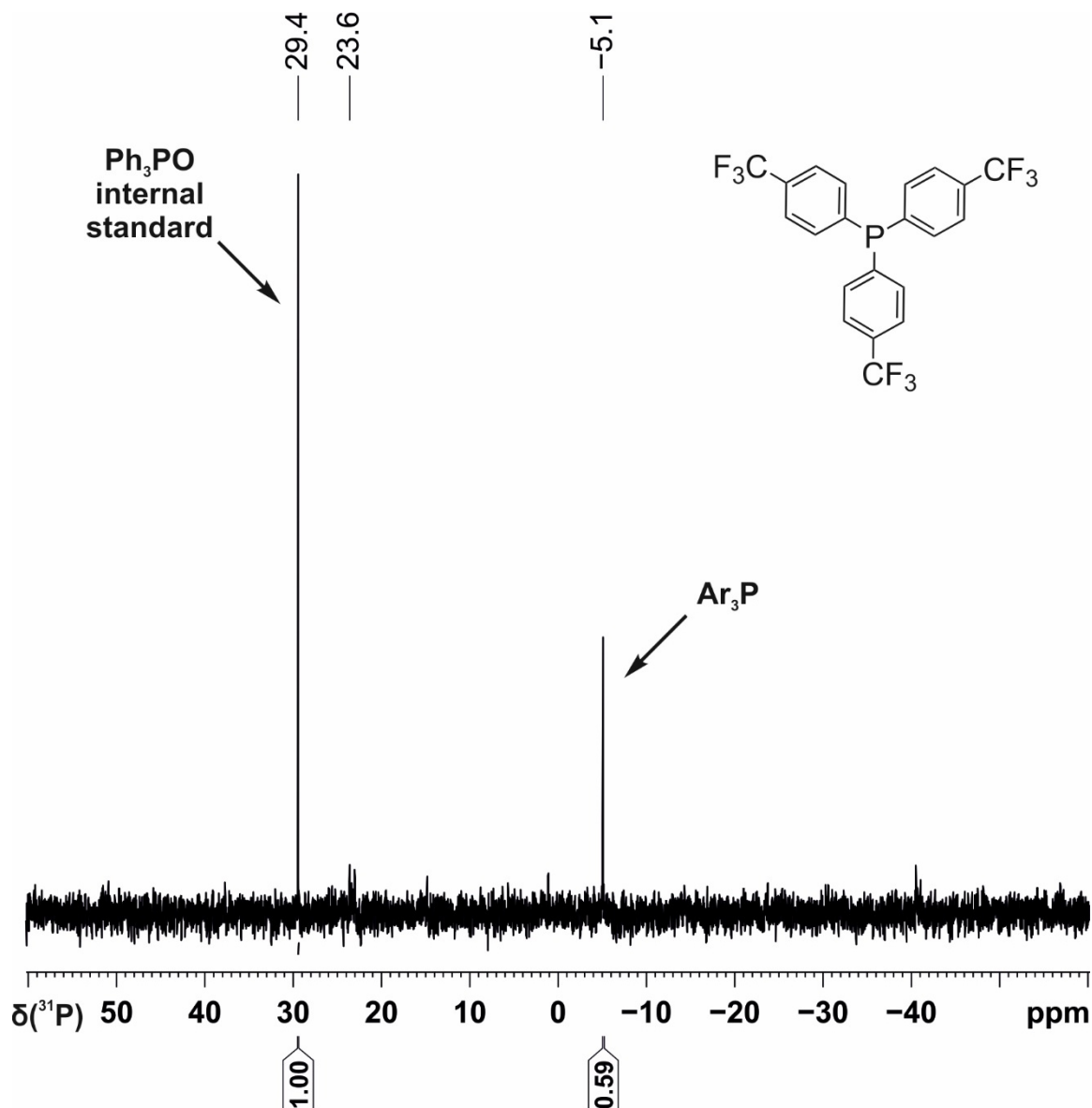
The general procedure was followed using methyl 4-iodobenzoate (156 μL , 1.1 mmol), which resulted in 39% conversion to tris(4-(methyl benzoate))phosphine as judged by quantitative $^{31}\text{P}\{^1\text{H}\}$ (zgpg) NMR spectroscopy (GC-MS: expected = 436 m/z; observed = 436 m/z).



Supplementary Figure 13. Qualitative single scan $^{31}\text{P}\{^1\text{H}\}$ (zgpg) NMR spectrum for the photocatalytic functionalisation of P_4 using methyl 4-iodobenzoate. Ar = 4-methylbenzoate. * marks the signal of an unknown by-product.

Tris-[4(trifluoromethyl)phenyl]phosphonium iodide (Table 3, Entry 6)

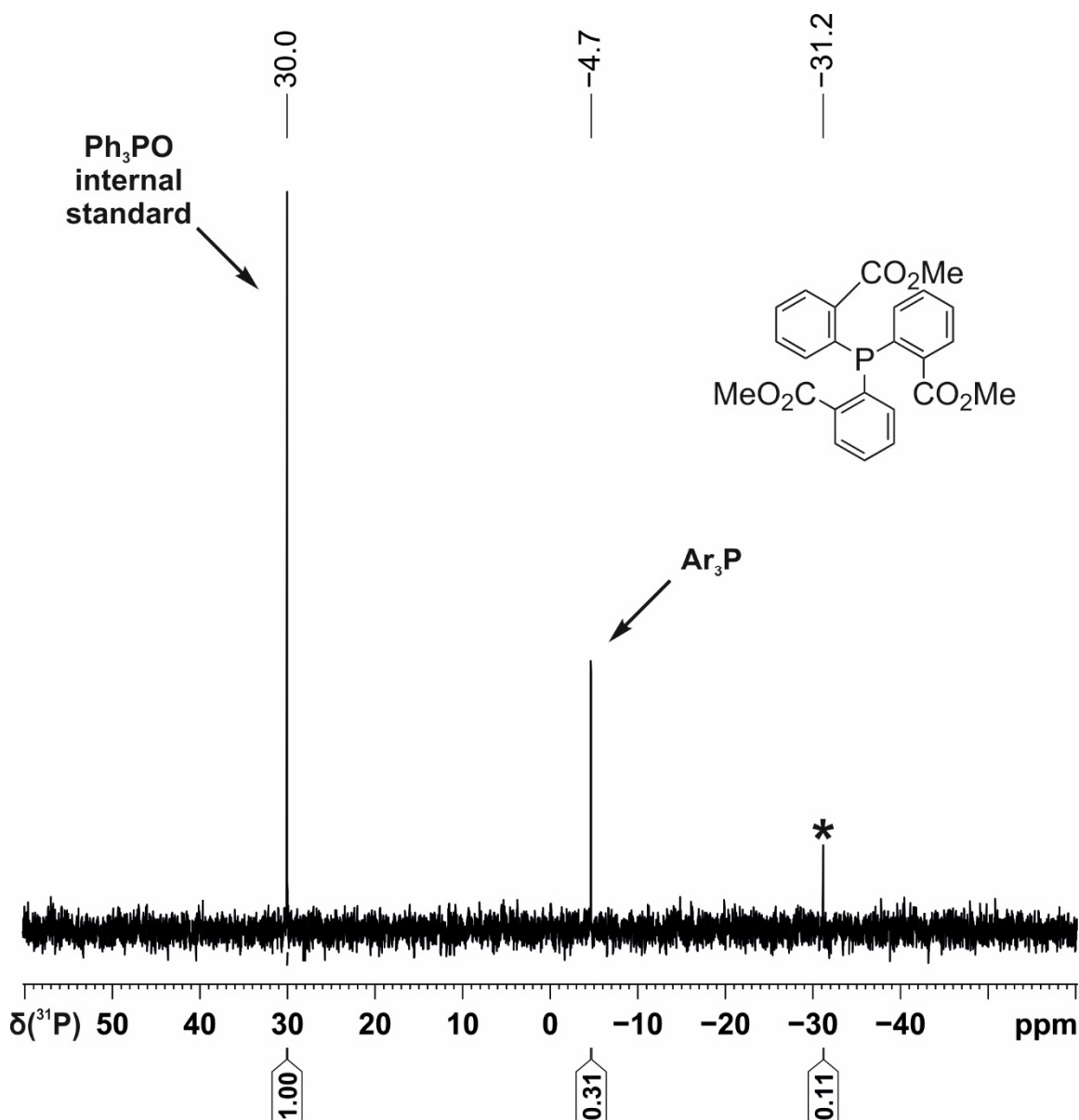
The general procedure was followed using 4-iodobenzotrifluoride (162 μL , 1.1 mmol), which resulted in 30% conversion to tris(4-(trifluoromethyl)phenyl)phosphine as judged by quantitative $^{31}\text{P}\{^1\text{H}\}$ (zgpg) NMR spectroscopy (GC-MS: expected = 466; observed = 466 m/z).



Supplementary Figure 14. Qualitative single scan $^{31}\text{P}\{^1\text{H}\}$ (zgpg) NMR spectrum for the photocatalytic functionalisation of P_4 using 4-iodobenzotrifluoride. Ar = 4-(trifluoromethyl)phenyl.

Tris[2-(methylbenzoate)]phosphine (Table 3, Entry 7)

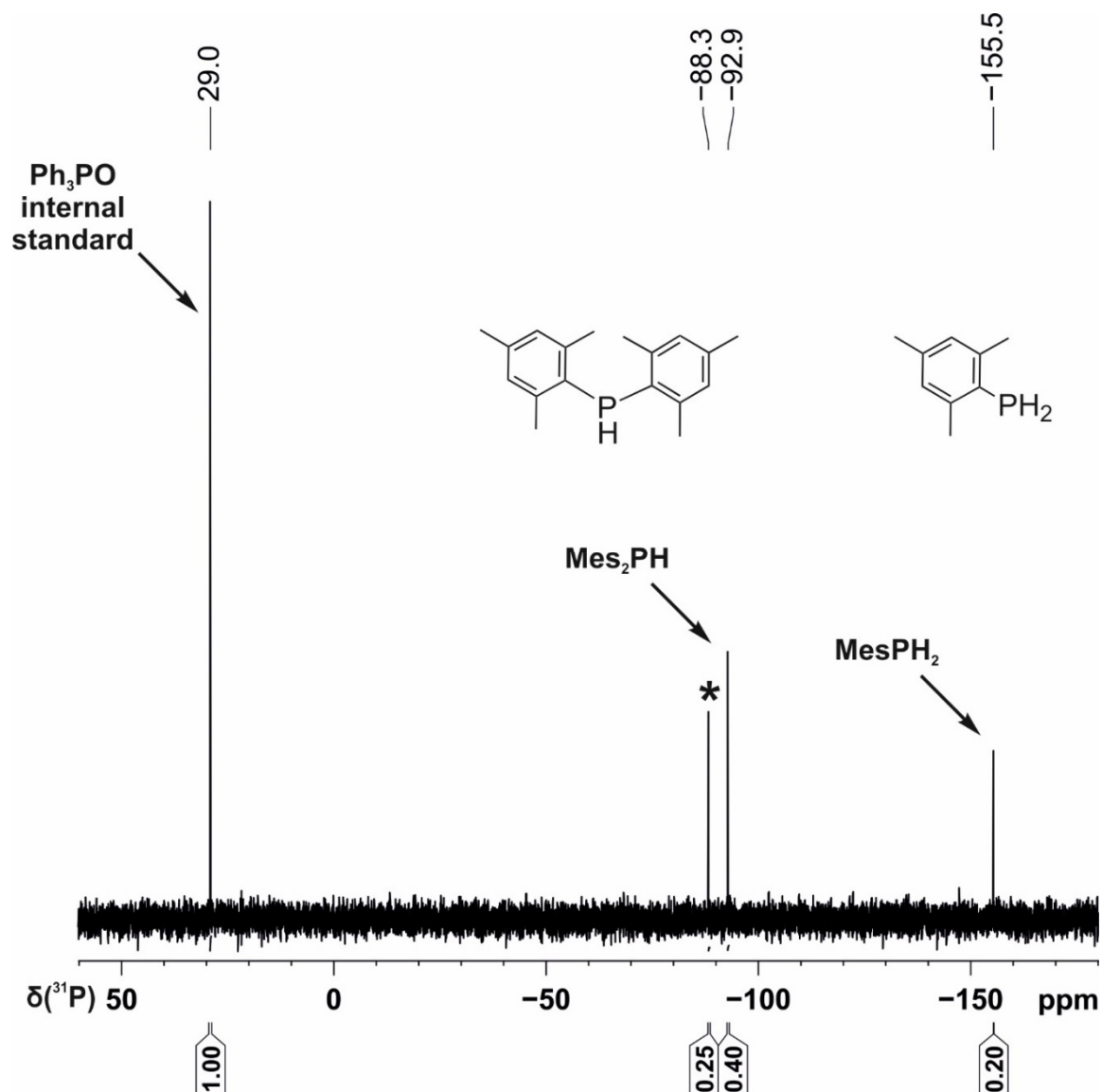
The general procedure was followed using methyl 2-iodobenzoate (161 μL , 1.1 mmol), which resulted in 11% conversion to tris(2-(methyl benzoate))phosphine as judged by quantitative $^{31}\text{P}\{^1\text{H}\}$ (zgpg) NMR spectroscopy (GC-MS: expected = 436 m/z; observed = 436 m/z).



Supplementary Figure 15. Qualitative single scan $^{31}\text{P}\{^1\text{H}\}$ (zgpg) NMR spectrum for the photocatalytic functionalisation of P_4 using methyl 2-iodobenzoate. Ar = 2-methylbenzoate. * marks the signal of an unknown by-product.

Mesityl- and Dimesityl-phosphine (Table 3, Entry 9)

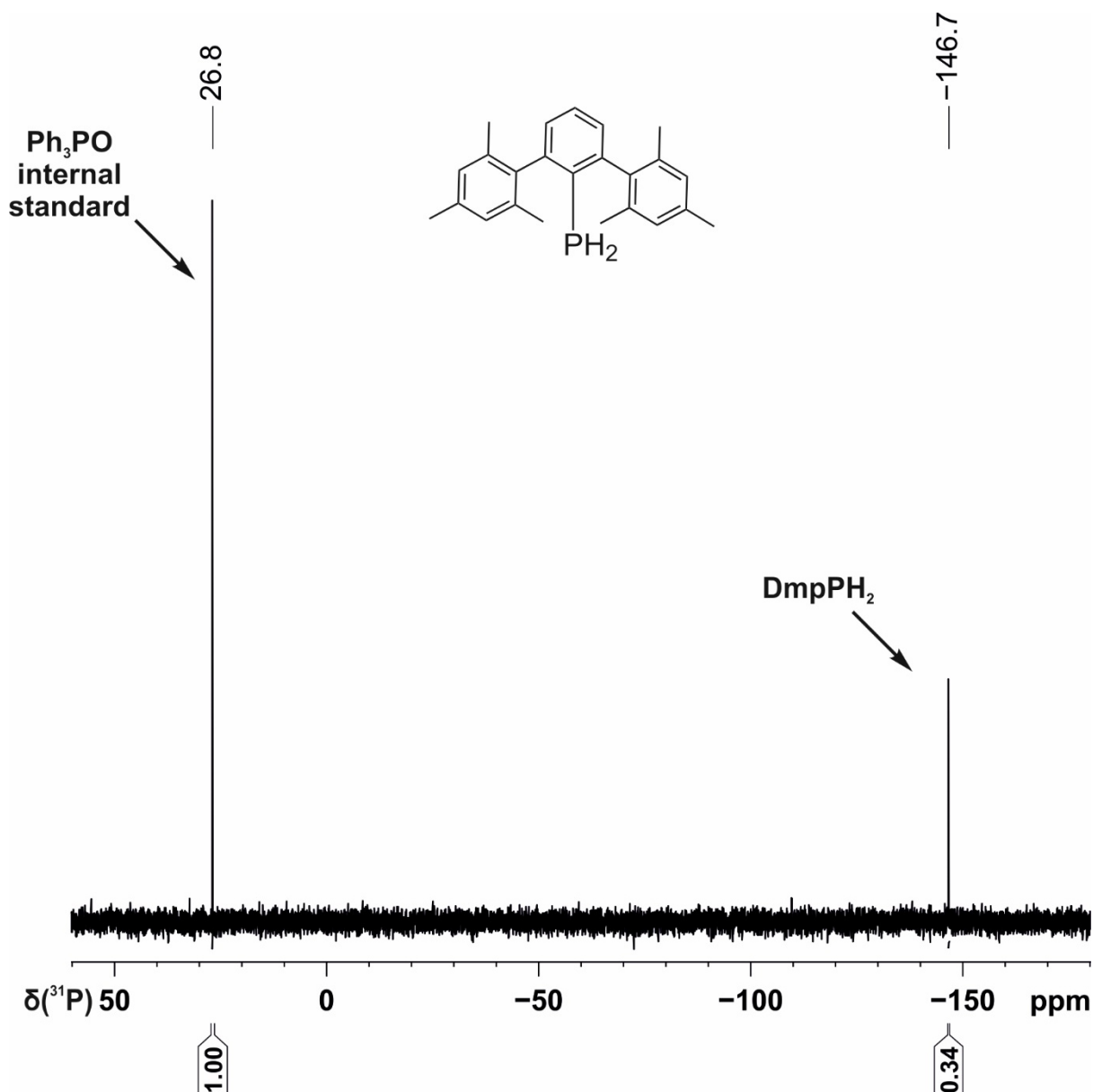
The general procedure was followed with mesityl iodide (2,4,6-trimethyliodobenzene, 271 mg, 1.1 mmol), which resulted in 3% conversion to each of mesitylphosphine and 24% conversion to dimesitylphosphine as judged by quantitative $^{31}\text{P}\{^1\text{H}\}$ (zgpg) NMR spectroscopy.



Supplementary Figure 16. Qualitative single scan $^{31}\text{P}\{^1\text{H}\}$ (zgpg) NMR spectrum for the photocatalytic functionalisation of P_4 using mesityl iodide. Mes = 2,4,6-trimethyliodobenzene. * marks the signal of an unknown by-product.

2,6-Dimesitylphenylphosphine (Table 3, Entry 10)

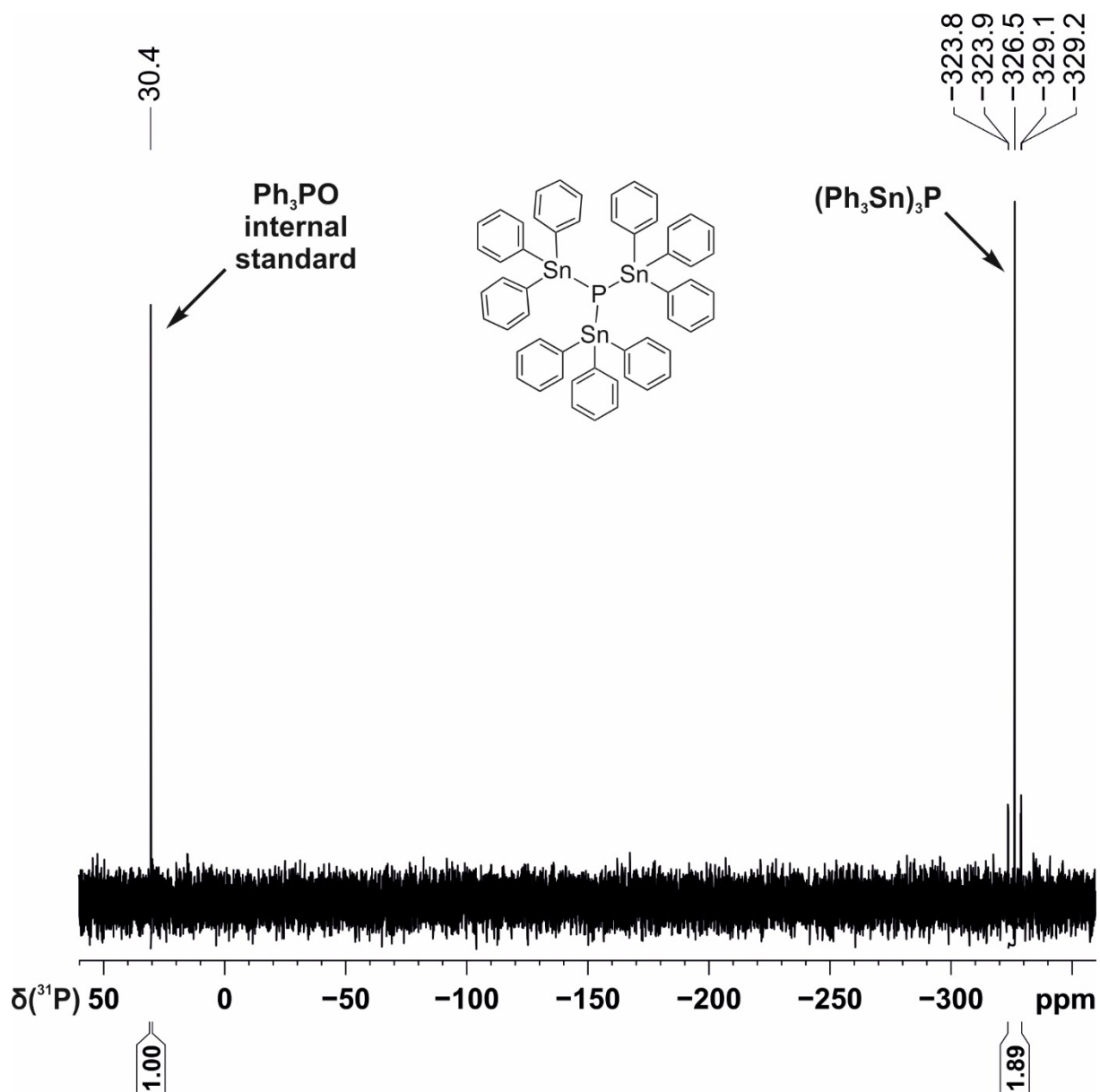
The general procedure was modified to use 1.5 mL benzene and 0.5 mL MeCN as solvent, and 2 equiv. 2,6-dimesityliodobenzene based on the phosphorus atom (88.1 mg, 0.2 mmol), which resulted in 12% conversion to (2,6-dimesitylphenyl)phosphine as judged by quantitative ^{31}P NMR (zg) spectroscopy.



Supplementary Figure 17. Qualitative single scan $^{31}\text{P}\{^1\text{H}\}$ (zgpg) NMR spectrum for the photocatalytic functionalisation of P_4 using 2,6-dimesityliodobenzene. DmP = 2,6-dimesitylphenyl.

Tris(triphenylstannyl)phosphine (Table 3, Entry 12)

The general procedure was followed with Ph_3SnCl (424 mg, 1.1 mmol), which resulted in 77% conversion to tris(triphenylstannyl)phosphine as judged by quantitative $^{31}\text{P}\{^1\text{H}\}$ (zgpg) NMR spectroscopy.



Supplementary Figure 18. Qualitative single scan $^{31}\text{P}\{^1\text{H}\}$ (zgpg) NMR spectrum for the photocatalytic functionalisation of P_4 using Ph_3SnCl .

2.5.3 Photocatalytic functionalisation of P₄ on a 1 mmol scale



Supplementary Figure 19. Illustration of the experimental setup used for photocatalytic reactions on a 1 mmol scale.

Supplementary Method 2. Photocatalytic preparation of tetraphenylphosphonium iodide from P₄ (1 mmol scale, Table 2, Entry 1)

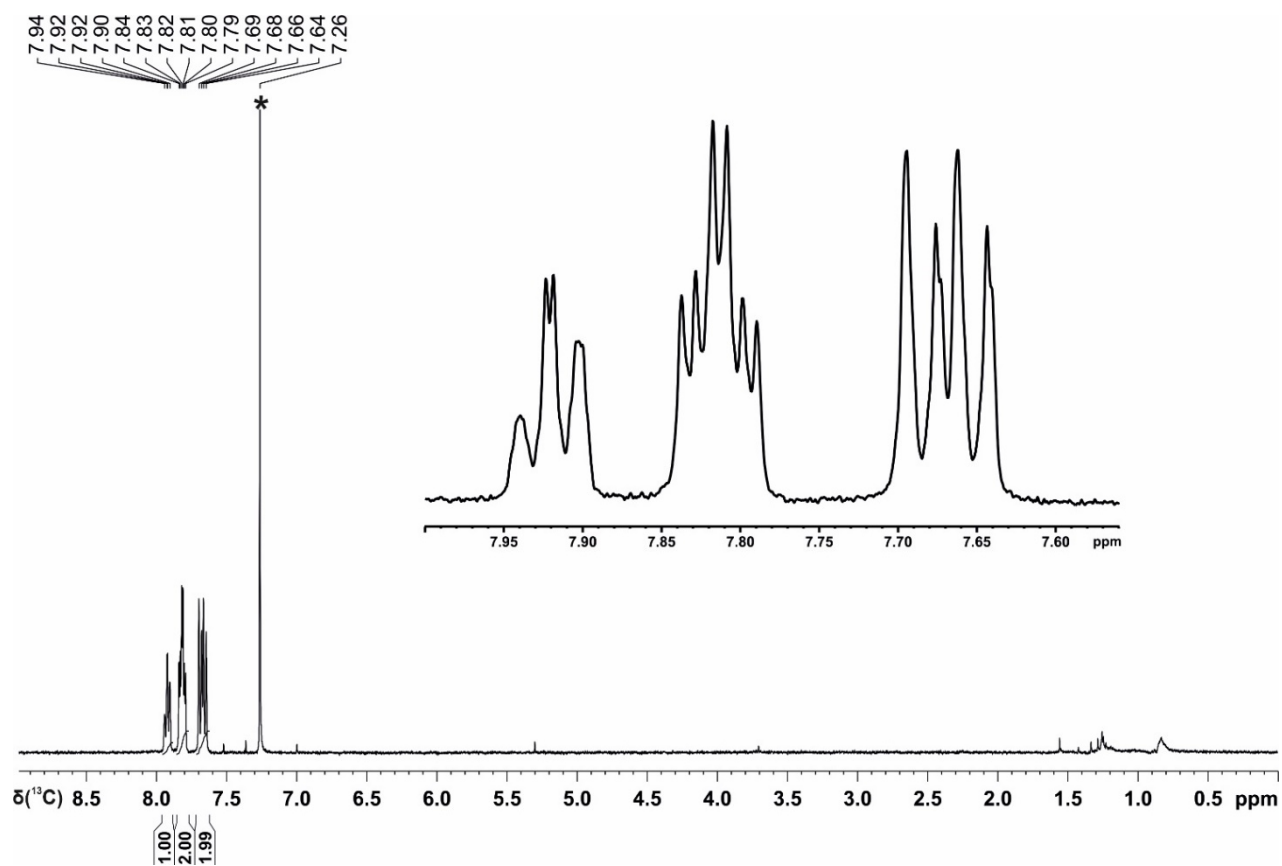
In a 50 ml stoppered tube equipped with a stirring bar, iodobenzene (1230 μ L, 11 mmol, 11 equiv. based on the phosphorus atom), Et₃N (2007 μ L, 14.4 mmol, 14.4 equiv.), catalyst [1]PF₆ (20.1 mg, 2.2 mol%), and P₄ (30.9 mg, 0.25 mmol, 1 equiv.) were added to 15 mL acetonitrile and 5 mL benzene in an N₂ filled glove box. The tube was sealed, placed in a water-cooled block to maintain near-ambient temperature (Supplementary Figure 19), and irradiated with blue light (7X Osram OSOLON SSL80, 455 nm (\pm 15 nm), 20.3 V 1000 mA) for 18 h. Subsequent work-up was performed under air. The reaction mixture was added to 1 L of water and the volume of the resulting yellow suspension was reduced to approx. 500 mL using a rotary evaporator at 50 °C, after which clearer separation of a yellow precipitate could be observed. The solution was filtered (sartorius, filter paper grade 1289) and the volume then further reduced until precipitation of a pale-yellow powder was observed to begin. Crude product was crystallised from the solution at 2 °C over the course of two days and isolated by filtration at 0 °C. Recrystallization from ethanol at –10 °C yielded a pale-yellow powder, which was dried under high vacuum (ca. 10⁻⁵ mbar) for 48 h (160 mg, 34%).

The characterization data of the product are consistent with the data found in the literature.^{S2}

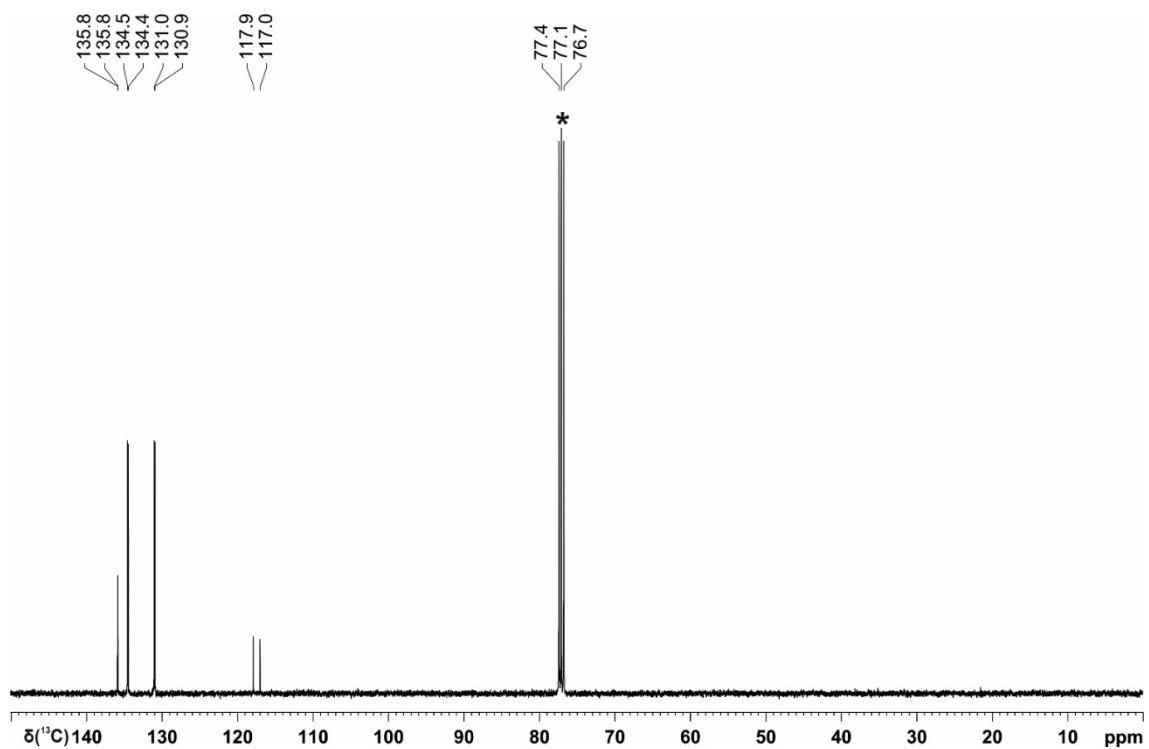
¹H NMR (400 MHz, CDCl₃): δ 7.94-7.90 (m, 4H), 7.81 (dt, J = 7.8, 3.6 Hz, 8H), 7.67 (dd, J = 12.7, 7.8 Hz, 8H).

¹³C{¹H} NMR (100 MHz, CDCl₃): δ 135.8 (d, J = 3.0 Hz), 134.5 (d, J = 10.3 Hz), 130.9 (d, J = 12.9 Hz), 117.5 (d, J = 89.5 Hz).

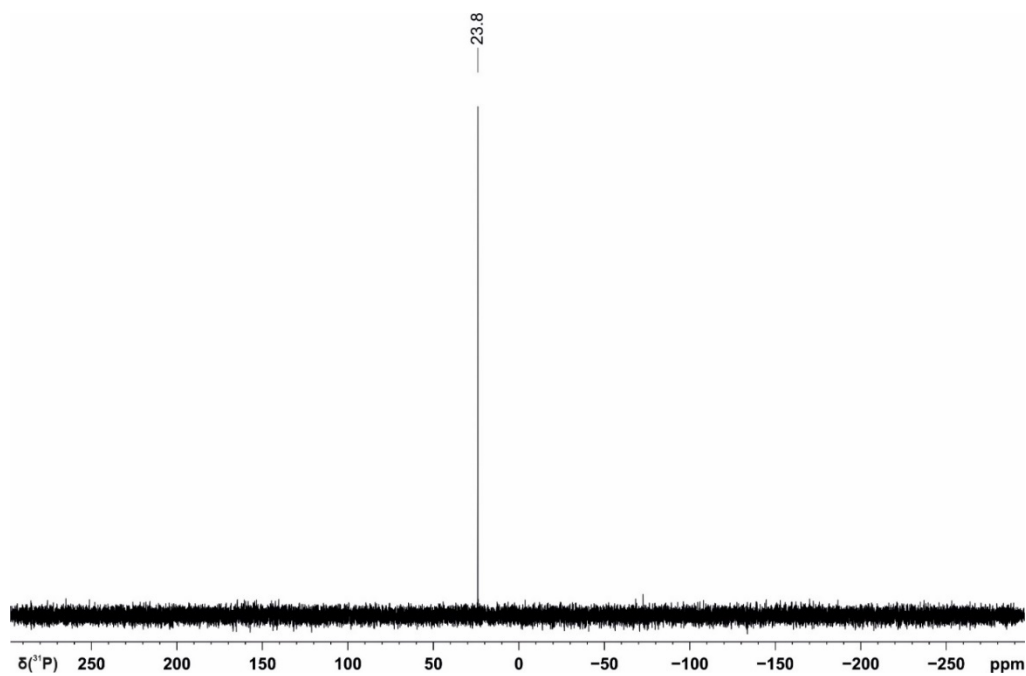
³¹P{¹H} NMR (162 MHz, CDCl₃): δ 23.8



Supplementary Figure 20. ^1H NMR spectrum in CDCl_3 of tetraphenylphosphonium iodide prepared photocatalytically from P_4 on a 1 mmol scale. $^*\text{CDCl}_3$.



Supplementary Figure 21. $^{13}\text{C}\{^1\text{H}\}$ NMR spectrum in CDCl_3 of tetraphenylphosphonium iodide prepared photocatalytically from P_4 on a 1 mmol scale. * CDCl_3 .



Supplementary Figure 22. $^{31}\text{P}\{^1\text{H}\}$ NMR spectrum in CDCl_3 of tetraphenylphosphonium iodide prepared photocatalytically from P_4 on a 1 mmol scale.

Supplementary Method 3. Photocatalytic preparation of tetra(*p*-tolyl)phosphonium iodide from P₄ (1 mmol scale, Table 2, Entry 2)

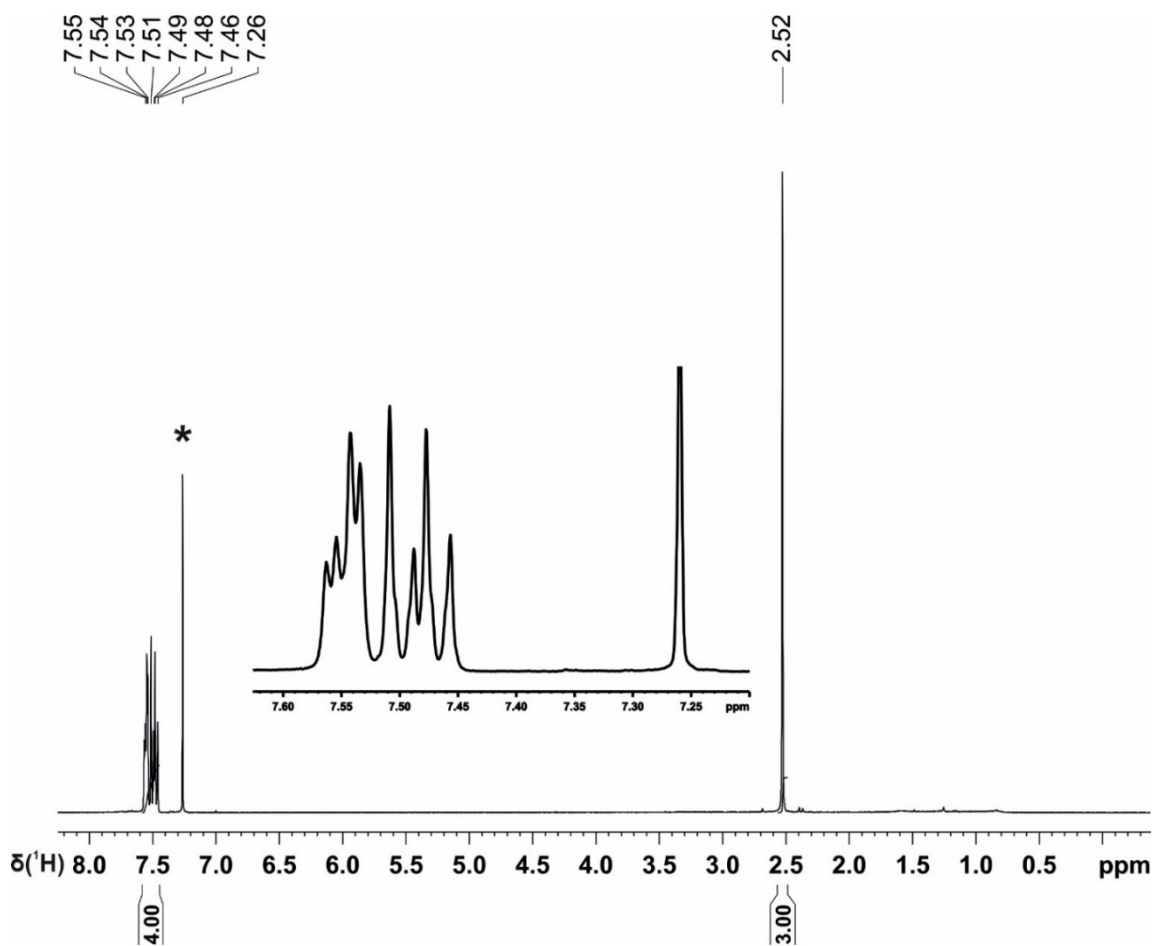
In a 50 ml stoppered tube equipped with a stirring bar, 4-iodotoluene (2398 mg, 11 mmol, 11 equiv. based on the phosphorus atom), Et₃N (2007 μ L, 14.4 mmol, 14.4 equiv.), catalyst [1]PF₆ (20.1 mg, 2.2 mol%), and P₄ (30.9 mg, 0.25 mmol, 1 equiv.) were added to 15 mL acetonitrile and 5 mL benzene in an N₂ filled glove box. The tube was sealed, placed in a water-cooled block to maintain near-ambient temperature (Supplementary Figure 19), and irradiated with blue light (7X Osram OSRON SSL80, 455 nm (\pm 15 nm), 20.3 V 1000 mA) for 30 h. Subsequent work-up was performed under air. The reaction mixture was added to 1 L of water and the volume of resulting yellow suspension was reduced to approx. 500 mL using a rotary evaporator at 50 °C, after which clearer separation of a yellow precipitate could be observed. The solution was filtered (sartorius, filter paper grade 1289) and the volume then further reduced until precipitation of a white powder was observed to begin. Crude product was crystallised from the solution at 2 °C over the course of two days and isolated by filtration at 0 °C. Drying of the resulting yellow material at 140 °C and high vacuum (ca. 10⁻⁵ mbar) yielded tetra(*p*-tolyl)phosphonium iodide as a spectroscopically clean, off-white powder (216 mg, 41%).

¹H NMR (400 MHz, CDCl₃): δ 7.56-7.53 (m, 8H), 7.51-7.46 (m, 8H), 2.52 (s, 12H).

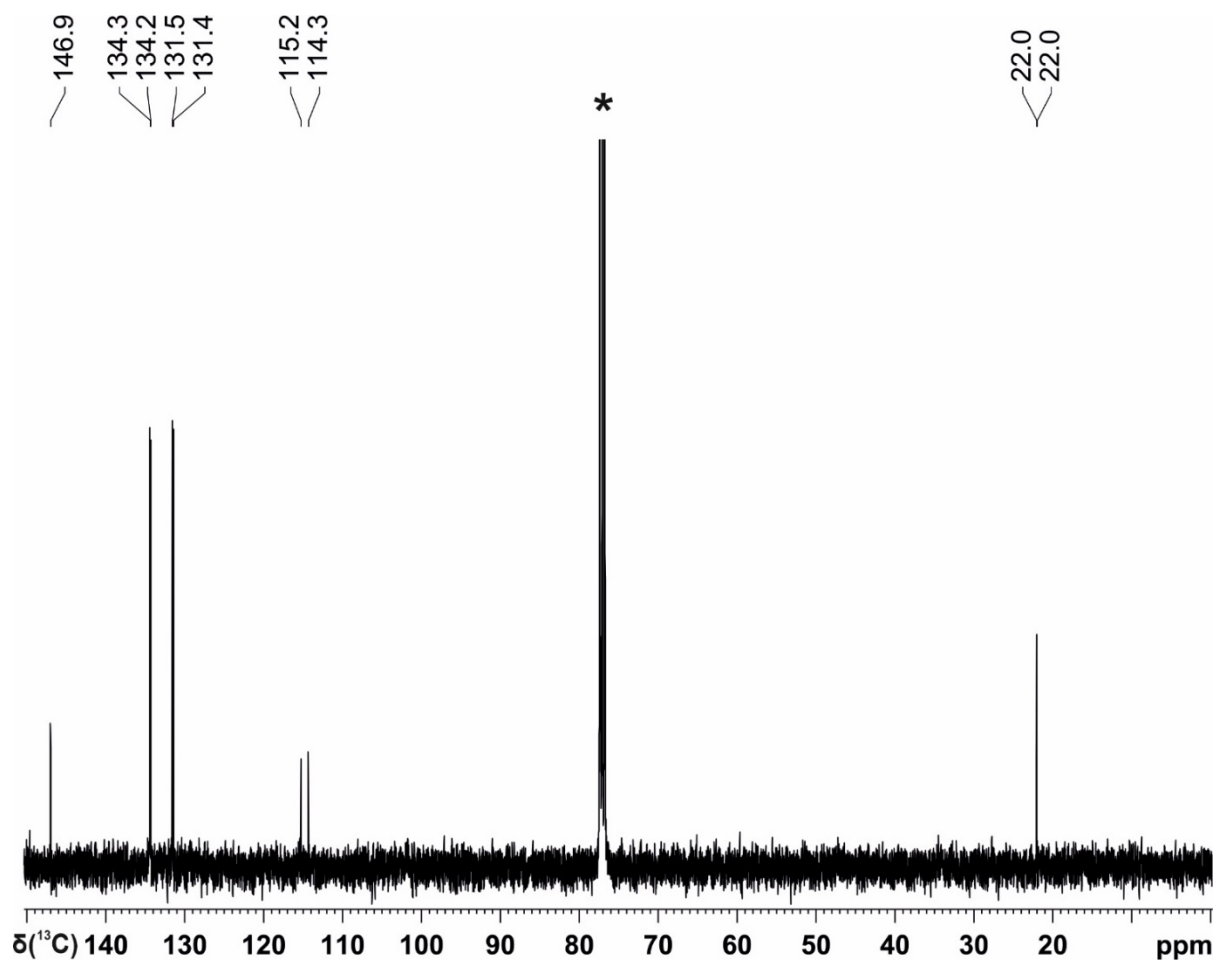
¹³C{¹H} NMR (100 MHz, CDCl₃): δ 146.9 (d, *J* = 3.0 Hz), 134.3 (d, *J* = 10.7 Hz), 131.4 (d, *J* = 13.3 Hz), 114.7 (d, *J* = 92.5 Hz), 22.0 (d, *J* = 1.4 Hz).

³¹P{¹H} NMR (162 MHz, CDCl₃): δ 22.8

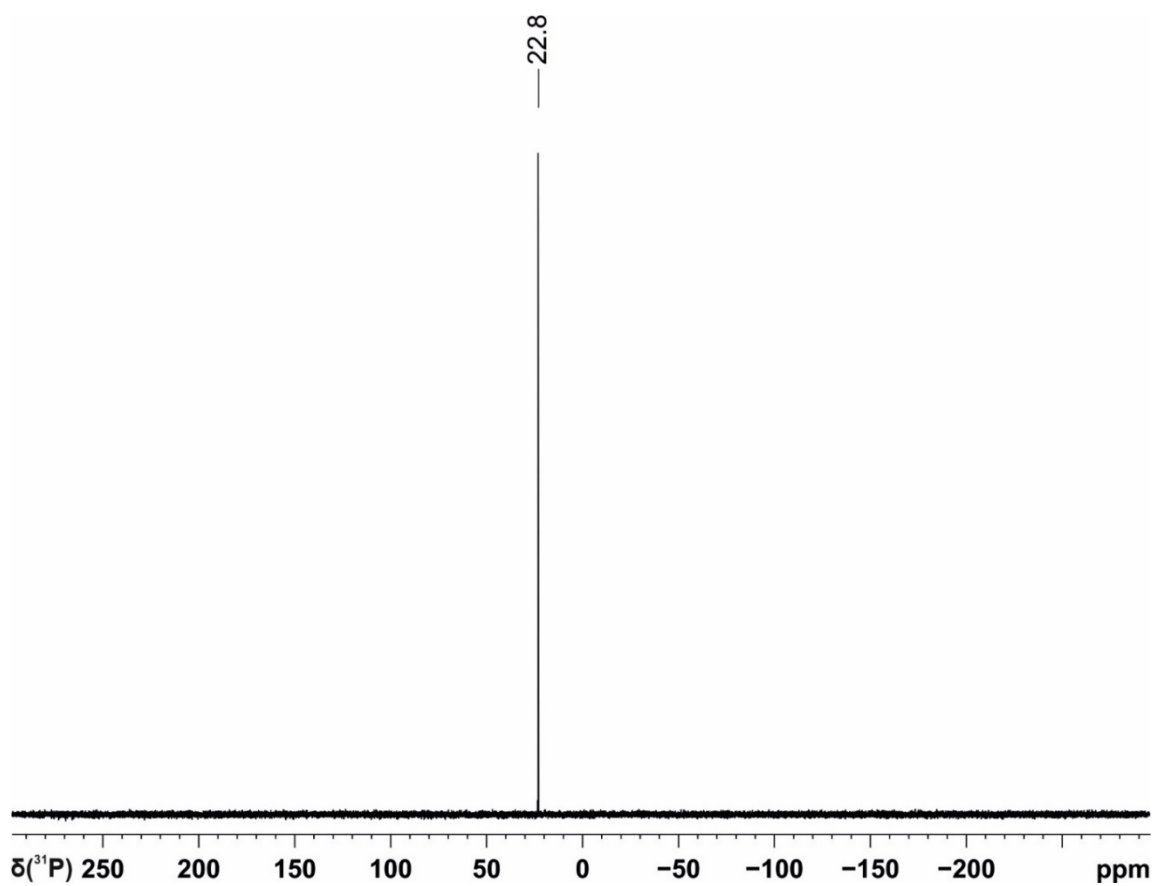
Elemental analysis: Calculated for C₂₈H₂₈IP: C, 64.38; H, 5.40; Found: C, 63.77; H, 5.55; N, 0.20.



Supplementary Figure 23. ^1H NMR spectrum in CDCl_3 of tetra(p-tolyl)phosphonium iodide prepared photocatalytically from P_4 on a 1 mmol scale. $^*\text{CDCl}_3$.



Supplementary Figure 24. $^{13}\text{C}\{^1\text{H}\}$ NMR spectrum in CDCl_3 of tetra(p-tolyl)phosphonium iodide prepared photocatalytically from P_4 on a 1 mmol scale. * CDCl_3 .



Supplementary Figure 25. $^{31}\text{P}\{^1\text{H}\}$ NMR spectrum in CDCl_3 of tetra(*p*-tolyl)phosphonium iodide prepared photocatalytically from P_4 on a 1 mmol scale.

Supplementary Method 4. Photocatalytic preparation of tetrakis(3-methoxyphenyl)phosphonium iodide from P₄ (1 mmol scale, Table 2, Entry 3)

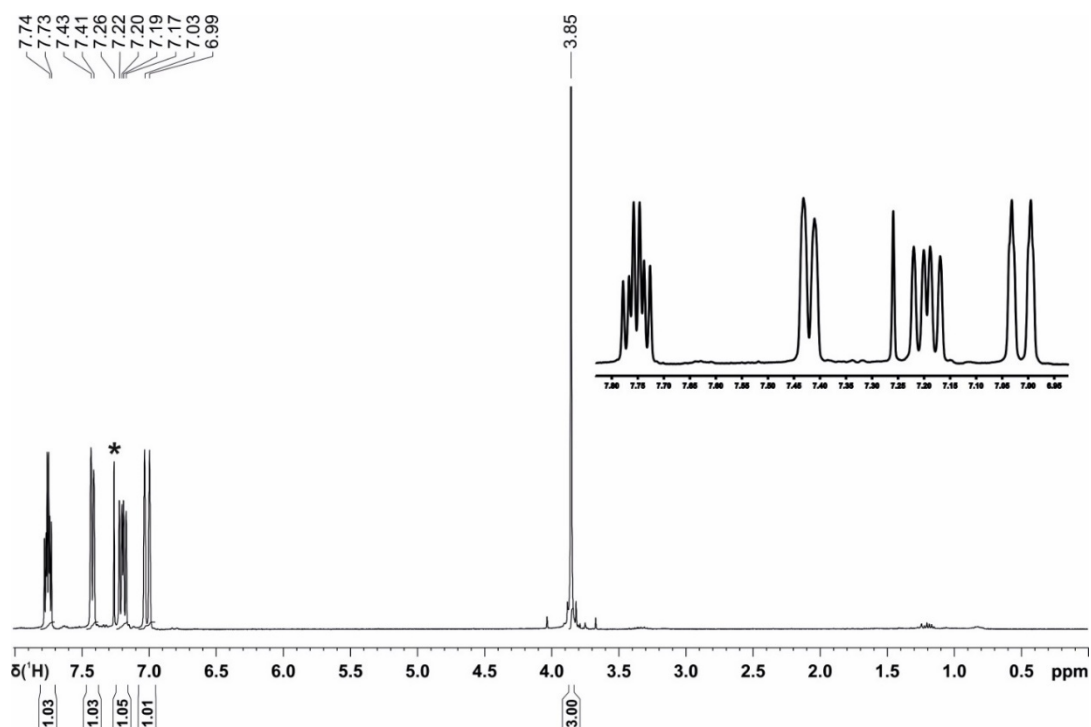
In a 50 ml stoppered tube equipped with a stirring bar, 3-iodoanisole (1310 μL , 11 mmol, 11 equiv. based on the phosphorus atom), Et₃N (2007 μL , 14.4 mmol, 14.4 equiv.), catalyst [1]PF₆ (20.1 mg, 2.2 mol%), and P₄ (30.9 mg, 0.25 mmol, 1 equiv.) were added to 15 mL acetonitrile and 5 mL benzene in an N₂ filled glove box. The tube was sealed, placed in a water-cooled block to maintain near-ambient temperature (Supplementary Figure 19), and irradiated with blue light (7X Osram OSRON SSL80, 455 nm (± 15 nm), 20.3 V 1000 mA) for 24 h. Subsequent work-up was performed under air. The reaction mixture was added to 1.5 L of water and the volume of resulting yellow suspension was reduced to approx. 500 mL using a rotary evaporator at 50 °C, after which clearer separation of a yellow precipitate could be observed. The solution was filtered (sartorius, filter paper grade 1289) and the solvent was removed *in vacuo*. Drying of the resulting yellow material at 140 °C and full vacuum (ca. 10⁻³ mbar) yielded tetrakis(3-methoxyphenyl)phosphonium iodide as a spectroscopically-clean off-white powder (350 mg, 60%).

¹H NMR (400 MHz, CDCl₃): δ 7.75 (dt, $J = 8.1, 4.6$ Hz, 4H), 7.42 (d, $J = 8.5$ Hz, 4H), 7.22-7.15 (m, 4H), 7.01-6.99 (m, 4H), 3.85 (s, 12H).

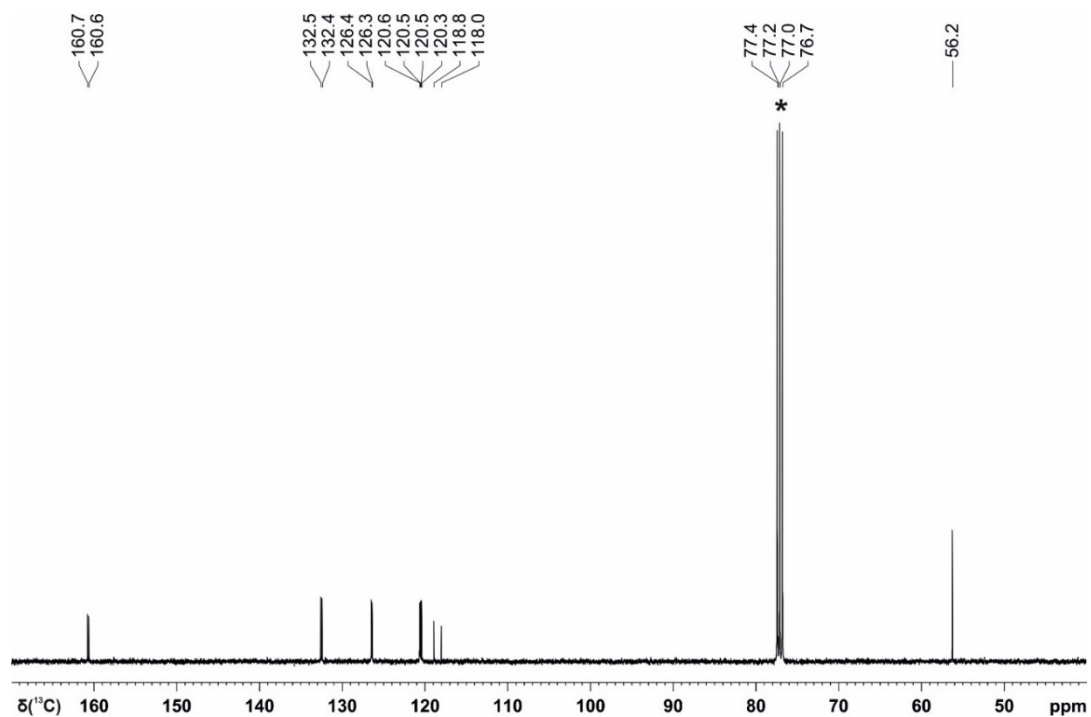
¹³C{¹H} NMR (100 MHz, CDCl₃): δ 160.6 (d, $J = 16.5$ Hz), 132.5 (d, $J = 15.2$ Hz), 126.4 (d, $J = 9.9$ Hz), 120.6 (d, $J = 2.9$ Hz), 120.4 (d, $J = 11.8$ Hz), 118.4 (d, $J = 89.2$ Hz), 56.2 (s).

³¹P{¹H} NMR (162 MHz, CDCl₃): δ 24.5

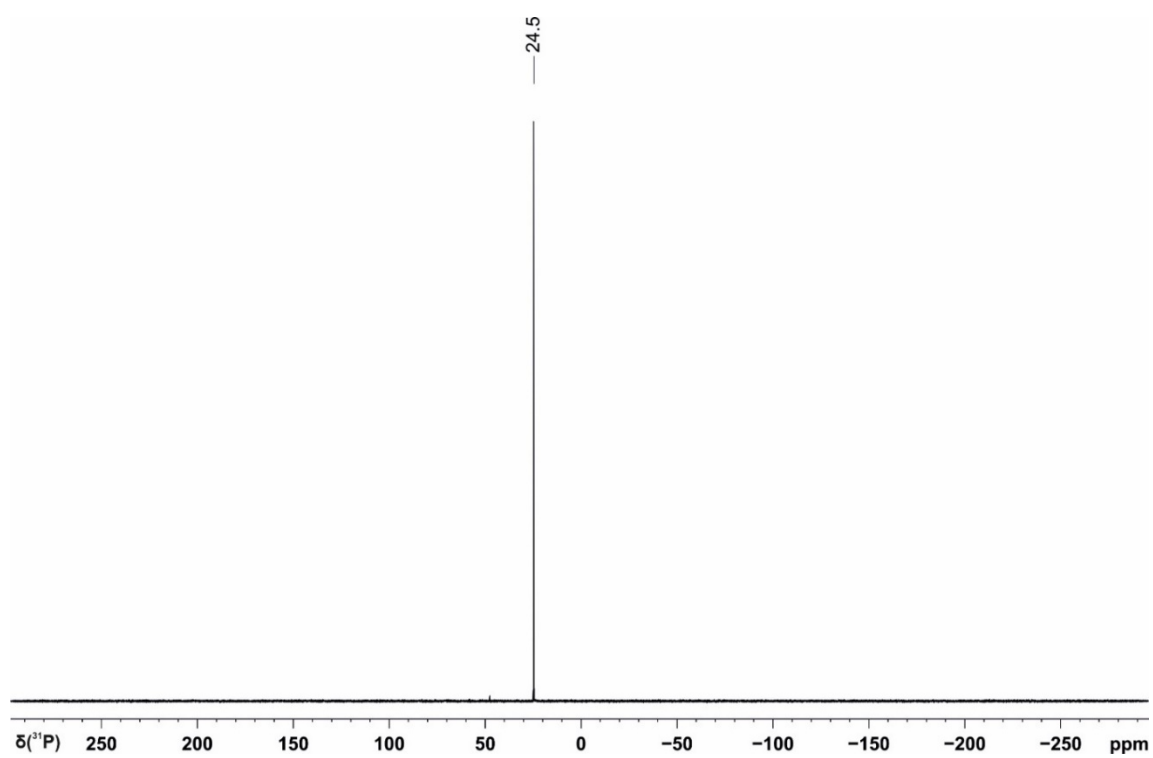
Elemental analysis: Calculated for C₂₈H₂₈IO₄P: C, 57.35; H, 4.81; Found: C, 57.49; H, 4.73, N, 0.00.



Supplementary Figure 26. ^1H NMR spectrum in CDCl_3 of tetrakis(3-methoxyphenyl)phosphonium iodide prepared photocatalytically from P_4 on a 1 mmol scale. $^*\text{CDCl}_3$.



Supplementary Figure 27. $^{13}\text{C}\{^1\text{H}\}$ NMR spectrum in CDCl_3 of tetrakis(3-methoxyphenyl)phosphonium iodide prepared photocatalytically from P_4 on a 1 mmol scale. $^*\text{CDCl}_3$.



Supplementary Figure 28. $^{31}\text{P}\{^1\text{H}\}$ NMR spectrum in CDCl_3 of tetrakis(3-methoxyphenyl)phosphonium iodide prepared photocatalytically from P_4 on a 1 mmol scale.

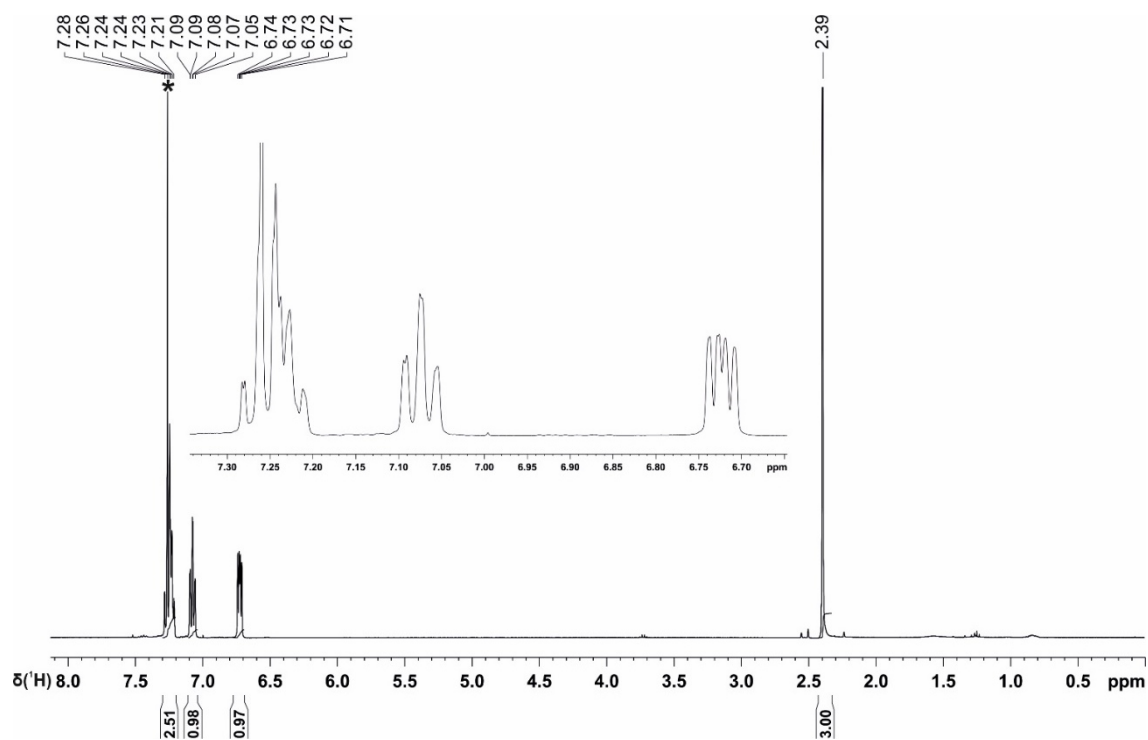
Supplementary Method 5. Photocatalytic preparation of tri(o-tolyl)phosphine from P₄ (1 mmol scale, Table 2, Entry 4)

In a 50 ml stoppered tube equipped with a stirring bar, 2-iodotoluene (1492 μ L, 11 mmol, 11 equiv. based on the phosphorus atom), Et₃N (2007 μ L, 14.4 mmol, 14.4 equiv.), catalyst [1]PF₆ (20.1 mg, 2.2 mol%), and P₄ (30.9 mg, 0.25 mmol, 1 equiv.) were added to 15 mL acetonitrile and 5 mL benzene in an N₂ filled glove box. The tube was sealed, placed in a water-cooled block to maintain near-ambient temperature (Supplementary Figure 19), and irradiated with blue light (7X Osram OSRON SSL80, 455 nm (\pm 15 nm), 20.3 V 1000mA) for 18 h. The solvent and other volatiles was evaporated *in vacuo* at 100 °C, and the residue kept under vacuum for 2 h. The resulting yellowish residue was sublimed (*ca.* 3 x 10⁻² mbar, 100 °C) twice to obtain tri(o-tolyl)phosphine as colorless solid (216 mg, 71%). The characterization data of the product are consistent with the data found in the literature.^{S3}

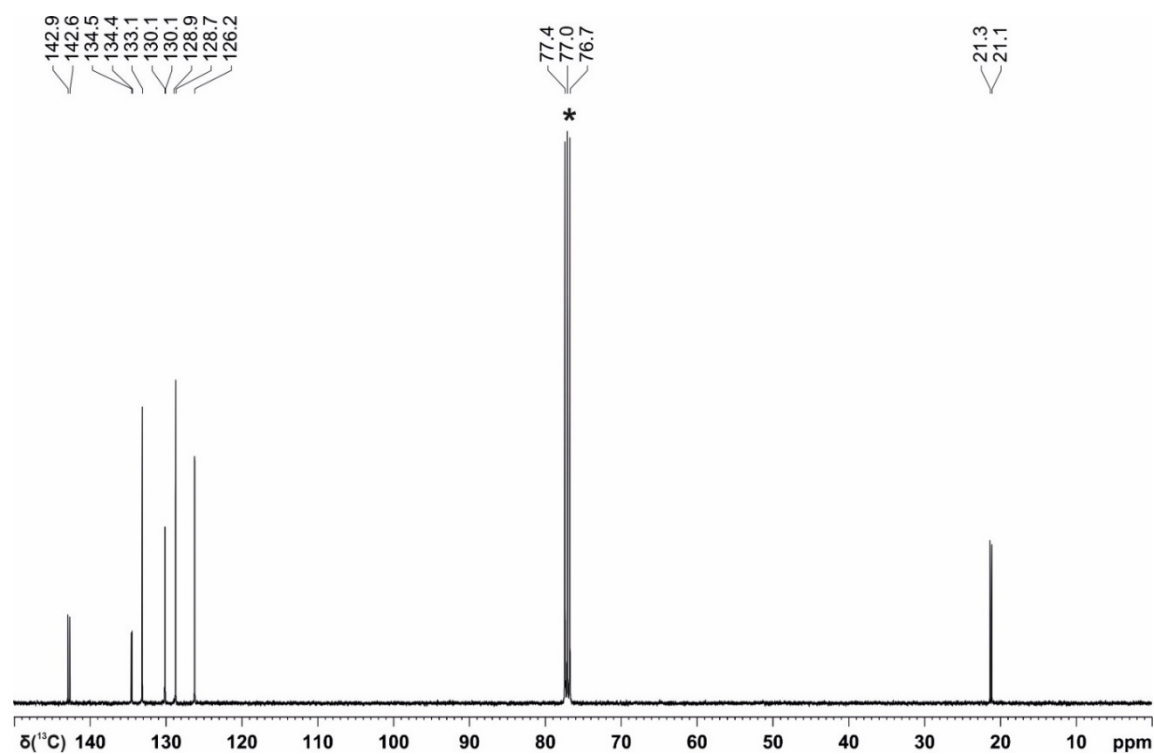
¹H NMR (400 MHz, CDCl₃): δ 7.28-7.21 (m, 6H), 7.09-7.05 (m, 3H), 6.74-6.71 (m, 3H), 2.39 (s, 9H).

¹³C{¹H} NMR (100 MHz, CDCl₃): δ 142.7 (d, *J* = 26.2 Hz), 134.5 (d, *J* = 10.7 Hz), 133.1, 130.1 (d, *J* = 4.8 Hz), 128.7, 126.2, 21.2 (d, *J* = 26.2 Hz).

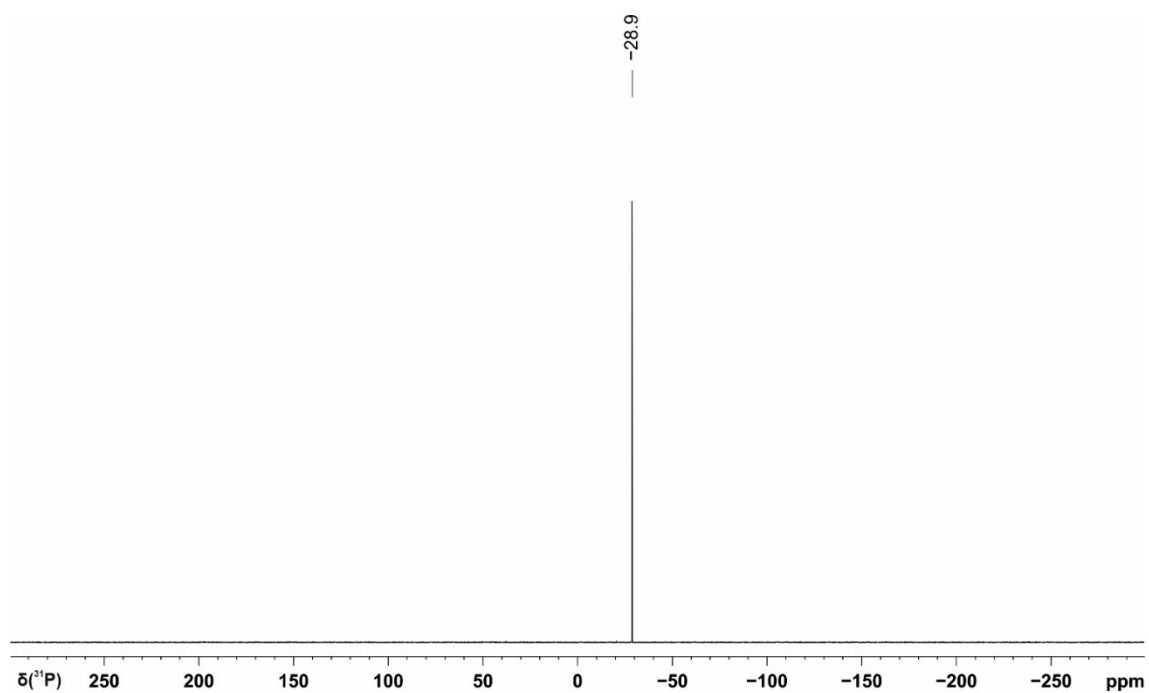
³¹P{¹H} NMR (162 MHz, CDCl₃): δ -28.9



Supplementary Figure 29. ^1H NMR spectrum in CDCl_3 of tri(*o*-tolyl)phosphine prepared photocatalytically from P_4 on a 1 mmol scale. * CDCl_3 .



Supplementary Figure 30. $^{13}\text{C}\{^1\text{H}\}$ NMR spectrum in CDCl_3 of tri(*o*-tolyl)phosphine prepared photocatalytically from P_4 on a 1 mmol scale. * CDCl_3 .



Supplementary Figure 31. $^{31}\text{P}\{^1\text{H}\}$ NMR spectrum in CDCl_3 of tri(*o*-tolyl)phosphine prepared photocatalytically from P_4 on a 1 mmol scale.

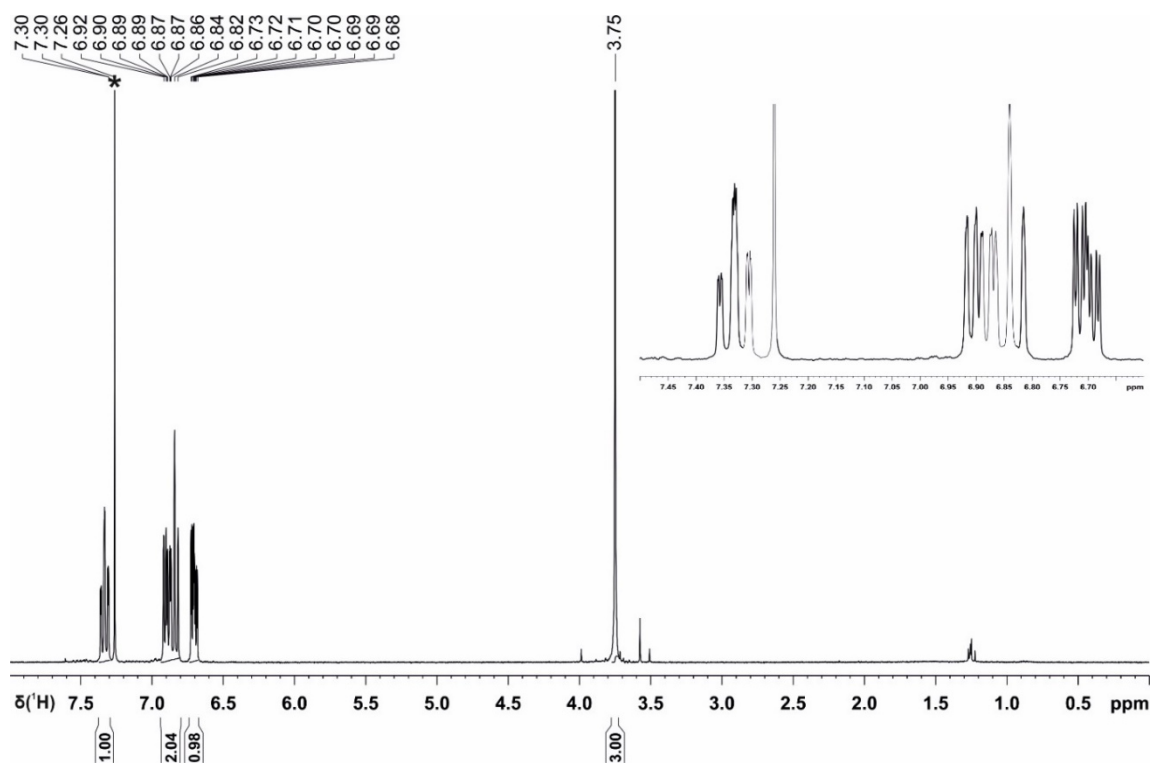
Supplementary Method 6. Photocatalytic preparation of tris(2-methoxyphenyl)phosphine from P₄ (1 mmol scale, Table 2, Entry 5)

In a 50 ml stoppered tube equipped with a stirring bar, 2-iodoanisole (1431 μL , 11 mmol, 11 equiv. based on the phosphorus atom), Et₃N (2007 μL , 14.4 mmol, 14.4 equiv.), catalyst [1]PF₆ (20.1 mg, 2.2 mol%), and P₄ (30.9 mg, 0.25 mmol, 1 equiv.) were added to 15 mL acetonitrile and 5 mL benzene in an N₂ filled glove box. The tube was sealed, placed in a water-cooled block to maintain near-ambient temperature (Supplementary Figure 19), and irradiated with blue light (7X Osram OSRON SSL80, 455 nm (± 15 nm), 20.3 V 1000 mA) for 30 h. The solvent and other volatiles was evaporated *in vacuo* at 120 °C, and the residue kept under vacuum for 2 h. The target compound crystallized from hot ethanol as pale yellow powder (129 mg, 37%). The characterization data of the product are consistent with the data found in the literature.³

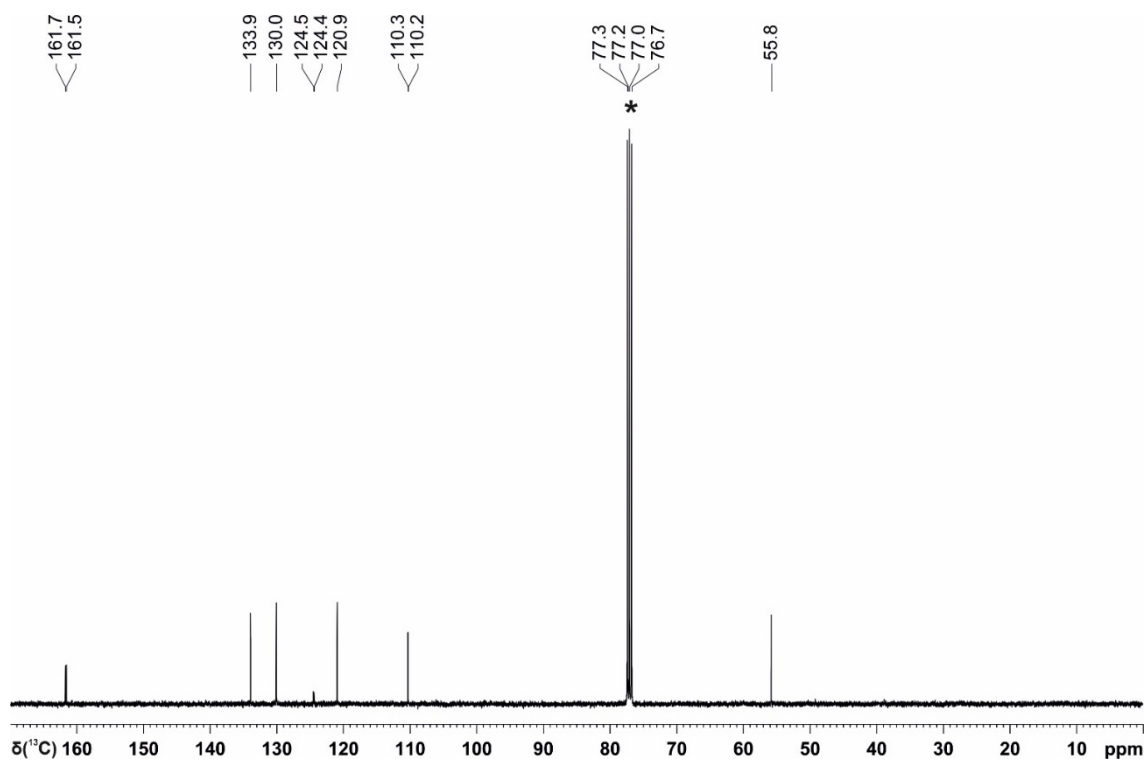
¹H NMR (400 MHz, CDCl₃): δ 7.36-7.30 (m, 3H), 6.92-6.82 (m, 6H), 6.73-6.68 (m, 3H), 3.74 (s, 9H).

¹³C{¹H} NMR (100 MHz, CDCl₃): δ 161.6 (d, J = 16.4 Hz), 133.9, 130.0, 124.4 (d, J = 11.0 Hz), 120.9, 110.2 (d, J = 1.7 Hz), 55.8

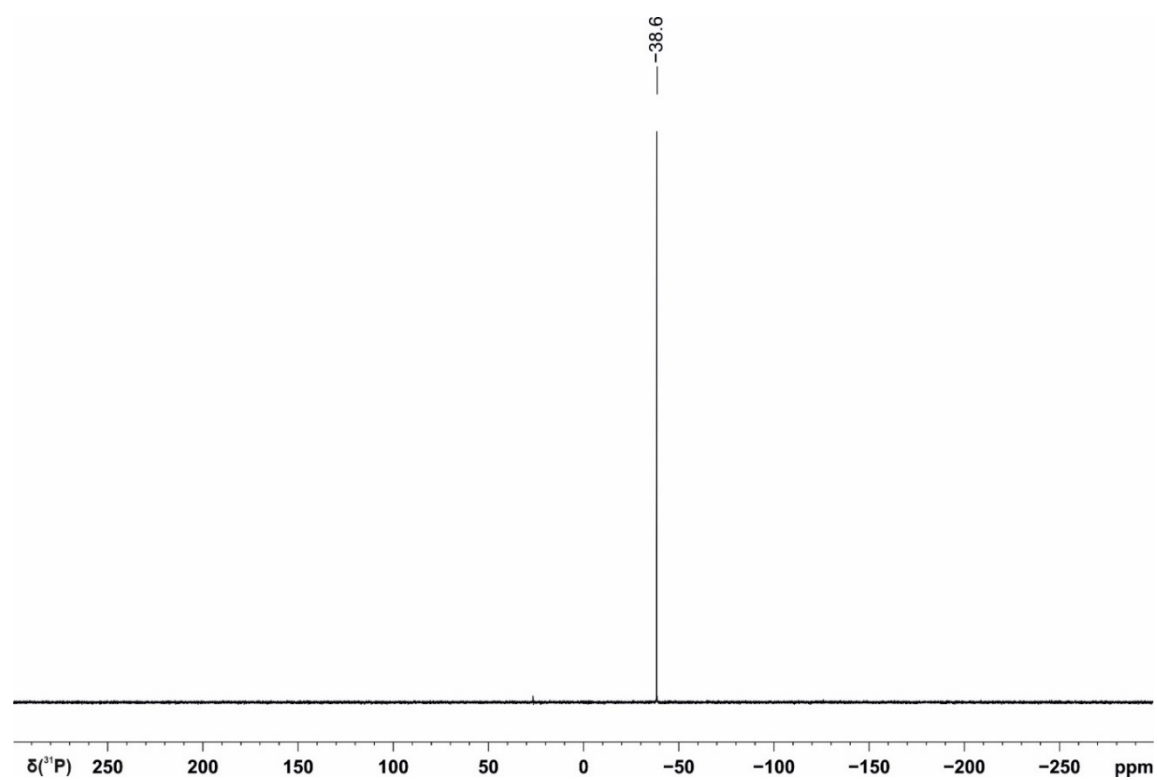
³¹P{¹H} NMR (162 MHz, CDCl₃): δ -38.6



Supplementary Figure 32. ^1H NMR spectrum in CDCl_3 of tris(2-methoxyphenyl)phosphine prepared photocatalytically from P_4 on a 1 mmol scale. $^*\text{CDCl}_3$.



Supplementary Figure 33. $^{13}\text{C}\{^1\text{H}\}$ NMR spectrum in CDCl_3 of tris(2-methoxyphenyl)phosphine prepared photocatalytically from P_4 on a 1 mmol scale. $^*\text{CDCl}_3$.



Supplementary Figure 34. $^{31}\text{P}\{^1\text{H}\}$ NMR spectrum in CDCl_3 of tris(2-methoxyphenyl)phosphine prepared photocatalytically from P_4 on a 1 mmol scale.

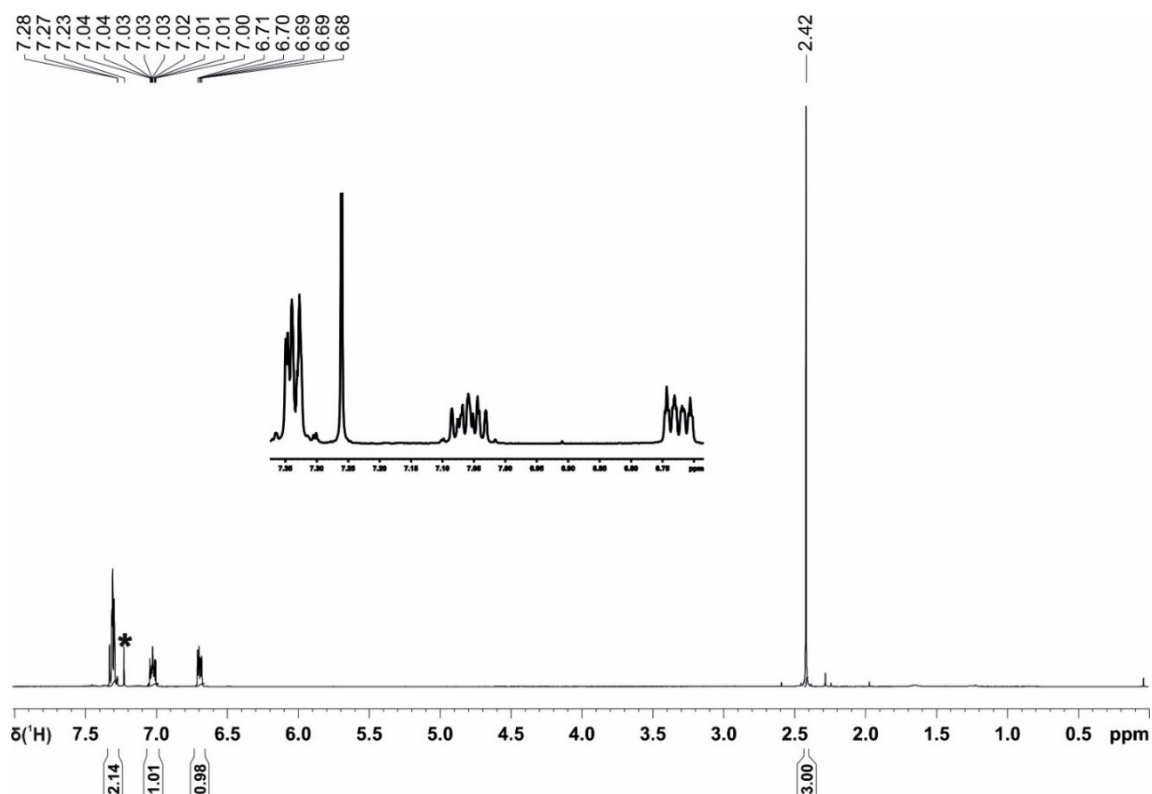
Supplementary Method 7. Photocatalytic preparation of tris(2-(methylthio)phenyl)phosphine from P₄ (1 mmol scale, Table 2, Entry 6)

In a 50 ml stoppered tube equipped with a stirring bar, 2-iodothioanisole (1600 μ L, 11 mmol, 11 equiv. based on the phosphorus atom), Et₃N (2007 μ L, 14.4 mmol, 14.4 equiv.), catalyst [1]PF₆ (20.1 mg, 2.2 mol%), and P₄ (30.9 mg, 0.25 mmol, 1 equiv.) were added to 15 mL acetonitrile and 5 mL benzene in an N₂ filled glove box. The tube was sealed, placed in a water-cooled block to maintain near-ambient temperature (Supplementary Figure 19), and irradiated with blue light (7X Osram OSOLON SSL80, 455 nm (\pm 15 nm), 20.3 V 1000 mA) for 18 h. The solvent and other volatiles was evaporated in vacuo at 120 °C, and the residue kept under vacuum for 2 h. The targeted compound was precipitated as a white powder (74 mg, 19%) from hot ethanol. The characterization data of the product are consistent with the data found in the literature.^{S4}

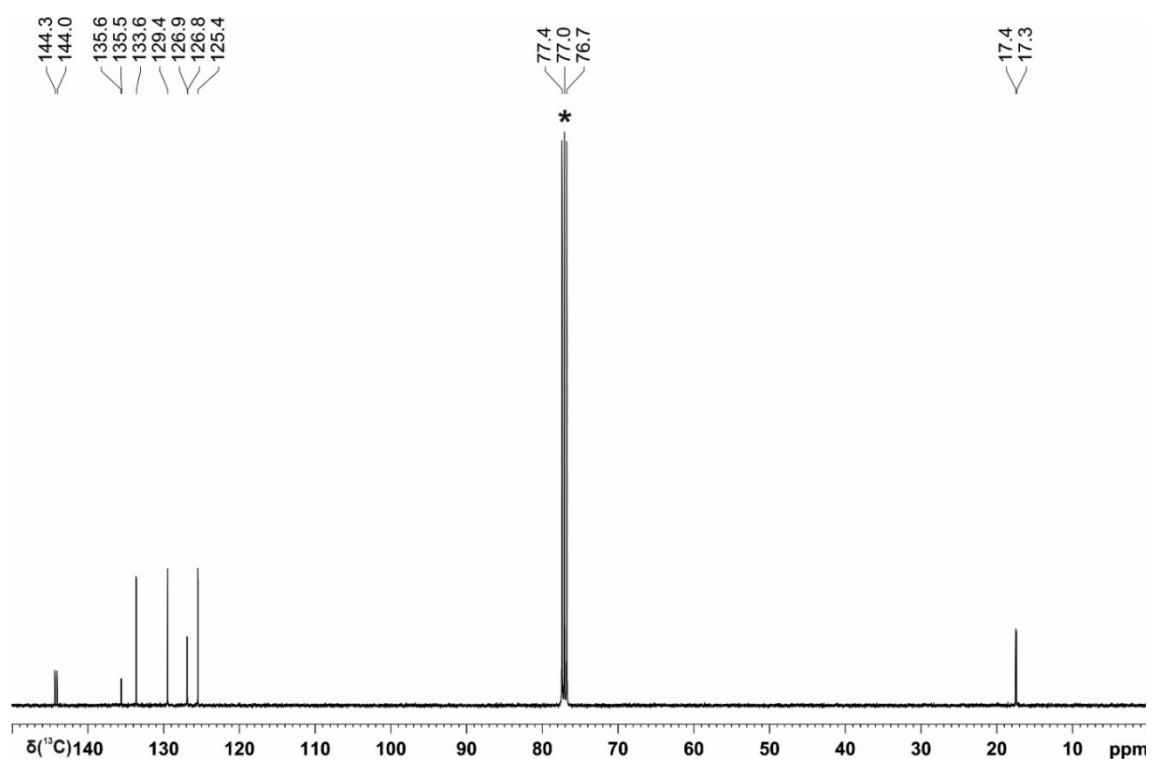
¹H NMR (400 MHz, CDCl₃): δ 7.35-7.33 (m, 6H), 7.08-7.03 (m, 3H), 6.75-6.71 (m, 3H), 2.45 (s, 9H).

¹³C{¹H} NMR (100 MHz, CDCl₃): δ 144.2 (d, J = 29.3 Hz), 135.6 (d, J = 9.6 Hz), 133.6, 129.4, 126.9 (d, J = 4.3 Hz), 125.4, 17.4 (d, J = 9.7 Hz).

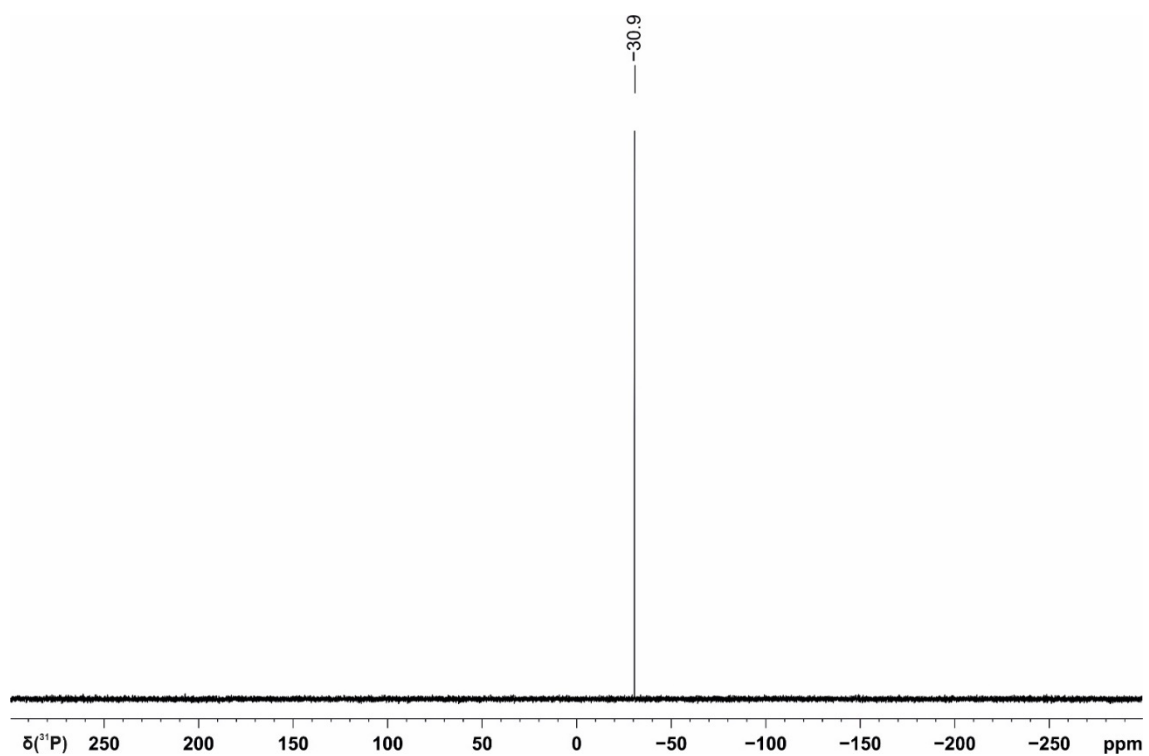
³¹P{¹H} NMR (162 MHz, CDCl₃): δ -30.9



Supplementary Figure 35. ^1H NMR spectrum in CDCl_3 of tris(2-(methylthio)phenyl)phosphine prepared photocatalytically from P_4 on a 1 mmol scale. $^*\text{CDCl}_3$.



Supplementary Figure 36. $^{13}\text{C}\{^1\text{H}\}$ NMR spectrum in CDCl_3 of tris(2-(methylthio)phenyl)phosphine prepared photocatalytically from P_4 on a 1 mmol scale. $^*\text{CDCl}_3$.



Supplementary Figure 37. $^{31}\text{P}\{^1\text{H}\}$ NMR spectrum in CDCl_3 of tris(2-(methylthio)phenyl)phosphine prepared photocatalytically from P_4 on a 1 mmol scale.

Supplementary Method 8. Photocatalytic preparation of tris(triphenylstannyl)phosphine from P₄ (1 mmol scale, Table 3, Entry 12)

In a 50 ml stoppered tube equipped with a stirring bar, Ph₃SnCl (4.24 g, 11 mmol, 11 equiv. based on the phosphorus atom), Et₃N (2007 μ L, 14.4 mmol, 14.4 equiv.), catalyst [1]PF₆ (20.1 mg, 2.2 mol%), and P₄ (30.9 mg, 0.25 mmol, 1 equiv.) were added to 15 mL acetonitrile and 5 mL benzene in an N₂ filled glove box. The tube was sealed, placed in a water-cooled block to maintain near-ambient temperature (Supplementary Figure 19), and irradiated with blue light (7X Osram OSOLON SSL80, 455 nm (\pm 15 nm), 20.3 V 1000 mA) for 18 h. The solvent was then removed *in vacuo*, and the resulting oily solid triturated with pentane over two days to give an off-white suspension. This suspension was filtered, and the resulting solid washed with further pentane. Extraction into benzene and removal of solvent *in vacuo* yielded another oily solid. The target product was isolated as a spectroscopically-pure white solid by fractional crystallization of this crude material from Et₂O: following precipitation of an initial ³¹P NMR silent fraction from a saturated solution at -35 °C, three separate crops of the product were obtained from the mother liquor at -80 °C (155 mg, 14%).

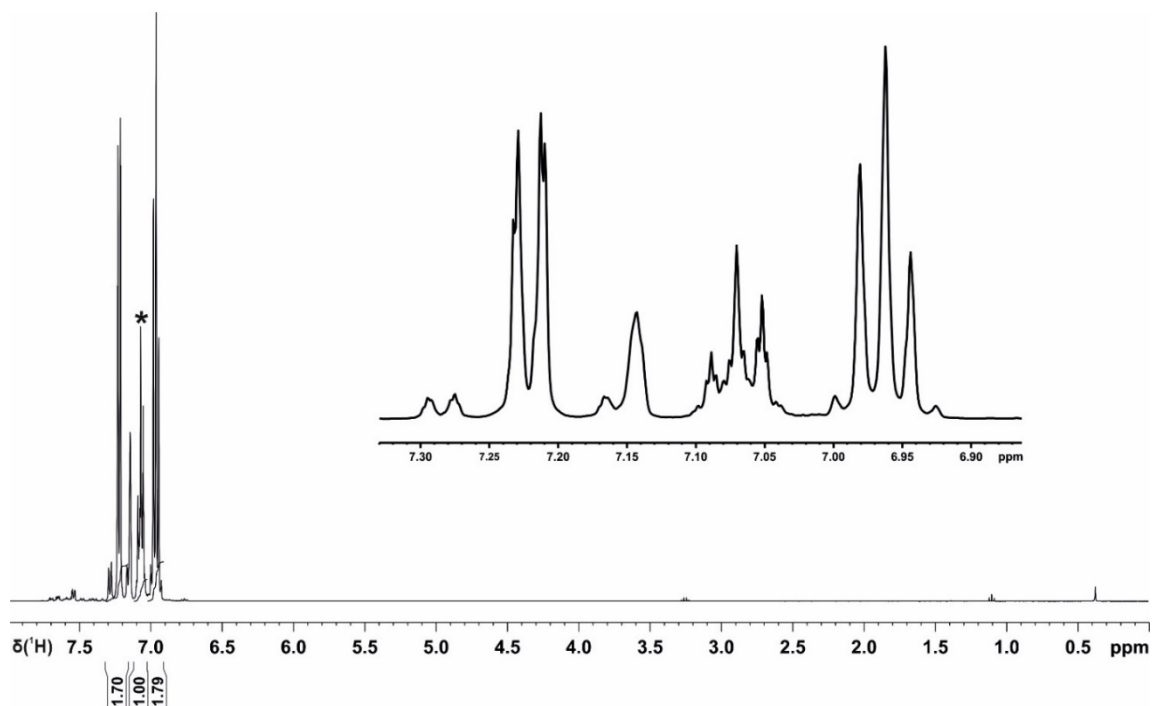
NMR spectroscopic data are consistent with previous literature reports.^{S5}

¹H NMR (400 MHz, C₆D₆): δ 7.29-7.17 (m, 18H), 7.10-7.04 (m, 9H), 7.00-6.93 (m, 18H).

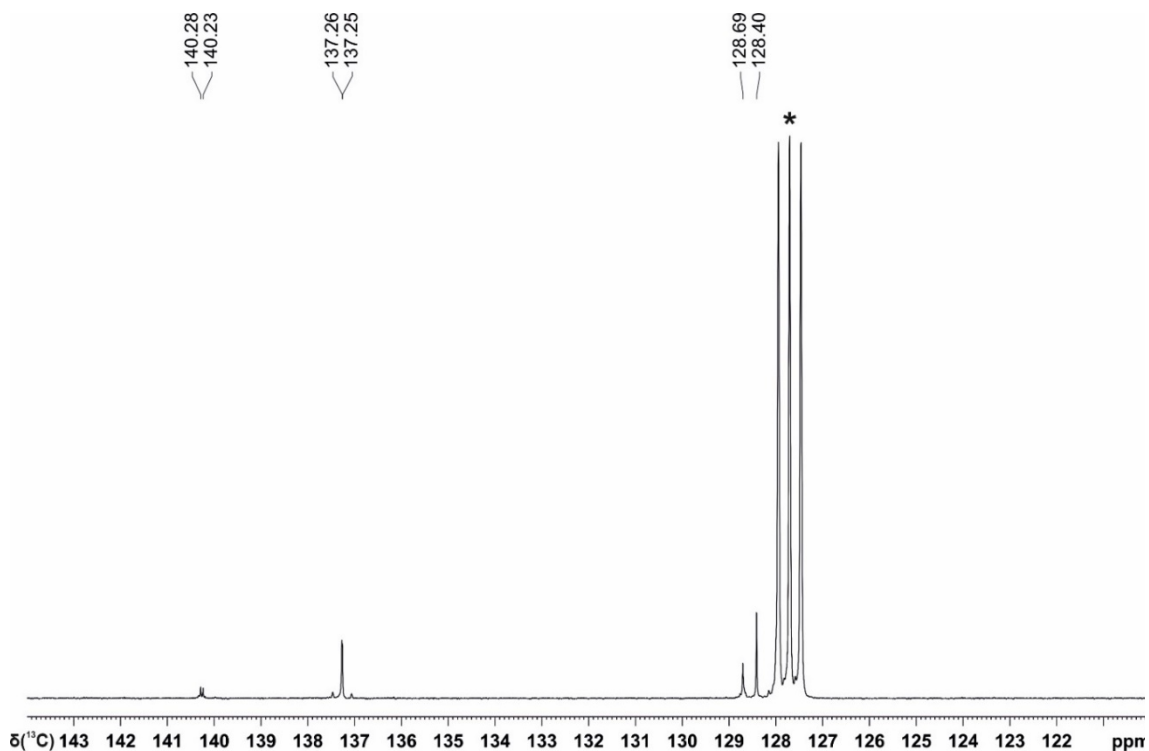
¹³C{¹H} NMR (100 MHz, C₆D₆): δ 140.3 (d, *J* = 5.4 Hz), 137.3 (d, *J* = 1.2 Hz), 128.7, 128.4.

³¹P{¹H} NMR (162 MHz, C₆D₆): δ -325.1 (d, *J*₁₁₉ = 885.5 Hz, *J*₁₁₇ = 847.4 Hz)

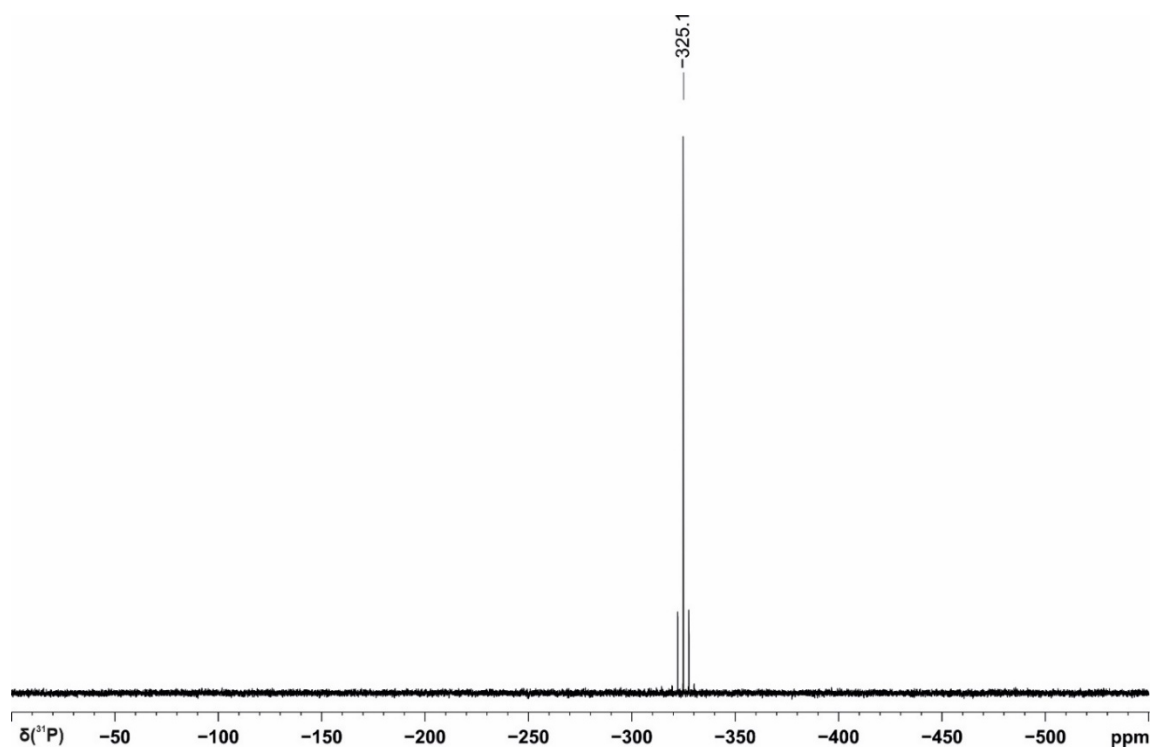
¹¹⁹Sn{¹H} NMR (149 MHz, C₆D₆): δ -67.6 (d, *J*₁₁₉ = 885.5 Hz)



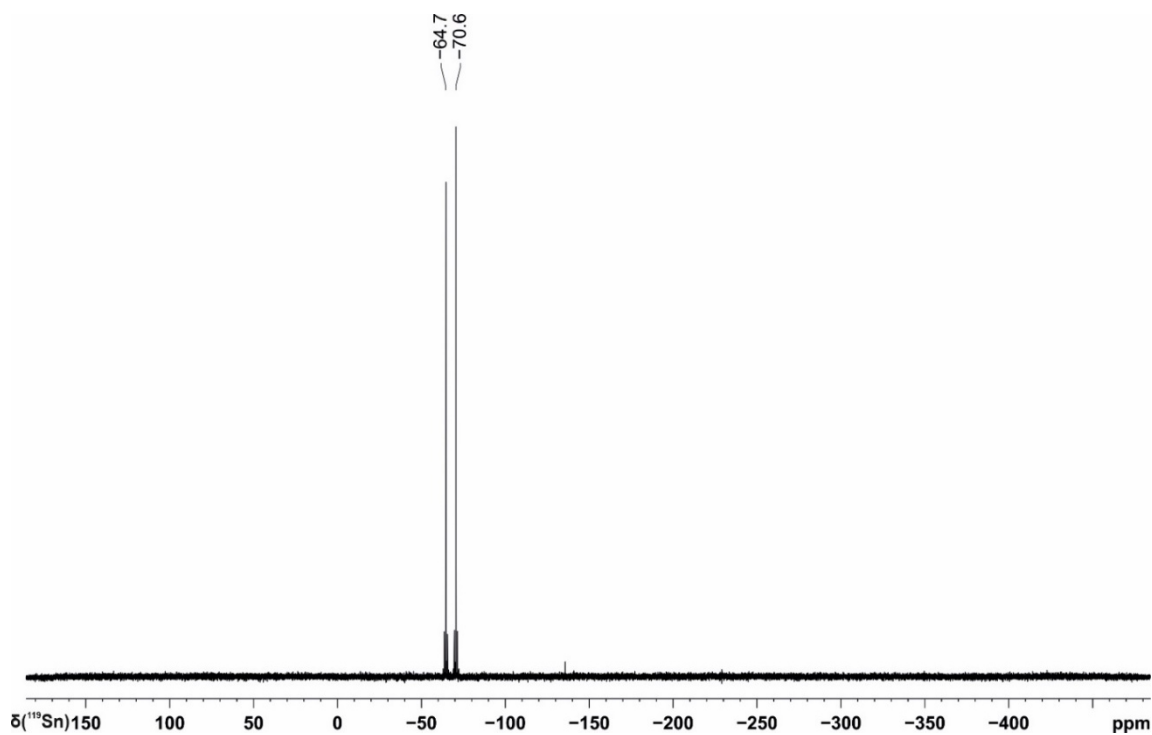
Supplementary Figure 38. ^1H NMR spectrum in C_6D_6 of tris(triphenylstannyl)phosphine prepared photocatalytically from P_4 on a 1 mmol scale. $^*\text{C}_6\text{D}_6$.



Supplementary Figure 39. $^{13}\text{C}\{^1\text{H}\}$ NMR spectrum in C_6D_6 of tris(triphenylstannyl)phosphine prepared photocatalytically from P_4 on a 1 mmol scale. $^*\text{C}_6\text{D}_6$.



Supplementary Figure 40. ^{31}P NMR spectrum in C_6D_6 of tris(triphenylstannyl)phosphine prepared photocatalytically from P_4 on a 1 mmol scale.



Supplementary Figure 41. $^{119}\text{Sn}\{^1\text{H}\}$ NMR spectrum in C_6D_6 of tris(triphenylstannyl)phosphine prepared photocatalytically from P_4 on a 1 mmol scale.

2.5.4 Supplementary Discussions

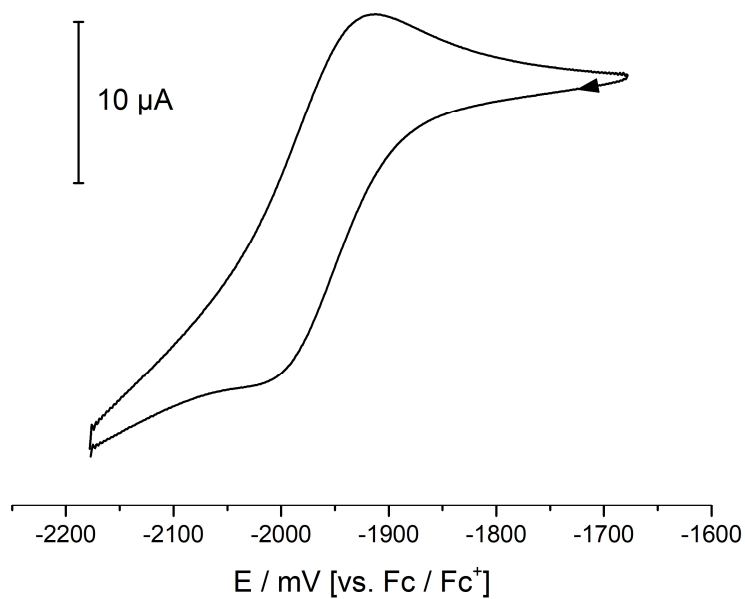
2.5.4.1 Cyclic voltammetry studies

Cyclic voltammetry experiments were performed in a single-compartment cell using a CH Instruments CHI600E potentiostat. The cell was equipped with a Pt disc working electrode (2 mm diameter) polished with 0.05 μm Al_2O_3 paste, a Pt wire counter electrode and an Ag/AgNO₃ reference electrode. The supporting electrolyte, *n*Bu₄NPF₆, was dried *in vacuo* at 110 °C for three days prior to use. All redox potentials are reported versus the ferrocene/ferrocenium (Fc/Fc⁺) couple. The scan rate is 100 mV s⁻¹ unless stated otherwise.

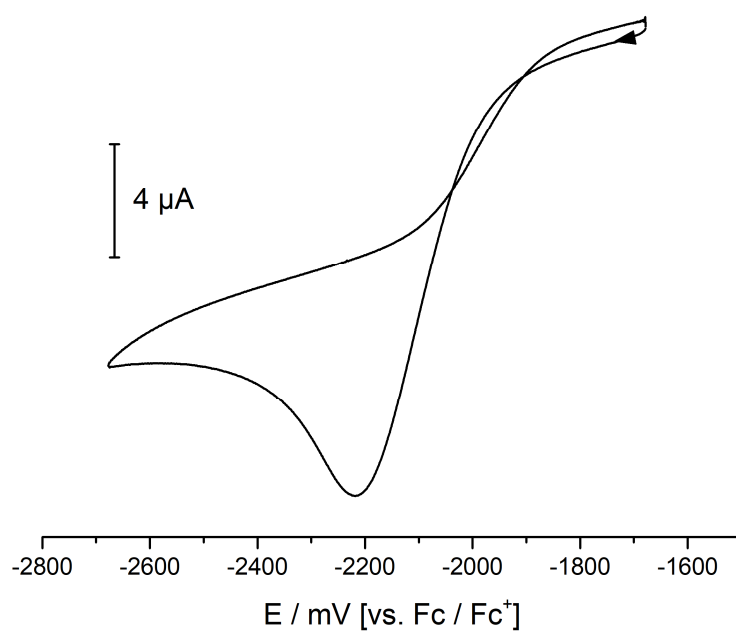
The cyclic voltammogram of Ir(dtbbpy)(ppy)₂PF₆ (**[1]**PF₆; dtbbpy = 4,4'-bis-*tert*butyl-2,2'-bipyridine, ppy = 2-(2-pyridyl)phenyl) recorded in MeCN/benzene (3:1) shows a fully reversible reduction wave at $E_{1/2} = -1.97$ V vs. Fc/Fc⁺ (Supplementary Figure 42). This value is in excellent agreement with the onset potential of the irreversible reduction wave observed for PhI under the same conditions: $E_{95} = -1.96$ V (Supplementary Figure 43; E_{95} is defined as the potential where the current is 95 % lower than at the peak of the wave, i.e. E_{95} occurs when $I = I_{\text{max}} - (0.95 \times \Delta I)$ where $\Delta I = I_{\text{max}} - I_{\text{baseline}}$). This clearly indicates the feasibility of electron transfer to PhI from the reduced catalyst **[1]**. By comparison, the redox potential for the **[1]**^{••}/**[1]**²⁺ couple has been reported to be approximately -1.4 V (in MeCN);^{S6} electron transfer to PhI from the photocatalyst excited state is therefore less likely.

The cyclic voltammogram of Et₃N has also been recorded in MeCN/benzene (3:1) and features an irreversible oxidation wave at $E_{95} = +0.24$ V vs. Fc/Fc⁺ (Supplementary Figure 44).^{S8} This is very similar to the potential reported for the **[1]**^{••}/**[1]** couple (in MeCN);^{S6} accordingly, reduction by Et₃N of the photocatalyst excited state to generate **[1]** during the catalytic cycle is expected to be feasible.

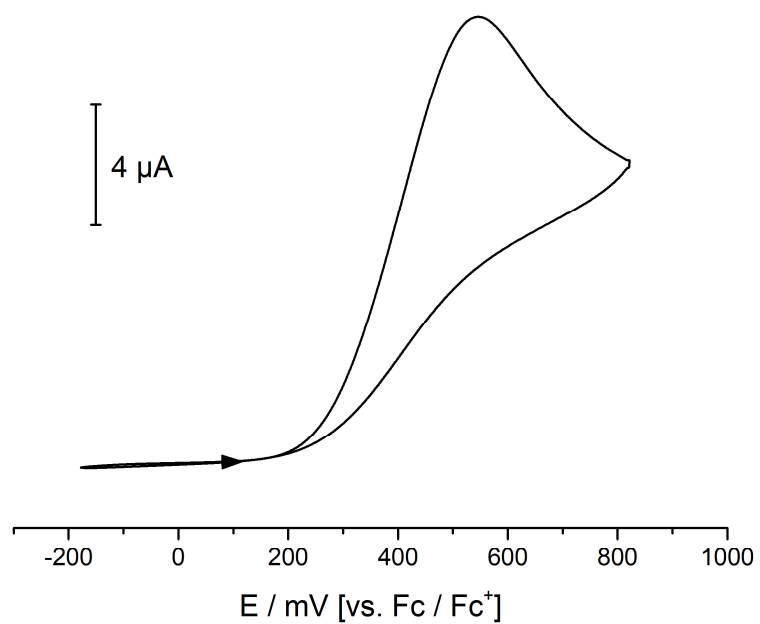
Note that attempts to observe a reduction wave for P₄ in MeCN/benzene (3:1) have been unsuccessful.



Supplementary Figure 42. Cyclic voltammogram of [1]PF₆ in MeCN/benzene (3:1) with *n*Bu₄NPF₆ supporting electrolyte (0.1 M). [1]PF₆ = Ir(dtbbpy)(ppy)₂PF₆.



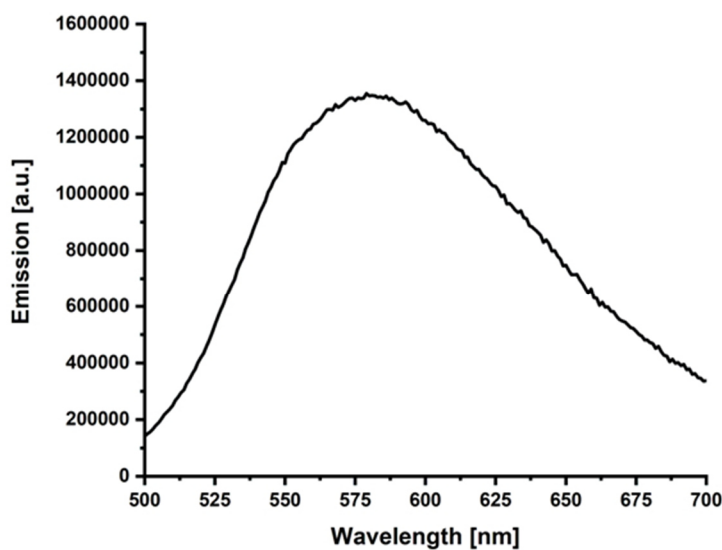
Supplementary Figure 43. Cyclic voltammogram of PhI in MeCN/benzene (3:1) with *n*Bu₄NPF₆ supporting electrolyte (0.1 M).



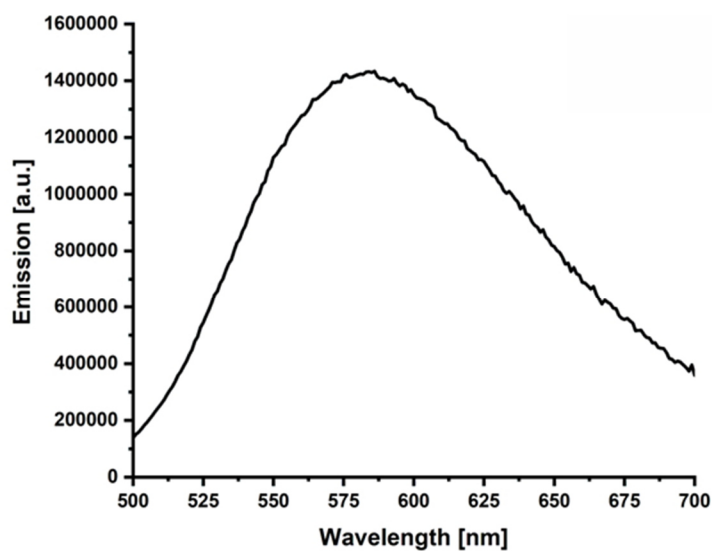
Supplementary Figure 44. Cyclic voltammogram of Et₃N in MeCN/benzene (3:1) with *n*Bu₄NPF₆ supporting electrolyte (0.1 M).

2.5.4.2 Emission quenching experiments

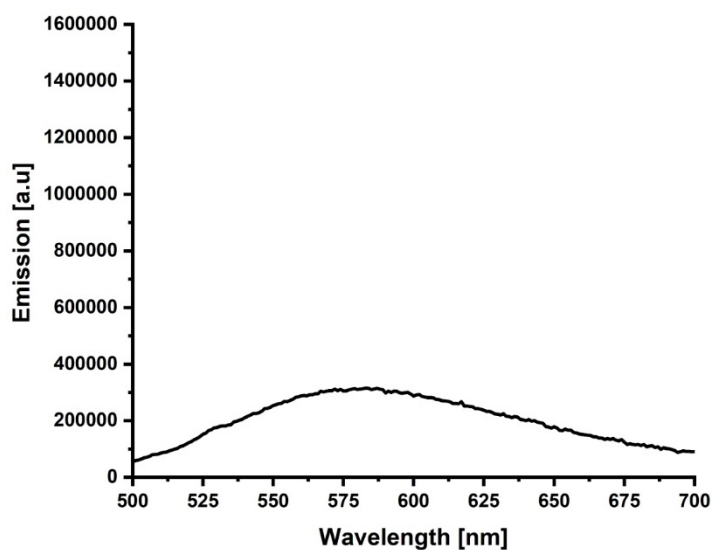
A fluorescence cuvette containing [1]PF₆ (3.9×10^{-6} M) in an MeCN/benzene mixture (3:1) was placed in a fluorescence spectrometer (Fluoromax-4 Spectrofluorometer). The solution was irradiated at 455 nm and the emission spectrum measured (Supplementary Figure 45). The maximum emission intensity was obtained at $\lambda_{\text{max}} = 584$ nm (*c.f.* 581 nm, reported in MeCN).⁶ The experiment was then repeated in the presence of potential quenchers (3180 equiv.; Supplementary Figure 46-51). Significant emission quenching was observed in the presence of Et₃N only (Supplementary Figure 47 and 52).



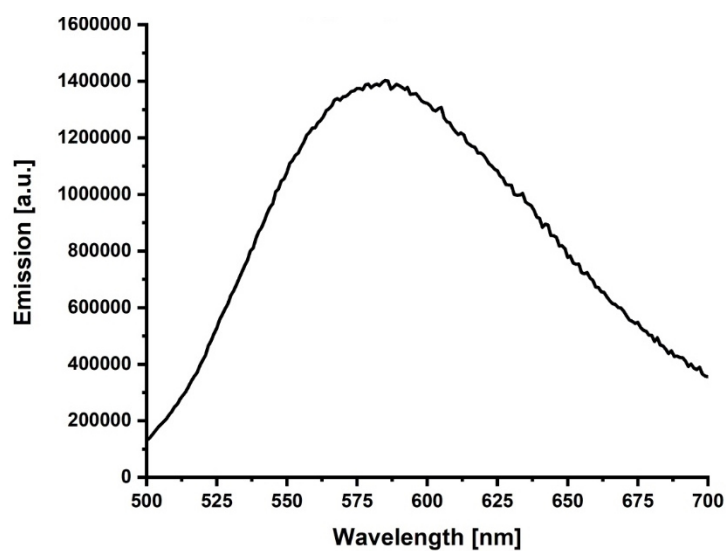
Supplementary Figure 45. Fluorescence emission spectrum for a 3.9×10^{-6} M solution of [1]PF₆ in MeCN/benzene (3:1). [1]PF₆ = Ir(dtbbpy)(ppy)₂PF₆.



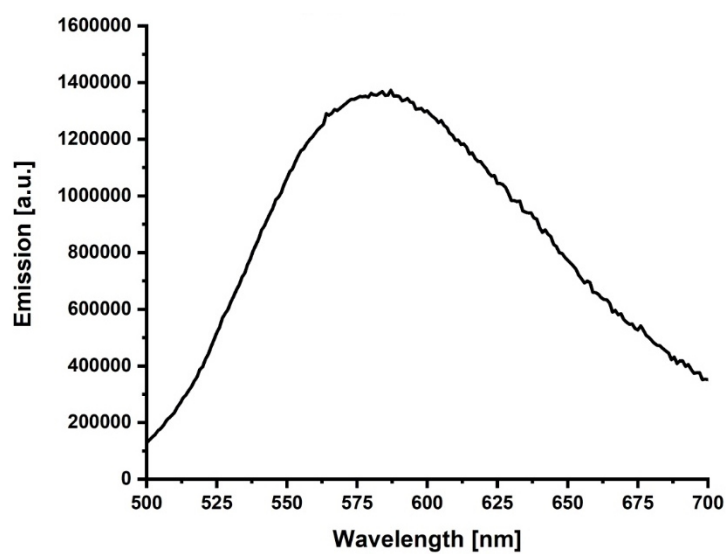
Supplementary Figure 46. Fluorescence emission spectrum for a 3.9×10^{-6} M solution of $[1]PF_6$ in MeCN/benzene (3:1) in the presence of P_4 (3180 equiv.). $[1]PF_6 = Ir(dtbbpy)(ppy)_2PF_6$.



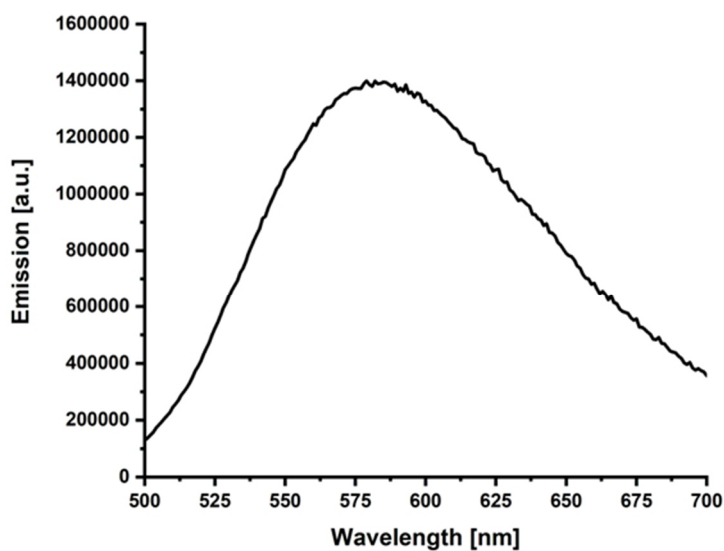
Supplementary Figure 47. Fluorescence emission spectrum for a 3.9×10^{-6} M solution of $[1]PF_6$ in MeCN/benzene (3:1) in the presence of Et_3N (3180 equiv.). $[1]PF_6 = Ir(dtbbpy)(ppy)_2PF_6$.



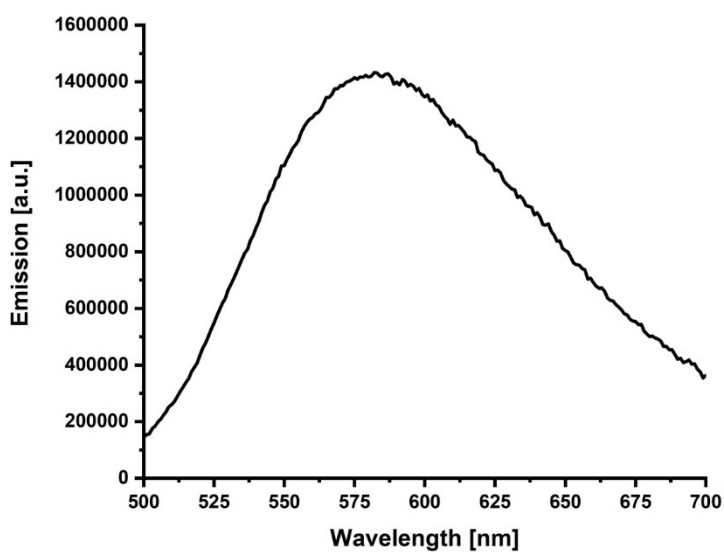
Supplementary Figure 48. Fluorescence emission spectrum for a 3.9×10^{-6} M solution of [1]PF₆ in MeCN/benzene (3:1) in the presence of PhI (3180 equiv.). [1]PF₆ = Ir(dtbbpy)(ppy)₂PF₆.



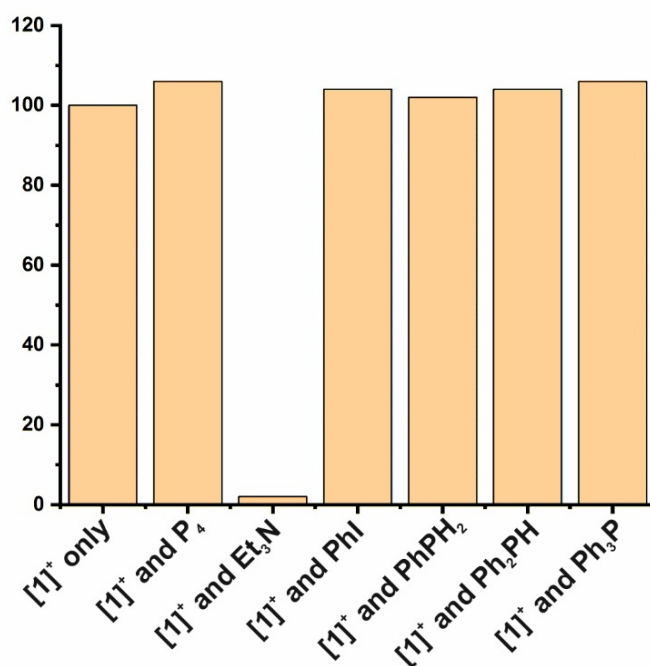
Supplementary Figure 49. Fluorescence emission spectrum for a 3.9×10^{-6} M solution of [1]PF₆ in MeCN/benzene (3:1) in the presence of PhPH₂ (3180 equiv.). [1]PF₆ = Ir(dtbbpy)(ppy)₂PF₆.



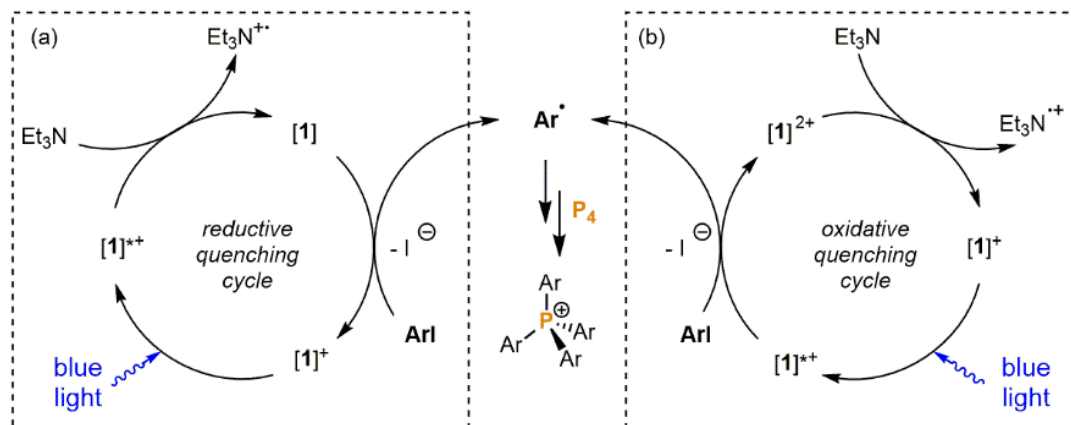
Supplementary Figure 50. Fluorescence emission spectrum for a 3.9×10^{-6} M solution of [1]PF₆ in MeCN/benzene (3:1) in the presence of Ph₂PH (3180 equiv.). [1]PF₆ = Ir(dtbbpy)(ppy)₂PF₆.



Supplementary Figure 51. Fluorescence emission spectrum for a 3.9×10^{-6} M solution of [1]PF₆ in MeCN/benzene (3:1) in the presence of Ph₃P (3180 equiv.). [1]PF₆ = Ir(dtbbpy)(ppy)₂PF₆.



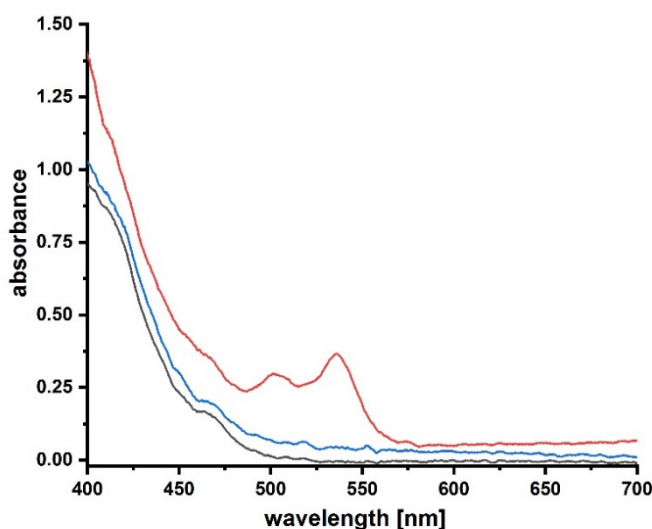
Supplementary Figure 52. Relative emission intensity of [1]PF₆ in MeCN/benzene (3:1) at 584 nm in the presence of potential quenchers (3180 equiv.). [1]PF₆ = Ir(dtbbpy)(ppy)₂PF₆.



Supplementary Figure 53. Possible catalytic cycles based on a) reductive b) oxidative quenching of the excited state [1]⁺*. Experimental evidence suggests only a) is mechanistically feasible. [1] = Ir(dtbbpy)(ppy)₂. Ar = phenyl.

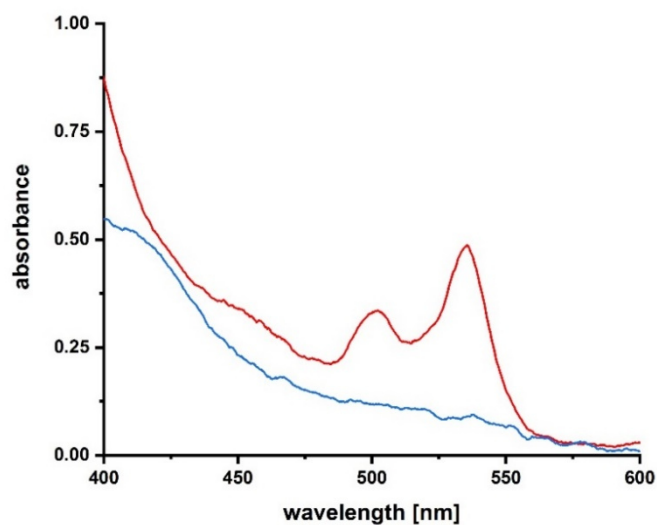
2.5.4.3 UV/VIS spectroscopic studies

A solution containing NEt_3 and $[\mathbf{1}]\text{PF}_6$ in MeCN/benzene showed a broad absorption band up to 500 nm in its UV/VIS spectrum. Two new bands ($\lambda_{\text{max}1} = 501 \text{ nm}$, $\lambda_{\text{max}2} = 537 \text{ nm}$) were formed upon irradiation with 455 nm blue light (a new orange/red coloration was also noticeable by eye), which was taken to indicate the formation of reduced $[\mathbf{1}]$ (Supplementary Figure 54). The initial spectrum was quickly recovered upon addition of excess PhI (neat) or excess P_4 (benzene solution). The $[\mathbf{1}]\text{PF}_6$ spectrum was also recovered without PhI after 20 minutes in the absence of blue LED irradiation, which is consistent with re-oxidation by (presumably) the previously-generated $[\text{Et}_3\text{N}]^+$ cation (or decomposition products thereof).



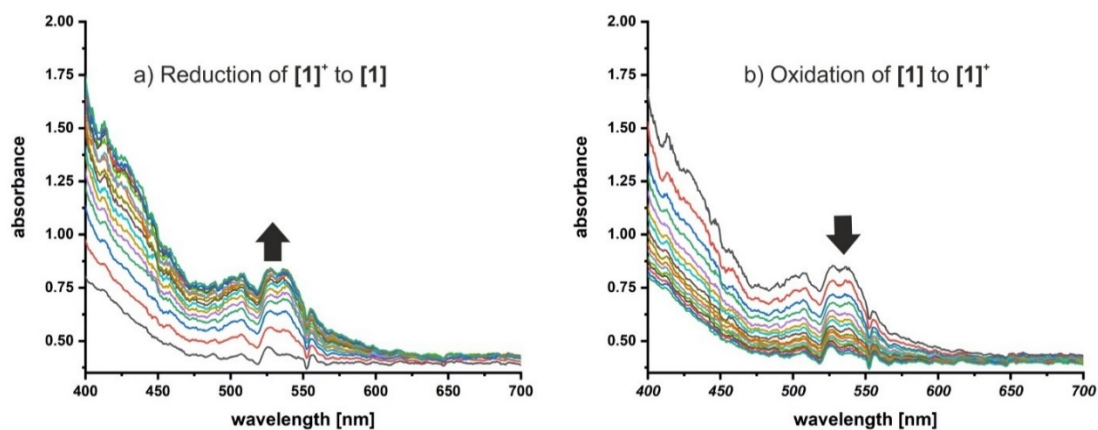
Supplementary Figure 54. UV/VIS spectra of $[\mathbf{1}]\text{PF}_6$ and Et_3N (excess) in 3:1 MeCN/benzene: initially (black), following irradiation with 455 nm light (red), following subsequent addition of excess PhI (blue). $[\mathbf{1}]\text{PF}_6 = \text{Ir}(\text{dtbbpy})(\text{ppy})_2\text{PF}_6$.

To further confirm the formation of reduced $[\mathbf{1}]$, $[\mathbf{1}]\text{PF}_6$ was treated with a single equivalent of KC_8 in THF (0.01 mmol scale in 0.5 mL THF). UV/VIS spectra of the resulting deep red solution (following separation of solids and dilution with further THF) showed features essentially identical to those previously assigned to $[\mathbf{1}]$ in MeCN/benzene (Supplementary Figure 55). Again, these disappeared immediately upon addition of PhI, or much more slowly upon addition of P_4 .



Supplementary Figure 55. UV/VIS spectrum of [1] in THF, prepared in situ through treatment of [1]PF₆ with KC₈ (red). After addition of excess PhI (blue). [1]PF₆ = Ir(dtbbpy)(ppy)₂PF₆.

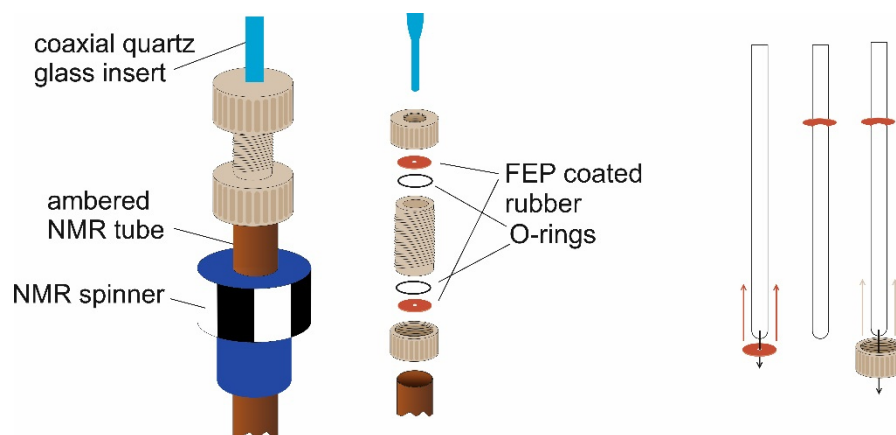
Finally, changes to the UV/VIS spectrum of [1]PF₆ (1.3 mM in 3:1 MeCN/benzene) were monitored by UV/VIS spectroelectrochemistry using an OTTLE cell. The stirred solution was exposed to a potential of -2.1 V (versus Fc/Fc⁺) for 80 s, during which time the two previously observed absorptions attributed to [1] were observed to steadily grow in (Supplementary Figure 56a). Subsequently a potential of -0.1 V was applied for 80 s, during which time the initial bands for [1]⁺ was reestablished (Supplementary Figure 56b).



Supplementary Figure 56. UV/VIS spectra showing electrochemical reduction of [1]⁺ to [1] (a), and subsequent reoxidation to [1]⁺ (b). [1] = Ir(dtbbpy)(ppy)₂.

2.5.4.4 *In situ* NMR experiments

The apparatus used for *in situ* NMR reaction monitoring with *in situ* illumination has been reported previously.⁸ The insert and the NMR tube were connected with the screw cap of a recently published UVNMR-illumination device to enable measurements under inert conditions.⁵⁹ Two FEP (fluorinated ethylene propylene) coated rubber septa increased the attachment between the insert and the tube. (Supplementary Figure 57).



Supplementary Figure 57. Schematic representation showing connection between the ambered NMR tube and illuminating insert used for *in situ* NMR reaction monitoring.

Measurements were conducted on a Bruker Avance III HD 500 MHz with a QXI probe (^1H , ^{13}C , ^{15}N , ^{31}P) or on a Bruker Avance III HD 600 MHz spectrometer with a fluorine selective TBIF probe. A high-power Cree XT-E 455 nm LED was employed for sample illumination. All spectra were recorded at 298 K. Spectrum acquisition and processing were managed with Bruker TopSpin 3.2 and TopSpin 4.0.3.

The reaction mixtures were prepared under inert atmosphere (N_2) in an ambered NMR-tube. The *in-situ* illumination device was inserted into the tube and fastened with the screw cap. The first NMR-spectra ($t = 0$) were recorded without illumination. The light source was then activated and NMR-measurements for reaction monitoring were simultaneously started. For runs where both nuclei were measured, ^1H and ^{31}P spectra were recorded alternately.

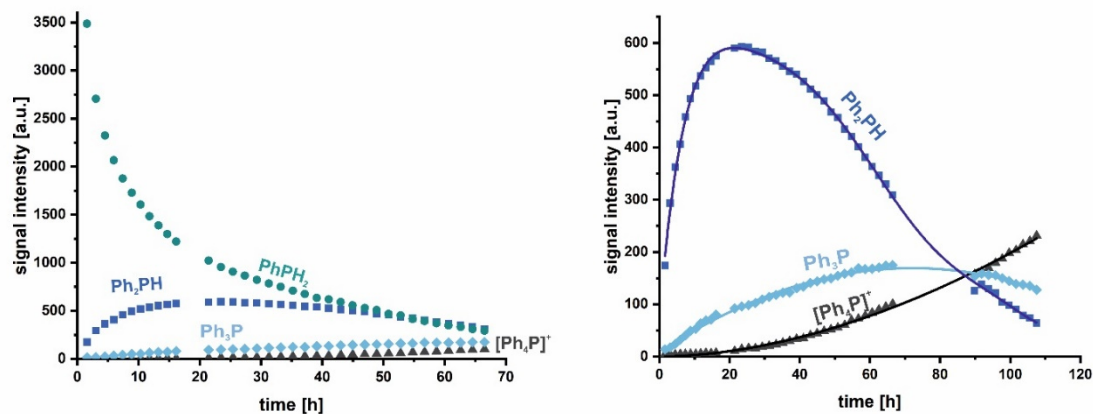
Supplementary Method 9. Procedure for ^{31}P and ^1H monitoring of the model reaction

The reaction mixture was prepared in accordance with the general procedure for photocatalytic functionalisation of P_4 in a 0.1 mmol scale (Supplementary Method 1) using iodobenzene as the substrate, with the exception that a 1:1 mixture of CD_3CN and C_6D_6 was used as solvent (the modified solvent ratio was used to ensure that complete homogeneity was maintained throughout the experiment). A 500 μL aliquot of this reaction mixture was then taken for NMR reaction monitoring.

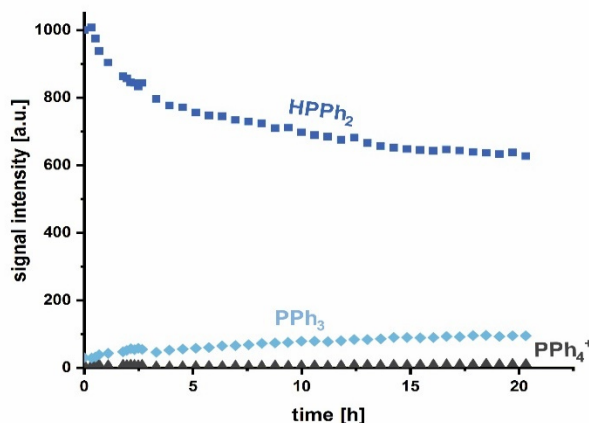
Measurements were conducted on a Bruker Avance III HD 500 MHz with a QXI probe (^1H , ^{13}C , ^{15}N , ^{31}P). For the ^1H NMR spectra the standard pulse program “zg30” was applied. For ^{31}P NMR reaction monitoring a modified “zgpg”-experiment was used, applying a broadband pulse (xyBEBOP) developed and provided by the group of Burkhard Luy. This enabled the recording of a sweep width (SW) of 1000 kHz within a single experiment and allowed for a simultaneous screening of reaction intermediates appearing within the SW of 1000 kHz. A sufficiently high time domain (TD) was adjusted to avoid wiggles in the foothills of the signals. The spectrum in the absence of light and the first two spectra of the reaction monitoring with light were recorded with an NS (number of scans) of 512. For the subsequent spectra, the NS was increased to 1024 to increase the S/N (signal to noise ratio) for small signals. The T_1 relaxation times of the ^{31}P signals were not determined. Hence, only qualitative statements about the sequence of the reaction intermediates and products can be made. After acquisition, a uniformly positive phasing of all signals was not possible. To investigate the presence of real negative signals or artefacts, standard “zgpg30” experiments were recorded of the regions of interest. The spectra resulting from the broadband excitation (xyBEBOP) were processed with magnitude calculation.

^{31}P and ^1H monitoring of photocatalytic PhPH_2 and Ph_2PH arylation reactions

The procedure used for monitoring of the model reaction (Supplementary Method 8) was followed, using the appropriate phosphine (PhPH_2 , Ph_2PH ; 0.01 mmol) instead of P_4 .



Supplementary Figure 58. *In situ* NMR reaction monitoring of the photocatalytic arylation of PhPH_2 . Left: Consumption of PhPH_2 and formation of Ph_2PH , Ph_3P , and $[\text{Ph}_4\text{P}]^+$. Right: Magnified view showing formation of Ph_2PH , Ph_3P , and $[\text{Ph}_4\text{P}]^+$. Polynomial curve fitting was used to illustrate qualitative trends.



Supplementary Figure 59. *In situ* qualitative NMR monitoring of the photocatalytic arylation of Ph_2PH .

³¹P and ¹H monitoring of solutions of P₄ and PhI

Solutions were prepared in a 1:1 mixture of CD₃CN and C₆D₆ (2.0 mL total), containing [1]PF₆ (2.0 mg, 2.2 μmol), Et₃N (200 μL, 1.44 mmol) and *either* P₄ (3.1 mg, 0.025 mmol) *or* iodobenzene (11.2 μL, 0.1 mmol) *or* both. For each solution, a 500 μL sample was taken for NMR monitoring.

Measurements were conducted on a Bruker Avance III HD 600 MHz spectrometer with a fluorine selective TBIF probe. For both ¹H NMR and ³¹P NMR spectra the standard pulse program “zg30” was applied. Acquisition parameters (except receiver gain) were held constant throughout the three experiments. Important acquisition parameters are as follows:

¹H: TD = 65536, DS = 0, NS = 16, D1 = 2 sec

³¹P: TD = 32768, DS = 4, NS = 32, D1 = 2 sec

A spectrum in absence of light was recorded resembling the starting point t = 0. The light was then activated and the reaction monitored by alternately measuring ¹H and ³¹P spectra. After the spectra were processed, the signals of the spectra t > 0 were referenced to their according signal in the spectrum t = 0.

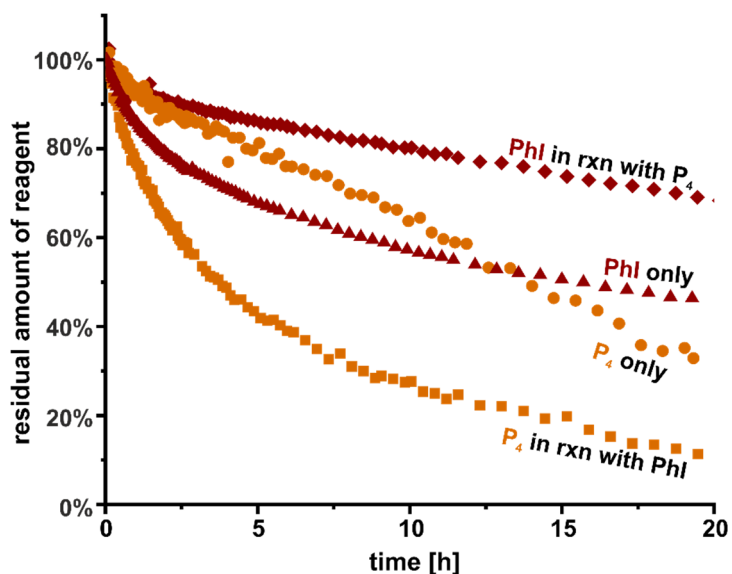
The results of these experiments are summarised in Supplementary Figure 60 and are broadly consistent with the mechanism proposed in Supplementary Figure 61. In particular, they provide yet further support for the proposal that the reduced state of the photocatalyst [1] (generated through Et₃N reduction of the photoexcited state [1]**) can be reoxidised through reaction with PhI (Supplementary Figure 61a). Nevertheless, it must be noted that these results also suggest the feasibility of direct P₄ reduction as a mechanism for regeneration of the ground state catalyst [1]⁺ (Supplementary Figure 61b). At this stage the possibility that this reaction may be mechanistically relevant cannot be conclusively ruled out. However, we note that:

1) Qualitatively, PhI appears to react more rapidly than P₄, and would be expected to react faster still during the catalytic reaction (where its concentration is an order of magnitude higher).

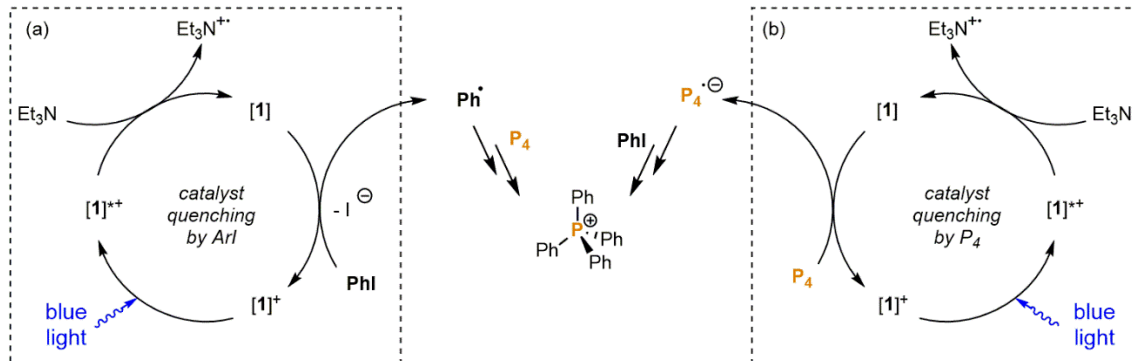
2) P₄ is consumed much more rapidly in the presence of PhI than in the absence, which is consistent with functionalisation of P₄ by Ph· radicals generated upon PhI reduction. In contrast, PhI consumption is *slower* in the presence of P₄, which suggests that the species generated upon P₄ reduction cannot react productively with PhI.

As such, we suggest that [1] oxidation by PhI remains a more likely mechanistically productive step than the analogous oxidation by P₄ (i.e. the cycle shown in

Supplementary Figure 61a is proposed to be mechanistically relevant, while that shown in Supplementary Figure 61b may be catalytically unproductive).



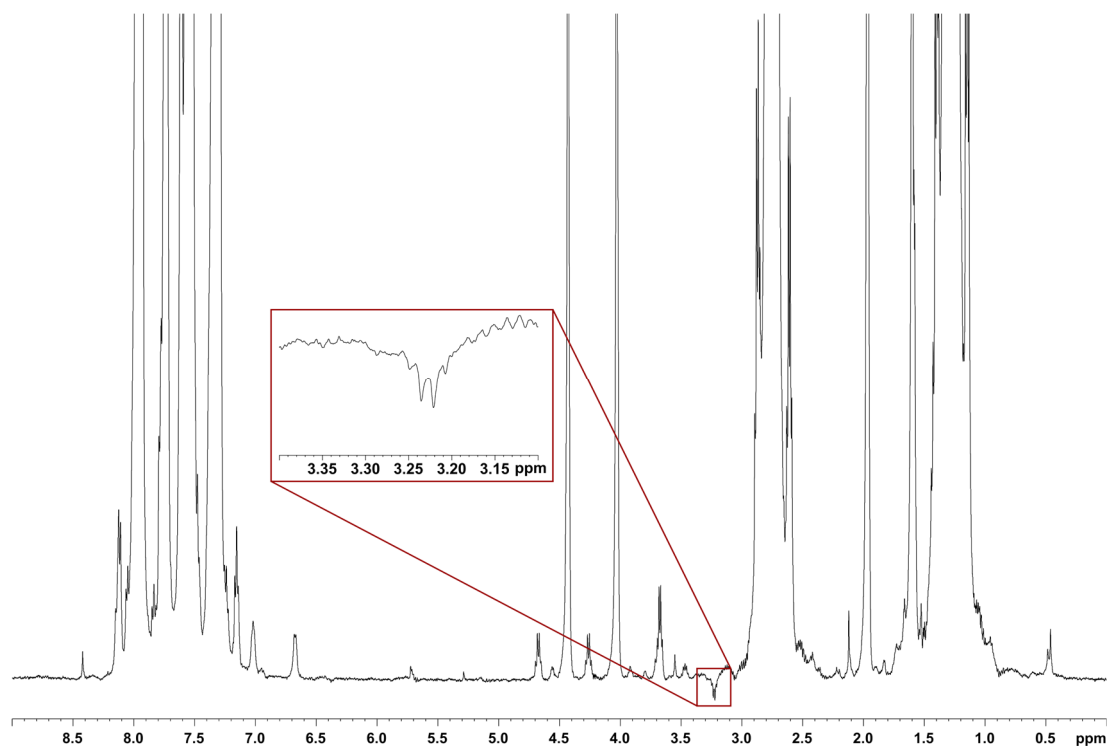
Supplementary Figure 60. Evolution of PhI and P_4 concentrations during in situ 455 nm irradiation in the presence of $[1]PF_6$ and Et_3N . Red traces indicate PhI concentration as measured for solutions of PhI alone (triangles) or as a 1:1 mixture with P_4 (diamonds). Orange traces indicate P_4 concentration as measured for solutions of P_4 alone (circles) and in the presence of PhI (squares). $[1]PF_6 = Ir(dtbbpy)(ppy)_2PF_6$.



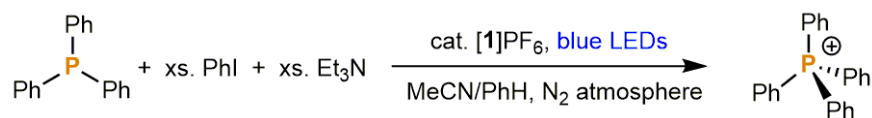
Supplementary Figure 61. Possible photoredox cycles involving $[1]^+$ regeneration through oxidation of PhI (a) or P_4 (b). $[1] = Ir(dtbbpy)(ppy)_2$.

Photo-CIDNP effect

During the *in situ* photocatalytic arylation of PhPH₂ a negative signal at 3.23 ppm was observed in the first ¹H NMR spectrum taken after starting to illuminate the mixture with 455 nm light (Supplementary Figure 62). This indicates the presence of a photo-CIDNP effect, which arises from the conversion of photogenerated radical species into diamagnetic reaction products.^{S10,S11} Considering the proposed mechanism (Supplementary Figure 61), in this case this effect may arise from the reaction of the excited photocatalyst [1]⁺⁺ with Et₃N, generating the reduced catalyst [1] and the radical cation of Et₃N^{•+}. Due to its chemical shift and multiplicity the negative signal probably belongs to the aliphatic CH₂-protons of the vinyl-substituted amine Et₂NCHCH₂ (which formally results from loss of H[•] from Et₃N^{•+}, followed by deprotonation) which was extensively investigated in an earlier CIDNP study as a product of a radical pair involving NEt₃^{•+}.^{S12}

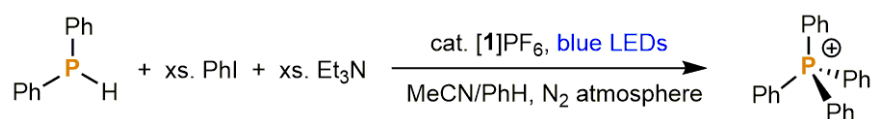


Supplementary Figure 62. Negative ¹H signal observed during *in situ* photocatalytic PhPH₂ arylation due to the photo-CIDNP effect.

2.5.4.5 Photocatalytic phenylation of Ph₃P, Ph₂PH and PhPH₂**Supplementary Table 4.** Photocatalytic functionalisation of Ph₃P to [Ph₄P]⁺

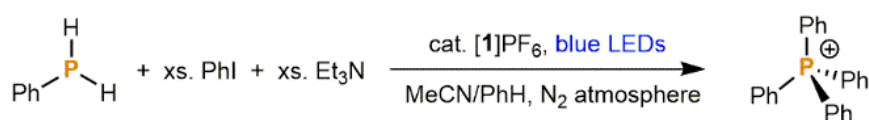
Entry	Conditions ^[a]	Conv. to [Ph ₄ P] ⁺ / %	Consumption of Ph ₃ P / %
1	standard	>99	100
2	no PhI	0	<3
3	no [1]PF ₆	7	15
4	no light	<5	>95
5	no Ph ₃ P	0	-
6	no Et ₃ N	4	4

[a] The general procedure for reactions at 0.1 mmol scale (Supplementary Method 1) was modified by replacing P₄ with Ph₃P (26.3 mg, 0.1 mmol). [1]PF₆ = Ir(dtbbpy)(ppy)₂PF₆.

Supplementary Table 5. Photocatalytic functionalisation of Ph₂PH to [Ph₄P]⁺.

Entry	Conditions ^[a]	Conv. to [Ph ₄ P] ⁺ / %	Consumption of Ph ₂ PH / %
1	standard	67	100
2	no PhI	0	<3
3	no [1]PF ₆	0	33
4	no light	0	0
5	no Ph ₂ PH	0	-
6	no Et ₃ N	... ^[b]	... ^[b]

[a] The general procedure for reactions at 0.1 mmol scale (Supplementary Method 1) was modified by replacing P₄ with Ph₂PH (17.5 μL mg, 0.1 mmol). [1]PF₆ = Ir(dtbbpy)(ppy)₂PF₆. [b] The standard procedure reproducibly gives a broad resonance for Ph₃PO which precludes accurate integration. Nevertheless, no conversion to [Ph₄P]⁺ was observed.

Supplementary Table 6. Photocatalytic functionalisation of PhPH₂ to [Ph₄P]⁺

Entry	Conditions ^[a]	Conv. to [Ph ₄ P] ⁺ / %	Consumption of PhPH ₂ / %
1	standard	85	100
2	no PhI	0	31
3	no [1]PF ₆	0	44
4	no light	0	19
5	no PhPH ₂	0	-
6	no Et ₃ N	0	73

[a] The general procedure for reactions at 0.1 mmol scale (Supplementary Method 1) was modified by replacing P₄ with PhPH₂ (11.0 μL mg, 0.1 mmol). [1]PF₆ = Ir(dtbbpy)(ppy)₂PF₆.

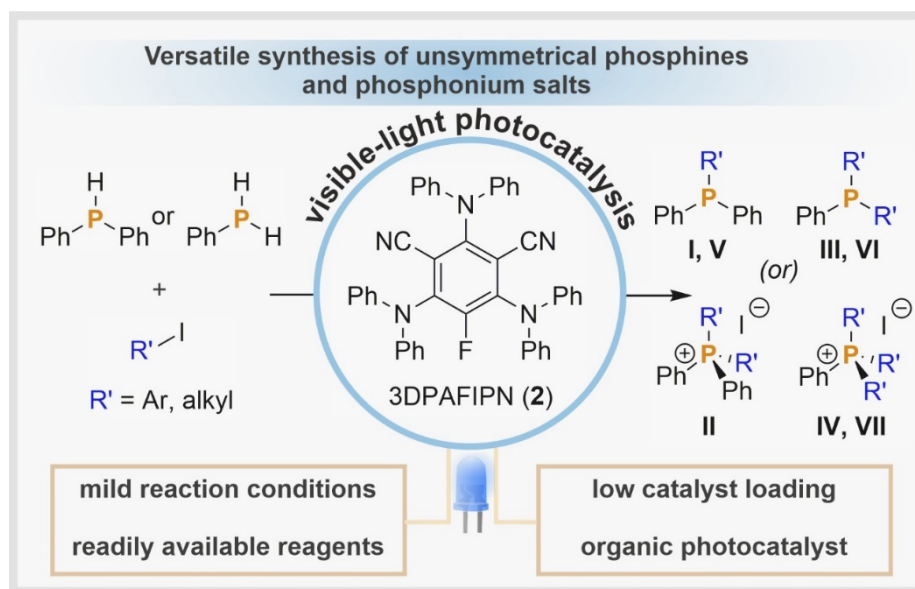
2.5.5 Supplementary References

- S1. Weitz, I. S. & Rabinovitz, M. The application of C₈K for organic synthesis: reduction of substituted naphthalenes. *J. Chem. Soc. Perkin 1* **0**, 117–120 (1993).
- S2. Marcoux, D., Charrette, A.B. Palladium-Catalyzed Synthesis of Functionalized Tetraarylphosphonium Salts. *J. Org. Chem.* **73**, 590-593 (2008).
- S3. Demchuk, O.M., Jasinski, R., Strelecka, D., Dziuba, K., Kula, K., Chrzanowski, J., Krasowska, D. A clean and simple method for deprotection of phosphines from borane complexes. *Pure Appl. Chem.* **90(1)**, 49-62 (2018).
- S4. Barnes, N. A., Godfrey, S. M., Halton, R. T. A., Mushtaq, I., Pritchard, R. G. The reaction of tertiary phosphines with(Ph₂Se₂l₂)₂-the influence of steric and electronic effects. *Dalton Trans.* **40**, 4795-4804 (2006).
- S5. Cummins, C.C., Huang, C., Miller, T. J., Reintinger, M. W., Stauber, J. M., Tannou, I., Tofan, D., Toubaei, A., Velian, A., Gang, W. The Stannylphosphide Anion Reagent Sodium Bis(triphenylstannyl) Phosphide: Synthesis, Structural Characterization, and Reactions with Indium, Tin, and Gold Electrophiles. *Inorg. Chem.* **53**, 3678-3687 (2014).

- S6. Prier, C. K., Rankic, D. A. & MacMillan, D. W. C. Visible Light Photoredox Catalysis with Transition Metal Complexes: Applications in Organic Synthesis. *Chem. Rev.* **113**, 5322–5363 (2013).
- S7. Krejčík, M., Daněk, M. & Hartl, F. Simple construction of an infrared optically transparent thin-layer electrochemical cell: Applications to the redox reactions of ferrocene, $\text{Mn}_2(\text{CO})_{10}$ and $\text{Mn}(\text{CO})_3(3,5\text{-di-}t\text{-butyl-catecholate})^-$. *J. Electroanal. Chem. Interfacial Electrochem.* **317**, 179–187 (1991).
- S8. Feldmeier, C., Bartling, H., Riedle, E. & Gschwind, R. M. LED based NMR illumination device for mechanistic studies on photochemical reactions – Versatile and simple, yet surprisingly powerful. *J. Magn. Reson.* **232**, 39–44 (2013).
- S9. Seegerer, A., Nitschke, P. & Gschwind, R. M. Combined In Situ Illumination-NMR-UV/Vis Spectroscopy: A New Mechanistic Tool in Photochemistry. *Angew. Chem. 1Int. Ed.* **57**, 7493–7497 (2018).
- S10. Goez, M. Chapter 3 Photo-CIDNP Spectroscopy. in *Annual Reports on NMR Spectroscopy* **66**, 77–147 (Academic Press, 2009).
- S11. Goez, M. & Sartorius, I. Photo-CIDNP investigation of the deprotonation of aminium cations. *J. Am. Chem. Soc.* **115**, 11123–11133 (1993).
- S12. Goez, M. & Sartorius, I. CIDNP Determination of the Rate of In-Cage Deprotonation of the Triethylamine Radical Cation. *J. Phys. Chem. A* **107**, 8539–8546 (2003).

3 VERSATILE VISIBLE-LIGHT-DRIVEN SYNTHESIS OF UNSYMMETRICAL PHOSPHINES AND PHOSPHONIUM SALTS

Percia Beatrice Arockiam, Ulrich Lennert, Christina Graf, Robin Rothfelder, Daniel J. Scott, Tillmann G. Fischer, Kirsten Zeitler, and Robert Wolf



Unsymmetrically substituted tertiary phosphines and quaternary phosphonium salts are used extensively in applications throughout industry and academia. Despite their significance, classical methods to synthesise such compounds demand either harsh reaction conditions, prefunctionalisation of starting materials, highly sensitive organometallic reagents, or expensive transition metal catalysts. Mild, practical methods thus remain elusive, despite being of great current interest. Herein, we describe a visible light-driven method to form these products from secondary and primary phosphines. Using an inexpensive organic photocatalyst and blue light irradiation, arylphosphines can be both alkylated and arylated using commercially available organohalides. In addition, the same organocatalyst can be used to transform white phosphorus (P_4) directly into symmetrical aryl phosphines and phosphonium salts in a single reaction step, which has previously only been possible using precious metal catalysis.

[I] Accepted in *Chem. Eur. J.*

[II] U.L. developed the catalytic procedure for arylation reactions; U.L., C.G. and R.R. performed the optimisation studies, investigated the substrate scope and U.L. isolated the products at increased scale. P.B.A. developed the catalytic procedure for alkylation reactions and performed the optimisation studies, substrate scope and further isolated the products at increased scale. P.B.A. carried out the mechanistic experiments and performed the reactions with diphosphines. P.B.A did the optimisation of P_4 functionalisation, investigated the substrate scope and isolation of products. K.Z. and T.G.F. provided organic photocatalyst for catalytic studies. P.B.A. and U.L prepared the manuscript, with input from all authors. D.J.S. read and revised the manuscript. R.W. oversaw and directed the project.

3.1 INTRODUCTION

Tertiary phosphines (PR_3) and the related quaternary phosphonium salts (PR_4^+) are of great significance in both industrial and academic chemistry. As such, the development of new methods for the synthesis of these compounds remains an important, ongoing research challenge. In particular, there is a strong desire to develop new routes for the preparation of unsymmetrically substituted PR_3 and PR_4^+ products, which find extensive uses throughout chemistry. For example, the former are ubiquitous in the fields of coordination chemistry and catalysis, where they are used as ‘designer’ and chelating ligands with well-defined and optimised steric and electronic properties.^[1] The latter, meanwhile, are used as phase transfer catalysts,^[2] and components of ionic liquids,^[3] among a number of other applications.^[4] Unfortunately, the number of practical methods for the preparation of these compounds remains limited, which creates a barrier to research and can curtail developments in these fields.

Classical methods for the preparation of unsymmetrical tertiary phosphines (I, III) involve the nucleophilic substitution of halophosphines with organometallic reagents, reaction of metal phosphides with organic halides, and reduction of mixed phosphine oxides (Fig. 1a).^[5] However, these methods suffer from the use of hazardous and highly-sensitive reagents, often accompanied by harsh reaction conditions, difficult procedures with problematic reproducibility and/or poor product yields. Transition metal (Pd, Ni, Cu) catalysed condensations of secondary phosphines with organic halides or pseudo halides may also be employed, but often require an expensive transition metal catalyst and forcing reaction conditions (Fig. 1b).^[6] Alternatively, hydrophosphination of alkenes or alkynes^[7] can be catalysed by transition metal complexes (Fe, Ni, Pd, Cu),^[8] or by rare-earth-metal complexes (La, Yb)^[9], or may proceed without a catalyst in certain cases (Fig. 1b).^[10] While sometimes very effective, these reactions can only be used to introduce alkyl substituents with a β -H atom, and often suffer from issues of regioselectivity. Very recently, radical cross-coupling of *N*-hydroxyphthalimide esters with chlorophosphines was reported, mediated either by a metal reductant (Zn) or an iridium photocatalyst.^[11] While this protocol provided a broad range of tertiary phosphines, pre-functionalisation steps were required to obtain the activated esters, which limits the attractiveness of these reactions.

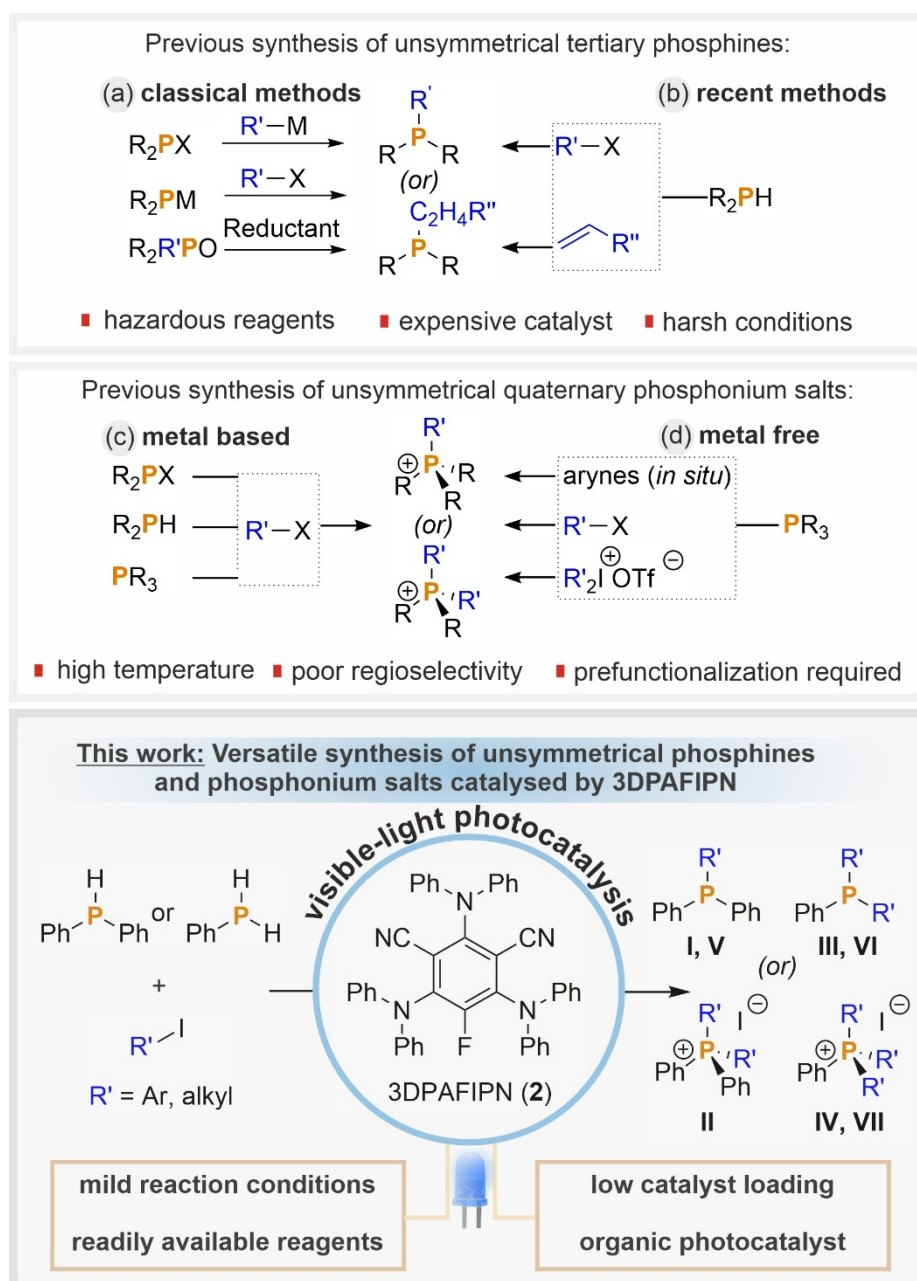


Fig. 1. General methods to synthesise unsymmetrical tertiary phosphines and quaternary phosphonium salts; R, R' = aryl, alkyl; M = metal; X = leaving group.

Unsymmetrical quaternary phosphonium salts (**II**, **IV**) are mostly synthesised from tertiary phosphines through nucleophilic attack on alkyl or aryl (pseudo) halides and transition metal catalysed (Pd, Ni) arylation using haloarenes at (very) high temperatures (>140 °C; Fig. 1c),^[12] although a small number of metal-free reactions have also been reported.^[13] One of these involves the trapping by tertiary phosphines of *in situ* generated arynes but provides only poor regioselectivity.^[13a] Another recently developed reaction of PPh₃ with bromoarenes in phenol requires very high temperature (180 °C).^[13b] Alternatively, visible light-driven reactions with iodonium salts have been reported, either mediated by a Ru-based photosensitiser,^[14] or using a metal free protocol facilitated by the formation of an electron donor-acceptor complex formed from iodonium salts and

tertiary phosphines (Fig. 1d).^[15] In both cases the need for prior synthesis of the iodonium salts places a limit on the overall usefulness of the reaction. On the other hand, there are only a very few examples which enable the synthesis of unsymmetrical quaternary phosphonium salts from secondary phosphines or chlorophosphines using the conventional strategy of exploiting transition metal (Pd, Ni) catalysts at elevated temperatures (>150 °C).^[16] Thus, despite a variety of methods having been reported for the synthesis of unsymmetrical tertiary phosphines and quaternary phosphonium salts, a mild, practical and general method for their formation from readily-available precursors remains elusive.

In recent years, visible-light photoredox catalysis has become a powerful synthetic tool that has enabled the development of many novel organic transformations.^[17] We recently demonstrated the visible light-driven, iridium-catalysed direct functionalisation of white phosphorus, which gives triarylphosphines and tetraarylphosphonium salts under mild reaction conditions.^[18] It was found that this method arylates P₄ in a stepwise manner, giving rise to H₂PAR, HPAR₂, PAR₃, and PAR₄⁺ products in a well-defined sequence. Building upon these observations, herein we report that the same reaction protocol can be used to provide convenient access to unsymmetrical tertiary phosphines and quaternary phosphonium salts, by starting from the commercially available primary and secondary phosphines H₂PPh and HPPh₂. Furthermore, we show that the previously-employed noble metal photocatalyst can be replaced by the inexpensive organic photocatalyst 3DPAFIPN, not only in these reactions but also in the direct arylation of P₄,^[19] providing simple and practical protocols for the synthesis of a broad range of symmetric and unsymmetric target products (Fig. 1, bottom box, Fig. 2).

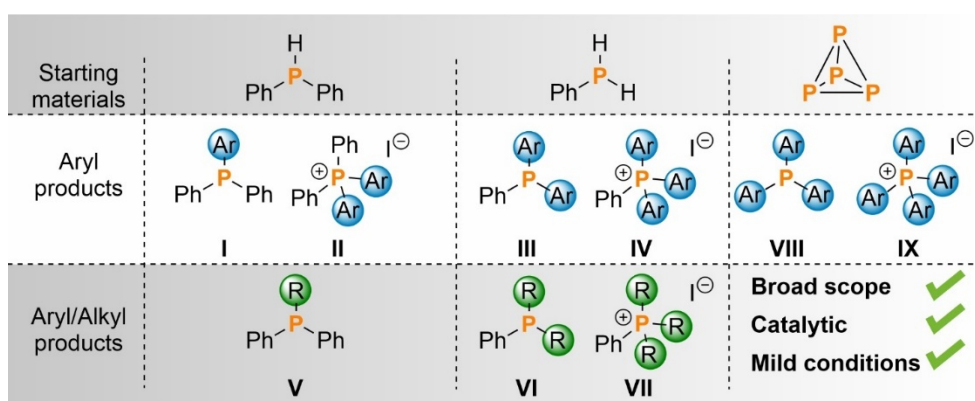
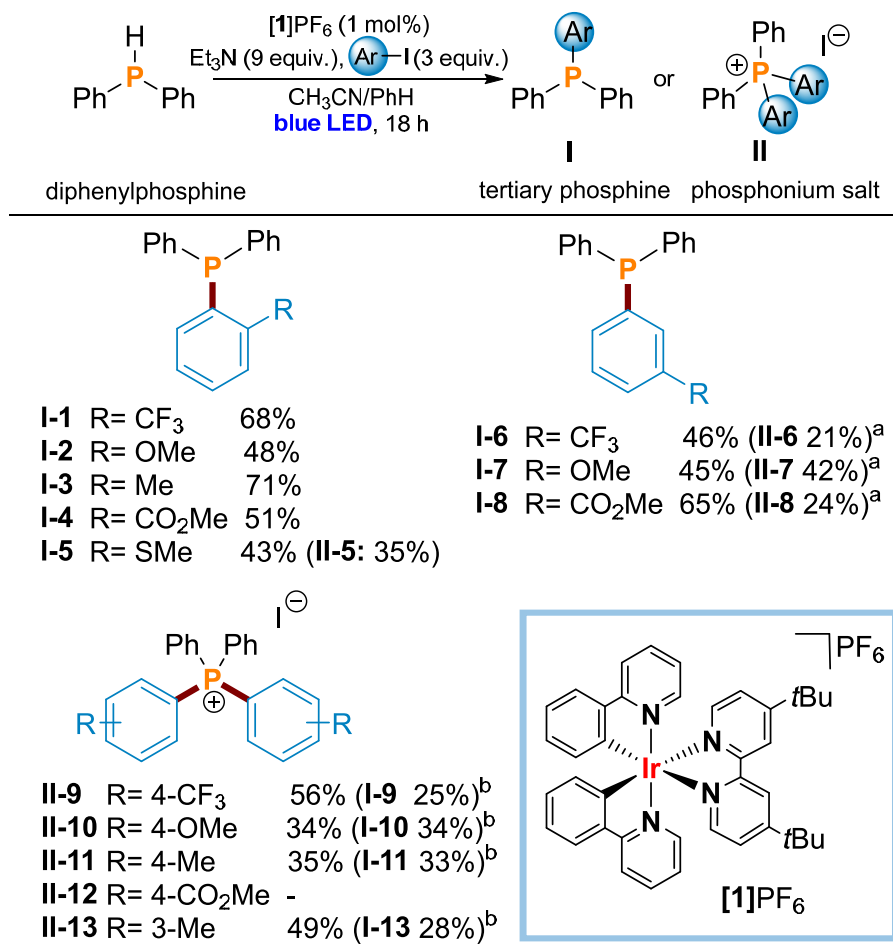


Fig. 2. An overview of the broad scope of symmetrically and unsymmetrically substituted phosphines and phosphonium salts accessed in this work, and the corresponding product numbering scheme. R = alkyl, Ar = aryl

3.2 RESULTS AND DISCUSSION

3.2.1 Arylation of diphenylphosphine mediated by [Ir(dtbbpy)(ppy)₂]PF₆

Based upon our previous observations,^[18] we reasoned that the commercially-available aryl phosphines HPPh₂ and H₂PPh could be transformed into unsymmetrical tertiary phosphines (RPPh₂ or R₂PPh) and quaternary phosphonium salts (R₂PPh₂⁺ or R₃PPh) through reaction with aryl iodides, mediated by the same photocatalytic system previously used for the arylation of P₄. Thus, a solution containing the photocatalyst [Ir(dtbbpy)(ppy)₂]PF₆ (**[1]**PF₆; dtbbpy = 4,4'-bis-*tert*-butyl-2,2'-bipyridine, ppy = 2-(2-pyridyl)phenyl; structure shown in Table 1), HPPh₂, the electron donor Et₃N, and a model substrate 2-iodotoluene in a CH₃CN/PhH mixture (3:1) was irradiated with blue LED light (λ_{max} = 455 nm) for 18 h. Gratifyingly, this reaction was indeed found to yield 63% of the desired tertiary phosphine product. Further investigations revealed that the yield could be further optimised to 71% by optimising the ratios of Et₃N, aryl iodide and **[1]**PF₆ (Table 1, **I-3**). Control experiments confirmed that the reaction proceeds only in the presence of all reaction components (Et₃N, aryl iodide, blue light irradiation, HPPh₂ and **[1]**PF₆; Supplementary Table 1). Meanwhile, a preliminary substrate screening showed that several other iodobenzene derivatives could also be employed in the reaction successfully (Table 1).

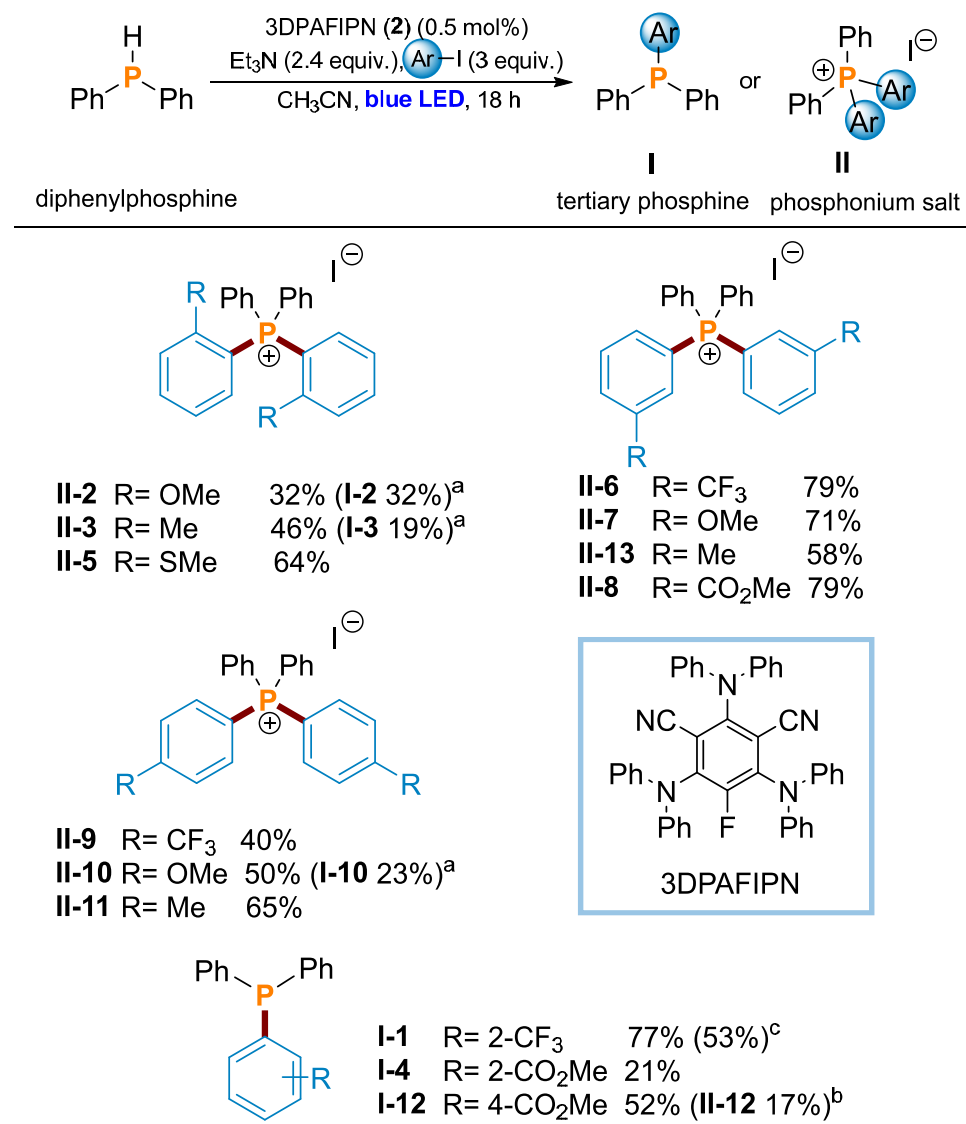
Table 1. Photocatalytic synthesis of unsymmetrically substituted aryldiphenylphosphines (**I**) and bisaryldiphenylphosphonium salts (**II**) from HPPPh₂ using [Ir(dtbbpy)(ppy)₂]PF₆ as a photoredox catalyst.

All reactions were carried out using HPPPh₂ (0.1 mmol, 1 equiv.), Ar-I (0.3 mmol, 3 equiv.), [1]PF₆ (1 mol%), and Et₃N (8.6 mmol, 8.6 equiv.) in CH₃CN/PhH (3:1 v/v, 2 mL) under an N₂ atmosphere and blue LED irradiation ($\lambda_{\text{max}} = 455 \text{ nm}$) for 18 h. Yields were determined by quantitative ³¹P{¹H} NMR analysis of the reaction mixture with PPh₃O as an internal standard. (a) Values in parentheses are the yields of the corresponding tetraaryldiphenylphosphonium salt **II** (b) Values in parentheses are the yields of the corresponding triaryldiphenylphosphines **I**.

While these initial results clearly confirmed the validity of our proposed reaction, it was unfortunately found that in most cases undesirable mixtures of phosphine (**I**) and phosphonium (**II**) products were obtained, in ratios typically between ca. 1:1 and 2:1. Interestingly, slightly higher selectivity was generally observed using electron-poor iodoarenes, regardless of whether the major product was a phosphine or phosphonium salt. This more controlled behaviour is presumably not due to difficulties in radical generation (Ar-I reduction should be more facile for electron-poor arenes) and may instead be due to reduced reactivity of less nucleophilic aryl radicals (e.g. towards electrophilic P₂Ph₄; *vide infra*). Only for ortho-substituted aryl iodides (with the exception of 2-iodothioanisole) were the phosphine products obtained selectively, presumably for steric reasons.

3.2.2 Arylation of diphenylphosphine mediated by 3DPAFIPN

Given the generally poor selectivity observed using $[1]PF_6$, it was decided to further optimise the $HPPh_2$ arylation reaction through investigation of alternative photocatalysts, which it was anticipated could yield cleaner product mixtures. In particular, it was decided to pursue the use of organic photocatalysts, in order to avoid the need to use expensive and scarce precious metals. To achieve similar reactivity, it was anticipated that a photocatalyst with comparable redox properties to $[1]^+$ would be required. Fortunately, the recently-developed organic photocatalyst 3DPAFIPN (**2**) has been reported to possess a reduction potential very similar to that of $[1]^+$, while also being a competent catalyst for other photoredox reactions.^[19] We were delighted to find that replacing $[1]PF_6$ by **2** gave not only comparable, but in fact notably superior results in the arylation of $HPPh_2$, including markedly improved selectivity for the phosphonium products **II** in most cases (Table 2 and *vide infra*). After further optimisation, it was found that only 0.5 mol% of **2**, and a much more modest excess of Et_3N (2.4 equiv.) and aryl iodide (3 equiv.) in pure CH_3CN under blue light irradiation transformed $HPPh_2$ into a variety of desired products with generally excellent selectivity. Hence, not only could $[1]PF_6$ be replaced with the readily available and inexpensive organophotocatalyst **2**, but this substitution additionally yielded a considerable improvement in reaction performance.

Table 2. Photocatalytic synthesis of unsymmetrically substituted aryldiphenylphosphines (**I**) and bisaryldiphenylphosphonium salts (**II**) from HPPh₂ using 3DPAFIPN as a photoredox catalyst.

All reactions were carried out using HPPh₂ (0.1 mmol, 1 equiv.), Ar-I (0.3 mmol, 3 equiv.), 3DPAFIPN (0.5 mol%) and Et₃N (0.24 mmol, 2.4 equiv.) in CH₃CN (2 mL) under an N₂ atmosphere and blue LED irradiation ($\lambda_{\text{max}} = 455 \text{ nm}$) for 18 h. Yields were determined by quantitative ³¹P{¹H} NMR analysis of the reaction mixture with PPh₃O as an internal standard. (a) Values in parentheses are the yield of the corresponding triaryldiphenylphosphine **I**. For simplicity, yields smaller than 10% are not given in the table (see the Supporting Information for further details). (b) Values in parentheses are the yield of the corresponding tetraaryldiphenylphosphonium salt **II**. (c) Value in parentheses is the isolated yield for **I-1** at 1 mmol scale.

Gratifyingly, this optimised reaction was found to be compatible with iodobenzene derivatives bearing both electron-donating and electron-withdrawing groups, with the nature of these substituents generally having relatively little impact on the reaction outcome (Table 2). Notably, and in contrast to results obtained using [1]PF₆, *meta*- and *para*-substituted substrates were found to furnish exclusively the corresponding phosphonium salts Ar₂PPh₂⁺ in almost all cases (Table 2, **II-6-11, 13**). Only for methyl 4-iodobenzoate (Table 2, **I-12**) was the tertiary phosphine (ArPPh₂) formed preferentially, which is in line with our previous observation that strongly electron-withdrawing groups

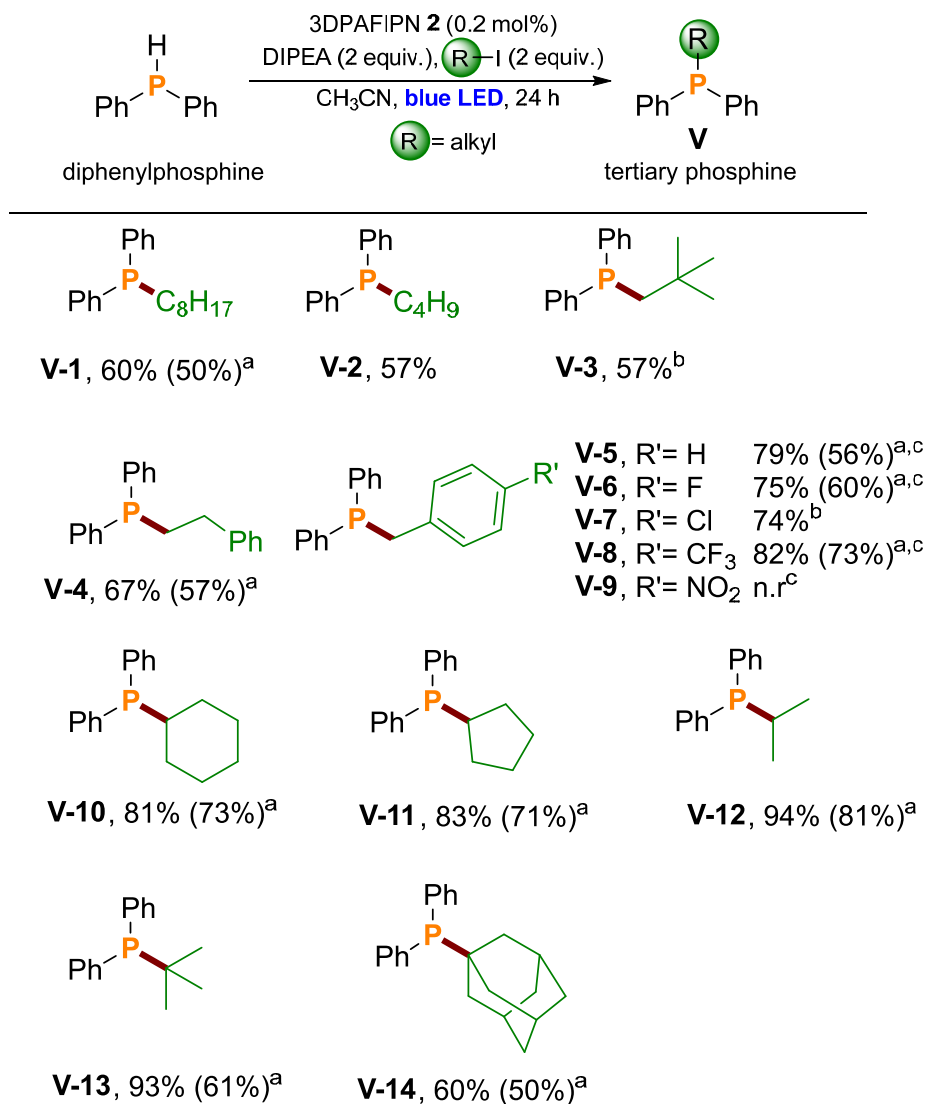
can disfavour formation of a phosphonium cation. Conversely, for *ortho*-substituted substrates significant Ar_2PPh formation was observed in all cases (**II-1-5**), in line with previous observations using $[\mathbf{1}]\text{PF}_6$ (*vide supra*). The reason(s) behind the increased preference for phosphonium salts **II** when using **2** rather than $[\mathbf{1}]\text{PF}_6$ are currently unclear, but are presumably related to slight differences in redox characteristics and/or electron transfer kinetics.^[20]

3.2.3 Arylation of phenylphosphine mediated by 3DPAFIPN

Having established the ability to arylate the secondary phosphine HPPH_2 , we proceeded to investigate the further extension of the scope of the arylation to the primary phosphine H_2PPh . Thus, after a modest increase in the amount of iodoarene, reductant and catalyst (to reflect the larger number of arylation steps required), various additional phosphines (Ar_2PPh , **III**) and phosphonium salts (Ar_3PPh^+ , **IV**) were conveniently accessible from H_2PPh in reasonable yields (Table 3). Similar patterns of functional group tolerance and selectivity were observed to the analogous reactions of HPPH_2 , although for *ortho*-substituted substrates a noticeably increased preference for the triarylphosphine product could be detected (**III-1-6**). This results in generally higher selectivity for these reactions (albeit with a slight cost in overall yield) and is consistent with the greater steric impact that results from the presence of two *ortho*-substituted aryl residues within the product structures.

of the alkyl substrates, which will limit alkyl radical formation and so may limit the extent of functionalisation.

Table 4. Photocatalytic synthesis of unsymmetrically substituted mixed alkyldiphenylphosphines (**V**) from HPPh₂ using 3DPAFIPN as a photoredox catalyst.



All reactions were carried out using HPPh₂ (0.2 mmol, 1 equiv.), R-I (0.4 mmol, 2 equiv.), 3DPAFIPN (0.2 mol%) and DIPEA (0.4 mmol, 2 equiv.) in CH₃CN (2 mL) under an N₂ atmosphere and blue LED irradiation ($\lambda_{\text{max}} = 455 \text{ nm}$) for 24 h. Yields were determined by quantitative ³¹P{¹H} NMR analysis of the reaction mixture with PPh₃O as an internal standard. (a) Values in parentheses are isolated yields for reactions at 1 mmol scale (for HPPh₂) using 0.5 mol% 3DPAFIPN. (b) The reaction was carried out with 0.5 mol% 3DPAFIPN for 38 h, (c) R-Br was used instead of R-I.

This transformation was found to be effective for primary long chain alkyl iodides such as *n*-octyl iodide and *n*-butyl iodide as well as for the more sterically encumbered neopentyl iodide. Excellent conversions were also achieved using various substituted benzyl bromide substrates,^[21] leading to formation of the corresponding benzylic phosphines. Such benzylic phosphines have recently found application as ligands within Ir- or Pt- complexes with potential uses in electroluminescent devices and OLEDs.^[22] A range of electron deficient groups (such as F (**V-6**), Cl (**V-7**), CF₃ (**V-8**)) at the 4-position

were tolerated, with the exception of NO_2 (**V-9**), possibly due to side-reactions at the NO_2 group itself. In addition to primary alkyl iodides, cyclic and acyclic secondary iodides could also be transformed into the corresponding tertiary phosphine products in reasonable yields, as could tertiary alkyl iodides. It should be noted that for the isopropyl and *tert*-butyl iodide substrates the corresponding products (**V-12**, **V-13**) could also be prepared in moderate yield (35%, 50%) in the absence of the photocatalyst **2**, although no product was observed upon exclusion of light (Supplementary Table 3). For other substrates, however, control experiments confirmed that a productive reaction is achieved only if all reaction components are present, including the photocatalyst.

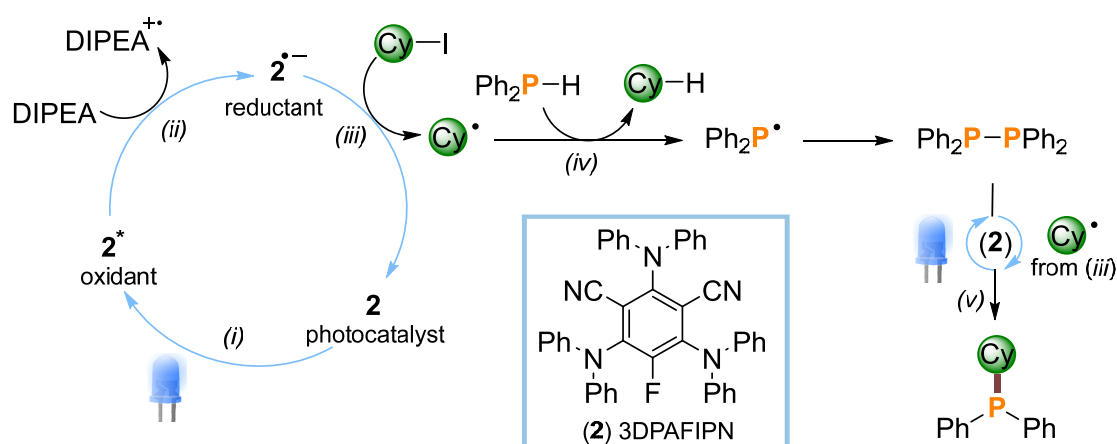
3.2.5 Alkylation of phenylphosphine mediated by 3DPAFIPN

Similar success was achieved for the alkylation of the primary phosphine H_2PPh , providing access to a broad range of dialkyl-substituted phenyl phosphines R_2PPh in good yields (Table 5). Again, a range of primary and secondary alkyl iodides could be employed as coupling partners, as could several benzyl bromides, although attempts to use *t*-butyl iodide were unsuccessful, presumably for steric reasons. In contrast to the formerly described alkylation of HPPh_2 , which gave exclusively tertiary phosphine products, here, in many cases triple alkylation of H_2PPh was found to furnish the phosphonium salts R_3PPh^+ with high selectivity. This is probably at least in part due to steric factors, given the small profile of most of the primary alkyl moieties. Notably, for the benzyl bromide substrates either the R_3PPh^+ or R_2PPh products can be accessed with high selectivity, simply by altering the molar ratio with H_2PPh .

3.2.6 Mechanistic investigations

To acquire mechanistic insights, the optimised reaction between HPPh₂ and cyclohexyl iodide (Cy-I) was chosen as a model system for further study. Radical inhibition experiments showed that addition of 2,2,6,6-tetramethyl-1-piperidinyloxy (TEMPO) as a radical scavenger to this reaction completely suppressed the formation of the expected product PPh₂Cy (**V-10**), supporting the involvement of a radical pathway (Supplementary Scheme 3).^[23] In addition, ³¹P{¹H} NMR monitoring of the model reaction showed complete consumption of HPPh₂ and rapid formation of the diphosphine P₂Ph₄ in less than 2 h. The same reaction gave only traces of product in the absence of photocatalyst **2**. Notably, no formation of P₂Ph₄ was observed in the absence of Cy-I, even with extended reaction times (Supplementary Table 4). These observations suggest that product formation may not proceed through direct alkylation of HPPh₂ *per se*, but rather through the intermediate formation of P₂Ph₄. this intermediate is presumably formed *via* dimerisation of Ph₂P• radicals that are in turn formed by abstraction of an H atom from HPPh₂ (Scheme 1, step iv) by photochemically-generated Cy• radicals.^[11] The formation of organyl radicals was confirmed by EPR measurements: when a CH₃CN solution of 2, DIPEA, Cy-I and the spin trap N-tert-butyl- α -phenylnitron (PBN) was irradiated with blue LED light the formation of a spin adduct with hyperfine couplings of $a^N = 15.2$ G, $a^H = 2.5$ G was observed which might correspond to the known spin adduct Cy-PBN or a related adduct (Supplementary Figure 3).^{[24][25]} Finally, fluorescence quenching experiments were performed to confirm that of the reaction components present in the model reaction mixture (DIPEA, Cy-I, H₂PPh, P₂Ph₄) only DIPEA effectively quenches the photoexcited state of photocatalyst **2** in CH₃CN (Supplementary Figure 4).

Based on our observations, a catalytic cycle can be proposed, which is summarised in Scheme 1. Irradiation of photocatalyst **2** with blue light generates the excited species **2*** [$E_{1/2}(PC^*/PC^{--}) = + 1.09$ V vs SCE] which undergoes reductive quenching in the presence of DIPEA ($E_{1/2}^{ox} = +0.65$ V vs SCE), resulting in the simultaneous formation of the DIPEA radical cation (DIPEA^{•+}) and the strong reductant **2⁻** [$E_{1/2}(PC/PC^{--}) = - 1.59$ V vs SCE] (step *i*, *ii*).^[19] This is capable of generating a cyclohexyl radical (Cy•, step iii) through one-electron reduction of Cy-I, which also closes the photoredox catalytic cycle.^[26] The radicals (Cy•) thus generated can then abstract a hydrogen radical from HPPh₂, producing Ph₂P• radicals that rapidly self-couple to form the intermediate diphosphine P₂Ph₄ (step *iv*, *v*). This step also accounts for the need for at least a 1equiv. excess of the organohalide in all reactions. Subsequent radicals Cy• can then react with P₂Ph₄, releasing the product tertiary phosphine PPh₂Cy (step *v*).

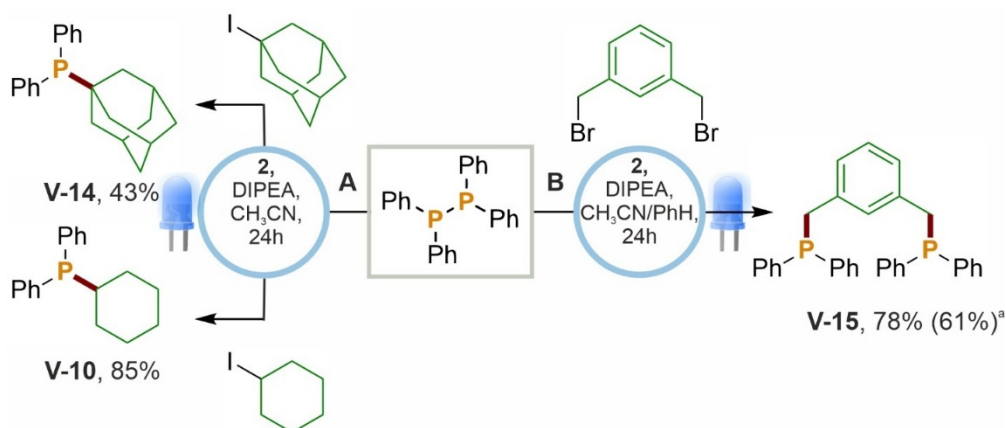


Scheme 1. Proposed mechanism for the formation of an unsymmetrical tertiary phosphine from Cy-I (cyclohexyl iodide) and HPPh₂.

Given the proposed involvement of P₂Ph₄ as an intermediate in the photocatalytic reaction, the direct reaction of P₂Ph₄ with selected alkyl iodides was also investigated. Thus, the reaction of P₂Ph₄ with Cy-I or 1-iodoadamantane and DIPEA in a 1:1.5:1.5 molar ratio (per phosphorus atom) was confirmed to provide the expected products **V-10** and **V-14**, in 89% and 43% yields, respectively (Scheme 2b). Unfortunately, the formation of tertiary phosphine was not observed with primary alkyl halides such as benzyl bromide and *n*-octyl iodide suggesting that different mechanisms may be operative in these cases (Supplementary Scheme 4).

3.2.7 Application to the synthesis of a PCP pincer ligand

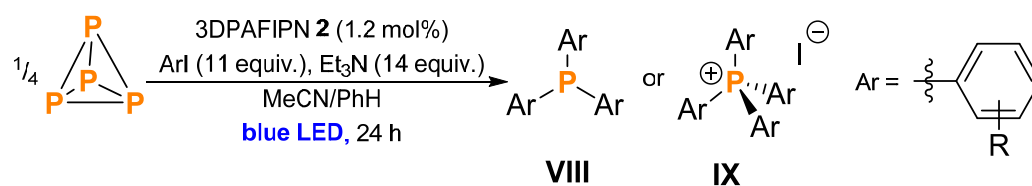
As a further demonstration of the utility of this method, we sought to synthesise a PCP pincer ligand starting from P₂Ph₄. These ligands are well known and widely exploited in organometallic chemistry.^[27] We had previously been disappointed to find that attempts to prepare these products starting from HPPh₂ were unsuccessful. However, to our satisfaction, blue LED irradiation of a 1:1.5:4 molar ratio of P₂Ph₄, 1,3-*bis*(bromomethyl)benzene and DIPEA in CH₃CN/PhH in the presence of 0.5 mol% of 3DPAFIPN led to selective formation of 1,3-*bis*(diphenylphosphinomethyl)benzene **V-15** in 61% isolated yield (Scheme 2a).



Scheme 2. Synthesis of tertiary phosphines and PCP pincer ligand from P_2Ph_4 . Reaction conditions: **(A)** P_2Ph_4 (0.2 mmol, 1 equiv.), **alkyl iodide** (0.6 mmol, 1.5 equiv. based on phosphorus atom), 3DPAFIPN (0.5 mol%), DIPEA (0.6 mmol, 1.5 equiv. based on phosphorus atom), CH_3CN (2 mL), N_2 atmosphere, blue LED ($\lambda_{max} = 455$ nm), 24 h. **(B)** P_2Ph_4 (0.15 mmol, 1.5 equiv.), **1,3-bis(bromomethyl)benzene** (0.1 mmol, 1 equiv.), 3DPAFIPN (0.5 mol%), DIPEA (0.4 mmol, 4 equiv.), CH_3CN (1.5 mL), PhH (0.5 mL), N_2 atmosphere, blue LED ($\lambda_{max} = 455$ nm), 24 h. a) Isolated yield for reactions at 0.5 mmol scale (for **1,3-bis(bromomethyl)benzene**).

3.2.8 Application of 3DPAFIPN in P_4 functionalisation

Finally, having demonstrated the ability of organic photocatalyst **2** to mediate the arylation (and alkylation) of primary and secondary phenyl phosphines, we were interested to establish whether the same catalyst could also mediate the formation of these phosphines from P_4 , and thus act as a competent catalyst for the direct transformation of P_4 into triarylphosphines and tetraarylphosphonium salts, in an analogous manner to the precious metal catalyst [**1**]⁺. Thus, our previously reported procedure for the catalytic phenylation of P_4 with iodobenzene was repeated using organic photocatalyst **2** (1.2 mol%, Supplementary Table 5). Direct catalyst replacement in this manner yielded the tetra-arylated phosphonium salt PPh_4I in 60% yield and with complete selectivity.

Table 6. Direct P₄ functionalisation using 3DPAFIPN as a photoredox catalyst.

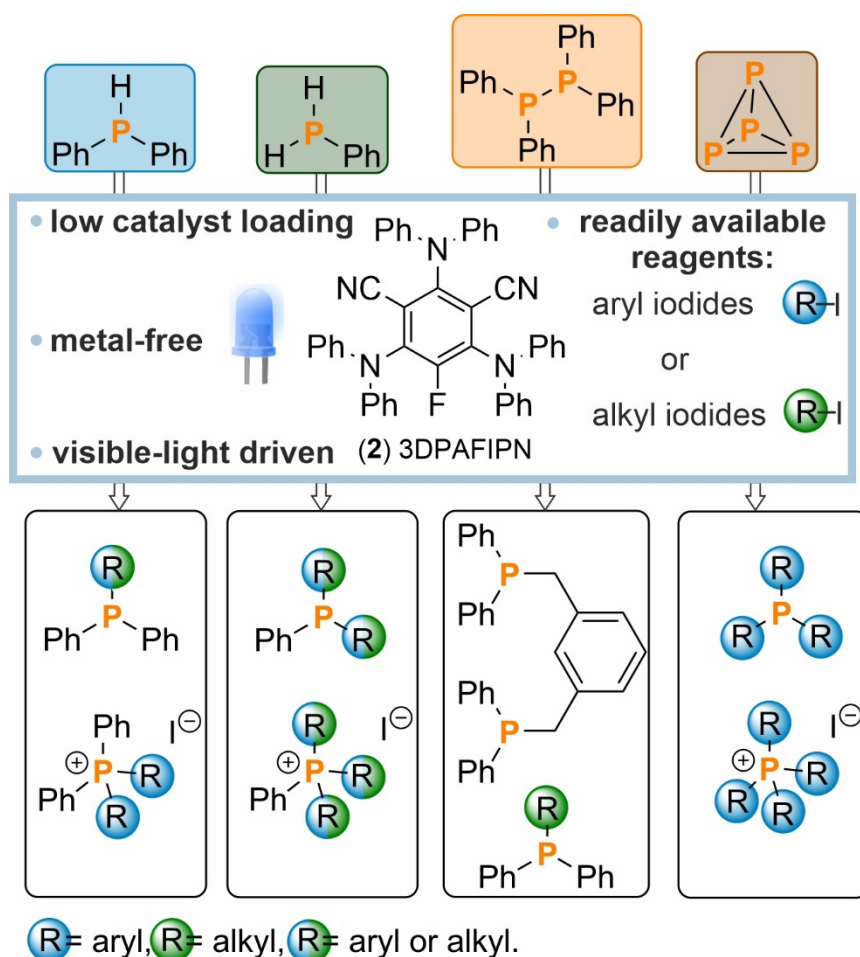
Entry	R	Product No.	[PAr ₄] ⁺ I ⁻	PAr ₃
1	H	IX-1	60 (24%)	-
2	3-Me	IX-2	37	-
3 ^a	4-Me	IX-3	29	-
4	3-OMe	IX-4	45	-
5	4-OMe	IX-5	19	-
6	3-COOMe	IX-6	20	-
7	4-COOMe	VIII-1	-	31
8	2-Me	VIII-2	-	54 (43%) ^b
9 ^a	2-OMe	VIII-3	-	24 (12%) ^b
10	2-SMe	VIII-4	-	24 (16%) ^b
11 ^c	Ph ₃ SnCl	VIII-5	-	56

All reactions were carried out using P₄ (0.025 mmol, 1 equiv.), Ar-I (1.1 mmol, 11 equiv. based on phosphorus atom), 3DPAFIPN (1.2 mol% based on phosphorus atom) and Et₃N (1.4 mmol, 14.4 equiv. based on phosphorus atom) in CH₃CN/PhH (3:1 v/v, 2 mL) under an N₂ atmosphere and blue LED irradiation ($\lambda_{\text{max}} = 455 \text{ nm}$) for 24 h. Yields were determined by quantitative ³¹P{¹H} NMR analysis of the reaction mixture with PPh₃O as an internal standard. (a) 30 h reaction time. (b) Values in parentheses are isolated yields for reactions at 1 mmol scale. (c) Ar-I was replaced by Ph₃SnCl.

As shown in Table 5, a range of substituted aryl iodides were amenable to this photocatalytic strategy, including both electron rich and electron deficient arenes. The scope and selectivity of the reaction were found to mirror those previously observed using [1]⁺ as a catalyst, again offering selective triarylphosphine formation for ortho substituted aryl iodides as well as for the electron-poor 4-CO₂Me derivative. By replacing the aryl iodide with Ph₃SnCl it was possible to prepare the potentially useful ‘P³⁻’ triply-stannylated synthon (Ph₃Sn)₃P. Although the yields of phosphines and phosphoniums obtained are typically slightly reduced compared to the analogous reactions catalysed by [1]⁺, the ability to use an inexpensive organic photocatalyst in place of a precious metal complex represents a significant improvement to the practicality and attractiveness of this synthetic method.

3.3 CONCLUSION

In summary, we have developed a mild and versatile, visible light-mediated approach for the selective formation of a broad scope of unsymmetrical aryl/aryl and aryl/alkyl tertiary phosphines and quaternary phosphonium salts, using stable, commercially available organic halides in combination with phenyl-substituted primary and secondary phosphines as starting materials (Scheme 3). Optimal results are obtained using low loadings of an inexpensive organic photocatalyst, resulting in a mild and versatile synthetic method for the preparation of these valuable compounds and providing an attractive alternative to previously developed Ir-photocatalysed protocols. The same organic photocatalyst can also be used to replace the precious metal photoredox catalyst in our previously reported photocatalytic arylation of P_4 , significantly improving the synthetic feasibility of this important transformation.



Scheme 3. Organic photocatalytic synthesis of unsymmetrically substituted tertiary phosphines and quaternary phosphonium salts

3.4 REFERENCES

- 1 a) N. Liu, X. Li, H. Sun, *J. Organomet. Chem.* **2011**, *696*, 2537-2542; b) H. Khan, A. Badshah, M. Said, G. Murtaza, J. Ahmad, B. J. Jean-Claude, M. Todorova, I. S. Butler, *Appl. Organomet. Chem.* **2013**, *27*, 387-395; c) H. Khan, A. Badshah, M. Said, G. Murtaza, M. Sirajuddin, J. Ahmad, I. S. Butler, *Inorg. Chim. Acta* **2016**, *447*, 176-182; d) K. Potgieter, Z. Engelbrecht, G. Naganagowda, M. J. Cronjé, R. Meijboom, *J. Coord. Chem.* **2017**, *70*, 2644-2658; e) V. T. Yilmaz, C. Icel, O. R. Turgut, M. Aygun, E. Evren, I. Ozdemir, *Inorg. Chim. Acta* **2020**, *500*, 119220.
- 2 a) D. Enders, T. V. Nguyen, *Org. Biomol. Chem.*, **2012**, *10*, 5327-5331; b) S. Liu, Y. Kumatabara, S. Shirakawa, *Green Chem.*, **2016**, *18*, 331-341; c) A. Golandaj, A. Ahmad, D. Ramjugernath, *Adv. Synth. Catal.* **2017**, *359*, 3676-3706.
- 3 a) J. McNulty, J. J. Nair, S. Cheekoori, V. Larichev, A. Capretta, A. J. Robertson, *Chem. Eur. J.* **2006**, *12*, 9314-9322; b) H. Cao, L. McNamee, H. Alper, *J. Org. Chem.* **2008**, *73*, 3530-3534; c) A. F. Ferreira, P. N. Simões, A. G. M. Ferreira, *J. Chem. Thermodynamics* **2012**, *45*, 16-27; d) C. G. Cassity, A. Mirjafari, N. Mobarrez, K. J. Strickland, R. A. O'Brien, J. H. Davis, *Chem. Commun.* **2013**, *49*, 7590-7592.
- 4 a) Z. Deng, J.-H. Lin, J.-C. Xiao, *Nat Commun* **2016**, *7*, 1-8; b) Y. Toda, S. Gomyou, S. Tanaka, Y. Komiyama, A. Kikuchi, H. Suga, *Org. Lett.* **2017**, *19*, 5786-5789; c) S. Guo, X. Mi, *Tetrahedron Lett.* **2017**, *58*, 2881-2884; d) M. Gupta, D. Yan, J. Xu, J. Yao, C. Zhan, *ACS Appl. Mater. Interfaces* **2018**, *10*, 5569-5576; e) M. Gupta, D. Yan, J. Yao, C. Zhan, *ACS Appl. Mater. Interfaces* **2018**, *10*, 35896-35903.
- 5 a) A. K. Bhattacharya, G. Thyagarajan, *Chem. Rev.* **1981**, *81*, 415-430; b) I. Wauters, W. Debrouwer, C. V. Stevens, *Beilstein J. Org. Chem.* **2014**, *10*, 1064-1096; c) D. Héroult, D. H. Nguyen, D. Nuel, G. Buono, *Chem. Soc. Rev.* **2015**, *44*, 2508-2528.
- 6 a) T. Oshiki, T. Imamoto, *J. Am. Chem. Soc.* **1992**, *114*, 3975-3977; b) D. Gelman, L. Jiang, S. L. Buchwald, *Org. Lett.* **2003**, *5*, 2315-2318; c) D. V. Allen, D. Venkataraman, *J. Org. Chem.* **2003**, *68*, 4590-4593; d) M. Sun, Y.-S. Zang, L.-K. Hou, X.-X. Chen, W. Sun, S.-D. Yang, *Eur. J. Org. Chem.* **2014**, 6796-6801; e) J. Yang, J. Xiao, T. Chen, L.-B. Han, *J. Organomet. Chem.* **2016**, *820*, 120-124; f) R. Yu, X. Chen, Z. Wang, *Tetrahedron Lett.* **2016**, *57*, 3404-3406; g) Y. Hirai, Y. Uozumi, *Synlett* **2017**, *28*, 2966-2970.
- 7 a) V. Koshti, S. Gaikwad, S. H. Chikkali, *Coord. Chem. Rev.* **2014**, *265*, 52-73; b) C. A. Bange, R. Waterman, *Chem. Eur. J.* **2016**, *22*, 12598-12605.

- 8 a) M. A. Kazankova, I. V. Efimova, A. N. Kochetkov, V. V. Afanas'ev, I. P. Beletskaya, P. H. Dixneuf, *Synlett* **2001**, 2001, 0497-0500; b) M. O. Shulyupin, M. A. Kazankova, I. P. Beletskaya, *Org. Lett.* **2002**, 4, 761-763; c) M. A. Kazankova, M. O. Shulyupin, A. A. Borisenko, I. P. Beletskaya, *Russ. J. Org. Chem.* **2002**, 38, 1479-1484; d) A. Leyva-Pérez, J. A. Vidal-Moya, J. R. Cabrero-Antonino, S. S. Al-Deyab, S. I. Al-Resayes, A. Corma, *J. Organomet. Chem.* **2011**, 696, 362-367; e) K. J. Gallagher, R. L. Webster, *Chem. Commun.* **2014**, 50, 12109-12111; f) K. J. Gallagher, M. Espinal-Viguri, M. F. Mahon, R. L. Webster, *Adv. Synth. Catal.* **2016**, 358, 2460-2468.
- 9 a) H. Hu, C. Cui, *Organometallics* **2012**, 31, 1208-1211; b) B. Liu, T. Roisnel, J.-F. Carpentier, Y. Sarazin, *Chem. Eur. J.* **2013**, 19, 13445-13462; c) A. A. Trifonov, I. V. Basalov, A. A. Kissel, *Dalton Trans.* **2016**, 45, 19172-19193; d) A. N. Selikhov, G. S. Plankin, A. V. Cherkasov, A. S. Shavyrin, E. Louyriac, L. Maron, A. A. Trifonov, *Inorg. Chem.* **2019**, 58, 5325-5334.
- 10 a) D. Mimeau, O. Delacroix, A.-C. Gaumont, *Chem. Commun.* **2003**, 2928-2929; b) D. Mimeau, O. Delacroix, B. Join, A.-C. Gaumont, *C. R. Chimie* **2004**, 7, 845-854; c) Y. Moglie, M. J. González-Soria, I. Martín-García, G. Radivoy, F. Alonso, *Green Chem.*, **2016**, 18, 4896-4907; d) D. Bissessar, J. Egly, T. Achard, P. Steffanut, S. Bellemin-Lapponnaz, *RSC Adv.* **2019**, 9, 27250-27256.
- 11 S. Jin, G. C. Haug, V. T. Nguyen, C. Flores-Hansen, H. D. Arman, O. V. Larionov, *ACS Catal.* **2019**, 9, 9764-9774.
- 12 a) T. Migita, T. Nagai, K. Kiuchi, M. Kosugi, *Bull. Chem. Soc. Jpn.* **1983**, 56, 2869-2870; b) O. I. Kolodiazhnyi, in *Phosphorus Ylides: Chemistry and Applications in Organic Synthesis*, Wiley-VCH: New York, **1999**, pp. 11-29; c) D. Marcoux, A. B. Charette, *Adv. Synth. Catal.* **2008**, 350, 2967-2974; d) D. Marcoux, A. B. Charette, *J. Org. Chem.* **2008**, 73, 590-593.
- 13 a) E. Rémond, A. Tessier, F. R. Leroux, J. Bayardon, S. Jugé, *Org. Lett.* **2010**, 12, 1568-1571; b) W. Huang, C.-H. Zhong, *ACS Omega* **2019**, 4, 6690-6696.
- 14 A. F. Fearnley, J. An, M. Jackson, P. Lindovska, R. M. Denton, *Chem. Commun.* **2016**, 52, 4987-4990.
- 15 D. I. Bugaenko, A. A. Volkov, M. V. Livantsov, M. A. Yurovskaya, A. V. Karchava, *Chem. Eur. J.* **2019**, 25, 12502-12506.
- 16 a) H.-J. Cristau, A. Chêne, H. Christol, *J. Organomet. Chem.* **1980**, 185, 283-295; b) N. Nowrouzi, S. Keshtgar, E. Bahman Jahromi, *Tetrahedron Lett.* **2016**, 57, 348-350; c) W. Wan, X. Yang, R. C. Smith, *Chem. Commun.* **2017**, 53, 252-254.
- 17 a) D. Ravelli, M. Fagnoni, A. Albini, *Chem. Soc. Rev.* **2013**, 42, 97-113; b) N. A. Romero, D. A. Nicewicz, *Chem. Rev.* **2016**, 116, 10075-10166; c) K. Luo, W.-C.

- Yang, L. Wu, *Asian J. Org. Chem.* **2017**, *6*, 350-367; d) J. Twilton, C. Le, P. Zhang, M. H. Shaw, R. W. Evans, D. W. C. MacMillan, *Nature Reviews Chemistry* **2017**, *1*, 0052; e) C.-S. Wang, P. H. Dixneuf, J.-F. Soulé, *Chem. Rev.* **2018**, *118*, 7532-7585; f) L. Marzo, S. K. Pagire, O. Reiser, B. König, *Angew. Chem. Int. Ed.* **2018**, *57*, 10034-10072.
- 18 U. Lennert, P. B. Arockiam, V. Streitferdt, D. J. Scott, C. Rödl, R. M. Gschwind, R. Wolf, *Nat Catal* **2019**, *2*, 1101-1106.
- 19 E. Speckmeier, T. G. Fischer, K. Zeitler, *J. Am. Chem. Soc.* **2018**, *140*, 15353-15365.
- 20 For example, the reduction potential of **2** is reported to be slightly lower than that of [1]⁺. Thus, Ar-I reduction may be more facile using this photocatalyst, which may promote complete arylation.
- 21 Attempts to use other alkyl bromides were unsuccessful, presumably due to their overly negative reduction potentials.
- 22 a) O. Akihiro, T. Yoshiaki, (Showa Denko K. K., Japan), JP 2007169475A, **2007**;
b) O. Akihiro, T. Yoshiaki, (Showa Denko K. K., Japan), JP 2008010647A, **2008**;
c) Y. Ch, L.-M. Huang, (National Tsing Hua University), US 8,722,885 B1, **2014**
- 23 Formation of the radical adduct TEMPO-Cy could be detected by GC-MS (see SI).
- 24 H. Iwahashi, Y.-i. Ishikawa, S. Sato, K. Koyano, *Bull. Chem. Soc. Jpn.* **1977**, *50*, 1278-1281.
- 25 Due to the line-broadening of the spectrum recorded at room temperature the formation of other alkyl or aryl radicals cannot be definitively excluded (see the Supporting Information for details).
- 26 An alternative mechanism could involve I atom abstraction mediated by DIPEA-derived radicals, as described recently by Leonori et al. doi: 10.1126/science.aba2419.
- 27 a) M. E. van der Boom, D. Milstein, *Chem. Rev.* **2003**, *103*, 1759-1792; b) W.-C. Shih, O. V. Ozerov, *Organometallics* **2015**, *34*, 4591-4597.

3.5 SUPPORTING INFORMATION

3.5.1 General Information

All reactions and manipulations were performed under an N₂ atmosphere (< 0.1 ppm O₂, H₂O) through use of an MBraun Unilab glovebox. All glassware was oven-dried (160 °C) overnight prior to use. Benzene was dried over Na and stored over molecular sieves (3 Å). Acetonitrile were distilled from CaH₂ and stored over molecular sieves (3 Å). Benzene was distilled from K and stored over molecular sieves (3 Å). C₆D₆ and CDCl₃ was stored over molecular sieves (3 Å). All other chemicals were purchased from major suppliers (Aldrich, ABCR, Alfa Aesar), liquids were purified by Kugelrohr distillation and freeze-pump-thaw degassed three times prior use; P₄ and Ph₃PO were purified by sublimation; all others were used as received.

GC-MS spectra were recorded using a mass detector model Agilent-5977B coupled with a GC oven 7820A and a Restek 5 Sil MS column with H₂ as carrier gas, using a 30 m × 0.25 mm × 0.25 μm column. Injection parameters: temperature of injection = 250 °C, split ratio = 25/1, volume injected = 1 μL, flow rate = 1.2 mL/ min. Oven parameters: starting temperature = 50 °C, rate = 15 °C/ min, end temperature = 300 °C, held for 5 min. Mass parameters: Temp source = 230 °C, Quad temperature = 150 °C, start mass = 50.00, end mass = 550.00.

NMR spectra were recorded at room temperature on Bruker Avance 400 (400 MHz) spectrometers and were processed using Topspin 3.2. Chemical shifts, δ, are reported in parts per million (ppm); ¹H NMR and ¹³C NMR shifts are reported relative to SiMe₄ and were referenced internally to residual solvent peaks, while ³¹P NMR shifts were referenced externally to 85 % H₃PO₄ (aq.). NMR samples were prepared in the glovebox using NMR tubes fitted with screw caps.

Quantitative ³¹P{¹H} NMR spectra were recorded using only a single scan (NS = 1, DS = 0, D1 = 2s). The accuracy of this method was confirmed by preparing solutions of (*o*-tolyl)₃P or Ph₄PCl and 0.05 mmol Ph₃PO in MeCN/benzene (1.5 mL, 0.5 mL, respectively), and comparing the measured and expected relative integrations (Chapter 2.5.1, Supplementary Figure 1).

3.5.2 Experimental Procedures

3.5.2.1 General procedures for small scale reactions

Supplementary Method 1. General procedure for photocatalytic synthesis of unsymmetrically substituted triarylphosphines and tetraarylphosphonium salts from HPPh₂ using [1]PF₆ (0.1 mmol scale)

In a 10 mL stoppered tube equipped with a stirring bar, the appropriate aryl iodides (0.30 mmol, 3 equiv. based on HPPh₂), Et₃N (8.6 mmol, 8.6 equiv.), catalyst [1]PF₆ (1 μmol, 1 mol%), and HPPh₂ (0.10 mmol, 1.0 equiv.) were added to 1.5 mL acetonitrile and 0.5 mL benzene in an N₂ filled glove box. The tube was sealed, placed in a water-cooled block to maintain near-ambient temperature (Chapter 2.5.2, Supplementary Figure 2), and irradiated with blue light (455 nm (±15 nm), 3.2 V, 700 mA, Osram OSRON SSL 80) for 18 h. A solution of Ph₃PO (0.05 mmol) in approximately 0.5 mL of benzene was subsequently added to act as an internal standard. The resulting mixture was subjected to NMR analysis.

Supplementary Method 2. General procedure for photocatalytic synthesis of unsymmetrically substituted triarylphosphines and tetraarylphosphonium salts from HPPh₂ using 3DPAFIPN (0.1 mmol scale)

In a 10 mL stoppered tube equipped with a stirring bar, the appropriate aryl iodide (0.30 mmol, 3.0 equiv. based on HPPh₂), Et₃N (2.4 mmol, 2.4 equiv.), catalyst 3DPAFIPN (0.5 μmol, 0.5 mol%), and HPPh₂ (0.10 mmol, 1.0 equiv.) were added to 2 mL acetonitrile in an N₂ filled glove box. The tube was sealed, placed in a water-cooled block to maintain near-ambient temperature (Chapter 2.5.2, Supplementary Figure 2), and irradiated with blue light (455 nm (±15 nm), 3.2 V, 700 mA, Osram OSRON SSL 80) for 18 h. A solution of Ph₃PO (0.050 mmol) in approximately 0.5 mL of benzene was subsequently added to act as an internal standard. The resulting mixture was subjected to NMR analysis.

Supplementary Method 3. General procedure for photocatalytic synthesis of unsymmetrically substituted triarylphosphines and tetraarylphosphonium salts from H₂PPh using 3DPAFIPN (0.1 mmol scale)

In a 10 mL stoppered tube equipped with a stirring bar, the appropriate aryl iodide derivative (0.50 mmol, 5.0 equiv. based on H₂PPh), Et₃N (5.0 mmol, 5.0 equiv.), catalyst 3DPAFIPN (2 μmol, 2 mol%), and H₂PPh (0.10 mmol, 1.0 equiv.) were added to 1.5 mL acetonitrile and 0.5 mL benzene in an N₂ filled glove box. The tube was sealed, placed in a water-cooled block to maintain near-ambient temperature (Chapter 2.5.2, Supplementary Figure 2), and irradiated with blue light (455 nm (±15 nm), 3.2 V, 700

mA, Osram OSOLON SSL 80) for 18 h. A solution of Ph_3PO (0.05 mmol) in approximately 0.5 mL of benzene was subsequently added to act as an internal standard. The resulting mixture was subjected to NMR analysis.

Supplementary Method 4. General procedure for photocatalytic synthesis of unsymmetrically substituted tertiary aryl/alkylphosphines from HPPh_2 using 3DPAFIPN (0.2 mmol scale)

In a 10 mL stoppered tube equipped with a stirring bar, the appropriate iodoalkane derivative (unless stated otherwise, refer to Table 4) (0.40 mmol, 2.0 equiv. based on HPPh_2), DIPEA (0.40 mmol, 2.0 equiv.), catalyst 3DPAFIPN (0.40 μmol , 0.20 mol%; unless stated otherwise, refer to Table 4), and HPPh_2 (0.10 mmol, 1.0 equiv.) were added to 2 mL acetonitrile in an N_2 filled glove box. The tube was sealed, placed in a water-cooled block to maintain near-ambient temperature (Chapter 2.5.2, Supplementary Figure 2), and irradiated with blue light (455 nm (± 15 nm), 3.2 V, 700 mA, Osram OSOLON SSL 80) for 24 h (unless stated otherwise, refer to Table 4). A solution of Ph_3PO (0.050 mmol) in approximately 0.5 mL of benzene was subsequently added to act as an internal standard. The resulting mixture was subjected to NMR analysis.

Supplementary Method 5. General procedure for photocatalytic synthesis of unsymmetrically substituted tertiary aryl/alkylphosphines and quaternary aryl/alkyl phosphonium salts from H_2PPh using 3DPAFIPN (0.2 mmol scale)

In a 10 mL stoppered tube equipped with a stirring bar, the appropriate iodoalkane derivative (unless stated otherwise, refer to Table 5) (0.80 mmol, 4.0 equiv. based on H_2PPh), DIPEA (6.0 mmol, 3.0 equiv.), catalyst 3DPAFIPN (0.40 μmol , 0.20 mol%; unless stated otherwise, refer to Table 5), and H_2PPh (0.20 mmol, 1.0 equiv.) were added to 2 mL acetonitrile in an N_2 filled glove box. The tube was sealed, placed in a water-cooled block to maintain near-ambient temperature (Chapter 2.5.2, Supplementary Figure 2), and irradiated with blue light (455 nm (± 15 nm), 3.2 V, 700 mA, Osram OSOLON SSL 80) for 24 h. A solution of Ph_3PO (0.05 mmol) in approximately 0.5 mL of benzene was subsequently added to act as an internal standard. The resulting mixture was subjected to NMR analysis.

Supplementary Method 6. General procedure for photocatalytic synthesis of unsymmetrically substituted tertiary aryl/alkylphosphines from P_2Ph_4 using 3DPAFIPN (0.2 mmol scale)

In a 10 mL stoppered tube equipped with a stirring bar, the appropriate iodoalkane derivative (0.60 mmol, 1.5 equiv. based on phosphorus atom), DIPEA (0.6 mmol, 1.5 equiv. based on phosphorus atom), catalyst 3DPAFIPN (0.40 μmol , 0.20 mol%), and P_2Ph_4 (0.20 mmol, 1.0 equiv.) were added to 2 mL acetonitrile in an N_2 filled glove box.

The tube was sealed, placed in a water-cooled block to maintain near-ambient temperature (Chapter 2.5.2, Supplementary Figure 2), and irradiated with blue light (455 nm (± 15 nm), 3.2 V, 700 mA, Osram OSOLON SSL 80) for 24 h. A solution of Ph_3PO (0.050 mmol) in approximately 0.5 mL of benzene was subsequently added to act as an internal standard. The resulting mixture was subjected to NMR analysis.

Supplementary Method 7. General procedure for photocatalytic synthesis of PCP pincer type ligand from P_2Ph_4 using 3DPAFIPN (0.1 mmol scale)

In a 10 mL stoppered tube equipped with a stirring bar, **1,3-bis(bromomethyl)benzene** (0.10 mmol, 1.0 equiv.), DIPEA (0.40 mmol, 4.0 equiv.), catalyst 3DPAFIPN (0.50 μmol , 0.50 mol%), and P_2Ph_4 (0.15 mmol, 1.5 equiv.) were added to 1.5 mL acetonitrile and 0.5 mL benzene in an N_2 filled glove box. The tube was sealed, placed in a water-cooled block to maintain near-ambient temperature (Chapter 2.5.2, Supplementary Figure 2), and irradiated with blue light (455 nm (± 15 nm), 3.2 V, 700 mA, Osram OSOLON SSL 80) for 24 h. A solution of Ph_3PO (0.050 mmol) in approximately 0.5 mL of benzene was subsequently added to act as an internal standard. The resulting mixture was subjected to NMR analysis.

Supplementary Method 8. General procedure for photocatalytic functionalisation of P_4 using 3DPAFIPN (0.1 mmol scale)

In a 10 mL stoppered tube equipped with a stirring bar, the appropriate aryl iodide (1.1 mmol, 11 equiv. based on the phosphorus atom), Et_3N (1.44 mmol, 14.4 equiv., based on the phosphorus atom), catalyst 3DPAFIPN (1.2 μmol , 1.2 mol%, based on the phosphorus atom), and P_4 (0.025 mmol, 1 equiv.) were added to 1.5 mL acetonitrile and 0.5 mL benzene in an N_2 filled glove box. The tube was sealed, placed in a water-cooled block to maintain near-ambient temperature (Chapter 2.5.2, Supplementary Figure 2), and irradiated with blue light (455 nm (± 15 nm), 3.2 V, 700 mA, Osram OSOLON SSL 80) for 24 h (unless stated otherwise, refer to Table 6). A solution of Ph_3PO (0.03 mmol) in approximately 0.3 mL of benzene was subsequently added to act as an internal standard. The resulting mixture was subjected to NMR analysis.

3.5.3 General procedures for increased scale reactions

Supplementary Method 9. Photocatalytic preparation of diphenyl((2-trifluoromethyl)phenyl)phosphine from HPPh₂ using 3DPAFIPN (1 mmol scale, Table 2, I-1)

In a 50 ml stoppered tube equipped with a stirring bar, 2-trifluoromethylphenyl iodide (421 μL , 3.00 mmol, 3.00 equiv. based on the phosphorus atom), Et₃N (335 μL , 2.40 mmol, 2.40 equiv.), catalyst 3 DPAFIPN (3.2 mg, 0.50 mol%), and HPPh₂ (174 μL , 1.00 mmol, 1.00 equiv.) were added to 20 mL acetonitrile in an N₂ filled glove box. The tube was sealed, placed in a water-cooled block to maintain near-ambient temperature (Chapter 2, Supplementary Figure 19), and irradiated with blue light (7X Osram OSRON SSL80, 455 nm (± 15 nm), 20.3 V 1000mA) for 18 h. The solvent and other volatiles were evaporated *in vacuo* at 100 °C, and the residue kept under vacuum for 2 h. The resulting yellowish residue was sublimed (*ca.* 1 x 10⁻² mbar, 120 °C and 100 °C) twice to obtain diphenyl((2-trifluoromethyl)phenyl)phosphine as colorless solid (175.5 mg, 53%).

Supplementary Method 10. General procedure for photocatalytic synthesis of unsymmetrically substituted tertiary aryl/alkylphosphines from HPPh₂ using 3DPAFIPN (1 mmol scale)

In a 50 mL stoppered tube equipped with a stirring bar, the appropriate haloalkane derivative (2.0 mmol, 2.0 equiv. based on HPPh₂), DIPEA (2.0 mmol, 2.0 equiv.), catalyst 3DPAFIPN (5.0 μmol , 0.50 mol%), and HPPh₂ (1.0 mmol, 1.0 equiv.) were added to 10 mL acetonitrile in an N₂ filled glove box. The tube was sealed, placed in a water-cooled block to maintain near-ambient temperature (Chapter 2.5.3, Supplementary Figure 19), and irradiated with blue light (7X Osram OSRON SSL80, 455 nm (± 15 nm), 20.3 V 1000 mA) for 24 h. After, the solvent was evaporated and purification by flash chromatography on silica gel eluted with 5 – 10% of Et₂O in hexane, provided the tertiary phosphine as pure compounds.

Supplementary Method 11. General procedure for photocatalytic synthesis of unsymmetrically substituted tertiary aryl/alkylphosphines from H₂PPh using 3DPAFIPN (1 mmol scale)

In a 50 mL stoppered tube equipped with a stirring bar, the appropriate haloalkane derivative (4.0 mmol, 4.0 equiv. based on HPPh₂), DIPEA (3.0 mmol, 3.0 equiv.), catalyst 3DPAFIPN (5.0 μmol , 0.50 mol%), and H₂PPh (1.0 mmol, 1.0 equiv.) were added to 10 mL acetonitrile in an N₂ filled glove box. The tube was sealed, placed in a water-cooled block to maintain near-ambient temperature (Chapter 2.5.3, Supplementary Figure 19), and irradiated with blue light (7X Osram OSRON SSL80, 455 nm (± 15 nm), 20.3 V 1000 mA) for 24 h. After, the solvent was evaporated and purification by flash

chromatography on silica gel eluted with 5 – 10% of Et₂O in hexane, provided the tertiary phosphine as pure compounds.

Supplementary Method 12. Photocatalytic preparation of 1,3-bis((diphenylphosphanyl)methyl) benzene from P₂Ph₄ (Scheme 2, V-15)

In a 50 ml stoppered tube equipped with a stirring bar, 1,3-bis(bromomethyl)benzene (0.50 mmol, 1.0 equiv.), DIPEA (2.0 mmol, 4.0 equiv.), catalyst 3DPAFIPN (2.5 μmol, 0.50 mol%), and P₂Ph₄ (0.75 mmol, 1.5 equiv.) were added to 7.5 mL acetonitrile and 2.5 mL benzene in an N₂ filled glove box. The tube was sealed, placed in a water-cooled block to maintain near-ambient temperature (Chapter 2.5.3, Supplementary Figure 19), and irradiated with blue light (7X Osram OSLOM SSL80, 455 nm (±15 nm), 20.3 V 1000mA) for 24 h. The solvent was evaporated and purification by flash chromatography on silica gel eluted with 5 – 10% of Et₂O in hexane provided 1,3-bis((diphenylphosphanyl)methyl)benzene as colourless oil in 61% yield (144.3 mg).

Supplementary Method 13. Photocatalytic preparation of tetraphenylphosphonium iodide from P₄ using 3DPAFIPN (1 mmol scale, Table 6, IX-1)

In a 50 ml stoppered tube equipped with a stirring bar, iodobenzene (1.23 mL, 11 mmol, 11 equiv. based on the phosphorus atom), Et₃N (2007 μL, 14.4 mmol, 14.4 equiv.), catalyst 3DPAFIPN (7.7 mg, 1.2 mol%), and P₄ (30.9 mg, 0.25 mmol, 1 equiv.) were added to 15 mL acetonitrile and 5 mL benzene in an N₂ filled glove box. The tube was sealed, placed in a water-cooled block to maintain near-ambient temperature (Chapter 2.5.3, Supplementary Figure 19), and irradiated with blue light (7X Osram OSLOM SSL80, 455 nm (±15 nm), 20.3 V 1000 mA) for 24 h. The solvent and other volatiles was evaporated *in vacuo* at 100 °C, and the residue kept under vacuum for 1 h. The product was crystallised twice from ethanol at 2 °C over the course of two days and isolated by filtration at 0 °C. The resulted off white powder was dried under high vacuum to obtain tetraphenylphosphoniumiodide in 24% yield (112.5 mg).

Supplementary Method 14. Photocatalytic preparation of tri(o-tolyl)phosphine from P₄ using 3DPAFIPN (1 mmol scale, Table 6, VIII-2)

In a 50 ml stoppered tube equipped with a stirring bar, 2-iodotoluene (1492 μL, 11.0 mmol, 11.0 equiv. based on the phosphorus atom), Et₃N (2007 μL, 14.4 mmol, 14.4 equiv.), catalyst 3DPAFIPN (7.7 mg, 1.2 mol%), and P₄ (30.9 mg, 0.25 mmol, 1 equiv.) were added to 15 mL acetonitrile and 5 mL benzene in an N₂ filled glove box. The tube was sealed, placed in a water-cooled block to maintain near-ambient temperature (Supplementary Figure 19), and irradiated with blue light (7X Osram OSLOM SSL80, 455 nm (±15 nm), 20.3 V 1000mA) for 24 h. The solvent and other

volatiles was evaporated *in vacuo* at 100 °C, and the residue kept under vacuum for 1 h. The resulting yellowish residue was sublimed (ca. 3×10^{-1} mbar, 100 °C) twice to obtain *tri(o-tolyl)phosphine* as colorless solid (131.7 mg, 43%).

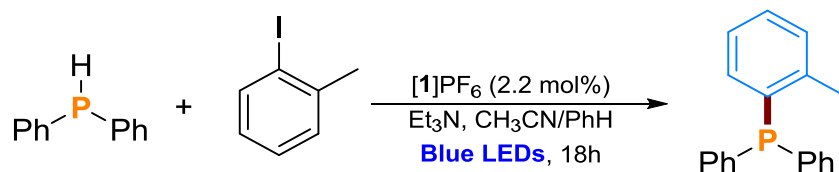
Supplementary Method 15. Photocatalytic preparation of tris(2-methoxyphenyl)phosphine from P₄ using 3DPAFIPN (1 mmol scale, Table 6, VIII-3)

In a 50 ml stoppered tube equipped with a stirring bar, 2-iodoanisole (1431 μ L, 11.0 mmol, 11.0 equiv. based on the phosphorus atom), Et₃N (2007 μ L, 14.4 mmol, 14.4 equiv.), catalyst 3DPAFIPN (7.70 mg, 1.20 mol%), and P₄ (30.9 mg, 0.250 mmol, 1.00 equiv.) were added to 15 mL acetonitrile and 5 mL benzene in an N₂ filled glove box. The tube was sealed, placed in a water-cooled block to maintain near-ambient temperature (Supplementary Figure 19), and irradiated with blue light (7X Osram OSLON SSL80, 455 nm (\pm 15 nm), 20.3 V 1000 mA) for 24 h. The solvent and other volatiles were evaporated *in vacuo* at 100 °C, and the residue kept under vacuum for 1 h. The target compound crystallised from hot ethanol as pale yellow powder (42.4 mg, 12%).

Supplementary Method 16. Photocatalytic preparation of tris(2-(methylthio)phenyl)phosphine from P₄ using 3DPAFIPN (1 mmol scale, Table 6, VIII-4)

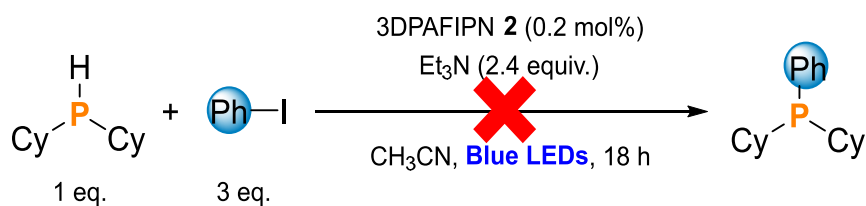
In a 50 ml stoppered tube equipped with a stirring bar, 2-iodothioanisole (1600 μ L, 11.0 mmol, 11.0 equiv. based on the phosphorus atom), Et₃N (2007 μ L, 14.4 mmol, 14.4 equiv.), catalyst 3DPAFIPN (7.7 mg, 1.20 mol%), and P₄ (30.9 mg, 0.250 mmol, 1.00 equiv.) were added to 15 mL acetonitrile and 5 mL benzene in an N₂ filled glove box. The tube was sealed, placed in a water-cooled block to maintain near-ambient temperature (Supplementary Figure 19), and irradiated with blue light (7X Osram OSLON SSL80, 455 nm (\pm 15 nm), 20.3 V 1000 mA) for 18 h. The solvent and other volatiles was evaporated *in vacuo* at 100 °C, and the residue kept under vacuum for 1 h. The targeted compound was precipitated as a white powder (63.8 mg, 16%) from hot ethanol.

3.5.4 Table for optimisation reactions

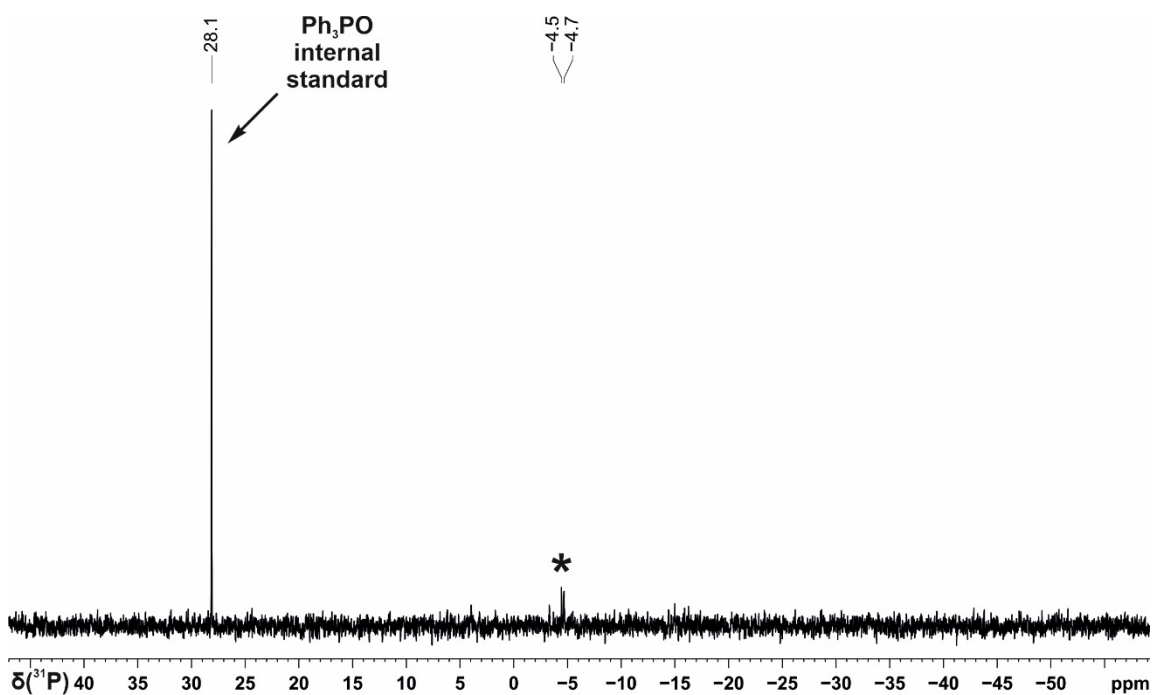
Supplementary Table 1. Photocatalytic arylation of Ph₂PH to Ph₂PAr catalysed by [1]PF₆.

Entry	Conditions ^[a]	Conv. to Ph ₂ PAr (%) ^[b]
1	standard	63
2	no ArI	0
3	no [1]PF ₆	0
4	no light	0
5	no Et ₃ N	0

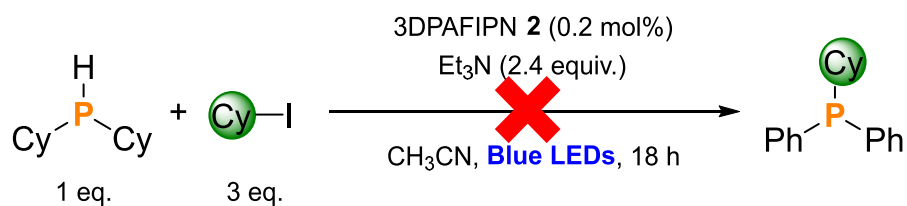
[a] All reactions were carried out using HPPH₂ (0.1 mmol, 1 equiv.), 2-iodotoluene (0.4 mmol, 4 equiv.), [1]PF₆ (2.2 mol%) and Et₃N (14 mmol, 14 equiv.) in CH₃CN/PhH (3:1 v/v, 2 mL) under an N₂ atmosphere and blue LED irradiation (λ_{max} = 455nm) for 18 h. [b] Yields were calculated using quantitative ³¹P{¹H} NMR experiments with PPh₃O as an internal standard. [1]PF₆ = [Ir(dtbbpy)(ppy)₂]PF₆.

Supplementary Scheme 1. Photocatalytic arylation of Cy₂PH with iodobenzene

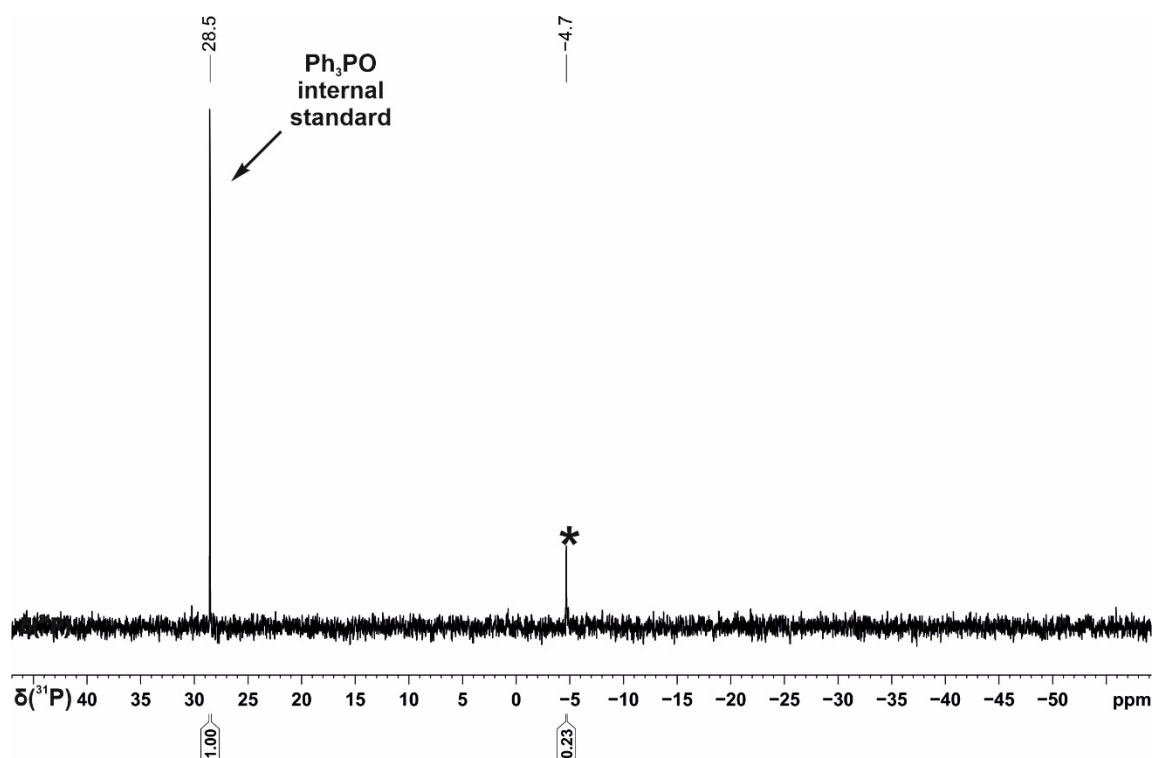
The general procedure 2 was followed using iodobenzene (34 μL , 0.3 mmol) and dicyclohexylphosphine (20 μL , 0.1 mmol) which resulted in degradation of dicyclohexylphosphine.



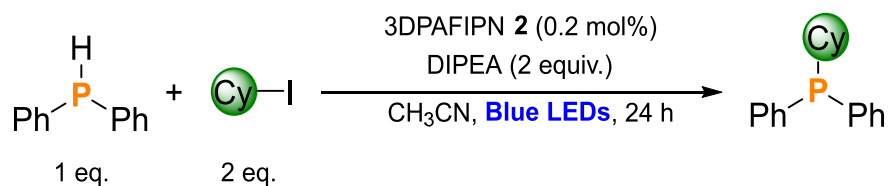
Supplementary Figure 1. Quantitative single scan $^{31}\text{P}\{^1\text{H}\}$ (zgig) NMR spectrum for the photocatalytic arylation of HPCy₂ using iodobenzene. * marks signal of unknown compound.

Supplementary Scheme 2. Photocatalytic alkylation of Cy₂PH with cyclohexyl iodide

The general procedure 2 was followed using cyclohexyl iodide (39 μL , 0.3 mmol) and dicyclohexylphosphine (20 μL , 0.1 mmol) which resulted in degradation of dicyclohexylphosphine.

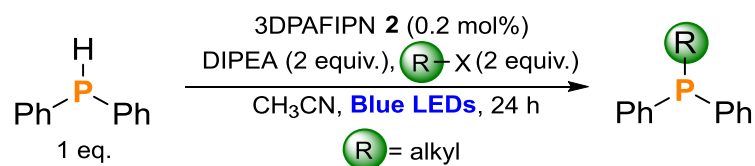


Supplementary Figure 2. Quantitative single scan $^{31}\text{P}\{^1\text{H}\}$ (zgig) NMR spectrum for the photocatalytic alkylation of dicyclohexylphosphine using cyclohexyl iodide. * marks signal of unknown compound.

Supplementary Table 2. Control experiments for the photocatalytic synthesis of PPh₂Cy from HPPh₂

Entry	Conditions ^[a]	Conv. to Ph ₂ PCy (%) ^[b]
1	standard	81
2	no Cy-I	0
3	no 3DPAFIPN	0
4	no irradiation	0
5	no DIPEA	0

[a] All reactions were carried out using HPPh₂ (0.2 mmol, 1 equiv.), Cy-I (0.4 mmol, 2 equiv.), 3DPAFIPN (0.2 mol%) and DIPEA (0.4 mmol, 2 equiv.) in CH₃CN (2 mL) under an N₂ atmosphere and blue LED irradiation ($\lambda_{\text{max}} = 455\text{nm}$) for 24 h. [b] Conversions were calculated using quantitative ³¹P{¹H} NMR experiments with PPh₃O as an internal standard.

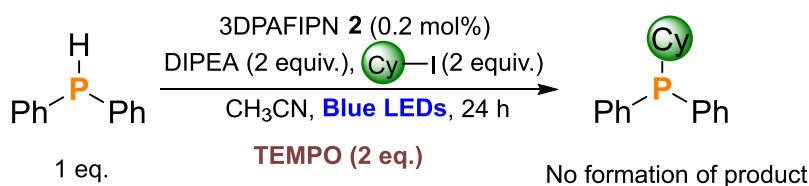
Supplementary Table 3. Control experiments for the photocatalytic synthesis of unsymmetrically substituted tertiary phosphines from HPPH_2 ^[a]

Entry	R-X	Conv. to Ph_2PR (%) ^[b]
1		0 ^[c] , 0 ^[d]
2		0 ^[c] , 0 ^[d]
3		0 ^[c] , 35 ^[d]
4		0 ^[c] , 50 ^[d]
5		0 ^[c] , 0 ^[d]
6		0 ^[c] , 0 ^[d]

[a] All reactions were carried out using HPPH_2 (0.2 mmol, 1 equiv.), R-I (0.4 mmol, 2 equiv.), 3DPAFIPN (0.2 mol%) and DIPEA (0.4 mmol, 2 equiv.) in CH_3CN (2 mL) under an N_2 atmosphere and blue LED irradiation ($\lambda_{\text{max}} = 455\text{nm}$) for 24 h. [b] Conversions were calculated using quantitative $^{31}\text{P}\{^1\text{H}\}$ NMR experiments with PPh_3O as an internal standard. [c] Reactions performed in absence of light. [d] Reactions performed in absence of photocatalyst 3DPAFIPN.

3.5.5 Mechanistic studies

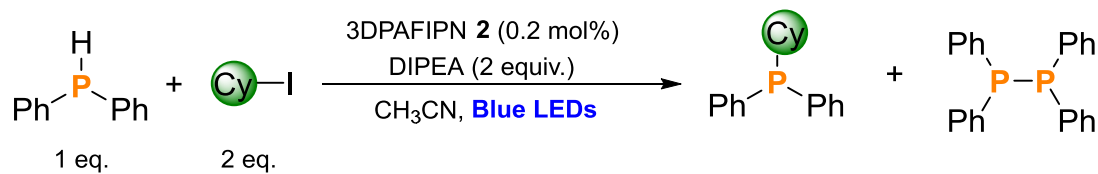
3.5.5.1 Radical trapping experiments



Supplementary Scheme 3. Standard reaction in the presence of radical scavenger TEMPO

In a 10 mL stoppered tube equipped with a stirring bar, cyclohexyl iodide (0.4 mmol, 2 equiv. based on HPPh₂), DIPEA (0.40 mmol, 2.0 equiv.), 3DPAFIPN (0.40 μmol, 0.20 mol%), TEMPO (0.40 mmol, 2.0 equiv.) and HPPh₂ (0.10 mmol, 1.0 equiv.) were added to 2 mL acetonitrile in an N₂ filled glove box. The tube was sealed, placed in a water-cooled block to maintain near-ambient temperature (Supplementary Figure 2), and irradiated with blue light (455 nm (±15 nm), 3.2 V, 700 mA, Osram OSOLON SSL 80) for 24 h. The resulting mixture was subjected to GC/MS analysis. After, a solution of Ph₃PO (0.050 mmol) in approximately 0.5 mL of benzene was subsequently added to act as an internal standard and recorded ³¹P{¹H} NMR spectroscopy. We observed that TEMPO completely inhibited the formation of PPh₂Cy, and a small amount of addition product TEMPO-Cy was observed in GC/MS indicating that a radical pathway was involved.

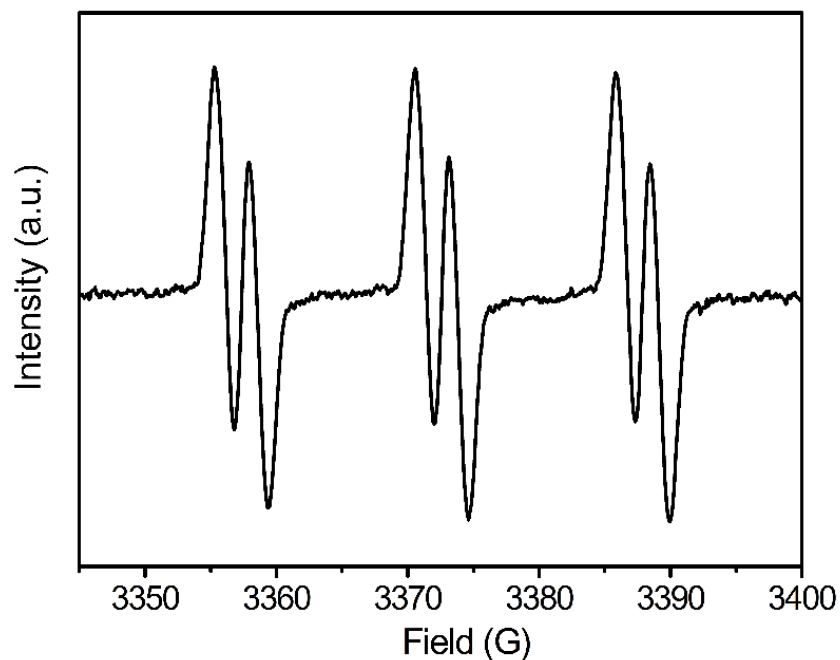
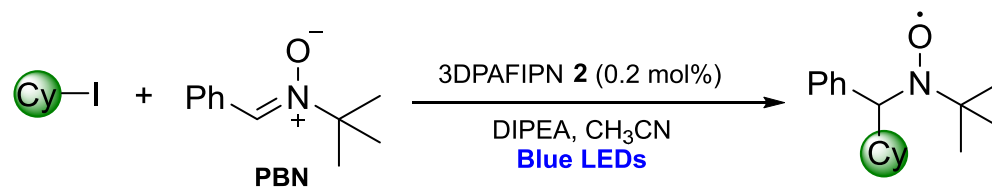
3.5.5.2 Analysis of intermediates

Supplementary Table 4. Formation of tetraphenyl diphosphine as intermediate in photocatalytic synthesis of PPh₂Cy from HPPh₂^[a]

Entry	Variation from standard conditions ^[a]	Time	Conv. to Ph ₂ PCy (%) ^[b]	Conv. to Ph ₄ P ₂ (%) ^[b]
1	none	18 h	81	0
2	none	2 h	2	86
3	no 3DPAFIPN	18 h	2	78
4	no 3DPAFIPN	2 h	0	5
5	no irradiation	2 h	0	3
6	no Cy-I	18 h	0	0
7	no DIPEA	18 h	0	0

[a] All reactions were carried out using HPPh₂ (0.2 mmol, 1 equiv.), Cy-I (0.4 mmol, 2 equiv.), 3DPAFIPN (0.2 mol%) and DIPEA (0.4 mmol, 2 equiv.) in CH₃CN (2 mL) under an N₂ atmosphere and blue LED irradiation ($\lambda_{\text{max}} = 455\text{nm}$) for respective time. [b] Conversions were calculated using quantitative ³¹P{¹H} NMR experiments with PPh₃O as an internal standard.

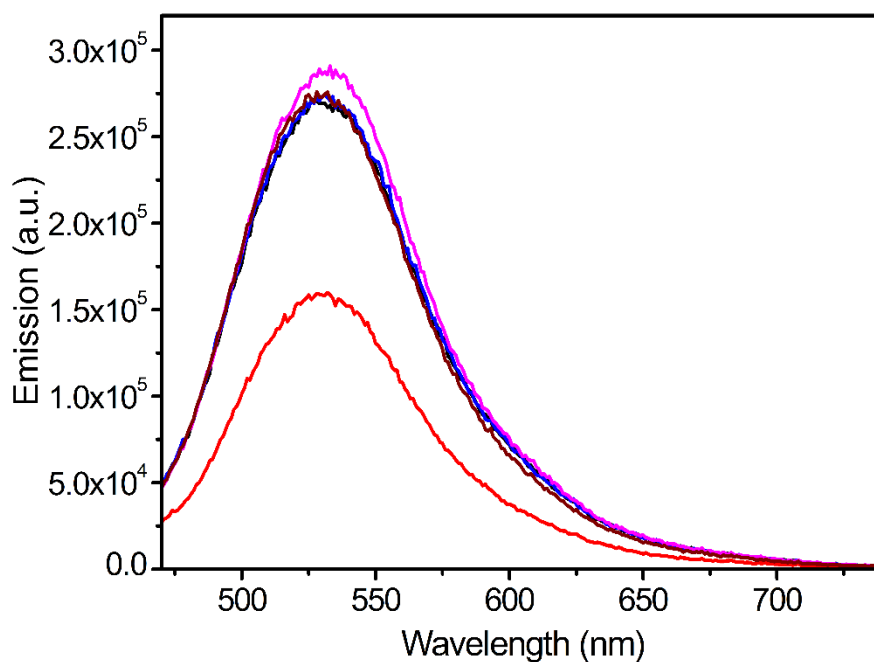
3.5.5.3 EPR studies



Supplementary Figure 3. EPR spectrum of the solution of 3DPAFIPN ($c = 0.0001$ M), DIPEA ($c = 0.015$ M), Cyclohexyl iodide ($c = 0.01$ M) and α -phenyl-*N*-*tert*-butylnitron (PBN) ($c = 0.001$ M) in acetonitrile at room temperature under an N_2 atmosphere and blue LED irradiation ($\lambda_{\text{max}} = 455\text{nm}$). The EPR spectrum is consistent with the previously reported spectrum.^[S1] Observed EPR parameters: $a^{\text{N}} = 15.2$ G, $a^{\text{H}} = 2.5$ G; Previously reported values for γ radiolysis of PBN in cyclohexane: $a^{\text{N}} = 14.5 \pm 0.2$ G, $a^{\text{H}} = 2.2 \pm 0.2$ G.

3.5.5.4 Emission quenching experiments

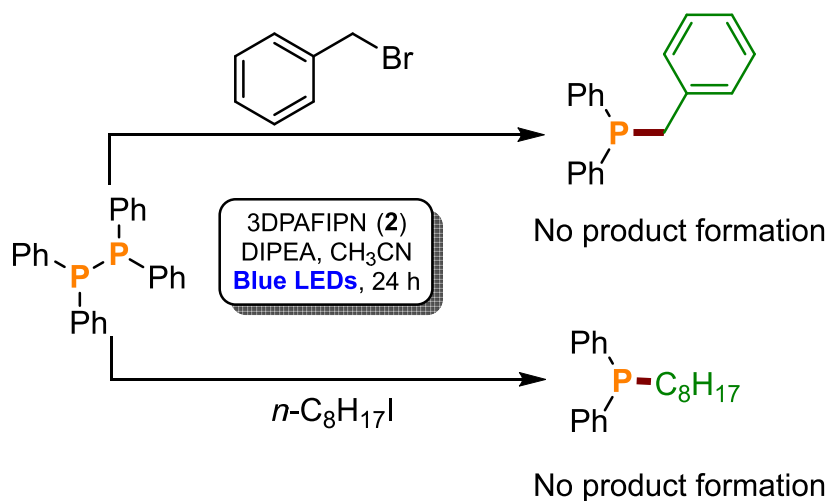
Emission quenching studies were performed using Fluoromax-4 Spectrofluorometer. A cuvette containing 3DPAFIPN (3.5×10^{-6} M) in an MeCN solution were irradiated at 455 nm and fluorescence was measured. The maximum emission intensity was obtained at $\lambda_{\text{max}} = 530$ nm (*c.f.* 525 nm, reported in MeCN).^[S2] The experiment was then repeated in the presence of potential quenchers (3500 equiv.). Significant emission quenching was only observed in the presence of DIPEA.



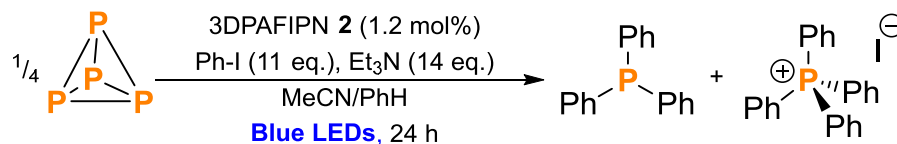
Supplementary Figure 4. Fluorescence emission spectrum for a 3.5×10^{-6} M solution of 3DPAFIPN in MeCN in the presence of potential quenchers (3500 equiv.). Emission spectrum of 3DPAFIPN in MeCN (black) and in the presence of DIPEA (red), iodocyclohexane (blue), HPPH₂ (magenta) and P₂Ph₄ (brown).

3.5.6 Reactions with tetraphenyl diphosphine with primary alkyl halides

The general procedure 6 was followed using benzyl bromide (36 μL , 0.30 mmol) or *n*-octyl iodide (54 μL , 0.3 mmol). No formation of corresponding tertiary phosphines was observed. These results suggest that there might be a different mechanism likely to be operative with primary halides.



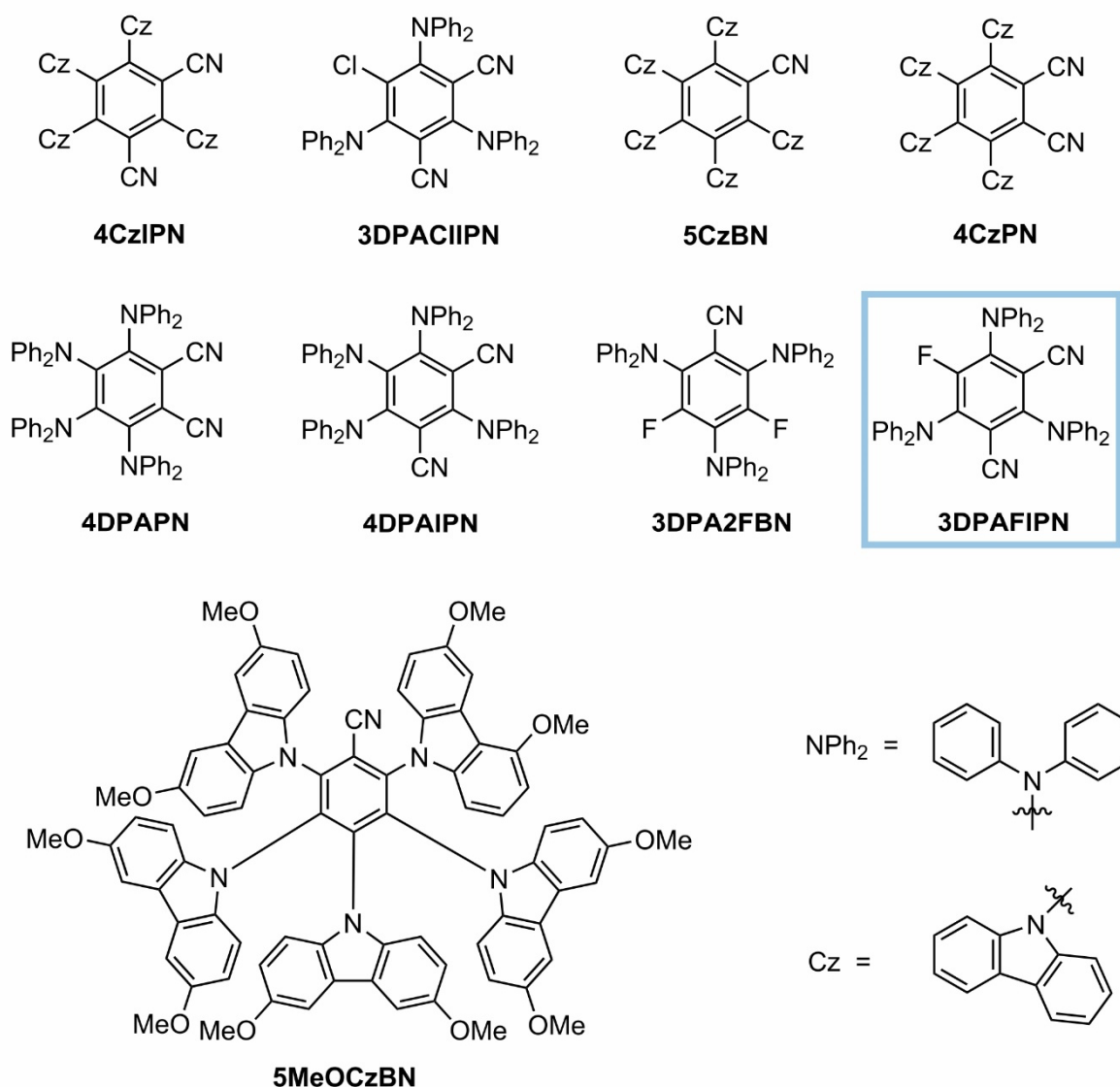
Supplementary Scheme 4. Reaction of tetraphenyl diphosphine with benzyl bromide or *n*-octyl iodide

3.5.7 Functionalisation of P₄ with organic photocatalyst**Supplementary Table 5.** Photocatalytic functionalisation of P₄ to [Ph₄P]⁺: screening of photocatalysts and control experiments^[a]

Entry	Variation from standard conditions ^[a]	Conv. to Ph ₃ P (%) ^[b]	Conv. to [Ph ₄ P] ⁺ I ⁻ (%) ^[b]
1	none	0	60
2	4CzIPN	20	22
3	3DPACIIPN	8	0
4	5CzBN	21	17
5	5MeOCzBN	8	0
6	4CzPN	0	0
7	4DPAPN	0	20
8	4DPAIPN	0	10
9	3DPA2FBN	10	11
11	no 3DPAFIPN	0	0
12	no P ₄	0	0
13	no PhI	0	0
14	no Et ₃ N	0	0
15	no light	0	0

[a] All the reactions was carried out using P₄ (0.025 mmol, 1 equiv.), Ph-I (1.1 mmol, 11 equiv. based on phosphorus atom), 3DPAFIPN (1.2 mol% based on phosphorus atom) and Et₃N (1.4 mmol, 14.4 equiv. based on phosphorus atom) in CH₃CN/PhH (3:1 v/v, 2 mL) under an N₂ atmosphere and blue LED irradiation (λ_{max} = 455 nm) for 18 h; [b] Yields were determined by quantitative ³¹P{¹H} NMR analysis of the reaction mixture with PPh₃O as an internal standard.

Organic photocatalysts



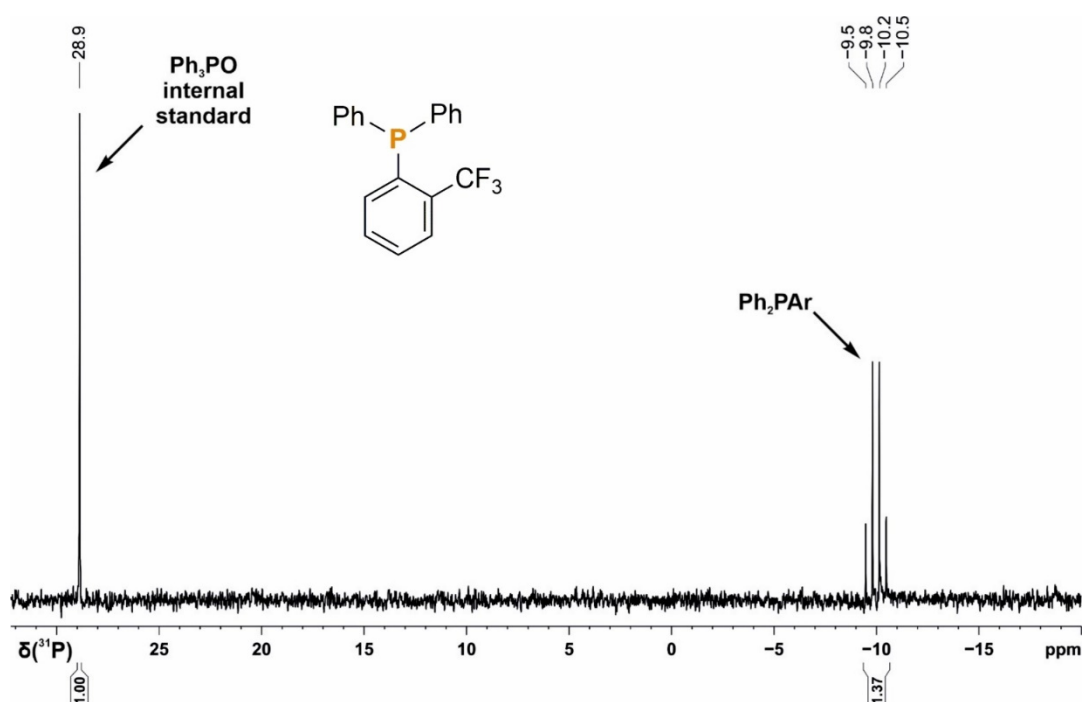
Supplementary Figure 5. Structural overview of organic photocatalyst. 4CzIPN = 1,2,3,5-tetrakis(carbazol-9-yl)-4,6-dicyanobenzene; 3DPACIIPN = 5-Chloro-2,4,6-tris(diphenylamino)isophthalonitrile; 5CzBN = 2,3,4,5,6-penta(9H-carbazol-9-yl)benzonitrile; 4CzPN = 1,2,3,4-tetrakis(carbazol-9-yl)-5,6-dicyanobenzene; 4DPAPN = 1,2,3,4-tetrakis(diphenylamino)-5,6-isophthalonitrile; 4DPAIPN = 1,2,3,5-tetrakis(diphenylamino)-4,6-isophthalonitrile; 3DPA2FBN = 2,4,6-tris(diphenylamino)-3,5-difluorobenzonitrile; 3DPAFIPN = 2,4,6-tris(diphenylamino)-5-fluoroisophthalonitrile; 5MeOCzBN = 2,3,4,5,6-pentakis(3,6-dimethoxy-9H-carbazol-9-yl)benzonitrile.

3.5.8 Crude $^{31}\text{P}\{^1\text{H}\}$ NMR spectra from optimisation screening of small scale reactions

The substrate screening was performed for each substrate at least twice to ensure reproducibility. The conversions were determined by quantitative ^{31}P NMR (zgig) experiments.

Diphenyl(2-trifluoromethyl)phenylphosphine, Table 1, compound I-1

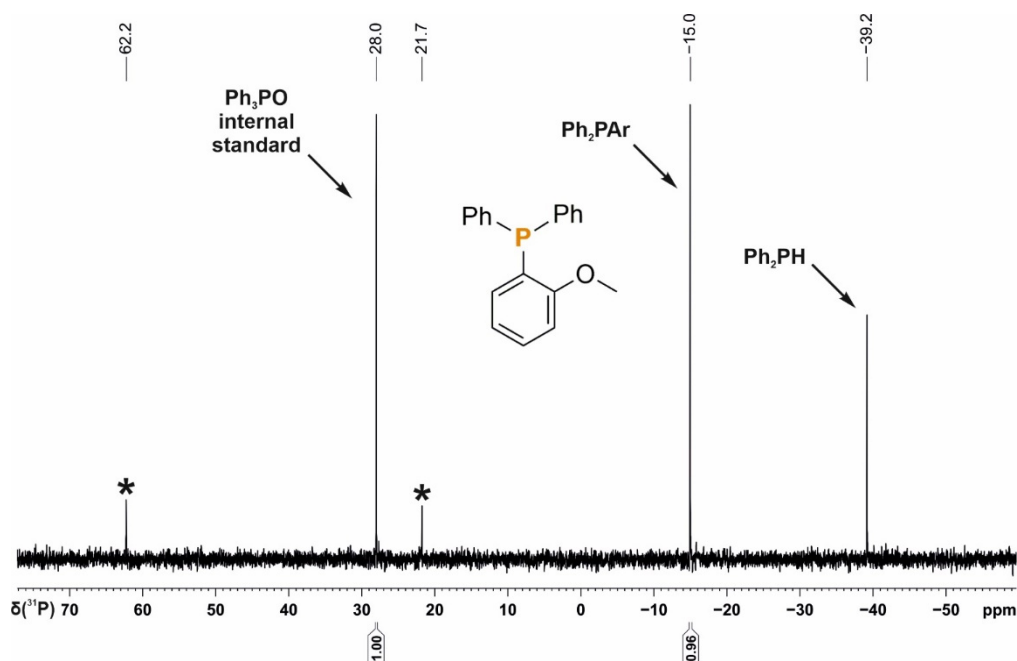
The general procedure 1 was followed using 2-trifluoromethylphenyl iodide (44 μL , 0.3 mmol), which resulted in 68% conversion to diphenyl ((2-trifluoromethyl)phenyl)phosphine as judged by quantitative $^{31}\text{P}\{^1\text{H}\}$ (zgig) NMR spectroscopy.



Supplementary Figure 6. Quantitative single scan $^{31}\text{P}\{^1\text{H}\}$ (zgig) NMR spectrum for the photocatalytic arylation of HPPH_2 using 2-trifluoromethylphenyl iodide. Ar = 2-trifluoromethylphenyl.

Diphenyl(2-methoxyphenyl)phosphine, Table 1, compound I-2

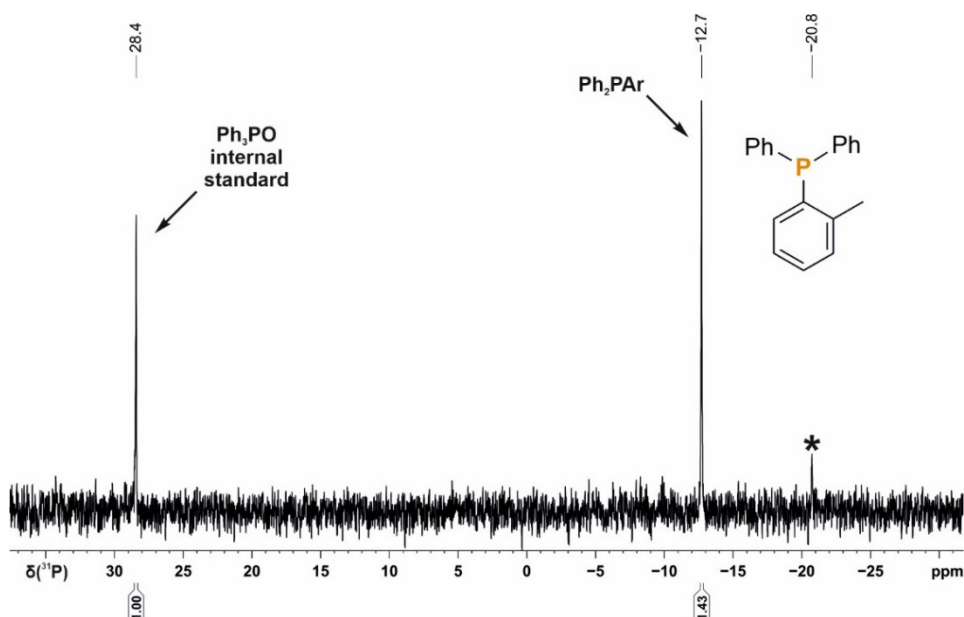
The general procedure 1 was followed using 2-iodoanisole (39 μL , 0.3 mmol), which resulted in 48% conversion to diphenyl(2-methoxyphenyl)phosphine as judged by quantitative $^{31}\text{P}\{^1\text{H}\}$ (zgif) NMR spectroscopy.



Supplementary Figure 7. Quantitative single scan $^{31}\text{P}\{^1\text{H}\}$ (zgif) NMR spectrum for the photocatalytic arylation of HPPH_2 using 2-iodoanisole. Ar = 2-methoxyphenyl. * marks the signal of an unknown by-product.

Diphenyl(2-methylphenyl)phosphine, Table 1, compound I-3

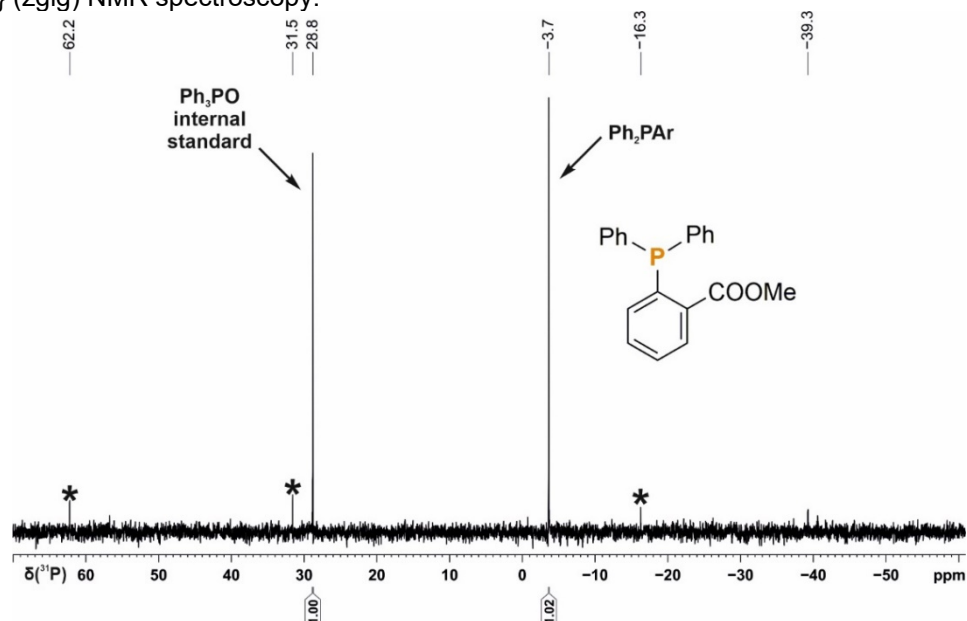
The general procedure 1 was followed using 2-iodotoluene (38 μL , 0.3 mmol), which resulted in 71% conversion to diphenyl(2-methylphenyl)phosphine as judged by quantitative $^{31}\text{P}\{^1\text{H}\}$ (zgif) NMR spectroscopy.



Supplementary Figure 8. Quantitative single scan $^{31}\text{P}\{^1\text{H}\}$ (zgif) NMR spectrum for photocatalytic arylation of HPPH_2 using 2-iodotoluene. Ar = 2-methylphenyl. * marks the signal of an unknown by-product.

Diphenyl(2-methylbenzoate)phosphine, Table 1, compound I-4

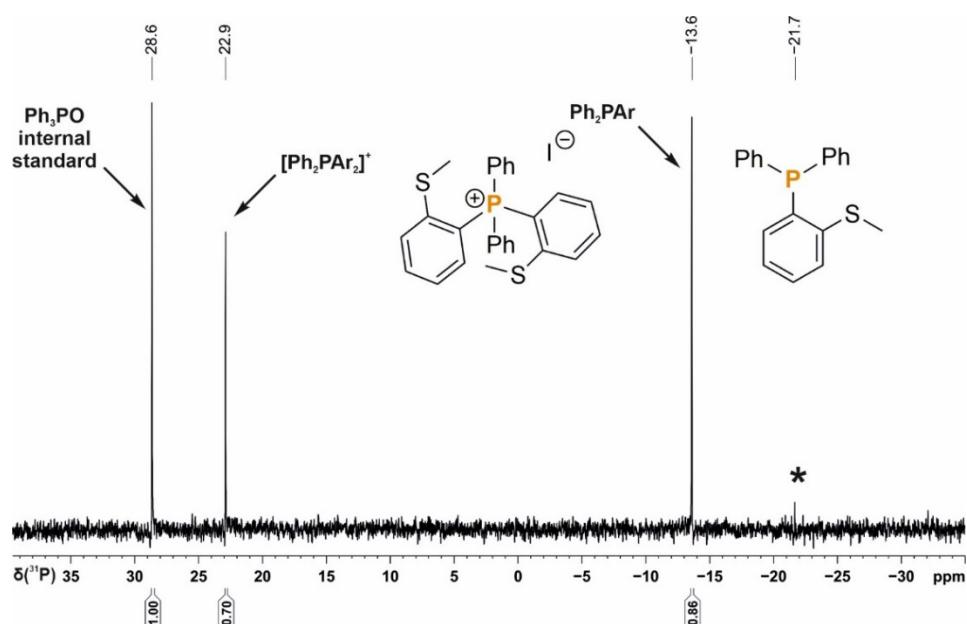
The general procedure 1 was followed using methyl 2-iodobenzoate (44 μ L, 0.3 mmol), which resulted in 51% conversion to diphenyl(2-methoxyphenyl)phosphine as judged by quantitative $^{31}\text{P}\{^1\text{H}\}$ (zgig) NMR spectroscopy.



Supplementary Figure 9. Quantitative single scan $^{31}\text{P}\{^1\text{H}\}$ (zgig) NMR spectrum for the photocatalytic arylation of HPPH_2 using methyl 2-iodobenzoate. Ar = 2-methylbenzoate. * marks the signal of an unknown by-product.

Diphenyl(2-methylthio(phenyl)phosphine and bis(2-methylthiophenyl)diphenylphosphonium iodide, Table 1, compound I-5 and II-5

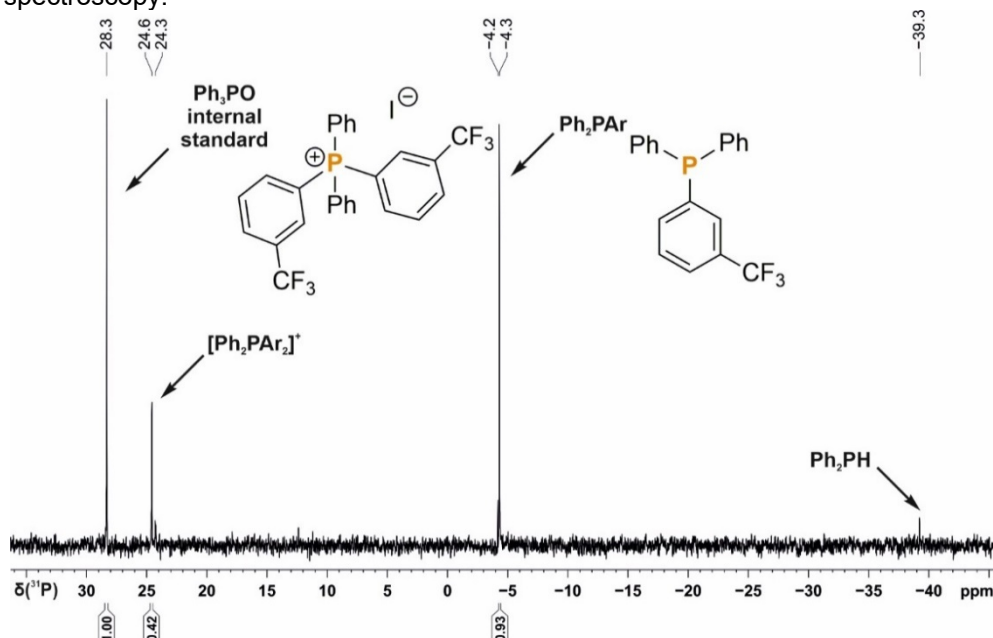
The general procedure 1 was followed using 2-iodothianisole (44 μ L, 0.3 mmol), which resulted in 43% conversion to diphenyl(2-methylthiophenyl)phosphine and 35% bis(2-methylthiophenyl)diphenyl phosphonium iodide as judged by quantitative $^{31}\text{P}\{^1\text{H}\}$ (zgig) NMR spectroscopy.



Supplementary Figure 10. Quantitative single scan $^{31}\text{P}\{^1\text{H}\}$ (zgig) NMR spectrum for the photocatalytic arylation of HPPH_2 using 2-iodothioanisole. Ar = 2-methylthiophenyl. * marks the signal of an unknown by-product.

Diphenyl(3-trifluoromethylphenyl)phosphine and bis(3-trifluoromethylphenyl)diphenylphosphonium iodide, Table 1, compound I-6 and II-6

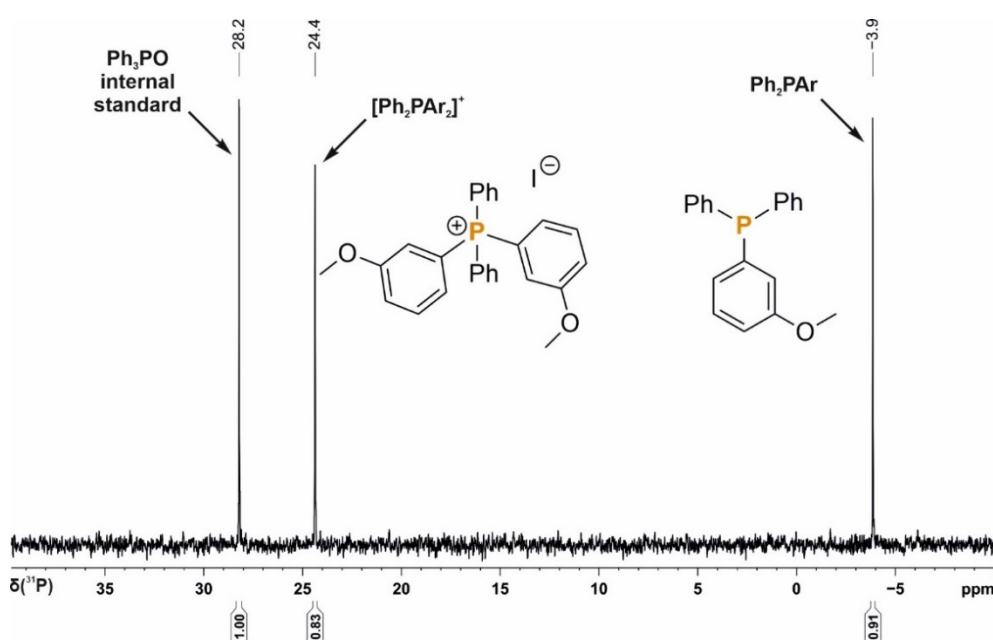
The general procedure 1 was followed using 3-trifluoromethylphenyl iodide (44 μL , 0.3 mmol), which resulted in 46% conversion to diphenyl(3-trifluoromethylphenyl)phosphine and 21% bis(3-trifluoromethylphenyl)diphenyl phosphonium iodide as judged by quantitative $^{31}\text{P}\{^1\text{H}\}$ (zgig) NMR spectroscopy.



Supplementary Figure 11. Quantitative single scan $^{31}\text{P}\{^1\text{H}\}$ (zgig) NMR spectrum for the photocatalytic arylation of HPPH_2 using 3-trifluoromethylphenyl iodide. Ar = 3-trifluoromethylphenyl.

Diphenyl(3-methoxyphenyl)phosphine and bis(3-methoxyphenyl)diphenylphosphonium iodide, Table 1, compound I-7 and II-7

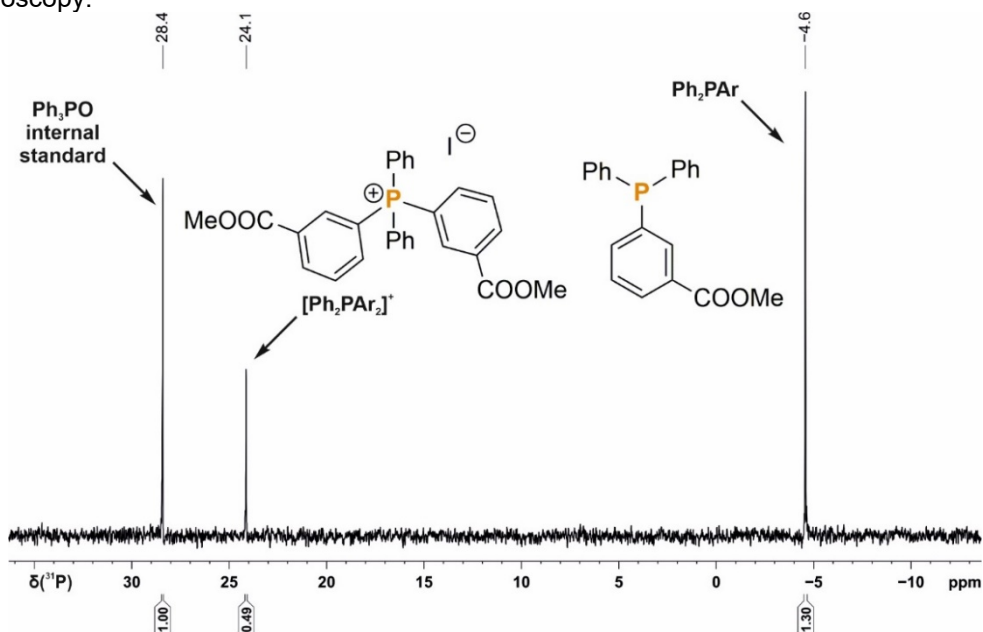
The general procedure 1 was followed using 3-iododanisole (36 μL , 0.3 mmol), which resulted in 45% conversion to diphenyl(3-methoxyphenyl)phosphine and 42% bis(3-methoxyphenyl)diphenyl phosphonium iodide as judged by quantitative $^{31}\text{P}\{^1\text{H}\}$ (zgig) NMR spectroscopy.



Supplementary Figure 12. Quantitative single scan $^{31}\text{P}\{^1\text{H}\}$ (zgig) NMR spectrum for the photocatalytic arylation of HPPH_2 using 3-iododanisole. Ar = 3-methoxyphenyl.

Diphenyl(3-methylbenzoate)phosphine and bis(3-methylbenzoate)diphenyl phosphonium iodide, Table 1, compound I-8 and II-8

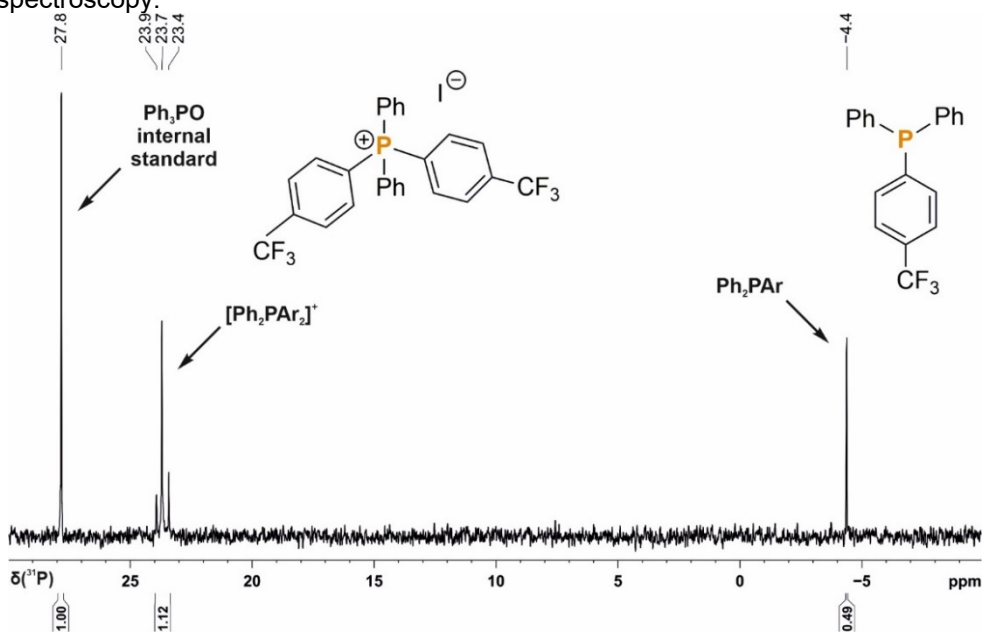
The general procedure 1 was followed using methyl 3-iodobenzoate (79 mg, 0.3 mmol), which resulted in 65% conversion to diphenyl(3-methoxyphenyl)phosphine and 24% bis(3-methoxyphenyl)diphenyl phosphonium iodide as judged by quantitative $^{31}\text{P}\{^1\text{H}\}$ (zgig) NMR spectroscopy.



Supplementary Figure 13. Quantitative single scan $^{31}\text{P}\{^1\text{H}\}$ (zgig) NMR spectrum for the photocatalytic arylation of HPPH_2 using methyl 3-iodobenzoate. Ar = 3-methylbenzoate.

Diphenyl(4-trifluoromethylphenyl)phosphine and bis(4-trifluoromethylphenyl)diphenylphosphonium iodide, Table 1, compound II-9 and I-9

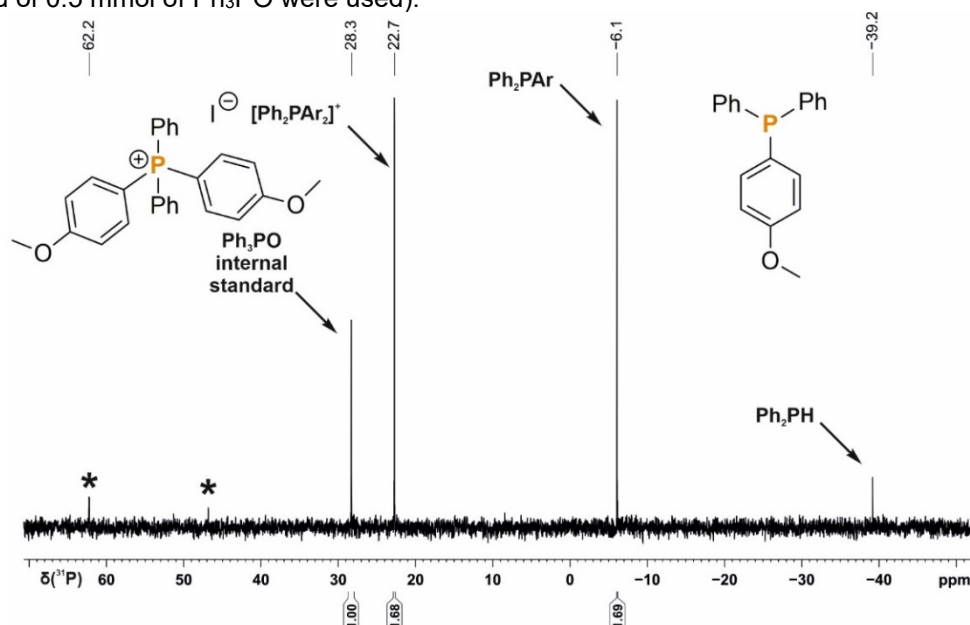
The general procedure 1 was followed using methyl 4-iodobenzotrifluoride (44 μL , 0.3 mmol), which resulted in 56% conversion to diphenyl(4-trifluoromethylphenyl)phosphine and 25% bis(4-trifluoromethylphenyl)diphenyl phosphonium iodide as judged by quantitative $^{31}\text{P}\{^1\text{H}\}$ (zgig) NMR spectroscopy.



Supplementary Figure 14. Quantitative single scan $^{31}\text{P}\{^1\text{H}\}$ (zgig) NMR spectrum for the photocatalytic arylation of HPPH_2 using 4-iodobenzotrifluoride. Ar = 3-trifluoromethylphenyl.

Diphenyl(4-methoxyphenyl)phosphine and bis(4-methoxyphenyl)diphenylphosphonium iodide, Table 1, compound II-10 and I-10

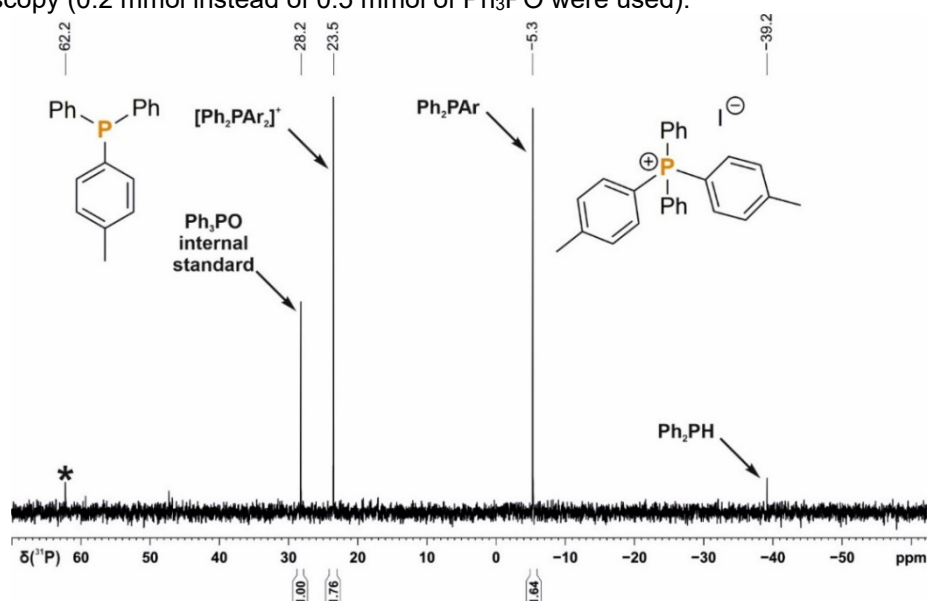
The general procedure 1 was followed using 4-iododanisole (70 mg, 0.3 mmol), which resulted in 34% conversion to diphenyl(4-methoxyphenyl)phosphine and 34% bis(4-methoxyphenyl)diphenyl phosphonium iodide as judged by quantitative $^{31}\text{P}\{^1\text{H}\}$ (zgig) NMR spectroscopy (0.2 mmol instead of 0.5 mmol of Ph_3PO were used).



Supplementary Figure 15. Quantitative single scan $^{31}\text{P}\{^1\text{H}\}$ (zgig) NMR spectrum for the photocatalytic arylation of HPPH_2 using 4-iododanisole. Ar = 4-methoxyphenyl. * marks the signal of an unknown by-product.

Diphenyl(4-trifluoromethylphenyl)phosphine and bis(4-trifluoromethylphenyl)diphenylphosphonium iodide, Table 1, compound II-11 and I-11

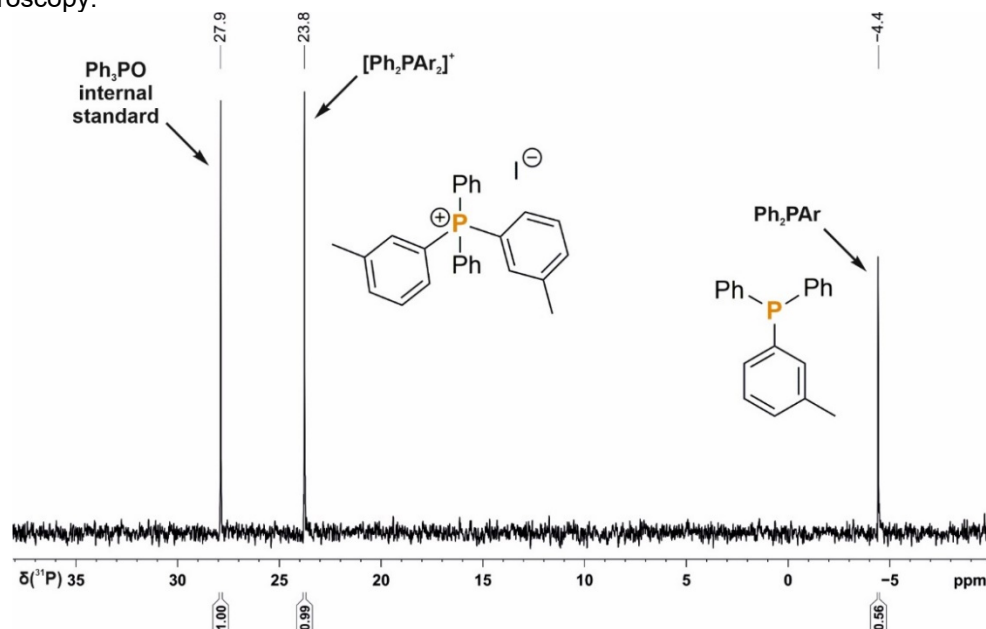
The general procedure 1 was followed using methyl 4-iodotoluene (65 mg, 0.3 mmol), which resulted in 33% conversion to diphenyl(4-methylphenylphenyl)phosphine and 35% bis(4-methylphenyl)diphenyl phosphonium iodide as judged by quantitative $^{31}\text{P}\{^1\text{H}\}$ (zgig) NMR spectroscopy (0.2 mmol instead of 0.5 mmol of Ph_3PO were used).



Supplementary Figure 16. Quantitative single scan $^{31}\text{P}\{^1\text{H}\}$ (zgig) NMR spectrum for the photocatalytic arylation of HPPH_2 using 4-iodotoluene. Ar = 4-methylphenyl. * marks the signal of an unknown by-product.

Diphenyl(3-methylphenyl)phosphine and bis(3-methylphenyl)diphenylphosphonium iodide, Table 1, compound II-13 and I-13

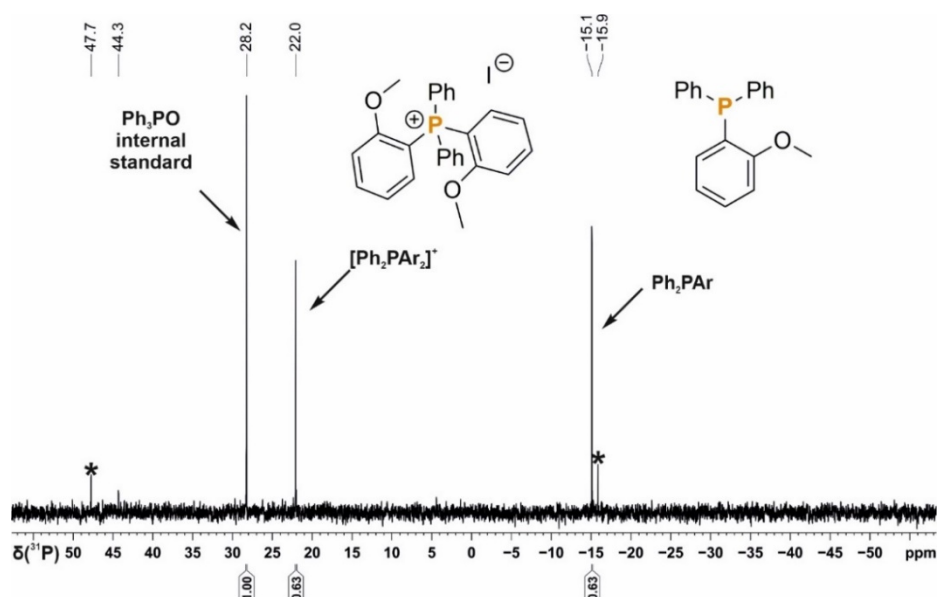
The general procedure 1 was followed using 3-iodotoluene (39 μL , 0.3 mmol), which resulted in 28% conversion to diphenyl(4-trifluoromethylphenyl)phosphine and 49% bis(4-trifluoromethylphenyl)diphenyl phosphonium iodide as judged by quantitative $^{31}\text{P}\{^1\text{H}\}$ (zgig) NMR spectroscopy.



Supplementary Figure 17. Quantitative single scan $^{31}\text{P}\{^1\text{H}\}$ (zgig) NMR spectrum for the photocatalytic arylation of HPPH₂ using 3-iodotoluene. Ar = 3-methylphenyl.

Bis(2-methoxyphenyl)diphenylphosphonium iodide and diphenyl(2-methoxyphenyl)phosphine, Table 2, compound II-2 and I-2

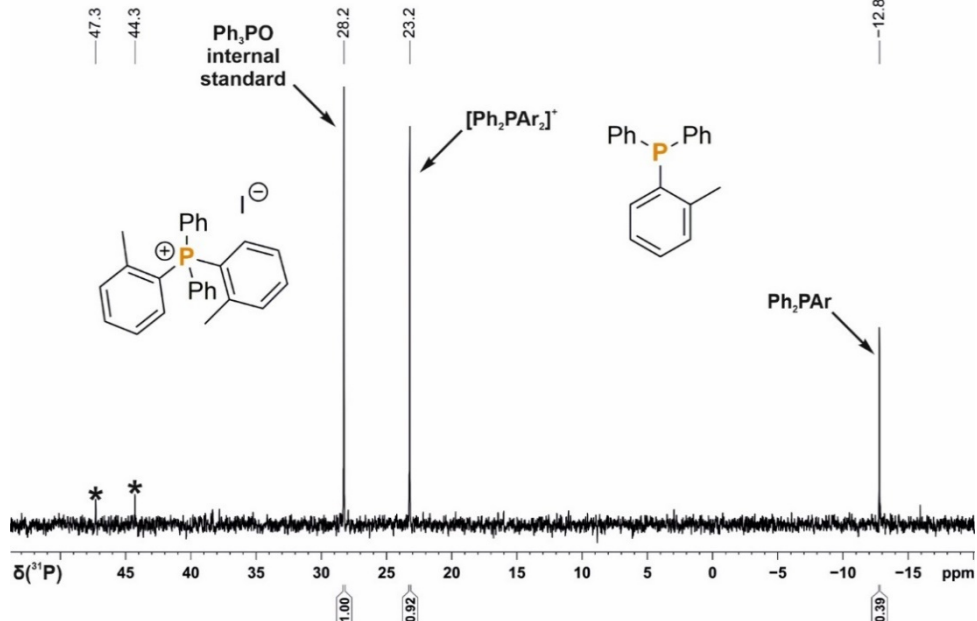
The general procedure 2 was followed using 2-iododanisole (39 μL , 0.3 mmol), which resulted in 32% conversion to bis(2-methoxyphenyl)diphenylphosphonium iodide and 32% diphenyl(2-methoxyphenyl)phosphine as judged by quantitative $^{31}\text{P}\{^1\text{H}\}$ (zgig) NMR spectroscopy.



Supplementary Figure 18. Quantitative single scan $^{31}\text{P}\{^1\text{H}\}$ (zgig) NMR spectrum for the photocatalytic arylation of HPPH₂ using 2-iododanisole. Ar = 2-methoxyphenyl. * marks the signal of an unknown by-product.

Bis(2-methylphenyl)diphenylphosphonium iodide and diphenyl(2-methylphenyl)phosphine, Table 2, compound II-3 and I-3

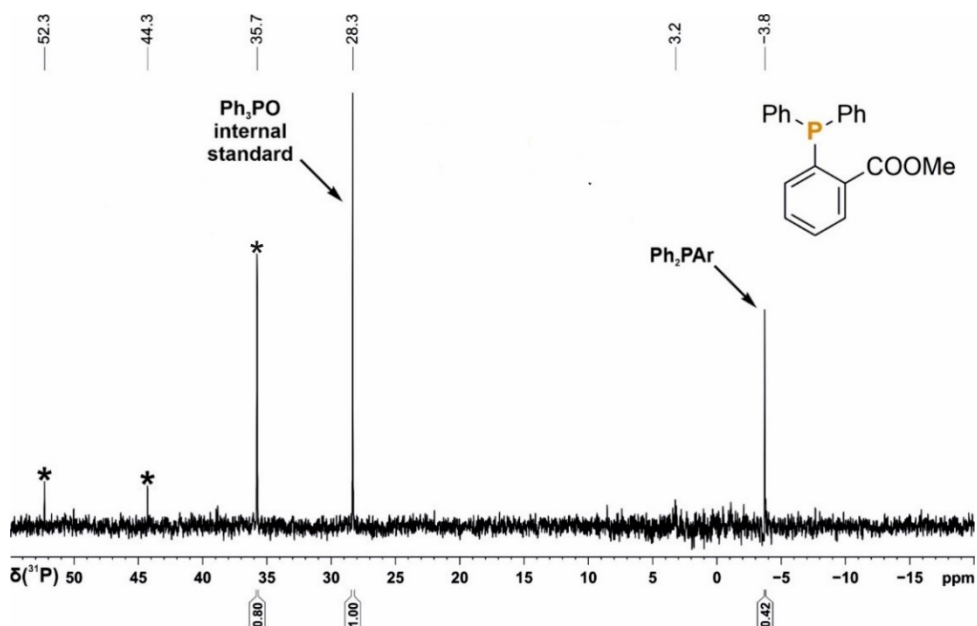
The general procedure 2 was followed using 2-iodotoluene (38 μ L, 0.3 mmol), which resulted in 46% conversion to bis(2-methylphenyl)diphenylphosphonium iodide and 19% diphenyl(2-methylphenyl)phosphine as judged by quantitative $^{31}\text{P}\{^1\text{H}\}$ (zgig) NMR spectroscopy.



Supplementary Figure 19. Quantitative single scan $^{31}\text{P}\{^1\text{H}\}$ (zgig) NMR spectrum for the photocatalytic arylation of HPPH₂ using 2-iodotoluene. Ar = 2-toluene. * marks the signal of an unknown by-product.

Bis(2-methylbenzoate)diphenylphosphonium iodide and diphenyl(2-methyl-carboxyphenyl)phosphine, Table 2, compound II-4 and I-4

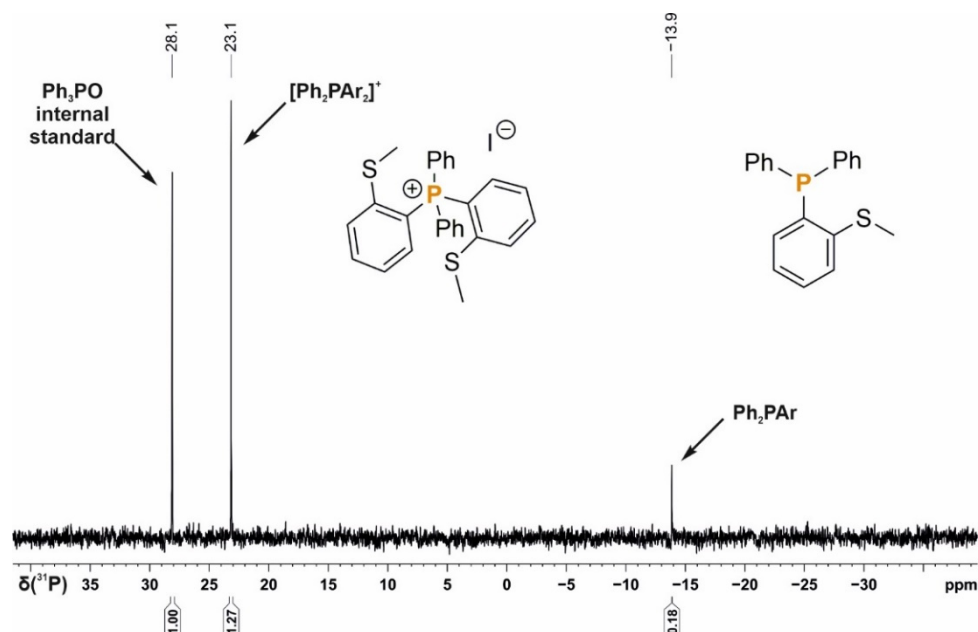
The general procedure 2 was followed using methyl 2-iodobenzoate (44 μ L, 0.3 mmol), which resulted in 21% conversion to diphenyl(2-methylphenyl)phosphine as judged by quantitative $^{31}\text{P}\{^1\text{H}\}$ (zgig) NMR spectroscopy.



Supplementary Figure 20. Quantitative single scan $^{31}\text{P}\{^1\text{H}\}$ (zgig) NMR spectrum for the photocatalytic arylation of HPPH₂ using methyl 2-iodobenzoate. Ar = 2-methylbenzoate * marks the signal of an unknown by-product.

Bis(2-methylthio)phenyl)diphenylphosphonium iodide, Table 2, compound II-5

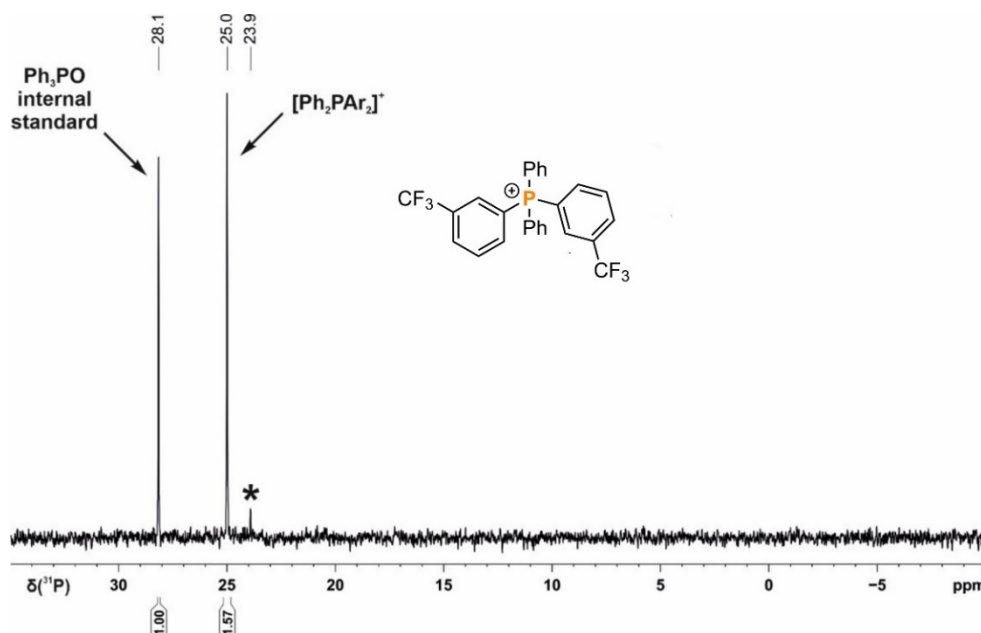
The general procedure 2 was followed using 2-iodothioanisole (42 μL , 0.3 mmol), which resulted in 64% conversion to bis(2-methylthio)phenyl)diphenylphosphonium iodide and 9% diphenyl((2-methylthio)phenyl)phosphine as judged by quantitative $^{31}\text{P}\{^1\text{H}\}$ (zgig) NMR spectroscopy.



Supplementary Figure 21. Quantitative single scan $^{31}\text{P}\{^1\text{H}\}$ (zgig) NMR spectrum for the photocatalytic arylation of HPPH₂ using 2-iodo-thioanisole. Ar = 2-thioanisole * marks the signal of an unknown by-product.

Bis(3-(trifluoromethyl)phenyl)diphenylphosphonium iodide, Table 2, compound II-6

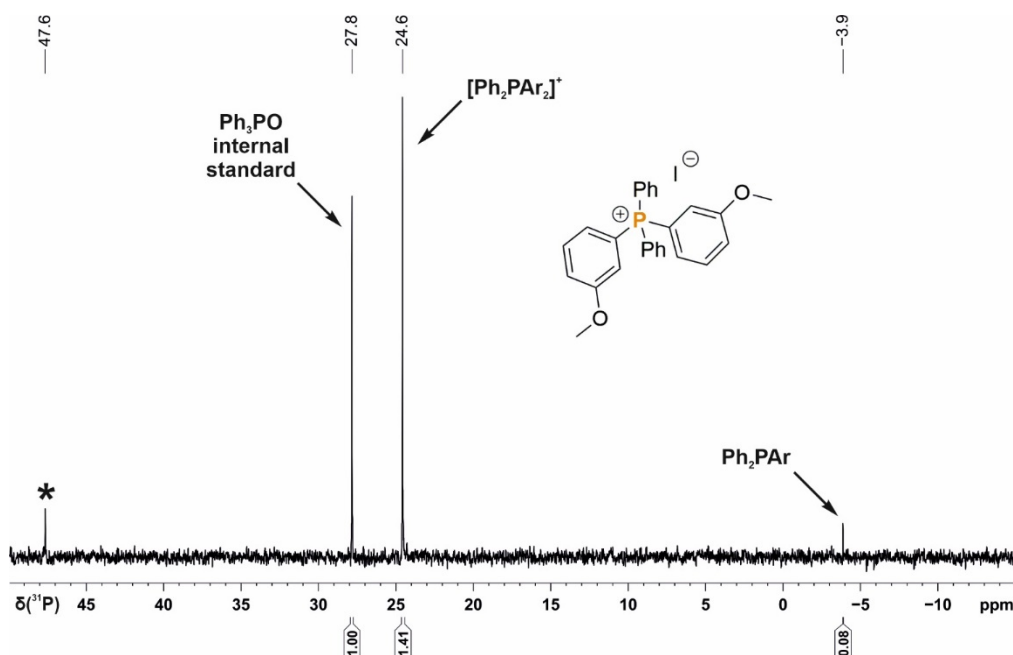
The general procedure 2 was followed using 3-iodobenzotrifluoride (43 μL , 0.3 mmol), which resulted in 79% conversion to bis(3-(trifluoromethyl)phenyl)diphenylphosphonium iodide as judged by quantitative $^{31}\text{P}\{^1\text{H}\}$ (zgig) NMR spectroscopy.



Supplementary Figure 22. Quantitative single scan $^{31}\text{P}\{^1\text{H}\}$ (zgig) NMR spectrum for the photocatalytic arylation of HPPH₂ using 3-iodobenzotrifluoride. Ar = 3-(trifluoromethyl)phenyl. * marks the signal of an unknown by-product.

Bis(3-methoxyphenyl)diphenylphosphonium iodide, Table 2, compound II-7

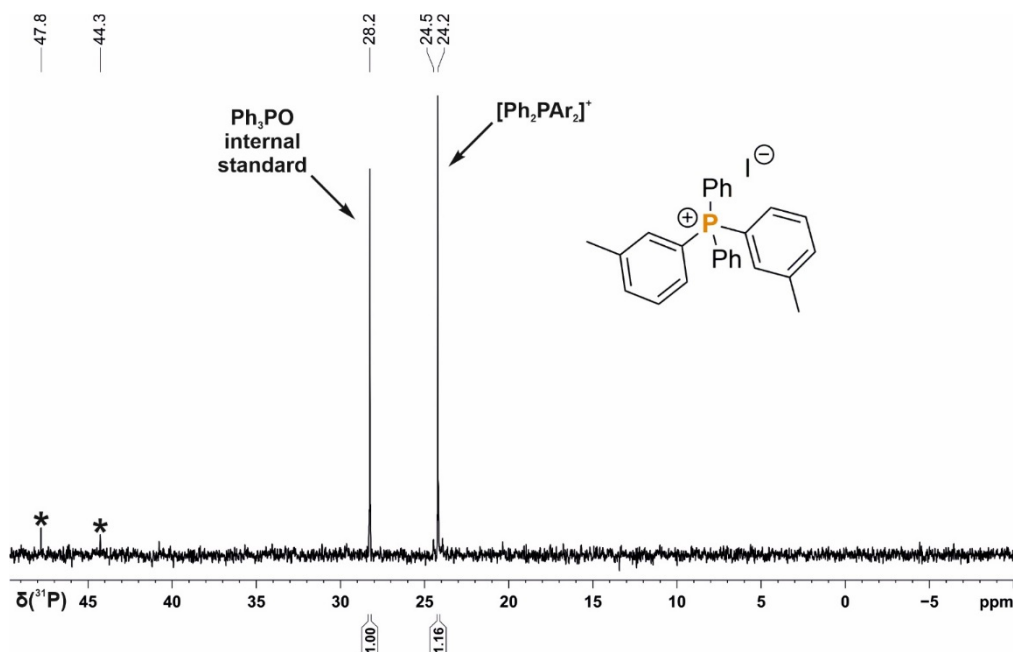
The general procedure 2 was followed using 3-iododanisole (36 μ L, 0.3 mmol), which resulted in 71% conversion to, bis(3-methoxyphenyl)diphenylphosphonium iodide and 4% diphenyl(3-methoxybenzoate)phosphine as judged by quantitative $^{31}\text{P}\{^1\text{H}\}$ (zgig) NMR spectroscopy.



Supplementary Figure 23. Quantitative single scan $^{31}\text{P}\{^1\text{H}\}$ (zgig) NMR spectrum for the photocatalytic arylation of HPPH_2 using 3-iododanisole. Ar = 3-methoxyphenyl * marks the signal of an unknown by-product.

Bis(3-methylphenyl)diphenylphosphonium iodide, Table 2, compound II-13

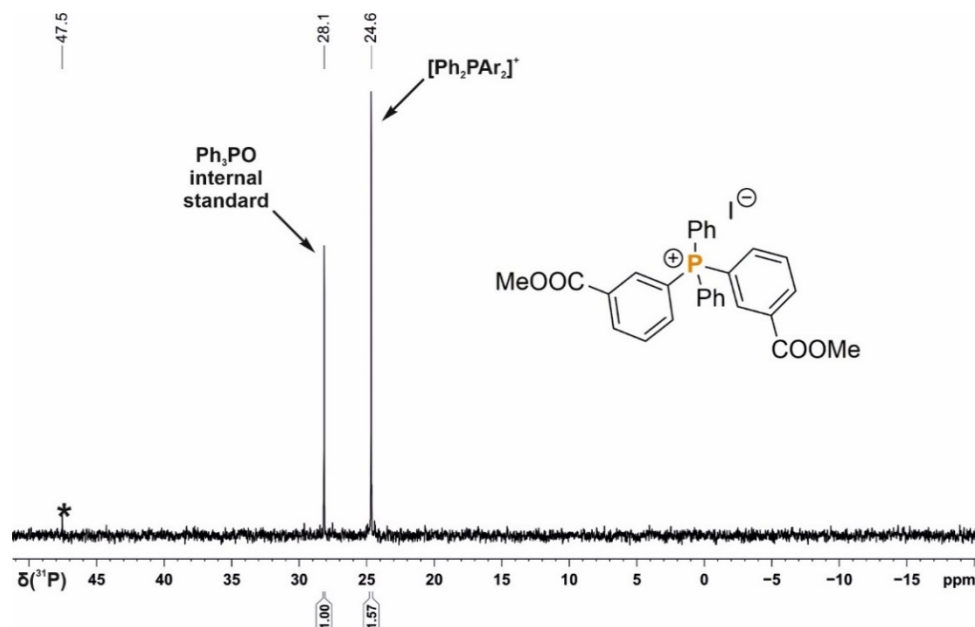
The general procedure 2 was followed using 3-iodotoluene (39 μ L, 0.3mmol), which resulted in 58% conversion to bis(3-methylphenyl)diphenylphosphonium iodide as judged by quantitative $^{31}\text{P}\{^1\text{H}\}$ (zgig) NMR spectroscopy.



Supplementary Figure 24. Quantitative single scan $^{31}\text{P}\{^1\text{H}\}$ (zgig) NMR spectrum for the photocatalytic arylation of HPPH_2 using 3-iodotoluene. Ar = 3-methylphenyl * marks the signal of an unknown by-product.

Bis(3-methylbenzoate)diphenylphosphonium iodide, Table 2, compound II-8

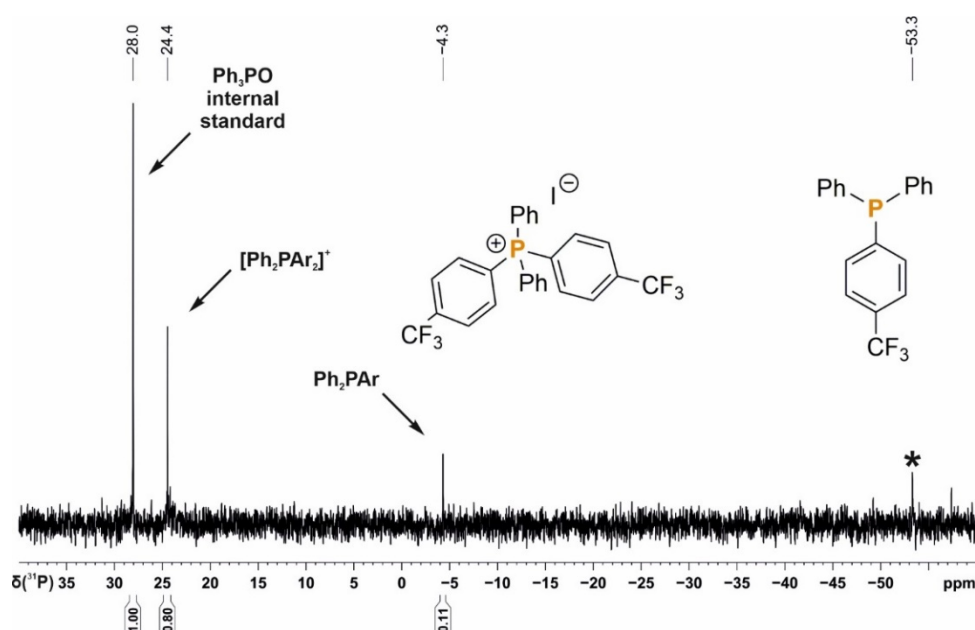
The general procedure 2 was followed using methyl 3-iodobenzoate (79 mg, 0.3 mmol), which resulted in 79% conversion to bis(3-methylbenzoate)diphenylphosphonium iodide as judged by quantitative $^{31}\text{P}\{^1\text{H}\}$ (zgig) NMR spectroscopy.



Supplementary Figure 25. Quantitative single scan $^{31}\text{P}\{^1\text{H}\}$ (zgig) NMR spectrum for the photocatalytic arylation of HPPH_2 using methyl 3-iodobenzoate. Ar = 3-methylbenzoate. * marks the signal of an unknown by-product.

Bis(4-trifluoromethylphenyl)diphenylphosphonium iodide, Table 2, compound II-9

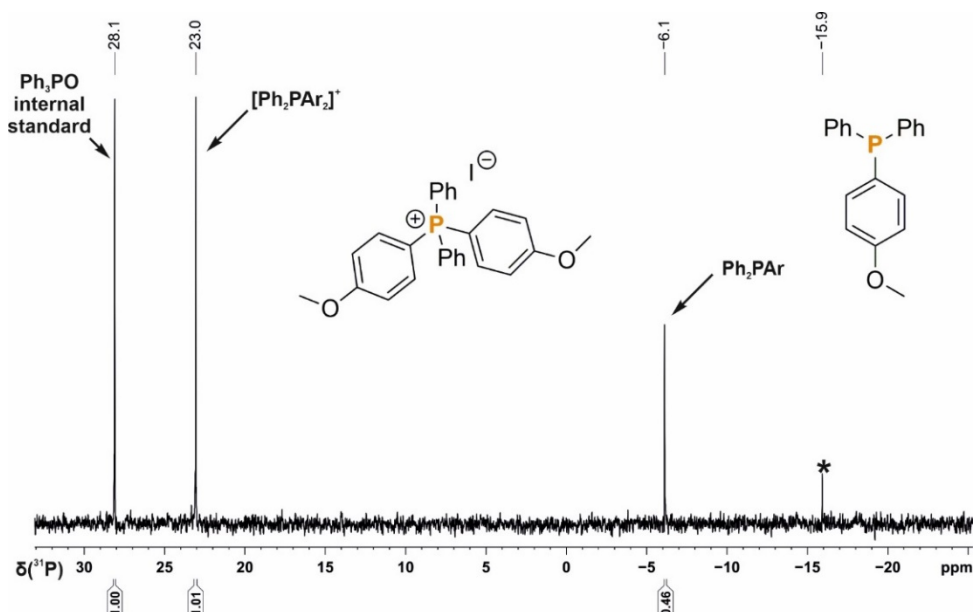
The general procedure 2 was followed using 3-iodobenzotrifluoride (43 μL , 0.3 mmol), which resulted in 40% conversion to bis(3-(trifluoromethyl)phenyl)diphenylphosphonium iodide and 6% diphenyl(4-(trifluoromethyl)phenyl)phosphine as judged by quantitative $^{31}\text{P}\{^1\text{H}\}$ (zgig) NMR spectroscopy.



Supplementary Figure 26. Quantitative single scan $^{31}\text{P}\{^1\text{H}\}$ (zgig) NMR spectrum for the photocatalytic arylation of HPPH_2 using 4-trifluoromethylphenyl iodide. Ar = 4-(trifluoromethyl)phenyl * marks the signal of an unknown by-product.

Bis(4-methoxyphenyl)diphenylphosphonium iodide and diphenyl(4-methoxyphenyl)phosphine, Table 2, compound II-10 and I-10

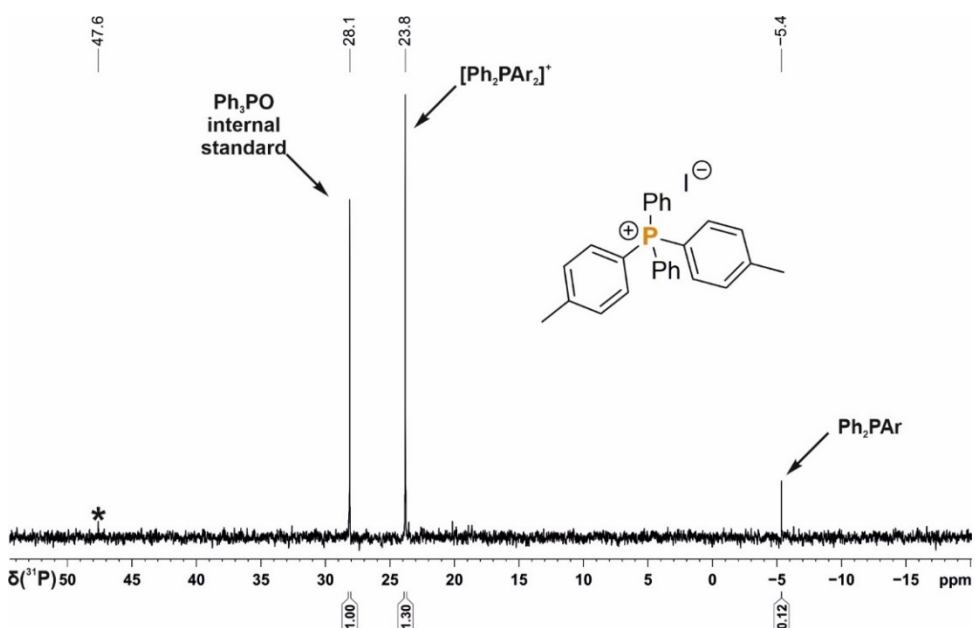
The general procedure 2 was followed using 4-iodoanisole (70 mg, 0.3 mmol), which resulted in 50% conversion bis(4-methoxyphenyl)diphenylphosphonium iodide and 23% diphenyl 4-methoxyphenylphosphine as judged by quantitative $^{31}\text{P}\{^1\text{H}\}$ (zgig) NMR spectroscopy.



Supplementary Figure 27. Quantitative single scan $^{31}\text{P}\{^1\text{H}\}$ (zgig) NMR spectrum for the photocatalytic arylation of HPPH_2 using 4-iodoanisole. Ar = 4-(methoxy)phenyl * marks the signal of an unknown by-product.

Bis(4-methylphenyl)diphenylphosphonium iodide, Table 2, compound II-11

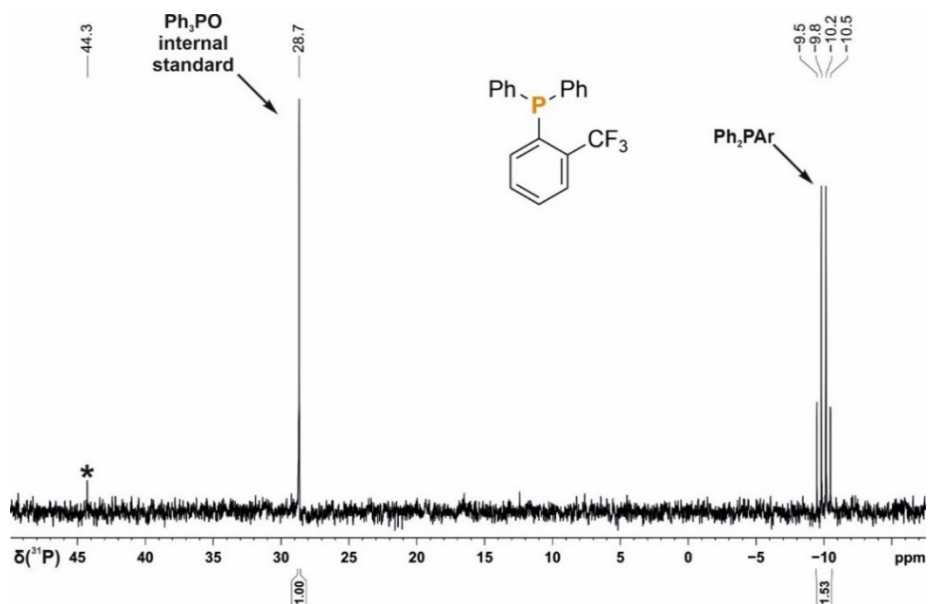
The general procedure 2 was followed using 4-iodotoluene (65 mg, 0.3 mmol), which resulted in 65% conversion bis(4-methylphenyl)diphenylphosphonium iodide and 6% diphenyl 4-methylphenylphosphine as judged by quantitative $^{31}\text{P}\{^1\text{H}\}$ (zgig) NMR spectroscopy.



Supplementary Figure 28. Quantitative single scan $^{31}\text{P}\{^1\text{H}\}$ (zgig) NMR spectrum for the photocatalytic arylation of HPPH_2 using 4-iodotoluene. Ar = 4-(methyl)phenyl * marks the signal of an unknown by-product.

Diphenyl[2-(trifluoromethyl)phenyl]phosphine, Table 2, compound I-1

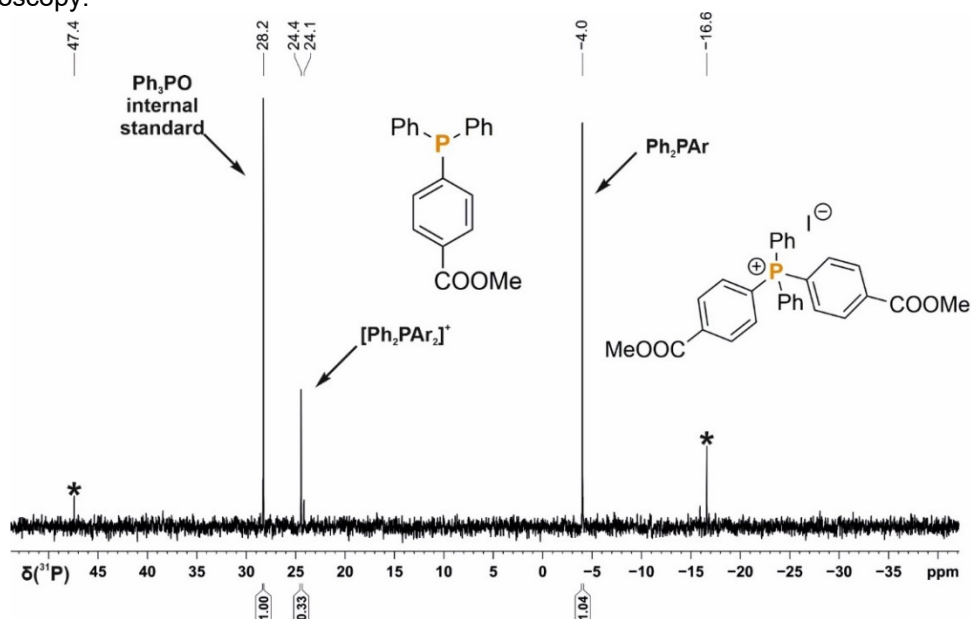
The general procedure 2 was followed using 2-iodobenzotrifluoride (42 μ L, 0.3 mmol), which resulted in 77% conversion to diphenyl(2-(trifluoromethyl)phenyl)phosphine as judged by quantitative $^{31}\text{P}\{^1\text{H}\}$ (zgig) NMR spectroscopy.



Supplementary Figure 29. Quantitative single scan $^{31}\text{P}\{^1\text{H}\}$ (zgig) NMR spectrum for the photocatalytic arylation of HPPH_2 using 2-iodobenzotrifluoride. Ar = 4-(trifluoromethyl)phenyl * marks the signal of an unknown by-product.

Diphenyl(4-methylbenzoate)phosphine and bis(4-methylbenzoate)diphenylphosphonium iodide, Table 2, compound I-12 and I-12

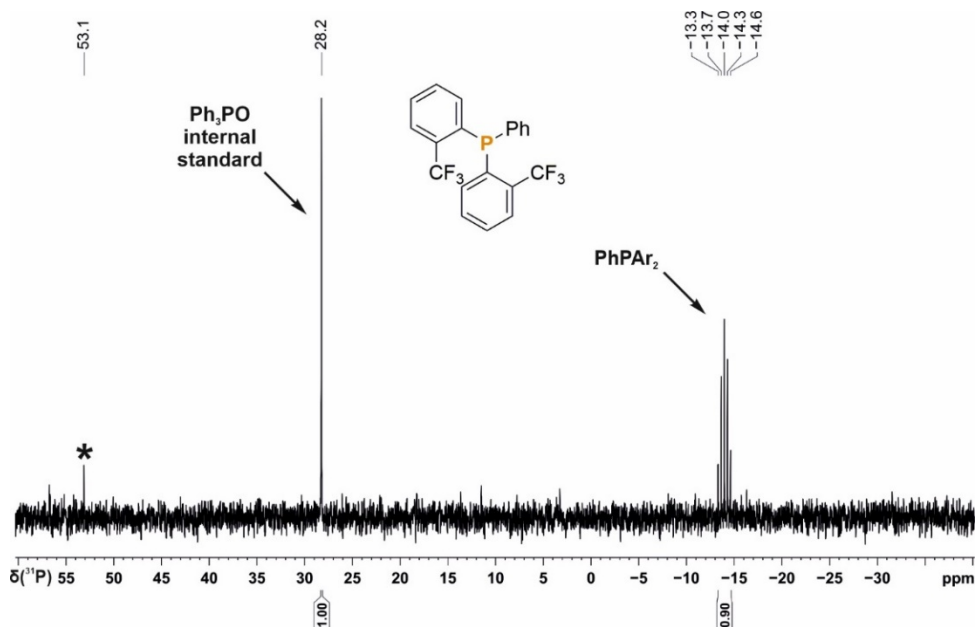
The general procedure 2 was followed using methyl 4-iodobenzoate (79 mg, 0.3 mmol), which resulted in 52% conversion to diphenyl(4-methylbenzoate)phosphine and 17% bis(4-methylbenzoate)diphenylphosphonium iodide as judged by quantitative $^{31}\text{P}\{^1\text{H}\}$ (zgig) NMR spectroscopy.



Supplementary Figure 30. Quantitative single scan $^{31}\text{P}\{^1\text{H}\}$ (zgig) NMR spectrum for the photocatalytic arylation of HPPH_2 using methyl 4-iodobenzoate. Ar = 4-methylbenzoate * marks the signal of an unknown by-product.

Bis(2-trifluoromethylphenyl)phenylphosphine, Table 3, compound III-1

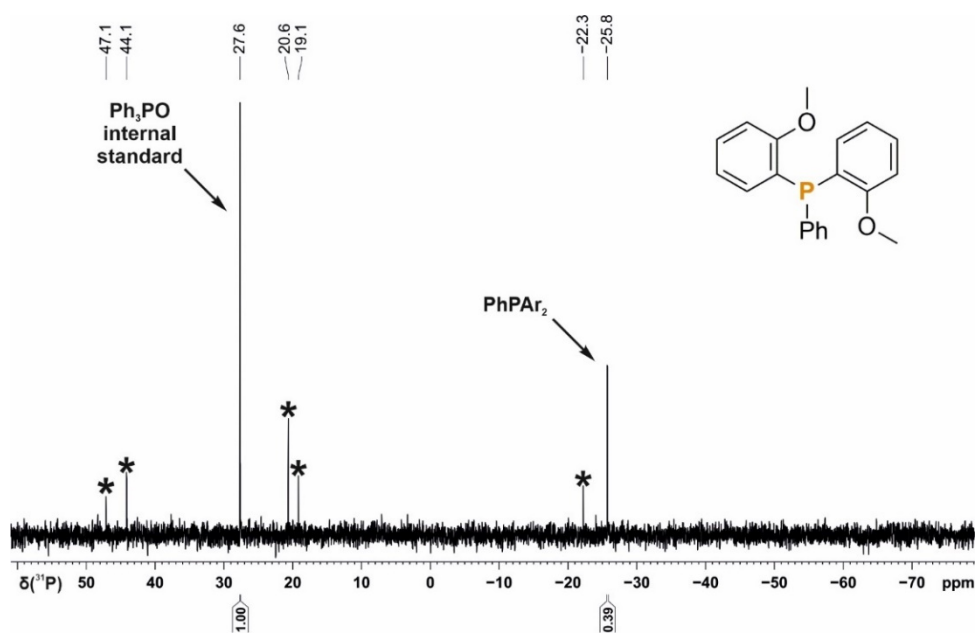
The general procedure 3 was followed using 2-iodobenzotrifluoride (70 μL , 0.5 mmol), which resulted in 45% conversion to bis(2-trifluoromethylphenyl)phenylphosphine as judged by quantitative $^{31}\text{P}\{^1\text{H}\}$ (zgig) NMR spectroscopy.



Supplementary Figure 31. Quantitative single scan $^{31}\text{P}\{^1\text{H}\}$ (zgig) NMR spectrum for the photocatalytic arylation of H_2PPh using 2-iodobenzotrifluoride. Ar = 2-trifluoromethylphenyl * marks the signal of an unknown by-product.

Bis(2-methoxyphenyl)phenylphosphine, Table 3, compound III-2

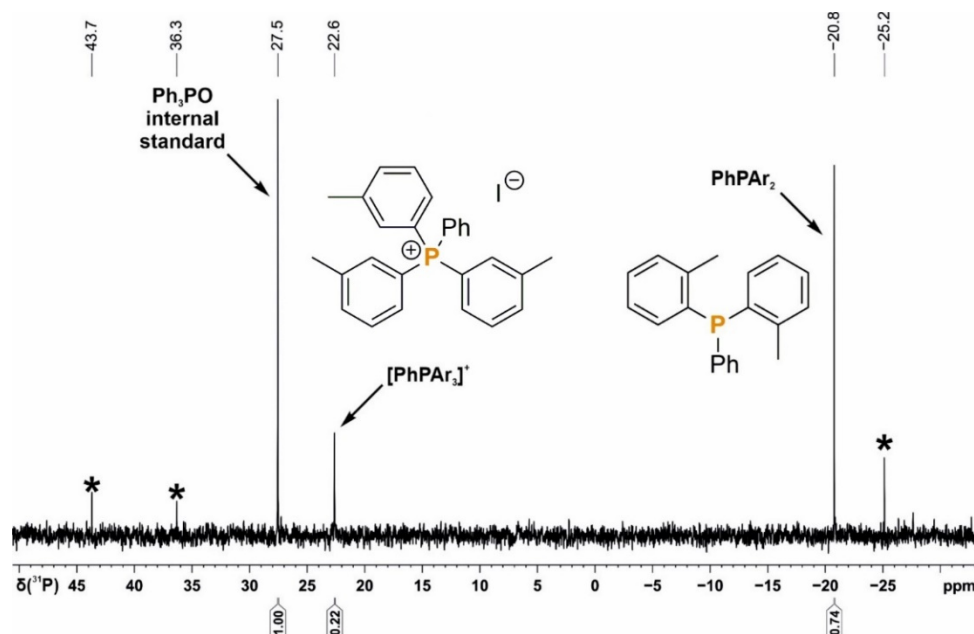
The general procedure 3 was followed using 2-iododanisole (65 μL , 0.5 mmol), which resulted in 20% conversion to bis(2-methoxyphenyl)phenylphosphine as judged by quantitative $^{31}\text{P}\{^1\text{H}\}$ (zgig) NMR spectroscopy



Supplementary Figure 32. Quantitative single scan $^{31}\text{P}\{^1\text{H}\}$ (zgig) NMR spectrum for the photocatalytic arylation of H_2PPh using 2-iododanisole. Ar = 2-methoxyphenyl * marks the signal of an unknown by-product.

Tris(2-methylphenyl)phenylphosphonium iodide and bis(2-methylphenyl)phenylphosphine, Table 3, compound III-3 and IV-3

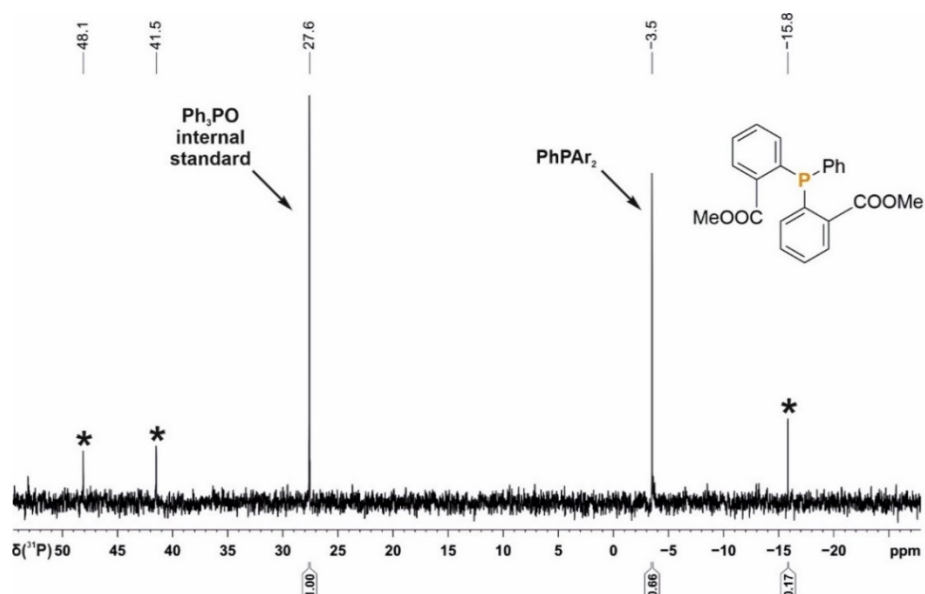
The general procedure 3 was followed using 2-iodotoluene (63 μL , 0.3 mmol), which resulted in 11% conversion to tris(2-methylphenyl)phenylphosphonium iodide and 37% bis(2-methylphenyl)phenylphosphine as judged by quantitative $^{31}\text{P}\{^1\text{H}\}$ (zgig) NMR spectroscopy.



Supplementary Figure 33. Quantitative single scan $^{31}\text{P}\{^1\text{H}\}$ (zgig) NMR spectrum for the photocatalytic arylation of H_2PPh using 2-iodotoluene. Ar = 2-methylphenyl * marks the signal of an unknown by-product.

Table 3, compound III-4, bis(2-methylbenzoate)phenylphosphine

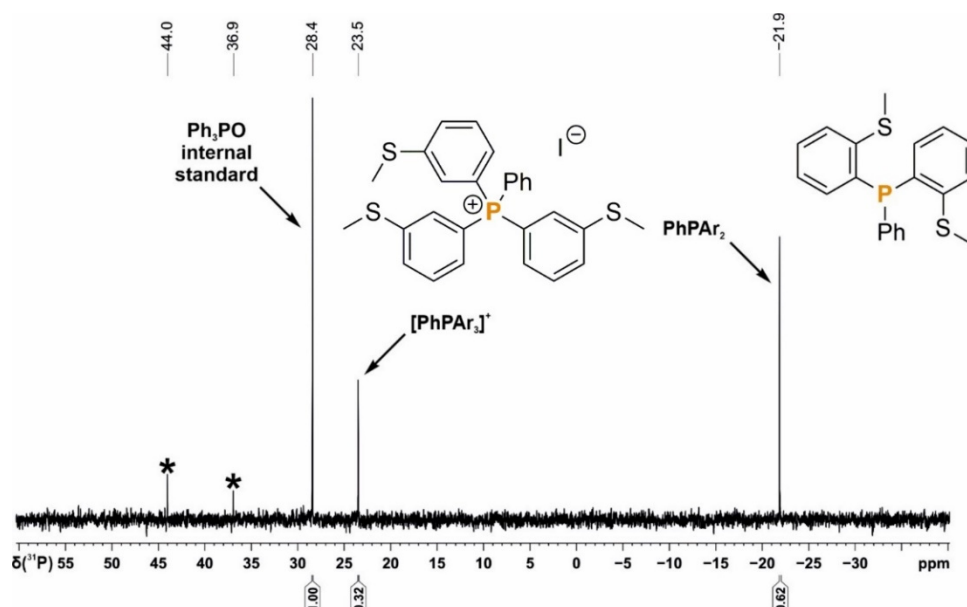
The general procedure 3 was followed using methyl 2-iodobenzoate (73 μL , 0.5 mmol), which resulted in 33% conversion to bis(2-methylbenzoate)phenylphosphine as judged by quantitative $^{31}\text{P}\{^1\text{H}\}$ (zgig) NMR spectroscopy.



Supplementary Figure 34. Quantitative single scan $^{31}\text{P}\{^1\text{H}\}$ (zgig) NMR spectrum for the photocatalytic arylation of H_2PPh using methyl 2-iodobenzoate. Ar = 2-methylbenzoate * marks the signal of an unknown by-product.

Bis(2-methylthio)phenyl)phenylphosphine and phenyl tris((2-methylthio)phenyl)-phosphonium iodide, Table 3, compound III-5 and IV-5

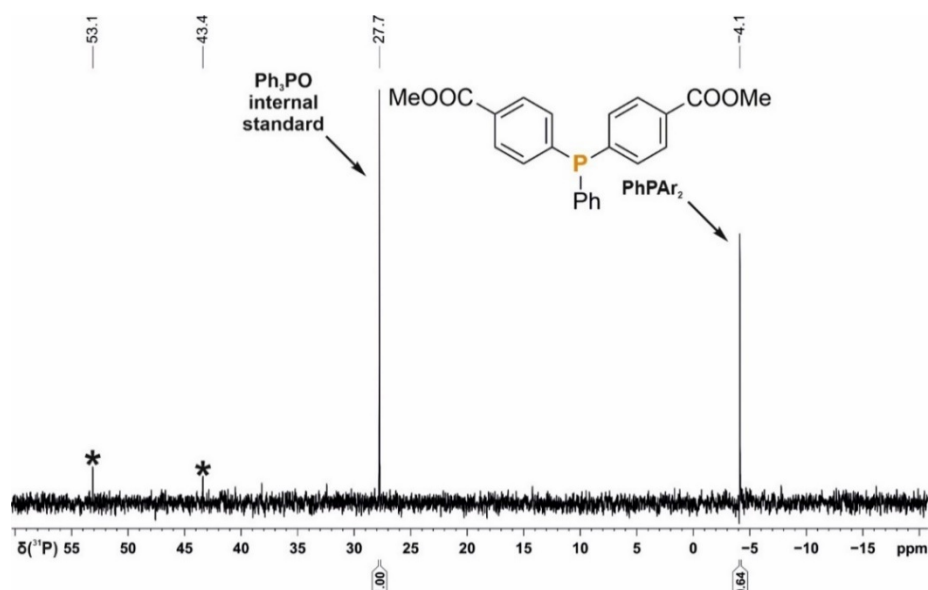
The general procedure 3 was followed using 2-iodothioanisole (70 μ L, 0.5 mmol), which resulted in 31% conversion to bis(2-methylthio)phenyl)phenylphosphine and 16% tris((2-methylthio)phenyl)phenylphosphonium iodide as judged by quantitative $^{31}\text{P}\{^1\text{H}\}$ (zlig) NMR spectroscopy.



Supplementary Figure 35. Quantitative single scan $^{31}\text{P}\{^1\text{H}\}$ (zlig) NMR spectrum for the photocatalytic arylation of H_2PPh using 2-iodothioanisole. Ar = 2-thioanisole * marks the signal of an unknown by-product.

Bis(4-methylbenzoate)phenyl)phenylphosphine, Table 3, compound III-6

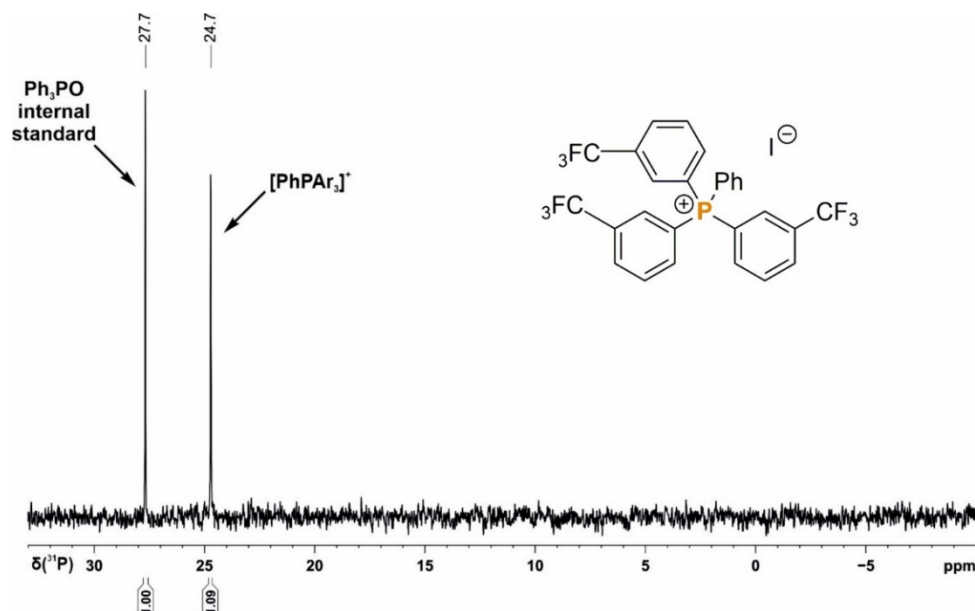
The general procedure 3 was followed using methyl 4-iodobenzoate (73 μ L, 0.5 mmol), which resulted in 32% conversion to tris(4-methylbenzoate)phenyl)phenylphosphine as judged by quantitative $^{31}\text{P}\{^1\text{H}\}$ (zlig) NMR spectroscopy.



Supplementary Figure 36. Quantitative single scan $^{31}\text{P}\{^1\text{H}\}$ (zlig) NMR spectrum for the photocatalytic arylation of H_2PPh using methyl 4-iodobenzoate. Ar = 4-methylbenzoate. * marks the signal of an unknown by-product.

Tris(3-trifluoromethyl)phenylphenylphosphonium iodide, Table 3, compound IV-7

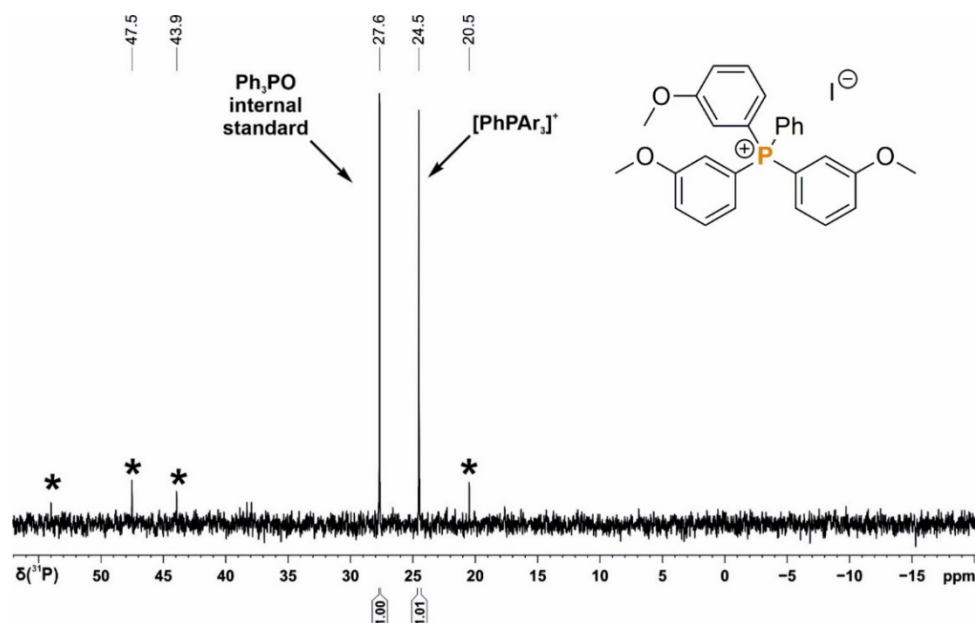
The general procedure 3 was followed using 3-iodobenzotrifluoride (72 μL , 0.5 mmol), which resulted in 55% conversion to tris((3-trifluoromethyl)phenyl)phenylphosphonium iodide as judged by quantitative $^{31}\text{P}\{^1\text{H}\}$ (zgig) NMR spectroscopy.



Supplementary Figure 37. Quantitative single scan $^{31}\text{P}\{^1\text{H}\}$ (zgig) NMR spectrum for the photocatalytic arylation of H_2PPh using 3-iodobenzotrifluoride. Ar = 3-trifluoromethylphenyl. * marks the signal of an unknown by-product.

Tris(3-methoxyphenyl)phenylphosphonium iodide, Table 3, compound IV-8

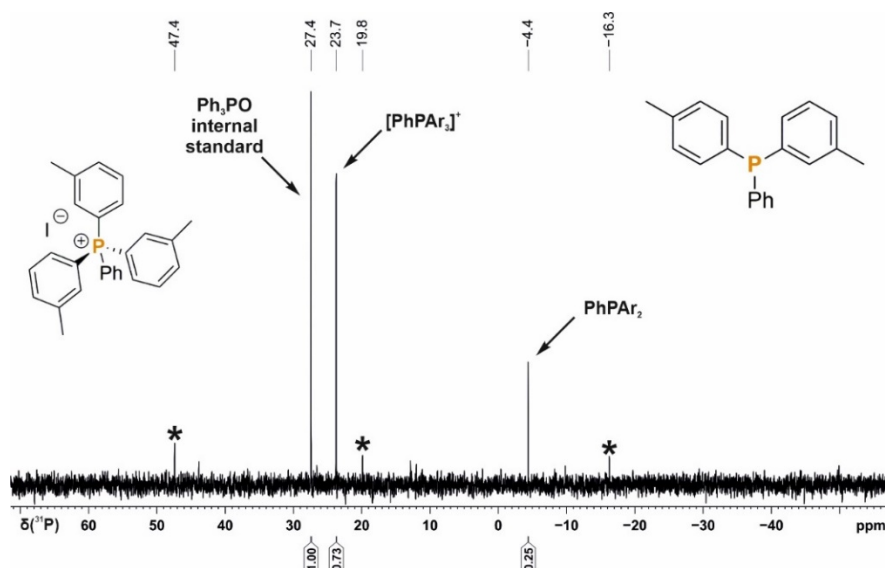
The general procedure 3 was followed using 3-iodoanisole (60 μL , 0.5 mmol), which resulted in 50% conversion to tris(3-methoxyphenyl)phenylphosphonium iodide as judged by quantitative $^{31}\text{P}\{^1\text{H}\}$ (zgig) NMR spectroscopy.



Supplementary Figure 38. Quantitative single scan $^{31}\text{P}\{^1\text{H}\}$ (zgig) NMR spectrum for the photocatalytic arylation of H_2PPh using 3-iodoanisole. Ar = 3-methoxyphenyl. * marks the signal of an unknown by-product.

Tris(3-methylphenyl)phenylphosphonium iodide and bis(3-methylphenyl)-phenylphosphine, Table 3, compound IV-9 and III-9

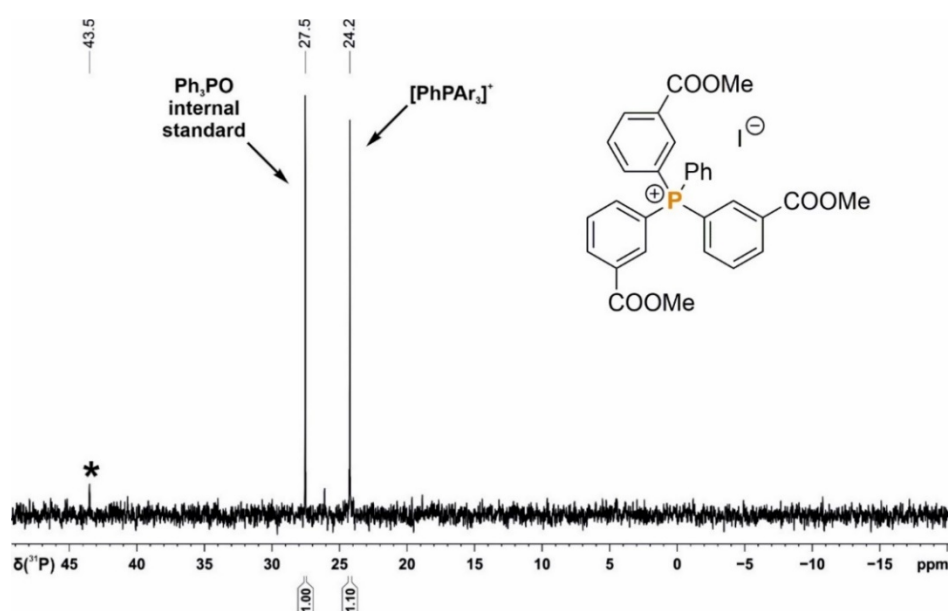
The general procedure 3 was followed using methyl 3-iodotoluene (60 μL , 0.5 mmol), which resulted in 36% conversion to tris(3-methylphenyl)phenylphosphonium iodide and 12 % conversion to bis(3-methylphenyl)phenylphosphine as judged by quantitative $^{31}\text{P}\{^1\text{H}\}$ (zgig) NMR spectroscopy.



Supplementary Figure 39. Quantitative single scan $^{31}\text{P}\{^1\text{H}\}$ (zgig) NMR spectrum for the photocatalytic arylation of H_2PPh using methyl 3-iodotoluene. Ar = 3-methylphenyl. * marks the signal of an unknown by-product.

Tris(3-methylbenzoate)phenylphosphonium iodide, Table 3, compound IV-10

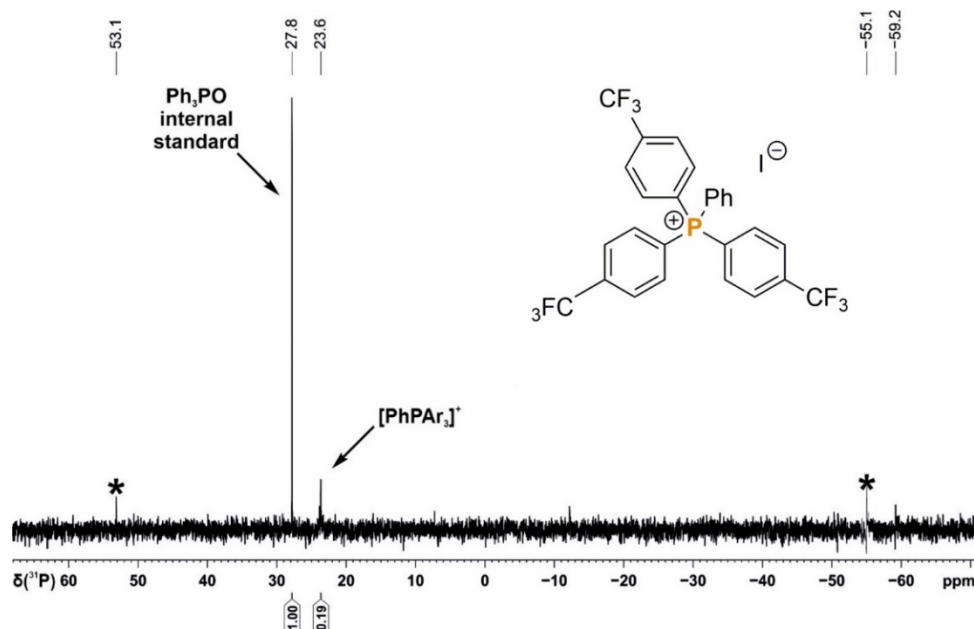
The general procedure 3 was followed using methyl 3-iodobenzoate (131 mg, 0.5 mmol), which resulted in 55% conversion to tris(3-methylbenzoate)phenylphosphonium iodide as judged by quantitative $^{31}\text{P}\{^1\text{H}\}$ (zgig) NMR spectroscopy.



Supplementary Figure 40. Quantitative single scan $^{31}\text{P}\{^1\text{H}\}$ (zgig) NMR spectrum for the photocatalytic arylation of H_2PPh using methyl 3-iodobenzoate. Ar = 3-methylbenzoate. * marks the signal of an unknown by-product.

Tris(4-trifluoromethyl)phenylphenylphosphonium iodide, Table 3, compound-IV-11

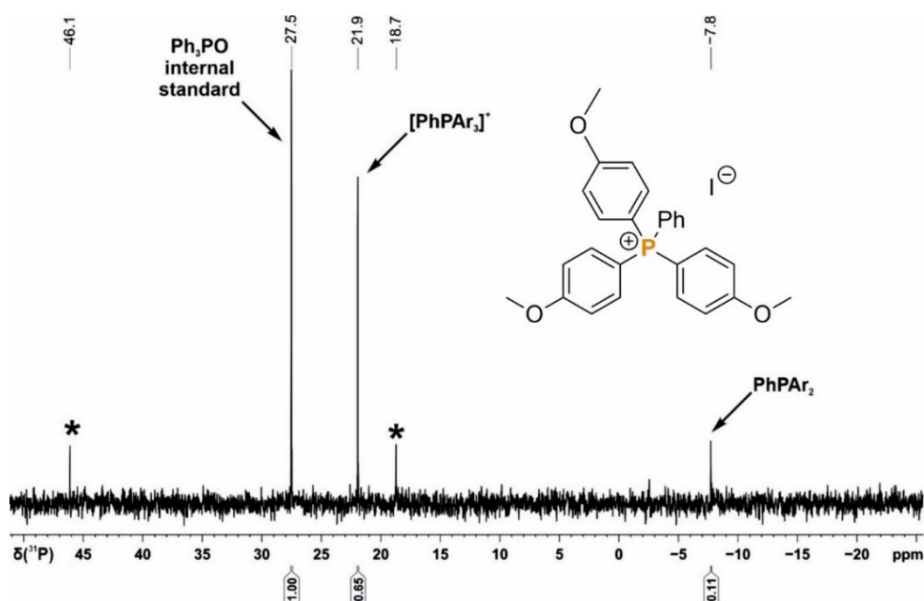
The general procedure 3 was followed using methyl 4-iodobenzyltrifluoride ((73 μ L, 0.3 mmol), which resulted in 10% conversion to tris((4-trifluoromethyl)phenyl)phenylphosphonium iodide as judged by quantitative $^{31}\text{P}\{^1\text{H}\}$ (zgig) NMR spectroscopy.



Supplementary Figure 41. Quantitative single scan $^{31}\text{P}\{^1\text{H}\}$ (zgig) NMR spectrum for the photocatalytic arylation of H_2PPh using 4-iodobenzotrifluoride. Ar = 4-trifluoromethylphenyl. * marks the signal of an unknown by-product.

Tris(4-methoxyphenyl)phenylphosphonium iodide, Table 3, compound IV-12

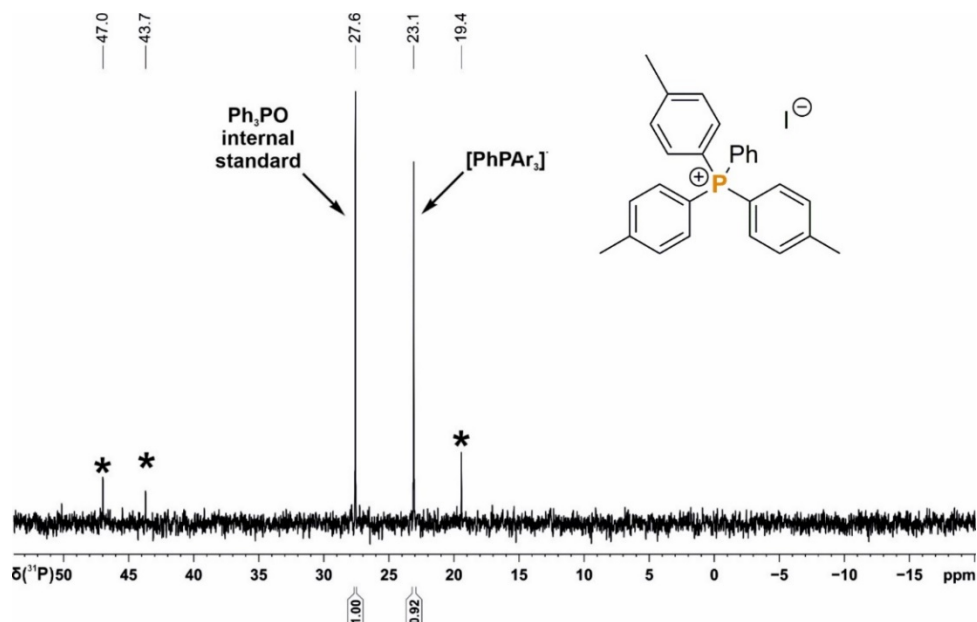
The general procedure 3 was followed using 4-iodoanisole (117 mg, 0.5 mmol), which resulted in 33% conversion to tris(4-methoxyphenyl)phenylphosphonium iodide and 5% di(4-methoxyphenyl)phenyl phosphine as judged by quantitative $^{31}\text{P}\{^1\text{H}\}$ (zgig) NMR spectroscopy.



Supplementary Figure 42. Quantitative single scan $^{31}\text{P}\{^1\text{H}\}$ (zgig) NMR spectrum for the photocatalytic arylation of H_2PPh using methyl 4-methoxyphenyl iodide. Ar = 4-methoxyphenyl. * marks the signal of an unknown by-product.

Tris(4-methylphenyl)phenylphosphonium iodide, Table 3, compound IV-13

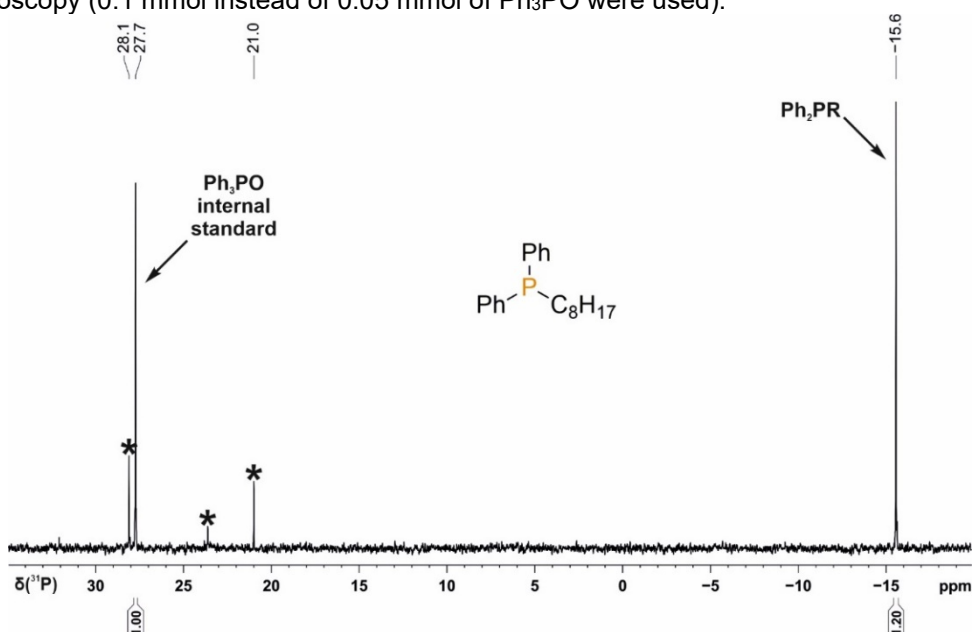
The general procedure 3 was followed using 4-iodotoluene (109 mg, 0.5 mmol), which resulted in 46% conversion to tris(4-methylphenyl)phenylphosphonium iodide as judged by quantitative $^{31}\text{P}\{^1\text{H}\}$ (zgig) NMR spectroscopy.



Supplementary Figure 43. Quantitative single scan $^{31}\text{P}\{^1\text{H}\}$ (zgig) NMR spectrum for the photocatalytic arylation of H_2PPh using 4-iodotoluene. Ar = 4-methylphenyl * marks the signal of an unknown by-product.

***n*-Octyldiphenylphosphine, Table 4, compound V-1,**

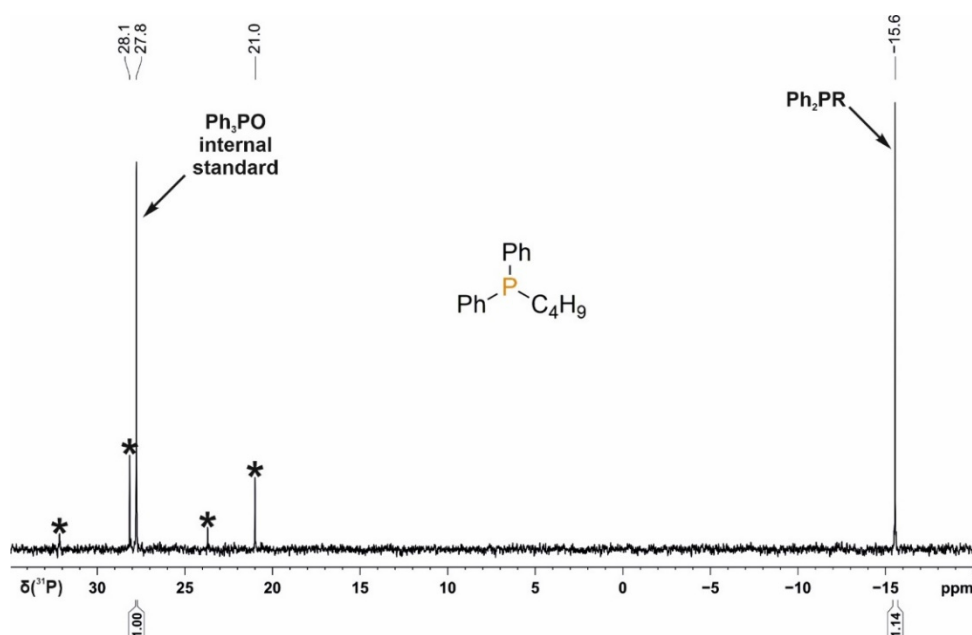
The general procedure 4 was followed using 1-iodooctane (72 μL , 0.4 mmol), which resulted in 60% conversion to *n*-octyldiphenylphosphine as judged by quantitative $^{31}\text{P}\{^1\text{H}\}$ (zgig) NMR spectroscopy (0.1 mmol instead of 0.05 mmol of Ph_3PO were used).



Supplementary Figure 44. Quantitative single scan $^{31}\text{P}\{^1\text{H}\}$ (zgig) NMR spectrum for the photocatalytic alkylation of HPPH_2 using 1-iodooctane. R = *n*-octyl * marks the signal of an unknown by-product.

***n*-Butyldiphenylphosphine, Table 4, compound V-2**

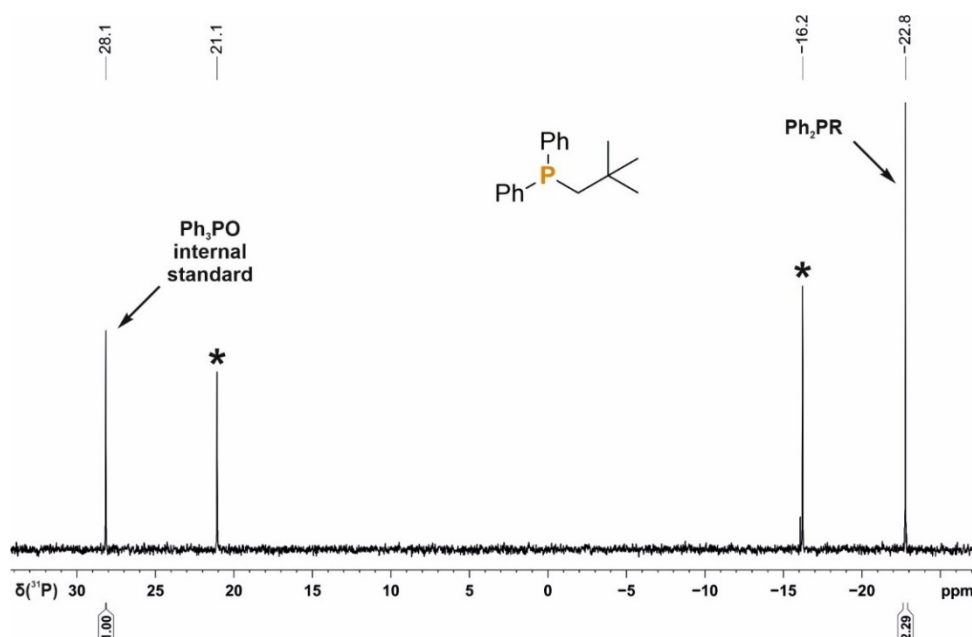
The general procedure 4 was followed using 1-iodobutane (46 μ L, 0.4 mmol), which resulted in 57% conversion to *n*-butyldiphenylphosphine as judged by quantitative $^{31}\text{P}\{^1\text{H}\}$ (zgig) NMR spectroscopy (0.1 mmol instead of 0.05 mmol of Ph_3PO were used).



Supplementary Figure 45. Quantitative single scan $^{31}\text{P}\{^1\text{H}\}$ (zgig) NMR spectrum for the photocatalytic alkylation of HPPH_2 using 1-iodobutane. R = *n*-butyl * marks the signal of an unknown by-product.

Neopentyldiphenylphosphine, Table 4, compound V-3

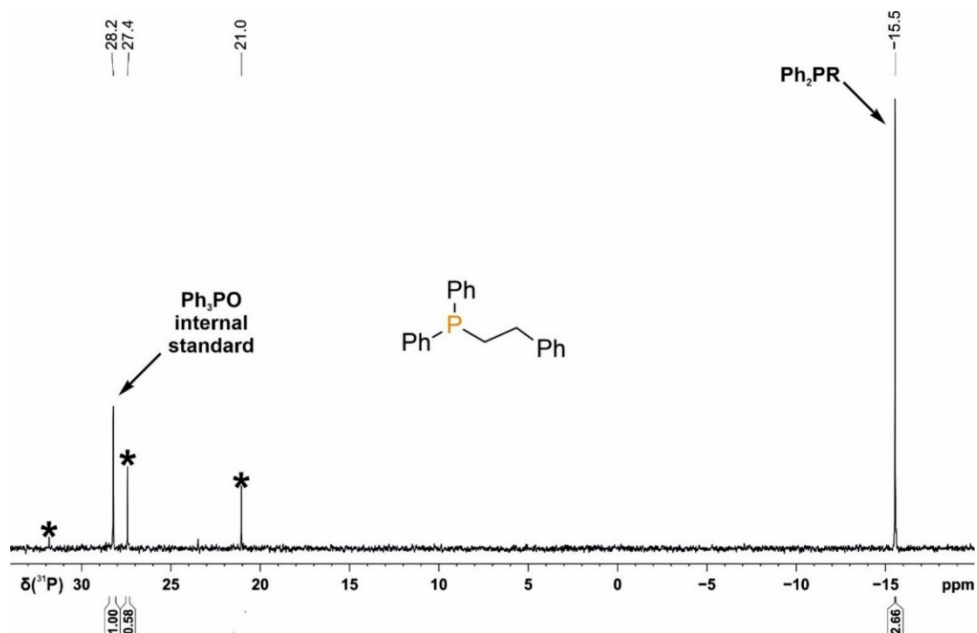
The general procedure 4 was followed using 1-iodo-2,2dimethylpropane (53 μ L, 0.4 mmol), which resulted in 57% conversion to neopentyldiphenylphosphine as judged by quantitative $^{31}\text{P}\{^1\text{H}\}$ (zgig) NMR spectroscopy.



Supplementary Figure 46. Quantitative single scan $^{31}\text{P}\{^1\text{H}\}$ (zgig) NMR spectrum for the photocatalytic alkylation of HPPH_2 using 1-iodo-2,2dimethylpropane. R = neopentyl. * marks the signal of an unknown by-product.

Phenethyldiphenylphosphine, Table 4, compound V-4

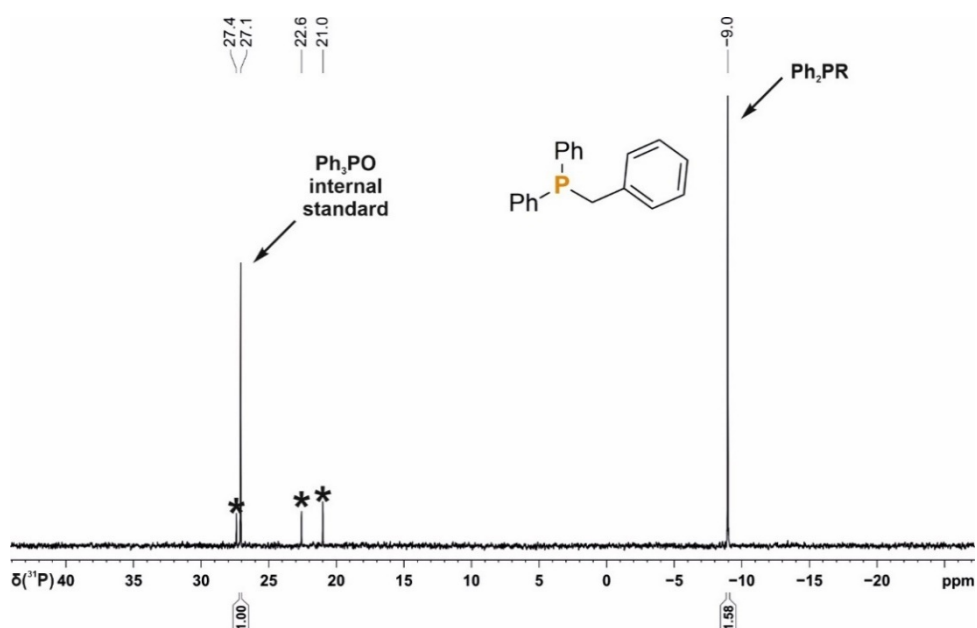
The general procedure 4 was followed using (2-iodoethyl)benzene (58 μL , 0.4 mmol), which resulted in 67% conversion to phenethyldiphenylphosphine as judged by quantitative $^{31}\text{P}\{^1\text{H}\}$ (zgig) NMR spectroscopy.



Supplementary Figure 47. Quantitative single scan $^{31}\text{P}\{^1\text{H}\}$ (zgig) NMR spectrum for the photocatalytic alkylation of HPPh_2 using (2-iodoethyl)benzene. R = 2-iodoethyl. * marks the signal of an unknown by-product.

Benzylidiphenylphosphine, Table 4, compound V-5

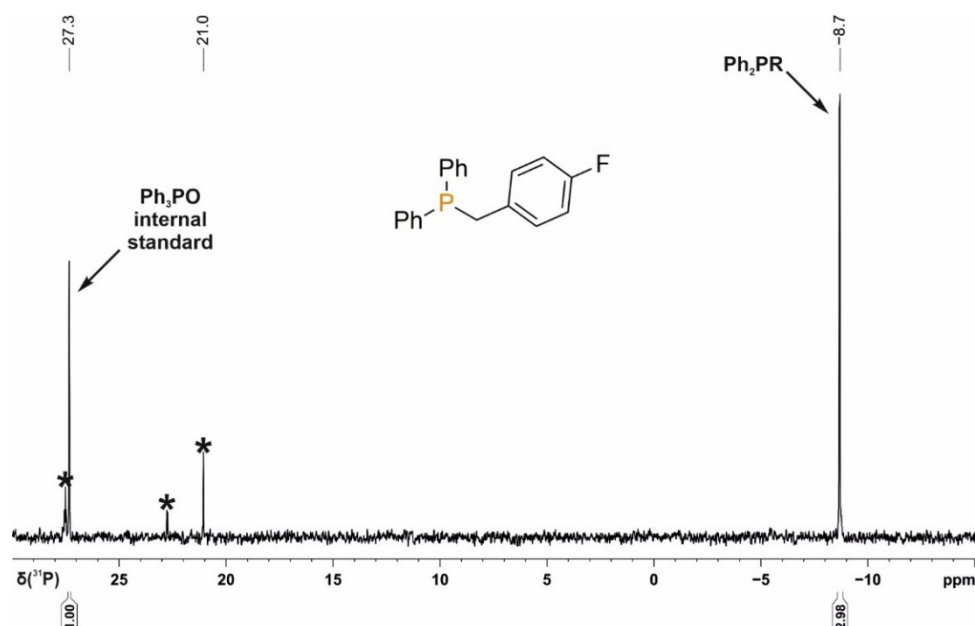
The general procedure 4 was followed using benzyl bromide (48 μL , 0.4 mmol), which resulted in 79% conversion to benzylidiphenylphosphine as judged by quantitative $^{31}\text{P}\{^1\text{H}\}$ (zgig) NMR spectroscopy (0.1 mmol instead of 0.05 mmol of Ph_3PO were used).



Supplementary Figure 48. Quantitative single scan $^{31}\text{P}\{^1\text{H}\}$ (zgig) NMR spectrum for the photocatalytic alkylation of HPPh_2 using benzyl bromide. R = benzyl. * marks the signal of an unknown by-product.

(4-Fluorobenzyl)diphenylphosphine, Table 4, compound V-6

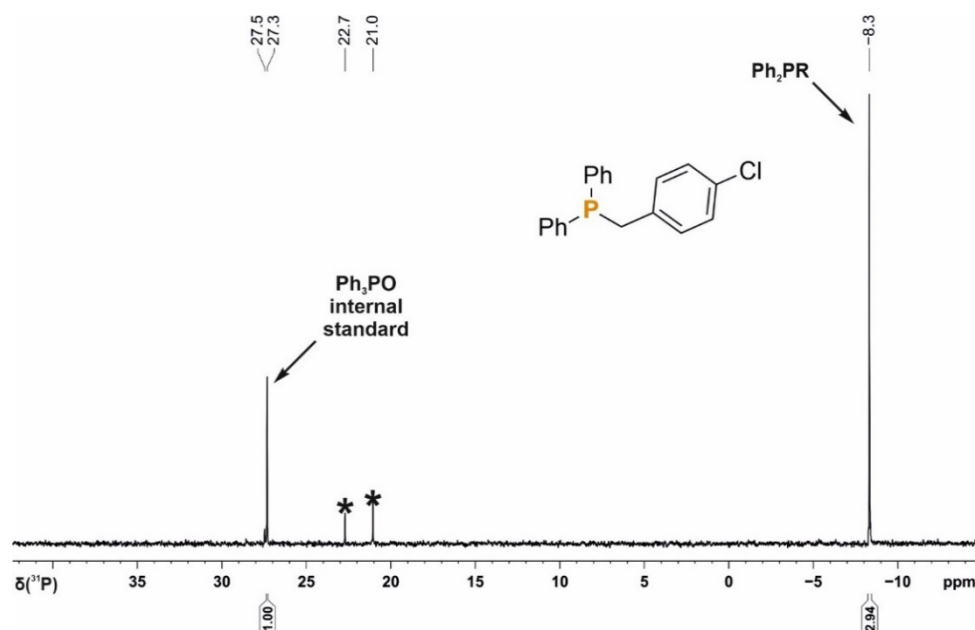
The general procedure 4 was followed using 4-fluorobenzyl bromide (50 μ L, 0.4 mmol), which resulted in 75% conversion to (4-fluorobenzyl)diphenylphosphine as judged by quantitative $^{31}\text{P}\{^1\text{H}\}$ (zgig) NMR spectroscopy.



Supplementary Figure 49. Quantitative single scan $^{31}\text{P}\{^1\text{H}\}$ (zgig) NMR spectrum for the photocatalytic alkylation of HPPH_2 using 4-fluorobenzyl bromide. R = 4-fluorobenzyl. *marks the signal of an unknown by-product.

(4-Chlorobenzyl)diphenylphosphine, Table 4, compound V-7

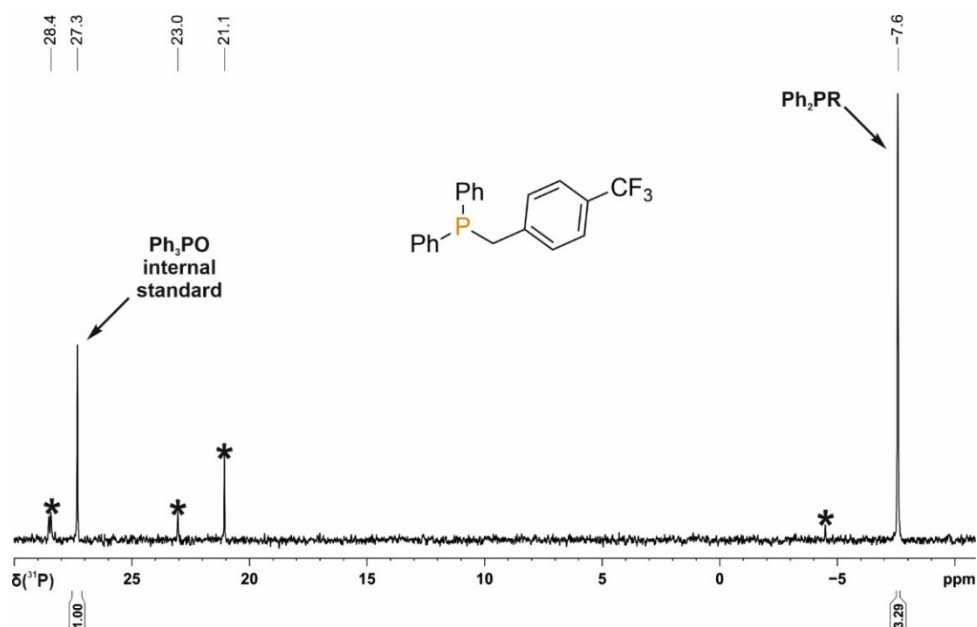
The general procedure 4 was followed using 4-chlorobenzyl bromide (82 mg, 0.4 mmol), which resulted in 74% conversion to (4-chlorobenzyl)diphenylphosphine as judged by quantitative $^{31}\text{P}\{^1\text{H}\}$ (zgig) NMR spectroscopy.



Supplementary Figure 50. Quantitative single scan $^{31}\text{P}\{^1\text{H}\}$ (zgig) NMR spectrum for the photocatalytic alkylation of HPPH_2 using 4-chlorobenzyl bromide. R = 4-chlorobenzyl. * marks the signal of an unknown by-product.

4-(Trifluoromethyl)benzylidiphenylphosphine, Table 4, compound V-8

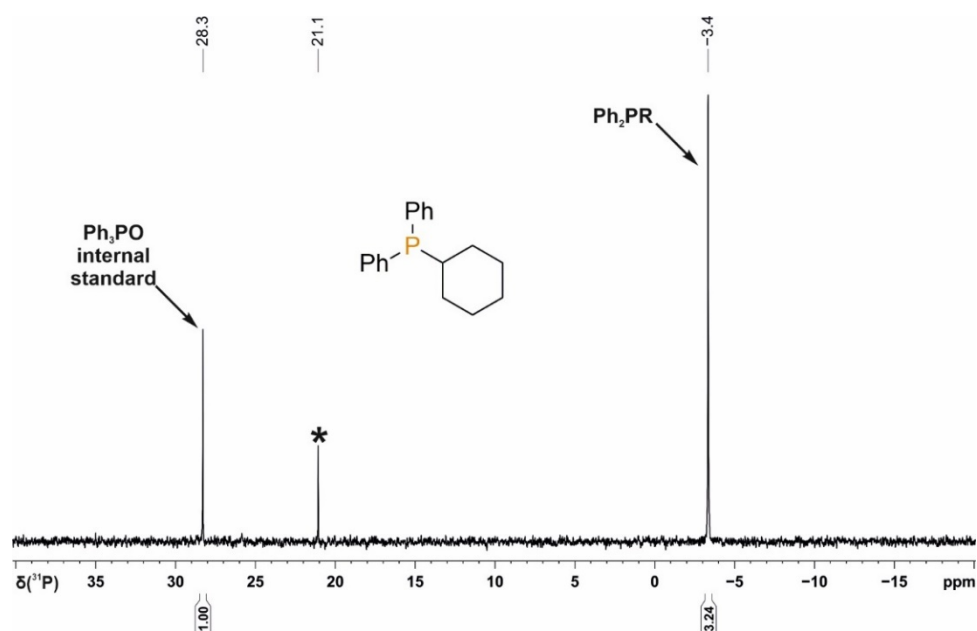
The general procedure 4 was followed using 4-(trifluoromethyl)benzyl bromide (96 mg, 0.4 mmol), which resulted in 82% conversion to as judged by quantitative $^{31}\text{P}\{^1\text{H}\}$ (zsig) NMR spectroscopy.



Supplementary Figure 51. Quantitative single scan $^{31}\text{P}\{^1\text{H}\}$ (zsig) NMR spectrum for the photocatalytic alkylation of HPPH_2 using 4-(trifluoromethyl)benzyl bromide. R = 4-(trifluoromethyl)benzyl. *marks the signal of an unknown by-product.

Cyclohexyldiphenylphosphine, Table 4, compound V-10

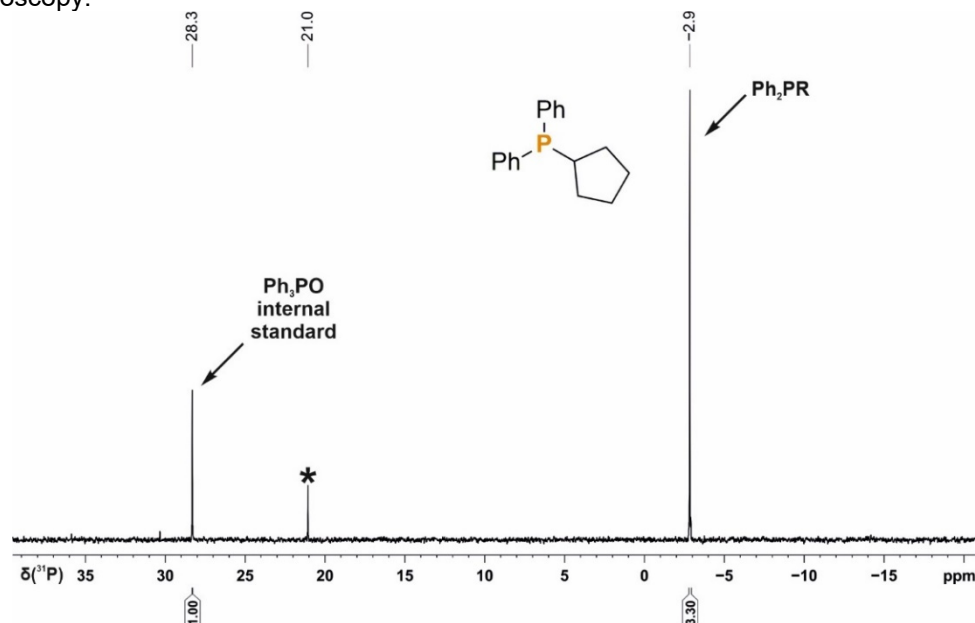
The general procedure 4 was followed using iodocyclohexane (52 μL , 0.4 mmol), which resulted in 81% conversion to cyclohexyldiphenylphosphine as judged by quantitative $^{31}\text{P}\{^1\text{H}\}$ (zsig) NMR spectroscopy.



Supplementary Figure 52. Quantitative single scan $^{31}\text{P}\{^1\text{H}\}$ (zsig) NMR spectrum for the photocatalytic alkylation of HPPH_2 using iodocyclohexane. R = cyclohexyl. *marks the signal of an unknown by-product.

Cyclopentylidiphenylphosphine, Table 4, compound V-11

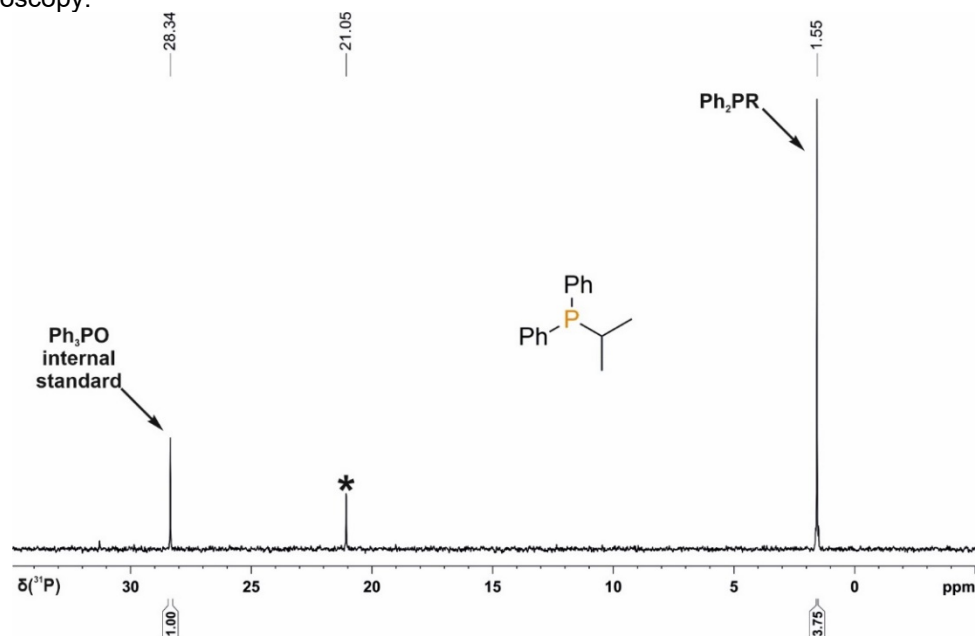
The general procedure 4 was followed using iodocyclopentane (46 μL , 0.4 mmol), which resulted in 83% conversion to cyclopentylidiphenylphosphine as judged by quantitative $^{31}\text{P}\{^1\text{H}\}$ (zgif) NMR spectroscopy.



Supplementary Figure 53. Quantitative single scan $^{31}\text{P}\{^1\text{H}\}$ (zgif) NMR spectrum for the photocatalytic alkylation of HPPH_2 using iodocyclopentane. R = cyclopentyl. *marks the signal of an unknown by-product.

Isopropylidiphenylphosphine, Table 4, compound V-12

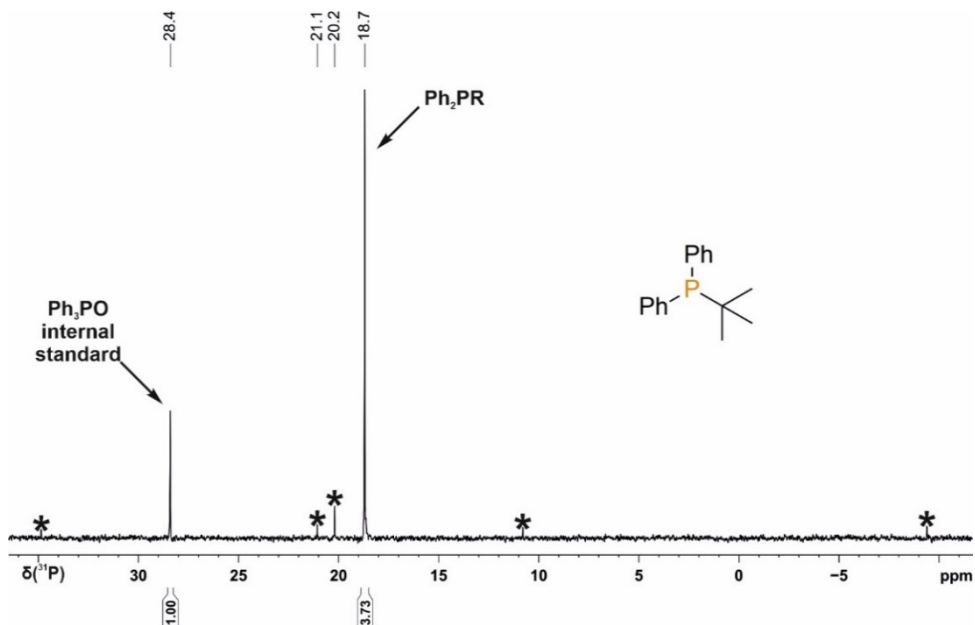
The general procedure 4 was followed using 2-iodopropane (40 μL , 0.4 mmol), which resulted in 95% conversion to isopropylidiphenylphosphine as judged by quantitative $^{31}\text{P}\{^1\text{H}\}$ (zgif) NMR spectroscopy.



Supplementary Figure 54. Quantitative single scan $^{31}\text{P}\{^1\text{H}\}$ (zgif) NMR spectrum for the photocatalytic alkylation of HPPH_2 using 2-iodopropane. R = isopropyl. *marks the signal of an unknown by-product.

***tert*-Butyldiphenylphosphine, Table 4, compound V-13**

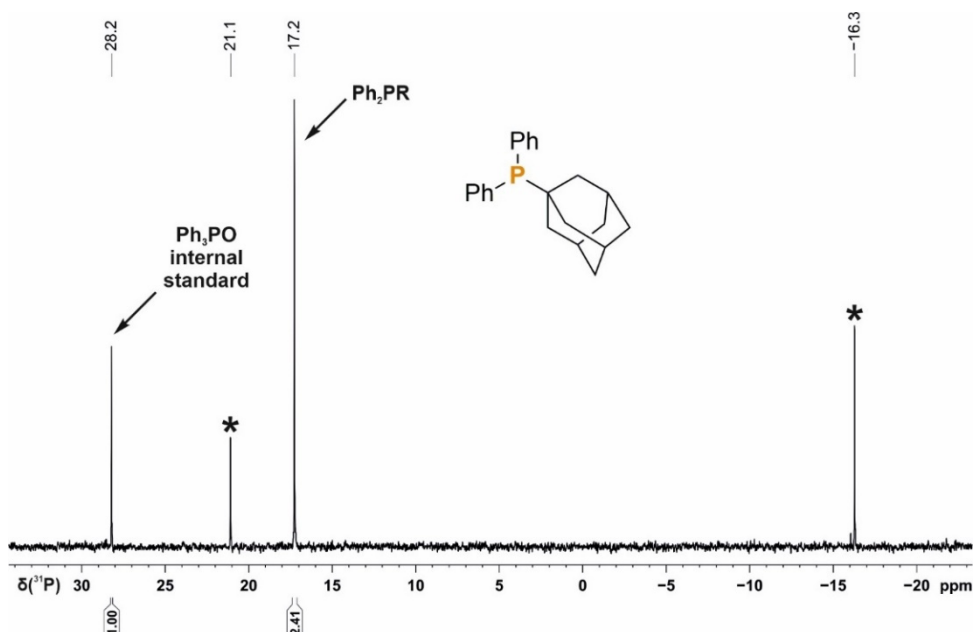
The general procedure 4 was followed using 2-iodo-2-methylpropane (48 μ L, 0.4 mmol), which resulted in 93% conversion to *tert*-butyldiphenylphosphine as judged by quantitative $^{31}\text{P}\{^1\text{H}\}$ (zlig) NMR spectroscopy.



Supplementary Figure 55. Quantitative single scan $^{31}\text{P}\{^1\text{H}\}$ (zlig) NMR spectrum for the photocatalytic alkylation of HPPH_2 using 2-iodo-2-methylpropane. R = *tert*-butyl. *marks the signal of an unknown by-product.

Adamantyldiphenylphosphine, Table 4, compound V-14

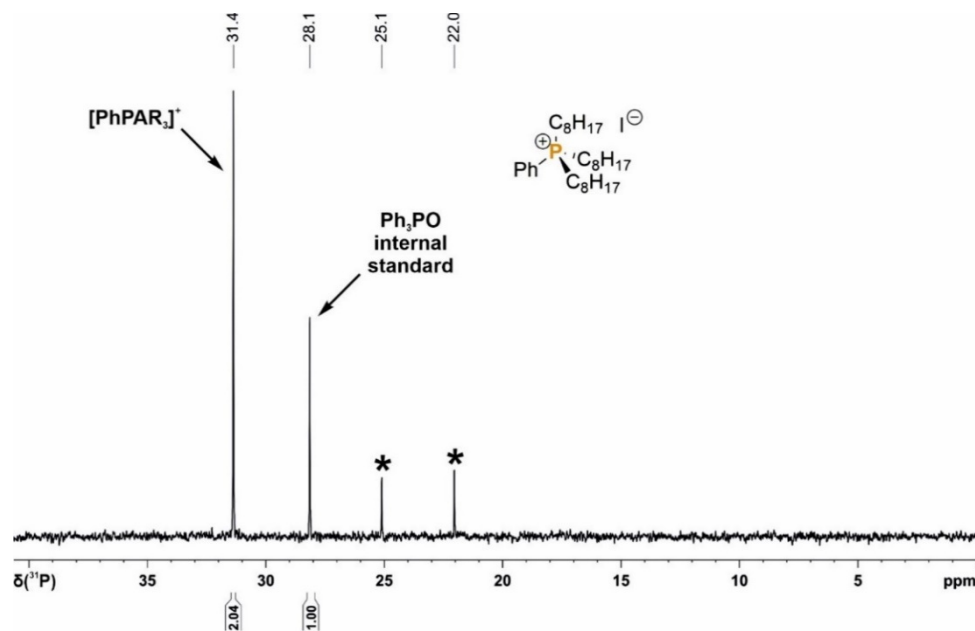
The general procedure 4 was followed using 1-iodoadamantane (105 mg, 0.4 mmol), which resulted in 60% conversion to adamantyldiphenylphosphine as judged by quantitative $^{31}\text{P}\{^1\text{H}\}$ (zlig) NMR spectroscopy.



Supplementary Figure 56. Quantitative single scan $^{31}\text{P}\{^1\text{H}\}$ (zlig) NMR spectrum for the photocatalytic alkylation of HPPH_2 using 1-iodoadamantane. R = 1-adamantyl. *marks the signal of an unknown by-product.

Tri(*n*-octyl)phenylphosphonium iodide, Table 5, compound VII-1

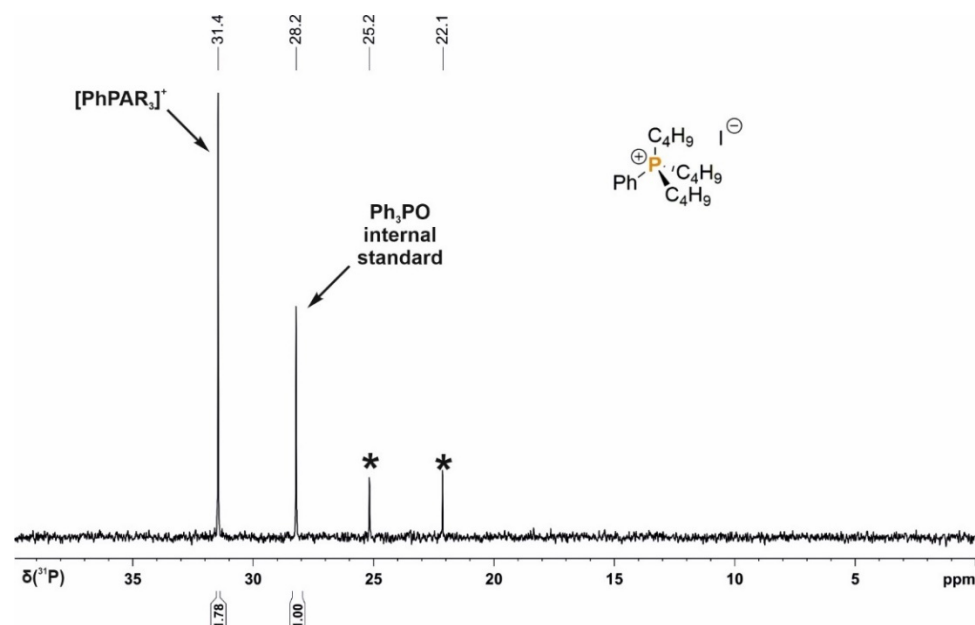
The general procedure 5 was followed using 1-iodooctane (144 μ L, 0.8 mmol), which resulted in 51% conversion to {tri(*n*-octyl)}(phenyl)phosphonium iodide as judged by quantitative $^{31}\text{P}\{^1\text{H}\}$ (zgig) NMR spectroscopy.



Supplementary Figure 57. Quantitative single scan $^{31}\text{P}\{^1\text{H}\}$ (zgig) NMR spectrum for the photocatalytic alkylation of H_2PPh using 1-iodooctane. R = *n*-octyl. *marks the signal of an unknown by-product.

Tributyl(phenyl)phosphonium iodide, Table 5, compound VII-2

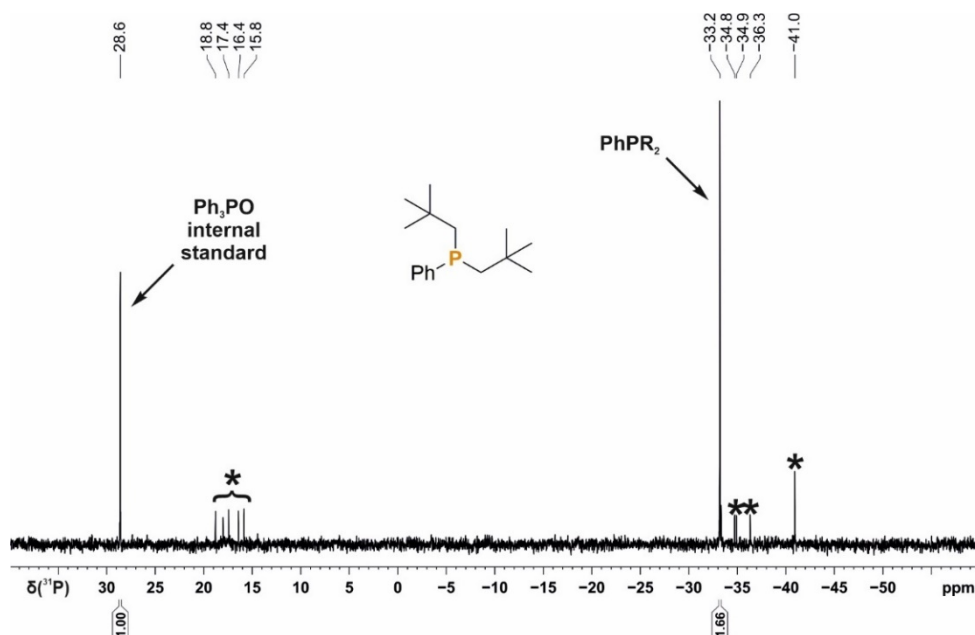
The general procedure 5 was followed using 1-iodobutane (72 μ L, 0.8 mmol), which resulted in 45% conversion to tributyl(phenyl)phosphonium iodide as judged by quantitative $^{31}\text{P}\{^1\text{H}\}$ (zgig) NMR spectroscopy.



Supplementary Figure 58. Quantitative single scan $^{31}\text{P}\{^1\text{H}\}$ (zgig) NMR spectrum for the photocatalytic alkylation of H_2PPh using 1-iodobutane. R = *n*-butyl * marks the signal of an unknown by-product.

Di(neopentyl)phenylphosphine, Table 5, compound VII-3

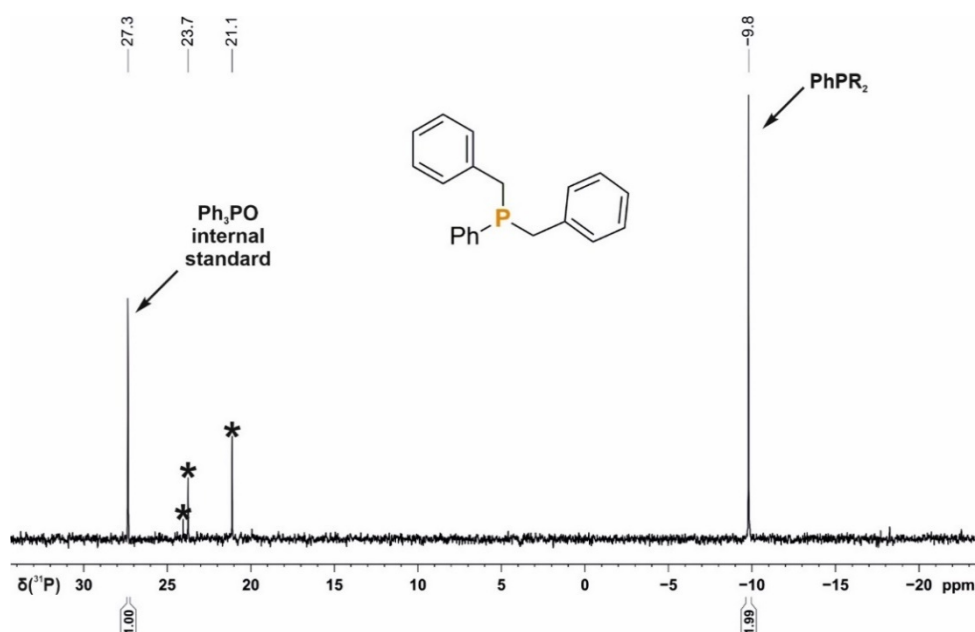
The general procedure 5 was followed using 1-iodo-2,2-dimethylpropane (106 μL , 0.8 mmol), which resulted in 42% conversion to di(neopentyl)phenylphosphine as judged by quantitative $^{31}\text{P}\{^1\text{H}\}$ (zgig) NMR spectroscopy.



Supplementary Figure 59. Quantitative single scan $^{31}\text{P}\{^1\text{H}\}$ (zgig) NMR spectrum for the photocatalytic alkylation of H_2PPh using 1-iodo-2,2-dimethylpropane. R = neopentyl * marks the signal of an unknown by-product.

Di(benzyl)phenylphosphine, Table 5, compound VI-4

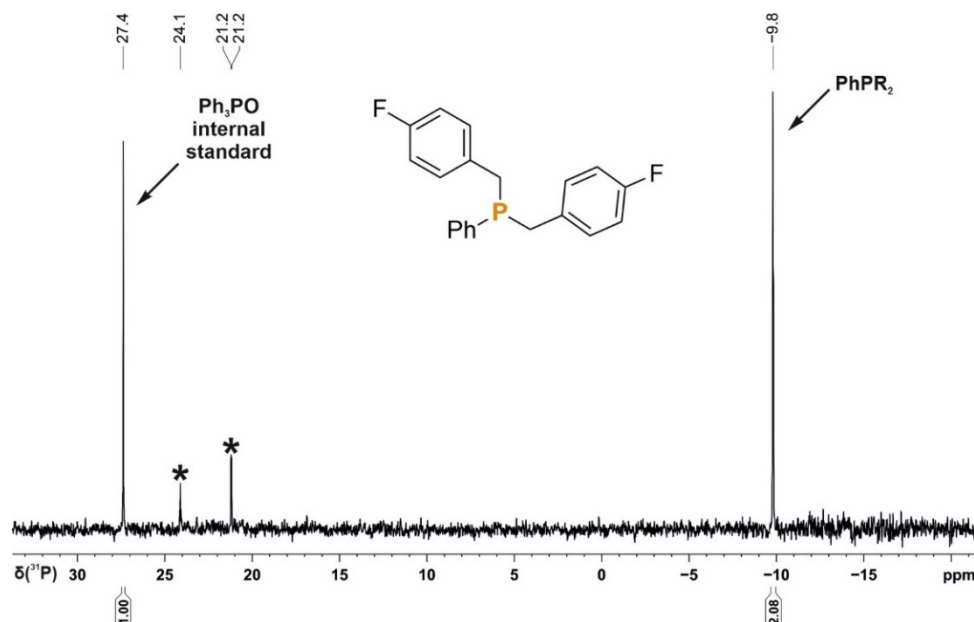
The general procedure 5 was followed using benzyl bromide (71 μL , 0.6 mmol), which resulted in 50% conversion to tris(4-methylphenyl)phenylphosphonium iodide as judged by quantitative $^{31}\text{P}\{^1\text{H}\}$ (zgig) NMR spectroscopy.



Supplementary Figure 60. Quantitative single scan $^{31}\text{P}\{^1\text{H}\}$ (zgig) NMR spectrum for the photocatalytic alkylation of H_2PPH using benzyl bromide. R = benzyl. * marks the signal of an unknown by-product.

Bis(4-fluorobenzyl)phenylphosphine, Table 5, compound VI-5

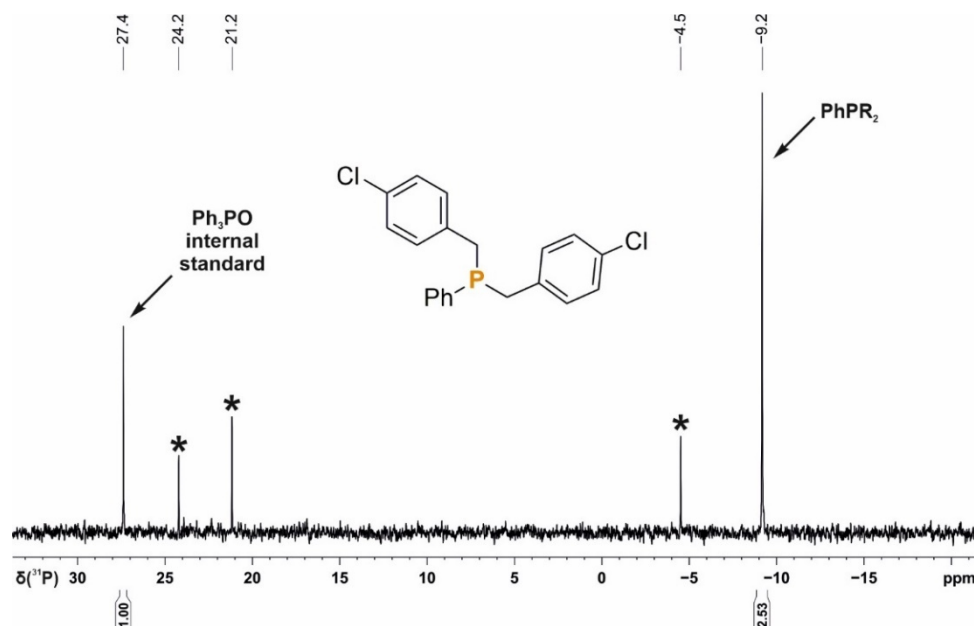
The general procedure 5 was followed using 4-fluorobenzyl bromide (75 μ L, 0.6 mmol), which resulted in 52% conversion to bis(4-fluorobenzyl)phenylphosphine as judged by quantitative $^{31}\text{P}\{^1\text{H}\}$ (zgig) NMR spectroscopy.



Supplementary Figure 61. Quantitative single scan $^{31}\text{P}\{^1\text{H}\}$ (zgig) NMR spectrum for the photocatalytic alkylation of H_2PPH using 4-fluorobenzyl bromide. R = 4-fluorobenzyl. *marks the signal of an unknown by-product.

Bis(4-chlorobenzyl)phenylphosphine, Table 5, compound VI-6

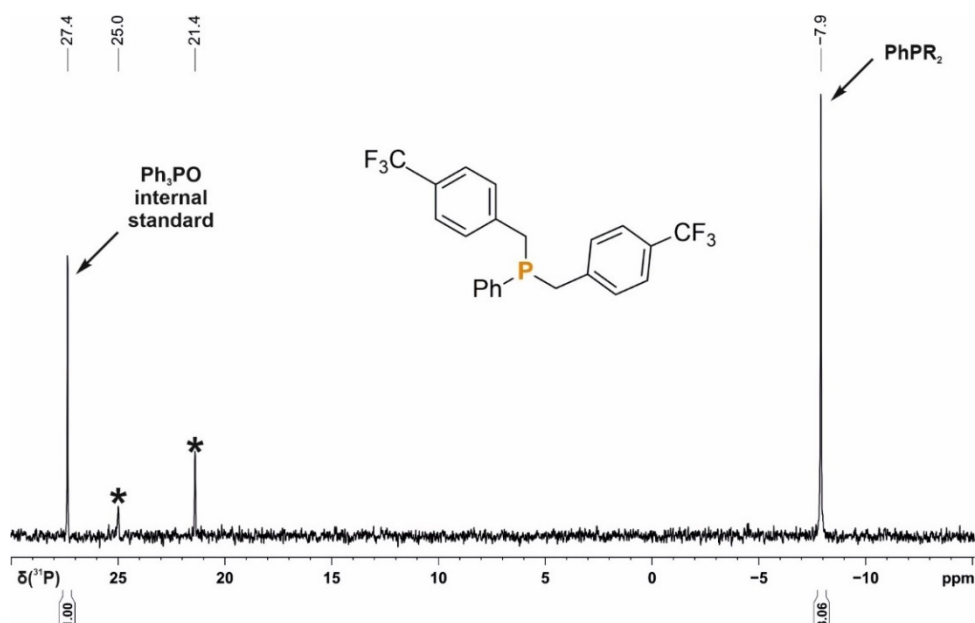
The general procedure 5 was followed using 4-chlorobenzyl bromide (123.3 mg, 0.6 mmol), which resulted in 63% conversion to bis(4-chlorobenzyl)phenylphosphine as judged by quantitative $^{31}\text{P}\{^1\text{H}\}$ (zgig) NMR spectroscopy.



Supplementary Figure 62. Quantitative single scan $^{31}\text{P}\{^1\text{H}\}$ (zgig) NMR spectrum for the photocatalytic alkylation of H_2PPH using 4-chlorobenzyl bromide. R = 4-chlorobenzyl. *marks the signal of an unknown by-product.

Bis-4-(trifluoromethyl)benzylphenylphosphine, Table 5, compound VI-7

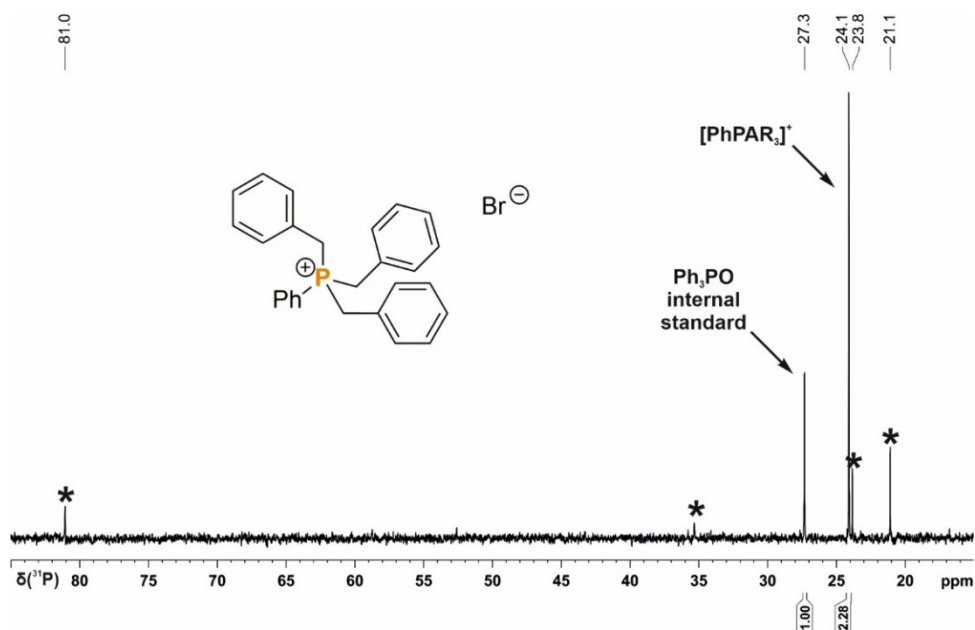
The general procedure 5 was followed using 4-(trifluoromethyl)benzyl bromide (143 mg, 0.6 mmol), which resulted in 77% conversion to bis(4-(trifluoromethyl)benzyl)phenylphosphine as judged by quantitative $^{31}\text{P}\{^1\text{H}\}$ (zgig) NMR spectroscopy.



Supplementary Figure 63. Quantitative single scan $^{31}\text{P}\{^1\text{H}\}$ (zgig) NMR spectrum for the photocatalytic alkylation of H_2PPH using 4-(trifluoromethyl)benzyl iodide. R = 4-(trifluoromethyl)benzyl * marks the signal of an unknown by-product.

Tribenzylphenylphosphonium bromide, Table 5, compound VII-4

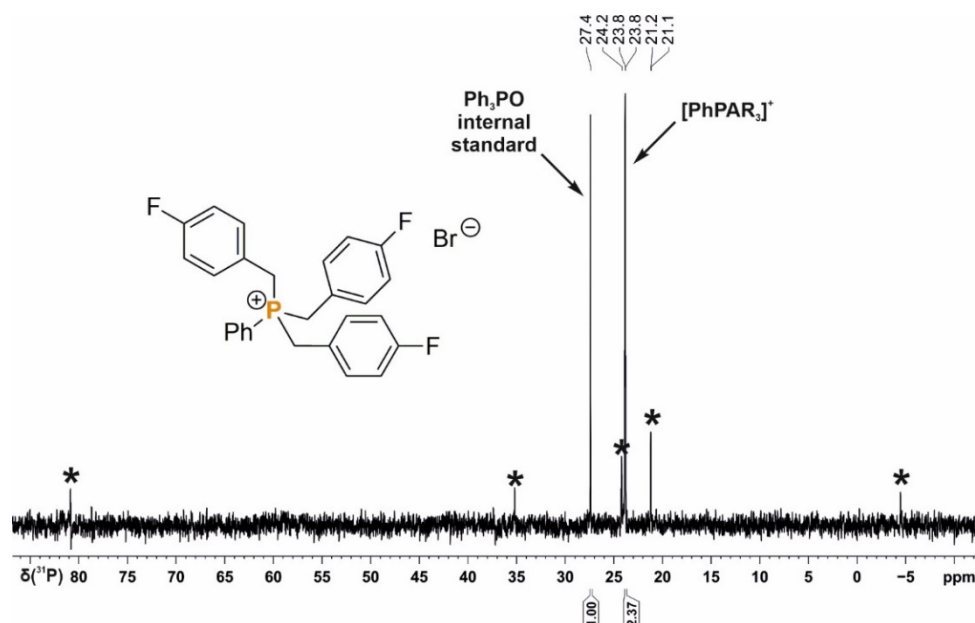
The general procedure 5 was followed using benzyl bromide (95 μL , 0.8 mmol), which resulted in 57% conversion to tribenzylphenylphosphonium bromide as judged by quantitative $^{31}\text{P}\{^1\text{H}\}$ (zgig) NMR spectroscopy.



Supplementary Figure 64. Quantitative single scan $^{31}\text{P}\{^1\text{H}\}$ (zgig) NMR spectrum for the photocatalytic alkylation of H_2PPH using benzyl bromide. R = benzyl. * marks the signal of an unknown by-product.

Tris(4-fluorobenzyl)phenylphosphonium bromide, Table 5, compound VII-5

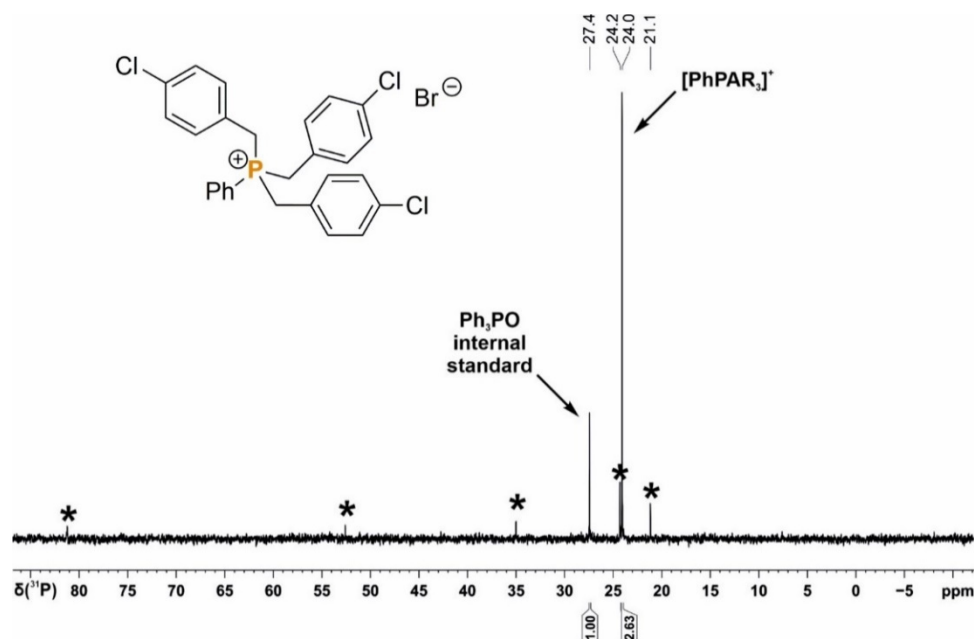
The general procedure 5 was followed using 4-fluorobenzyl bromide (100 μ L, 0.8 mmol), which resulted in 59% conversion to tris(4-fluorobenzyl)phenylphosphonium bromide as judged by quantitative $^{31}\text{P}\{^1\text{H}\}$ (zgig) NMR spectroscopy.



Supplementary Figure 65. Quantitative single scan $^{31}\text{P}\{^1\text{H}\}$ (zgig) NMR spectrum for the photocatalytic alkylation of H_2PPh using 4-fluorobenzyl bromide. R = 4-fluorobenzyl. *marks the signal of an unknown by-product.

Tris(4-chlorobenzyl)phenylphosphonium bromide, Table 5, compound VII-6

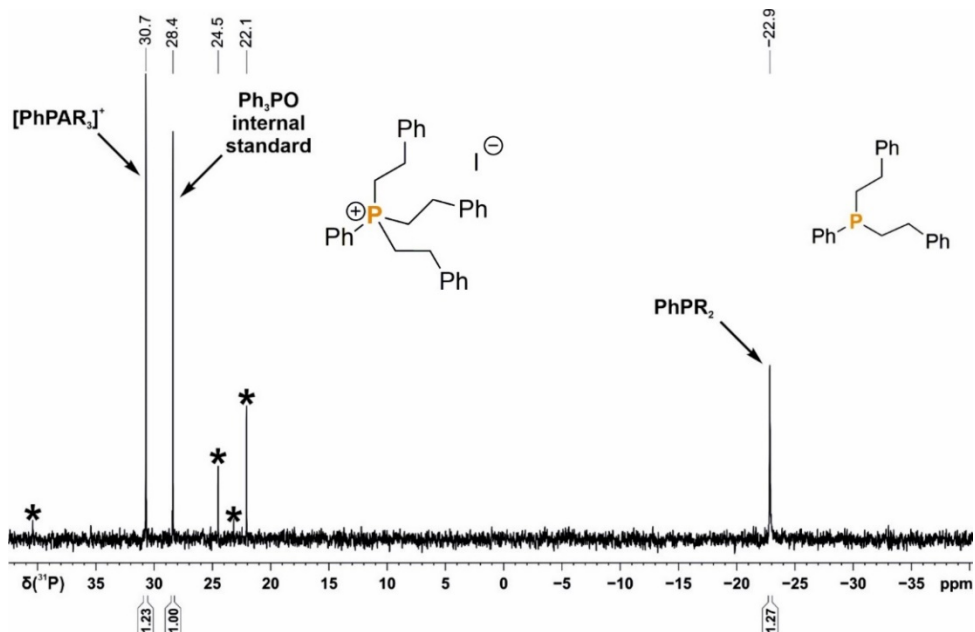
The general procedure 5 was followed using 4-chlorobenzyl bromide (164 mg, 0.8 mmol), which resulted in 66% conversion to tris(4-chlorobenzyl)phenylphosphonium bromide as judged by quantitative $^{31}\text{P}\{^1\text{H}\}$ (zgig) NMR spectroscopy.



Supplementary Figure 66. Quantitative single scan $^{31}\text{P}\{^1\text{H}\}$ (zgig) NMR spectrum for the photocatalytic alkylation of H_2PPh using 4-chlorobenzyl bromide. R = 4-chlorobenzyl. *marks the signal of an unknown by-product.

Tris(phenethyl)phenylphosphonium iodide and di(phenethyl)phenylphosphine, Table 5, compound VII-8 and VI-8

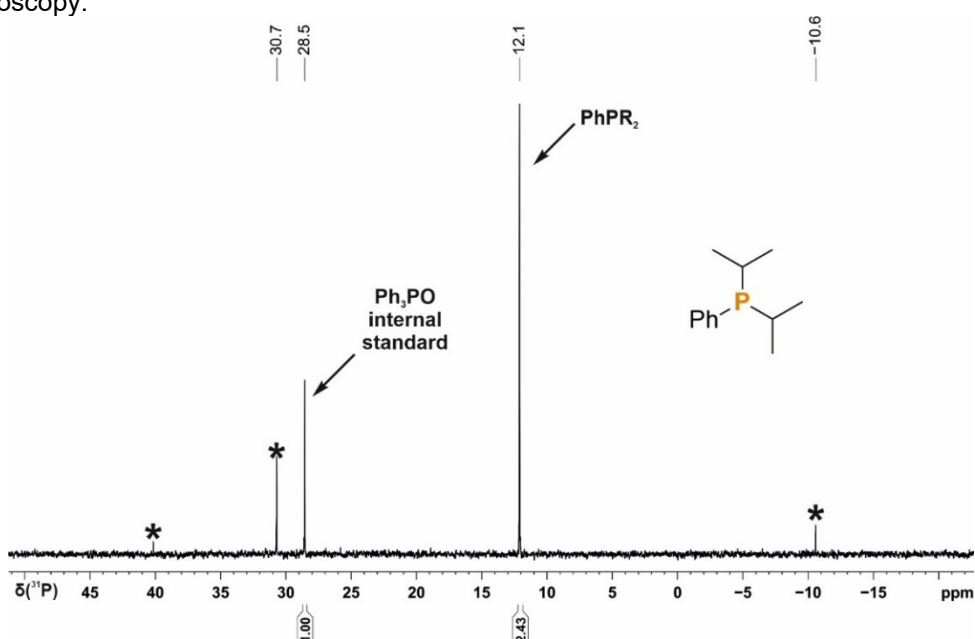
The general procedure 5 was followed using (2-iodoethyl)benzene (116 μL , 0.8 mmol), which resulted in 31% conversion to tris(phenethyl)phenylphosphonium iodide and 32% di(phenethyl)phenylphosphine as judged by quantitative $^{31}\text{P}\{^1\text{H}\}$ (zgig) NMR spectroscopy.



Supplementary Figure 67. Quantitative single scan $^{31}\text{P}\{^1\text{H}\}$ (zgig) NMR spectrum for the photocatalytic alkylation of H_2PPh using 2-iodoethylbenzene. R = 2-ethylbenzyl. * marks the signal of an unknown by-product.

Diisopropyl(phenyl)phosphine, Table 5, compound VI-9

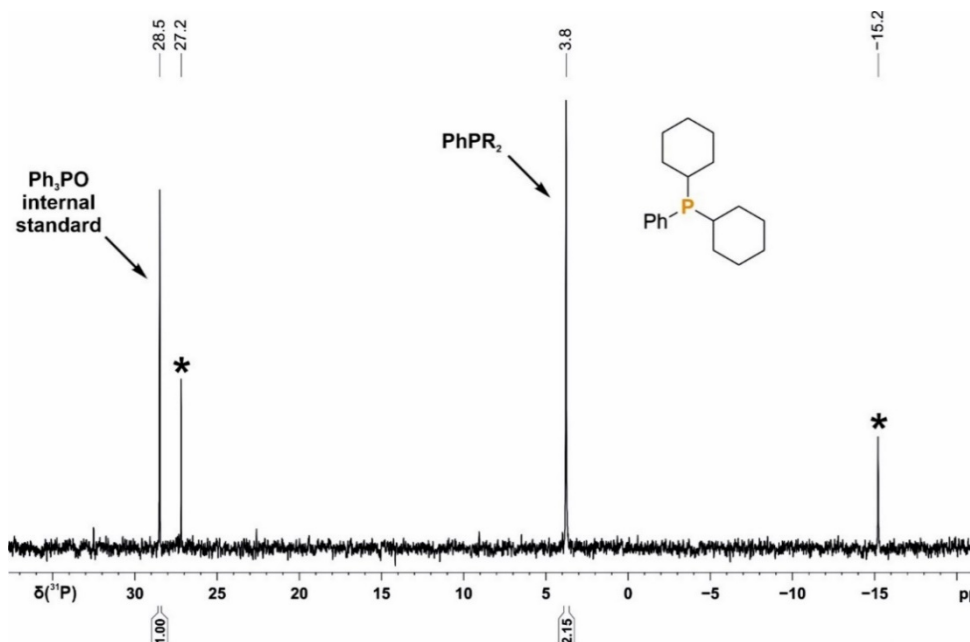
The general procedure 5 was followed using 2-iodopropane (80 μL , 0.8 mmol), which resulted in 61% conversion to diisopropyl(phenyl)phosphine as judged by quantitative $^{31}\text{P}\{^1\text{H}\}$ (zgig) NMR spectroscopy.



Supplementary Figure 68. Quantitative single scan $^{31}\text{P}\{^1\text{H}\}$ (zgig) NMR spectrum for the photocatalytic alkylation of H_2PPH using 2-iodopropane. R = isopropyl. * marks the signal of an unknown by-product.

Dicyclohexyl(phenyl)phosphine, Table 5, compound VI-10

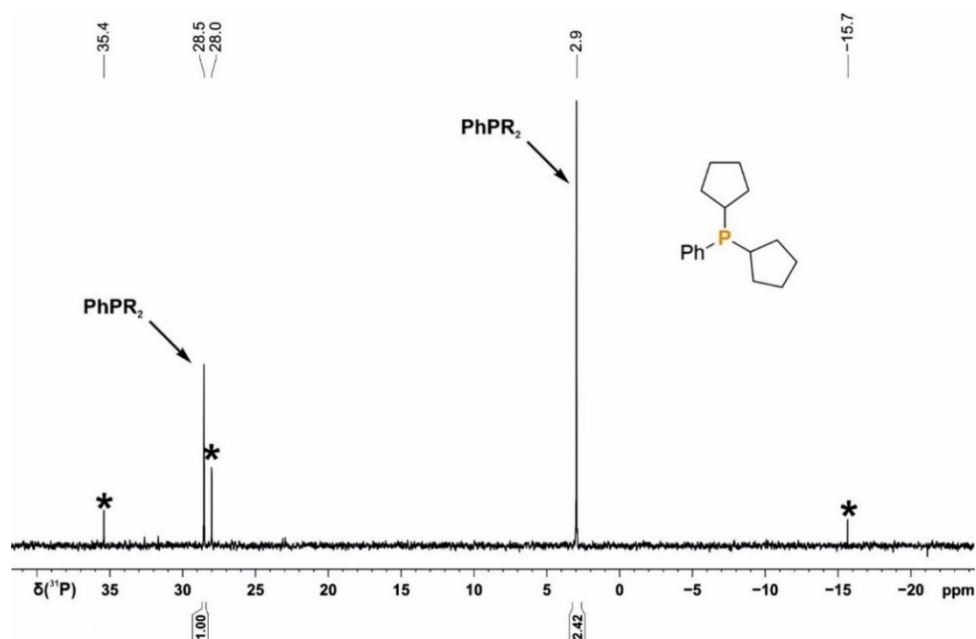
The general procedure 5 was followed using iodocyclohexane (103 μL , 0.8 mmol), which resulted in 54% conversion to dicyclohexyl(phenyl)phosphine as judged by quantitative $^{31}\text{P}\{^1\text{H}\}$ (zlig) NMR spectroscopy.



Supplementary Figure 69. Quantitative single scan $^{31}\text{P}\{^1\text{H}\}$ (zlig) NMR spectrum for the photocatalytic alkylation of H_2PPh using iodocyclohexane. R = cyclohexyl. * marks the signal of an unknown by-product.

Dicyclopentyl(phenyl)phosphine, Table 5, compound VI-11

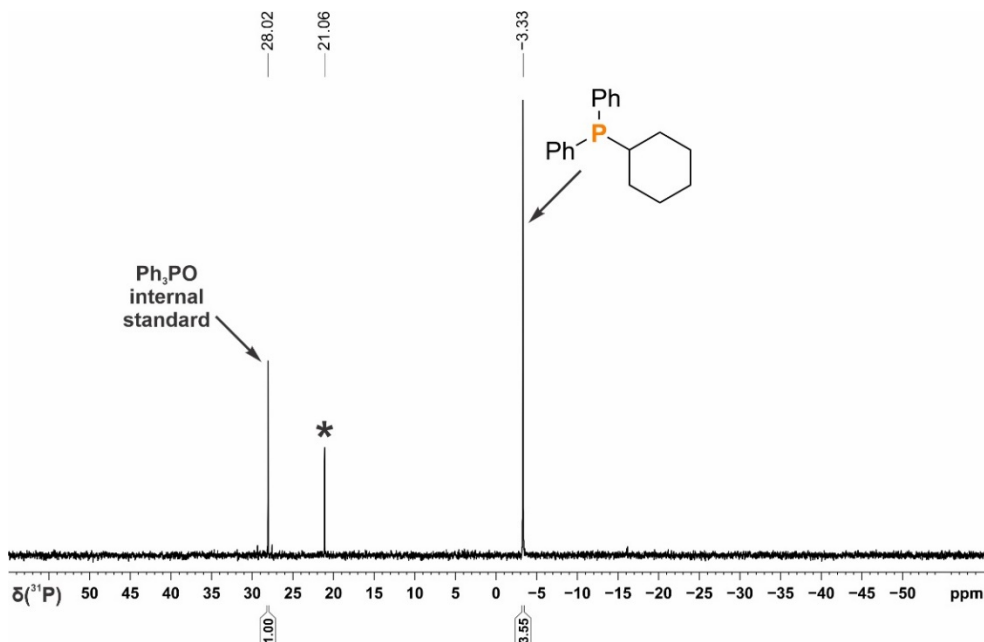
The general procedure 5 was followed using iodocyclopentyl (93 μL , 0.8 mmol), which resulted in 61% conversion to dicyclopentyl(phenyl)phosphine as judged by quantitative $^{31}\text{P}\{^1\text{H}\}$ (zlig) NMR spectroscopy.



Supplementary Figure 70. Quantitative single scan $^{31}\text{P}\{^1\text{H}\}$ (zlig) NMR spectrum for the photocatalytic alkylation of H_2PPh using iodocyclopentane. R = cyclopentyl * marks the signal of an unknown by-product.

Cyclohexyldiphenylphosphine, Scheme 2, compound V10

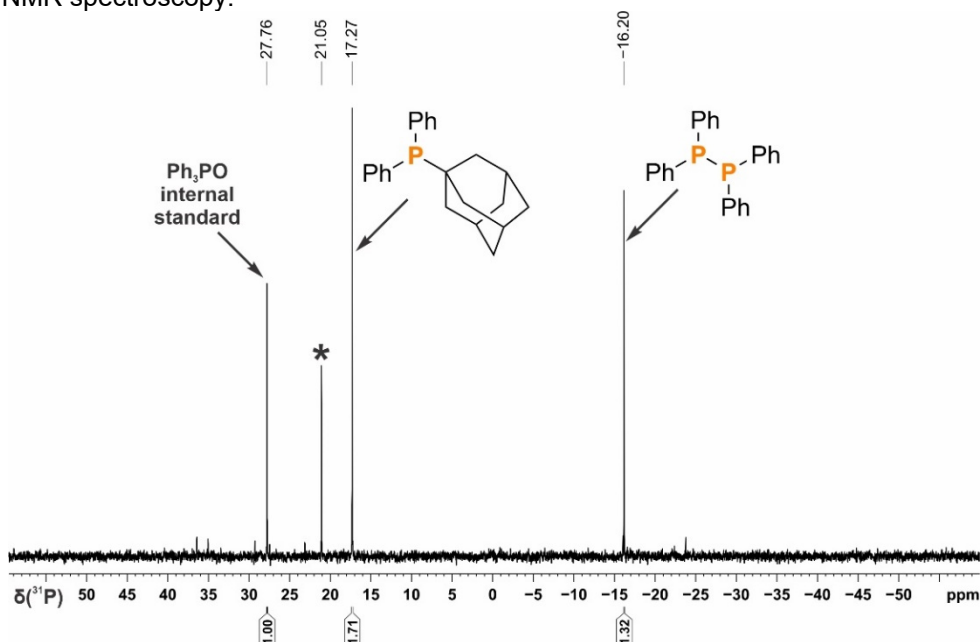
The general procedure 6 was followed using iodocyclohexane (78 μ L, 0.6 mmol), which resulted in 85% conversion to cyclohexyldiphenylphosphine as judged by quantitative $^{31}\text{P}\{^1\text{H}\}$ (zgig) NMR spectroscopy.



Supplementary Figure 71. Quantitative single scan $^{31}\text{P}\{^1\text{H}\}$ (zgig) NMR spectrum for the photocatalytic alkylation of P_2Ph_4 using iodocyclohexane. R = cyclohexyl * marks the signal of an unknown by-product.

Adamantyldiphenylphosphine, Scheme 2, compound V-14

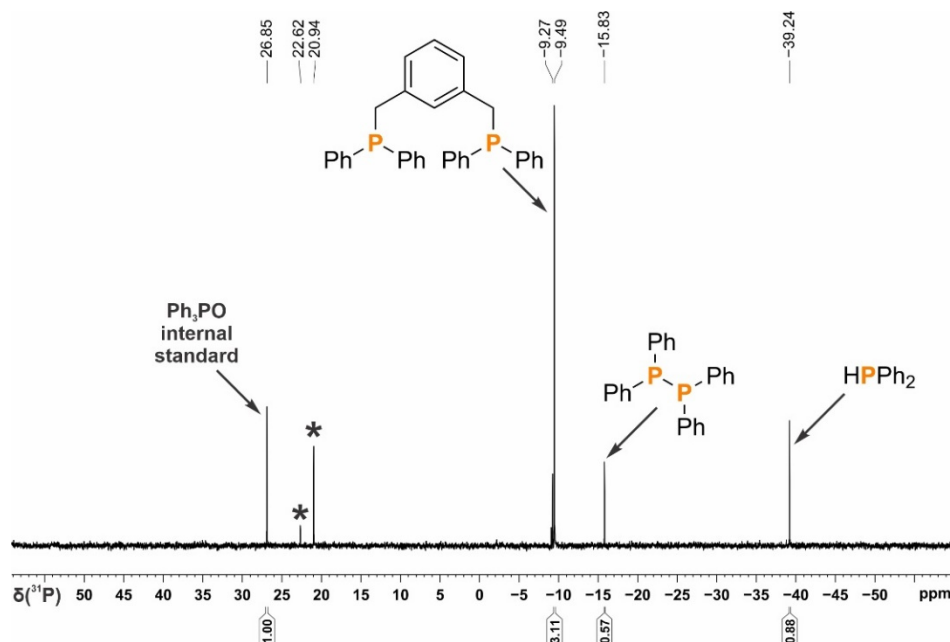
The general procedure 6 was followed using 1-iodoadamantane (157 mg, 0.6 mmol), which resulted in 43% conversion to adamantyldiphenylphosphine as judged by quantitative $^{31}\text{P}\{^1\text{H}\}$ (zgig) NMR spectroscopy.



Supplementary Figure 72. Quantitative single scan $^{31}\text{P}\{^1\text{H}\}$ (zgig) NMR spectrum for the photocatalytic alkylation of P_2Ph_4 using iodoadamantane. R = adamantyl * marks the signal of an unknown by-product.

1,3-Bis(diphenylphosphinomethyl)benzene, Scheme 2, compound V-15

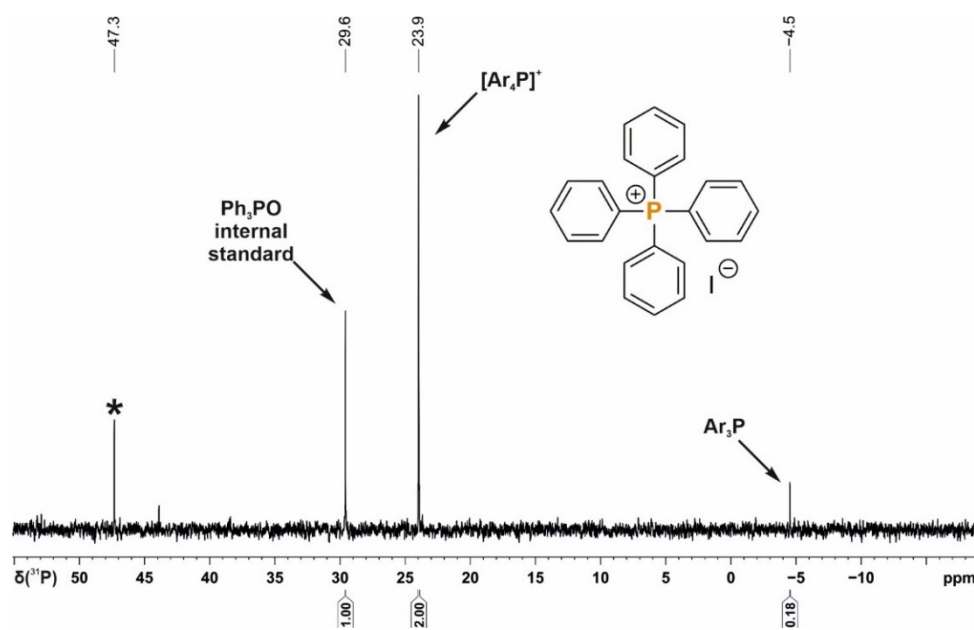
The general procedure 7 was followed using 1,3-bis(bromomethyl)benzene (27 mg, 0.1 mmol), which resulted in 78% conversion to 1,3-bis((diphenylphosphaneyl)methyl)benzene as judged by quantitative $^{31}\text{P}\{^1\text{H}\}$ (zgig) NMR spectroscopy.



Supplementary Figure 73. Quantitative single scan $^{31}\text{P}\{^1\text{H}\}$ (zgig) NMR spectrum for the photocatalytic alkylation of P_2Ph_4 using 1,3-bis(bromomethyl)benzene. * marks the signal of an unknown by-product.

Tetraphenylphosphonium iodide, Table 6, compound IX-1

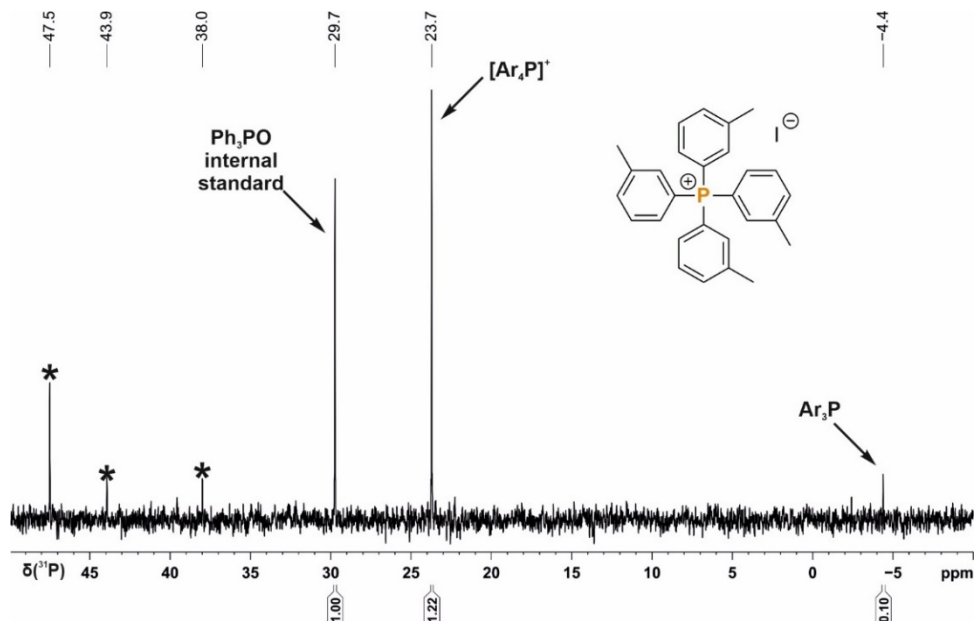
The general procedure 8 was followed using iodobenzene (128 μL , 1.1 mmol), which resulted in 60% conversion to tetraphenylphosphonium iodide as judged by quantitative $^{31}\text{P}\{^1\text{H}\}$ (zgig) NMR spectroscopy.



Supplementary Figure 74. Quantitative single scan $^{31}\text{P}\{^1\text{H}\}$ (zgig) NMR spectrum for the photocatalytic functionalization of P_4 using iodobenzene. Ar = phenyl. * marks the signal of an unknown by-product.

Tetrakis(3-methylphenyl)phosphonium iodide, Table 6, compound IX-2

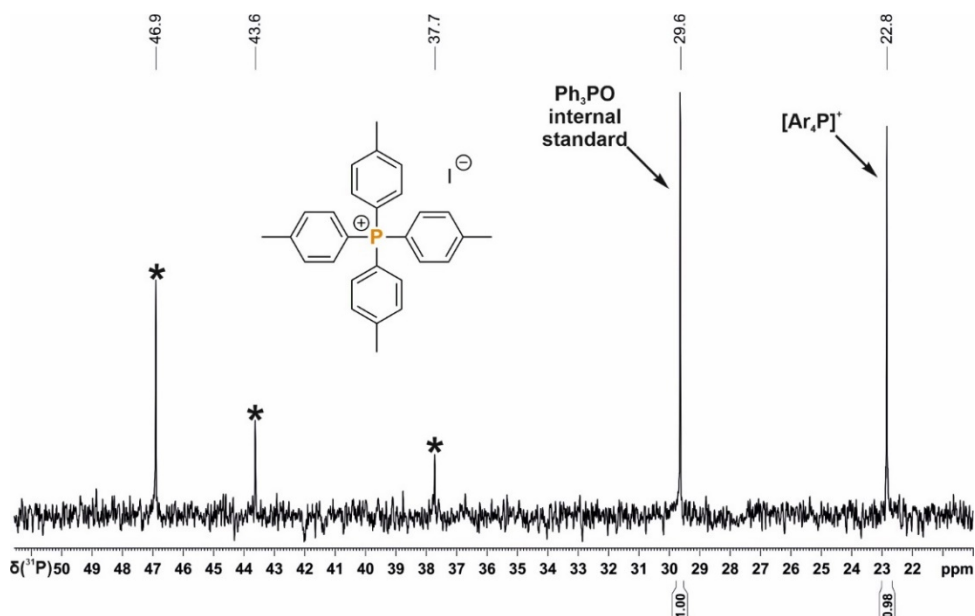
The general procedure 8 was followed using 3-iodotoluene (140 μ L, 1.1 mmol), which resulted in 37% conversion to tetrakis(3-methylphenyl)phosphonium iodide as judged by quantitative $^{31}\text{P}\{^1\text{H}\}$ (zgig) NMR spectroscopy.



Supplementary Figure 75. Quantitative single scan $^{31}\text{P}\{^1\text{H}\}$ (zgig) NMR spectrum for the photocatalytic functionalization of P_4 using 3-iodotoluene. Ar = 3-methylphenyl. * marks the signal of an unknown by-product.

Tetrakis(4-methylphenyl)phosphonium iodide, Table 6, compound IX-3

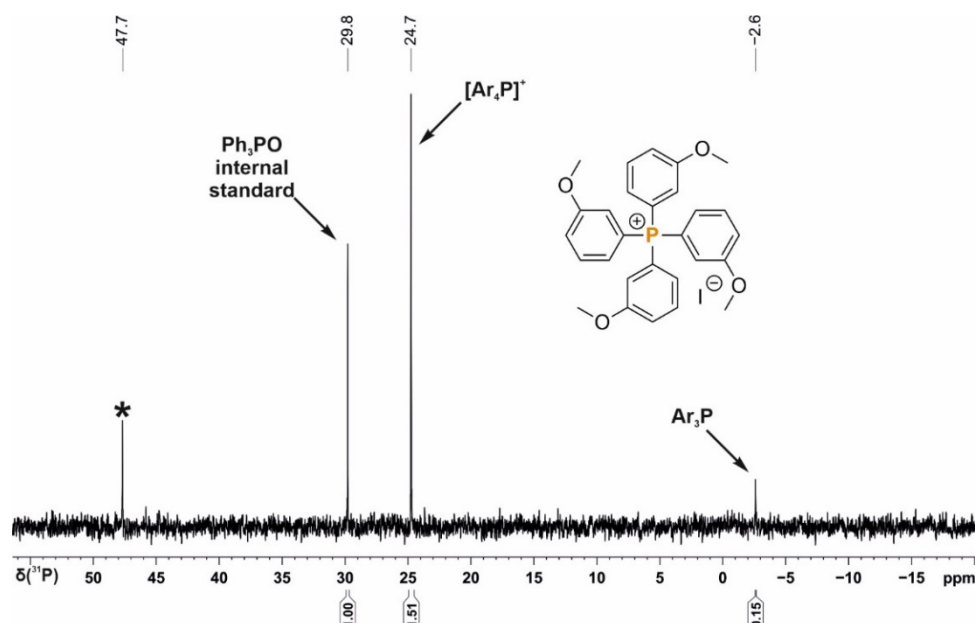
The general procedure 8 was followed using 4-iodotoluene (240 mg, 1.1 mmol), which resulted in 29% conversion to tetrakis(4-methylphenyl)phosphonium iodide as judged by quantitative $^{31}\text{P}\{^1\text{H}\}$ (zgig) NMR spectroscopy.



Supplementary Figure 76. Quantitative single scan $^{31}\text{P}\{^1\text{H}\}$ (zgig) NMR spectrum for the photocatalytic functionalisation of P_4 using 4-iodotoluene. Ar = 4-methylphenyl * marks the signal of an unknown by-product.

Tetrakis(3-methoxyphenyl)phosphonium iodide, Table 6, compound IX-4

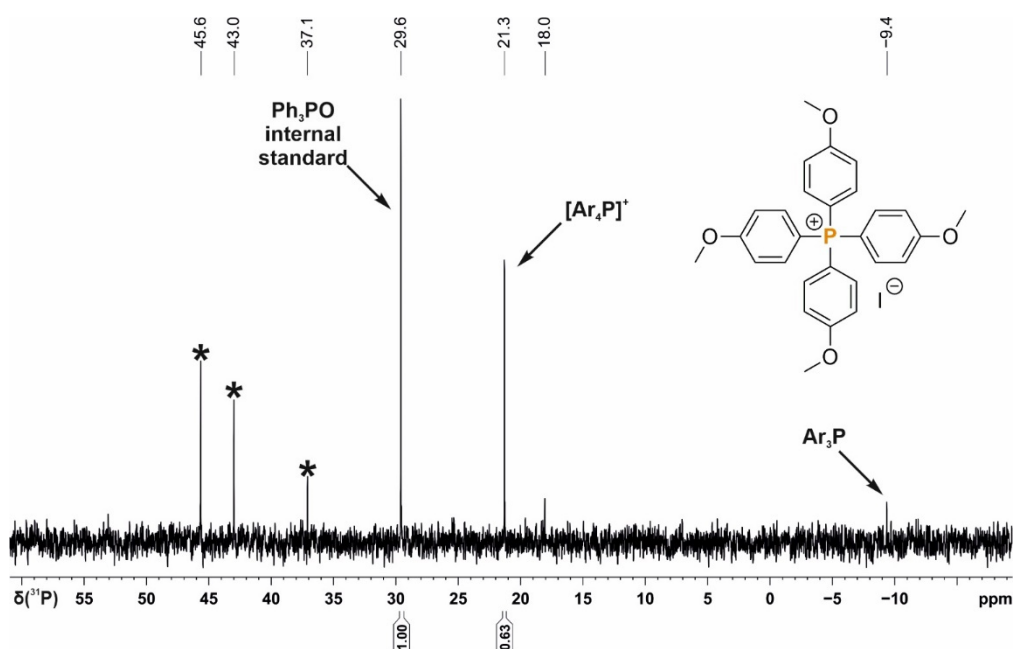
The general procedure 8 was followed using 3-iododanisole (131 μL , 1.1 mmol), which resulted in 45% conversion to tetrakis(3-methoxyphenyl)phosphonium iodide as judged by quantitative $^{31}\text{P}\{^1\text{H}\}$ (zgig) NMR spectroscopy.



Supplementary Figure 77. Quantitative single scan $^{31}\text{P}\{^1\text{H}\}$ (zgig) NMR spectrum for the photocatalytic functionalization of P_4 using 3-iododanisole. Ar = 3-methoxyphenyl. * marks the signal of an unknown by-product.

Tetrakis(4-methoxyphenyl)phosphonium iodide, Table 6, compound IX-5

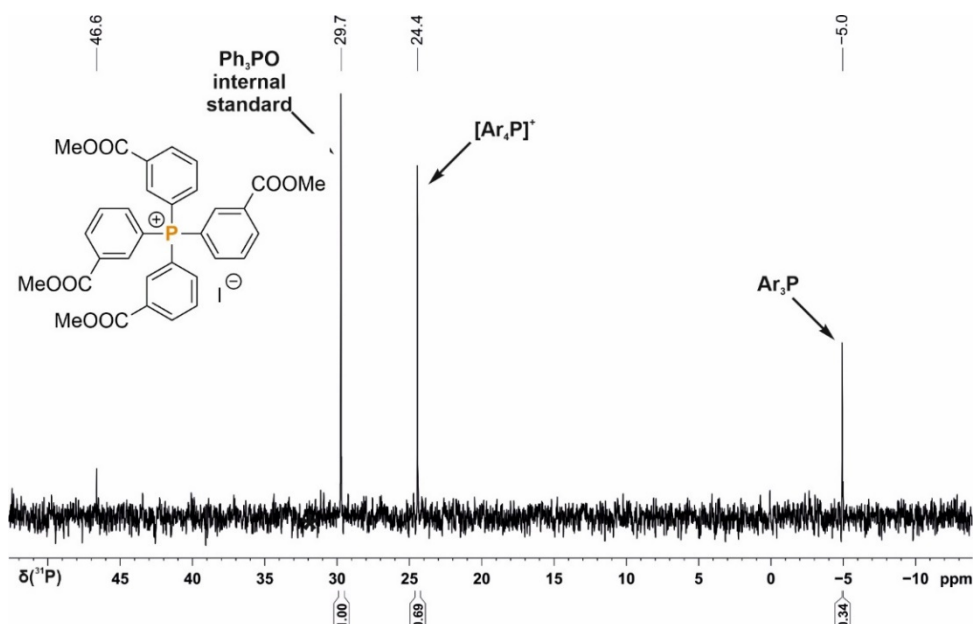
The general procedure 8 was followed using 4-iodoanisole (258 mg, 1.1 mmol), which resulted in 19% conversion to tetrakis(4-methoxyphenyl)phosphonium iodide as judged by quantitative $^{31}\text{P}\{^1\text{H}\}$ (zgig) NMR spectroscopy.



Supplementary Figure 78. Quantitative single scan $^{31}\text{P}\{^1\text{H}\}$ (zgig) NMR spectrum for the photocatalytic functionalization of P_4 using 4-iodoanisole. Ar = 4-methoxyphenyl. * marks the signal of an unknown by-product.

Tetrakis(3-(methyl benzoate)phosphonium iodide, Table 6, compound IX-6

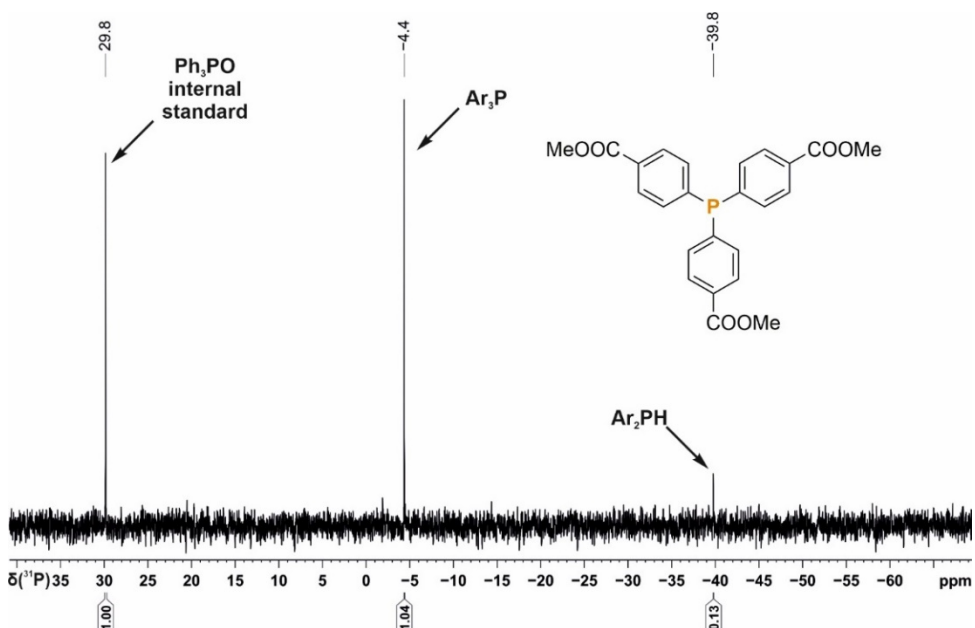
The general procedure 8 was followed using methyl 3-iodobenzoate (288 mg, 1.1 mmol), which resulted in 20% conversion to tetrakis(3-(methyl benzoate)phosphonium iodide as judged by quantitative $^{31}\text{P}\{^1\text{H}\}$ (zgig) NMR spectroscopy.



Supplementary Figure 79. Quantitative single scan $^{31}\text{P}\{^1\text{H}\}$ (zgig) NMR spectrum for the photocatalytic functionalization of P_4 using methyl 3-iodobenzoate. Ar = 3-methylbenzoate. * marks the signal of an unknown by-product.

Tris(4-carboxymethyl)phosphine, Table 6, compound VIII-1

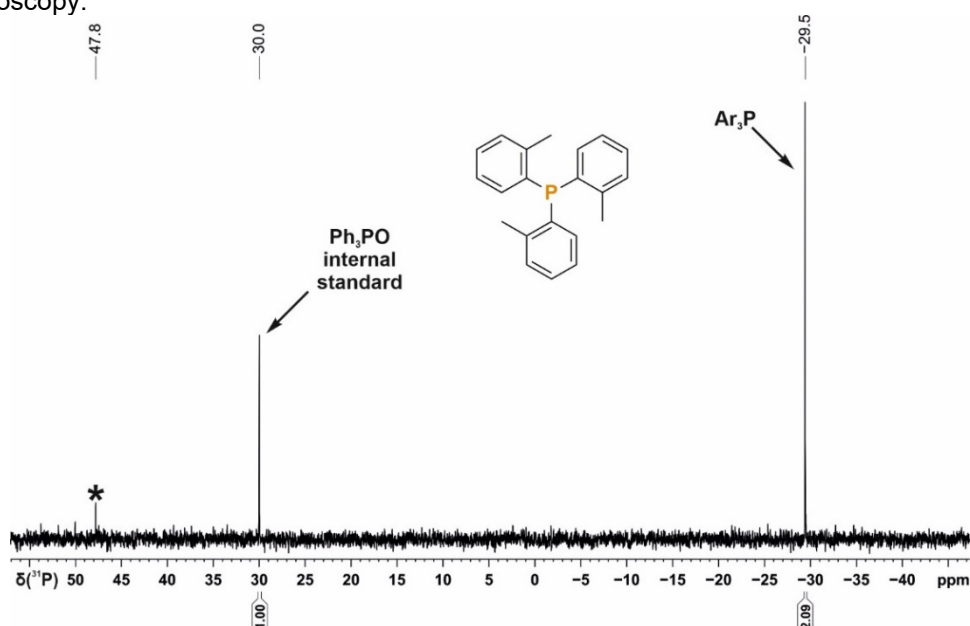
The general procedure 8 was followed using methyl 4-iodobenzoate (288 mg, 1.1 mmol), which resulted in 31% conversion to tris(4-carboxymethyl)phosphine as judged by quantitative $^{31}\text{P}\{^1\text{H}\}$ (zgig) NMR spectroscopy.



Supplementary Figure 80. Quantitative single scan $^{31}\text{P}\{^1\text{H}\}$ (zgig) NMR spectrum for the photocatalytic functionalization of P_4 using methyl 4-iodobenzoate. Ar = 4-methylbenzoate. * marks the signal of an unknown by-product.

Tris(2-methylphenyl)phosphine, Table 6, compound VII-2

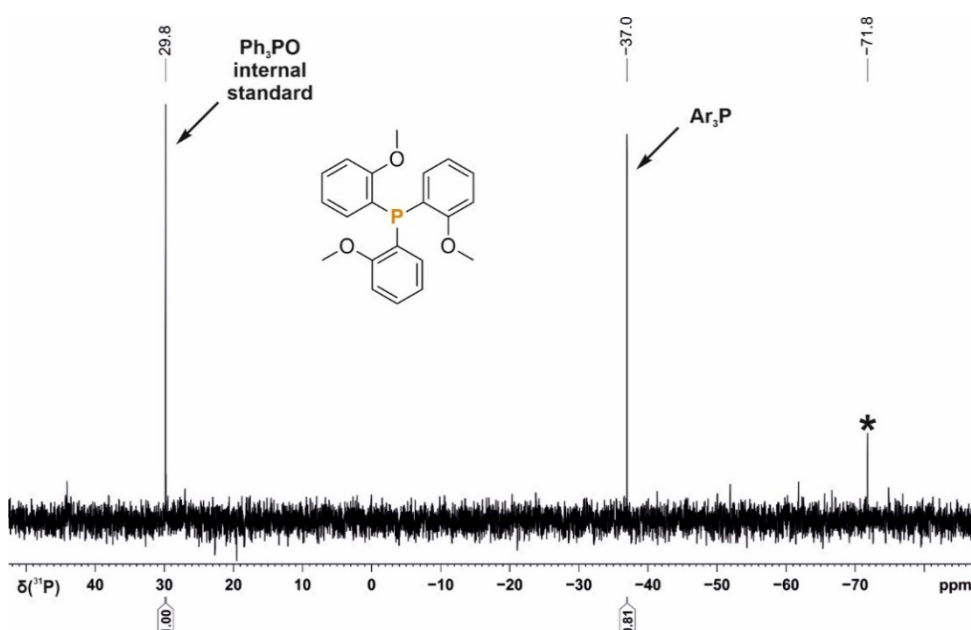
The general procedure 8 was followed using 2-iodotoluene (140 μL , 1.1 mmol), which resulted in 54% conversion to tris(2-methylphenyl)phosphine as judged by quantitative $^{31}\text{P}\{^1\text{H}\}$ (zgig) NMR spectroscopy.



Supplementary Figure 81. Quantitative single scan $^{31}\text{P}\{^1\text{H}\}$ (zgig) NMR spectrum for the photocatalytic functionalization of P_4 using 2-iodotoluene. Ar = 2-methylphenyl. * marks the signal of an unknown by-product.

Tris(2-methoxyphenyl)phosphine, Table 6, compound VIII-3

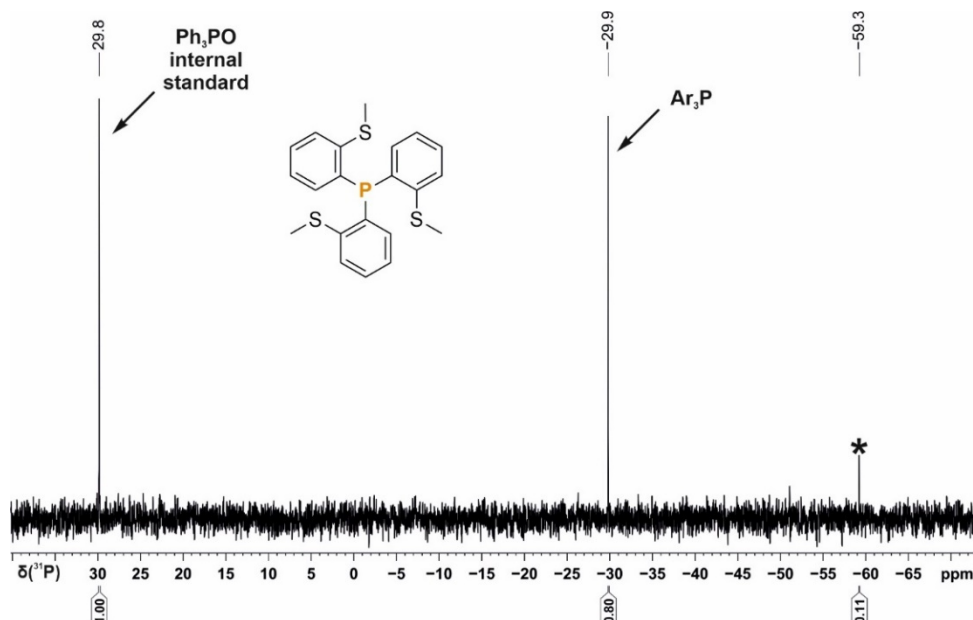
The general procedure 8 was followed using 2-iodoanisole (143 μL , 1.1 mmol), which resulted in 24% conversion to tris(2-methoxyphenyl)phosphine as judged by quantitative $^{31}\text{P}\{^1\text{H}\}$ (zgig) NMR spectroscopy.



Supplementary Figure 82. Quantitative single scan $^{31}\text{P}\{^1\text{H}\}$ (zgig) NMR spectrum for the photocatalytic functionalization of P_4 using 2-iodoanisole. Ar = 2-methoxyphenyl. * marks the signal of an unknown by-product.

Tris(2-(methylthiophenyl)phenyl)phosphine, Table 6, compound VIII-4

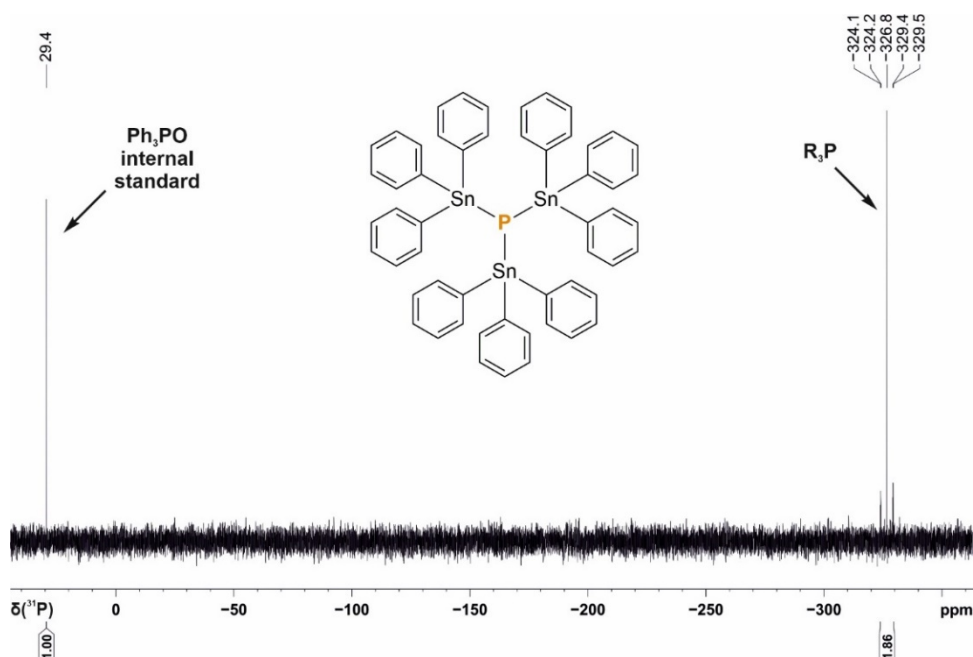
The general procedure 8 was followed using methyl 2-iodothioanisole (160 μ L, 1.1 mmol), which resulted in 24% conversion to tris(2-(methylthiophenyl)phenyl)phosphine as judged by quantitative $^{31}\text{P}\{^1\text{H}\}$ (zgig) NMR spectroscopy.



Supplementary Figure 83. Quantitative single scan $^{31}\text{P}\{^1\text{H}\}$ (zgig) NMR spectrum for the photocatalytic functionalization of P_4 using methyl 2-iodothioanisole. Ar = 2-methylthiophenyl. * marks the signal of an unknown by-product.

Tris(triphenylstannyl)phosphine, Table 6, compound VIII-5

The general procedure 7 was followed using Ph_3SnCl (424 mg, 1.1 mmol), which resulted in 56% conversion to tris(triphenylstannyl)phosphine as judged by quantitative $^{31}\text{P}\{^1\text{H}\}$ (zgig) NMR spectroscopy.



Supplementary Figure 84. Quantitative single scan $^{31}\text{P}\{^1\text{H}\}$ (zgig) NMR spectrum for the photocatalytic functionalization of P_4 using Ph_3SnCl . R = triphenylstannyl. * marks the signal of an unknown by-product.

3.5.9 Characterisation spectra and data of isolated compounds in 1 mmol scale

Diphenyl-2-(trifluoromethyl)phenylphosphine from HPPh₂ (1 mmol scale, Table 2, I-1)

The general procedure 9 was followed using 2-trifluoromethylphenyl iodide (421 μ L, 3.00 mmol) which provided diphenyl-2-(trifluoromethyl)phenylphosphine as colorless solid in 53% yield (175.5 mg, 53%).

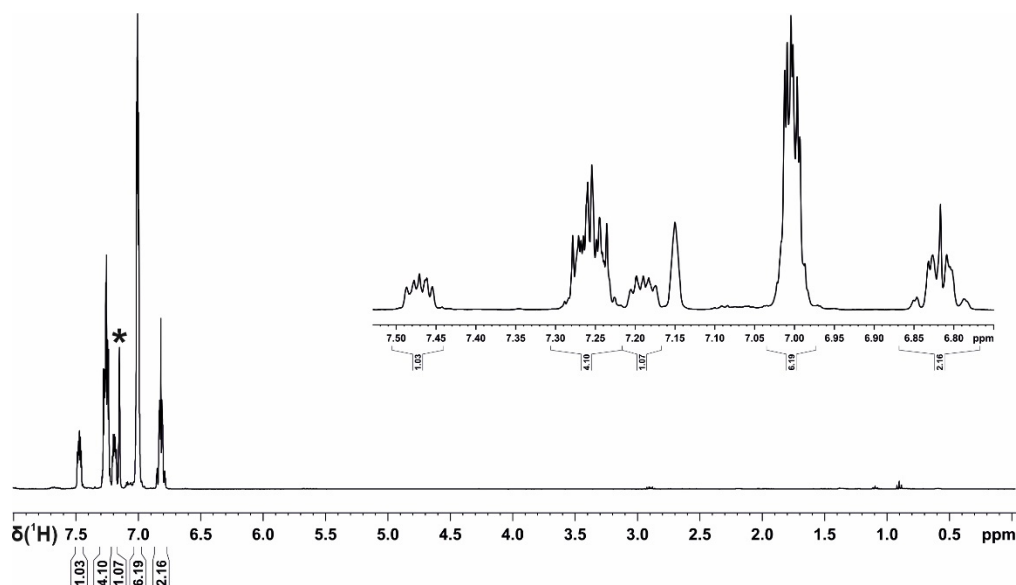
¹H NMR (400 MHz, C₆D₆): δ 7.49-7.45 (m, 1H), 7.28-7.24 (m, 4H), 7.21-7.17 (m, 1H), 7.01-6.99 (m, 6H), 7.21-7.17 (m, 1H), 6.85-6.79 (m, 2H).

¹³C{¹H} NMR (100 MHz, C₆D₆): δ 137.5 (d, J = 31.4 Hz), 137.1 (dd, J = 12.8, 1.22 Hz), 136.8 (d, J = 1.9 Hz), 135.6 (dd, J = 25.5, 4.9 Hz), 134.4 (d, J = 20.5 Hz), 132.0, 129.4, 129.3, 129.1 (d, J = 6.8 Hz), 127.0 (p, J = 5.6 Hz), 124.2.

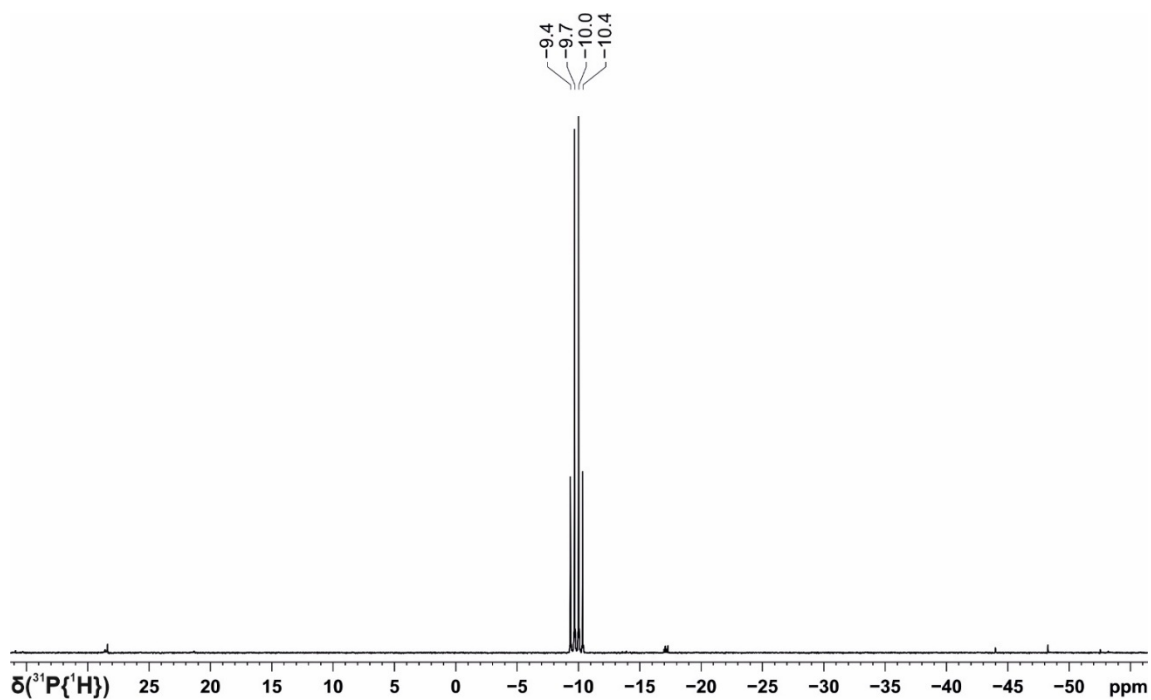
³¹P{¹H} NMR (162 MHz, C₆D₆): δ -9.9 (q, ⁴ J_{P-F} = 53.3 Hz).

¹⁹F{¹H} NMR (366 MHz, C₆D₆): δ -56.6 (d, ⁴ J_{P-F} = 53.3 Hz).

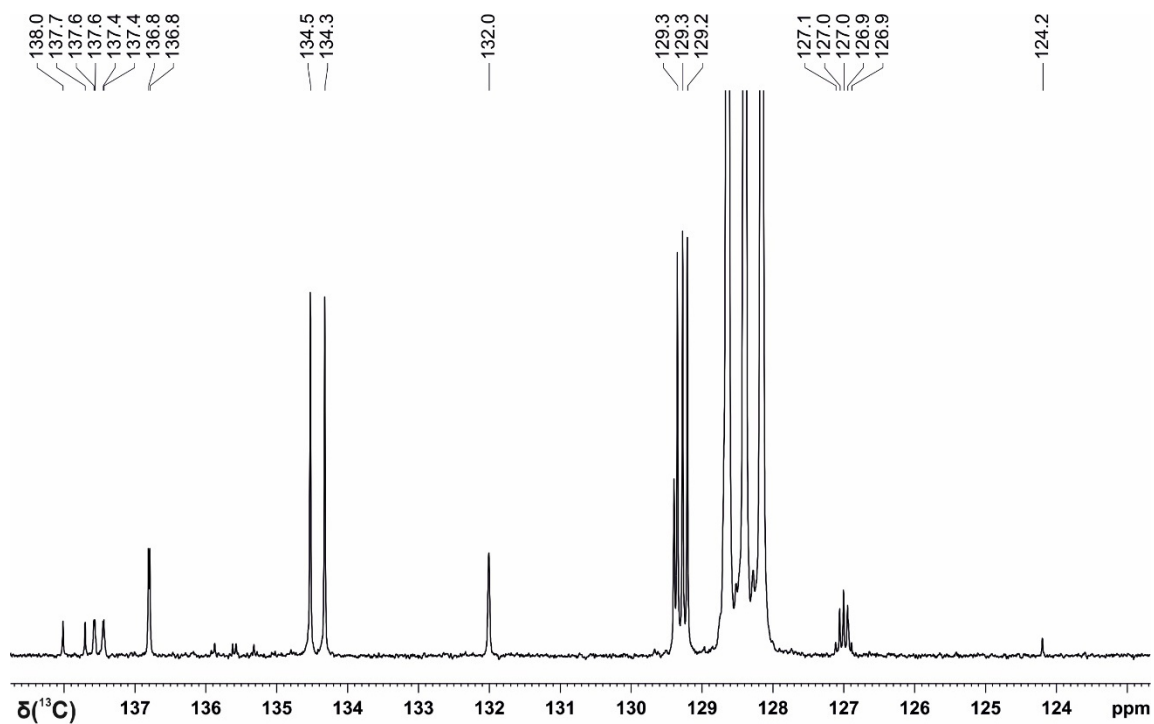
Elemental analysis: Calculated for C₁₉H₁₄F₃P: C, 69.09; H, 4.27; Found: C, 68.89; H, 4.43.



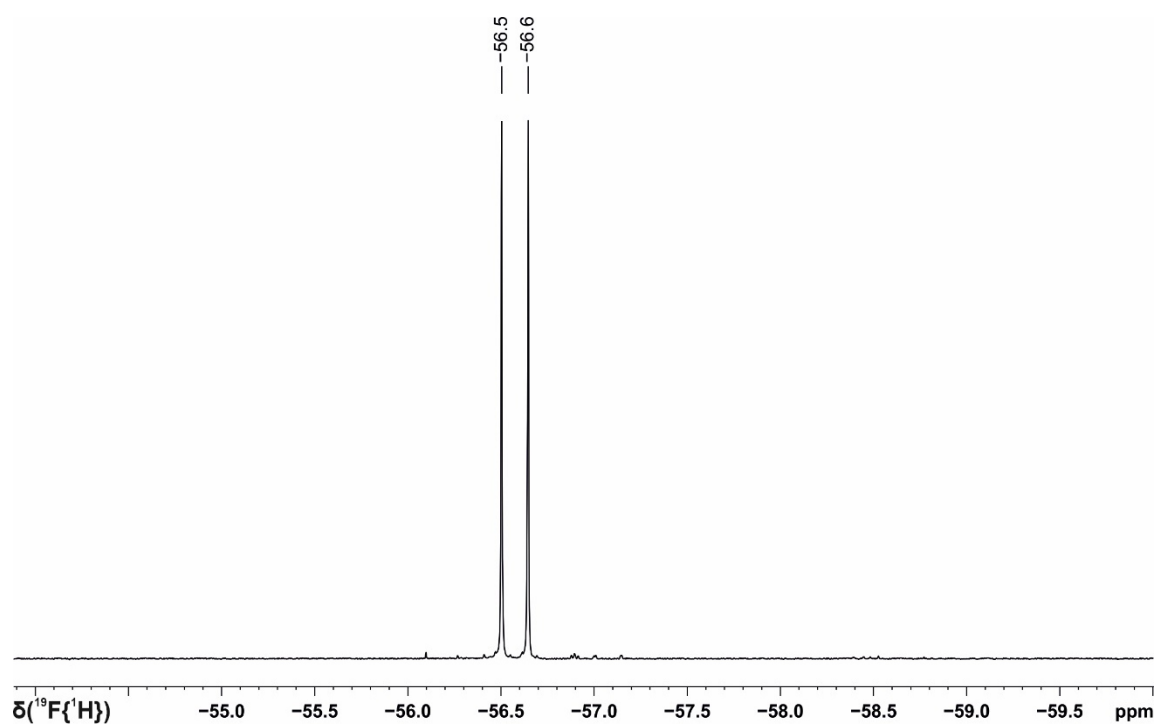
Supplementary Figure 85 ¹H NMR spectrum in C₆D₆ of diphenyl((2-trifluoromethyl)phenyl)phosphine prepared photocatalytically from HPPh₂ on a 1 mmol scale. *CDCl₃.



Supplementary Figure 86. $^{31}\text{P}\{^1\text{H}\}$ NMR spectrum in C_6D_6 of diphenyl((2-trifluoromethyl)phenyl)phosphine prepared photocatalytically from HPPH_2 on a 1 mmol scale.



Supplementary Figure 87. ^{13}C NMR spectrum in C_6D_6 of diphenyl((2-trifluoromethyl)phenyl)phosphine prepared photocatalytically from HPPH_2 on a 1 mmol scale.



Supplementary Figure 88. ^{19}F NMR spectrum in C_6D_6 of diphenyl((2-trifluoromethyl)phenyl)phosphine prepared photocatalytically from HPPH_2 on a 1 mmol scale.

***n*-Octyldiphenylphosphine (Table 4, V-1)**

The general procedure 10 was followed using 1-iodooctane (361 μL , 2 mmol) which provided *n*-octyldiphenylphosphine as colourless oil in 50% yield (147.8 mg).

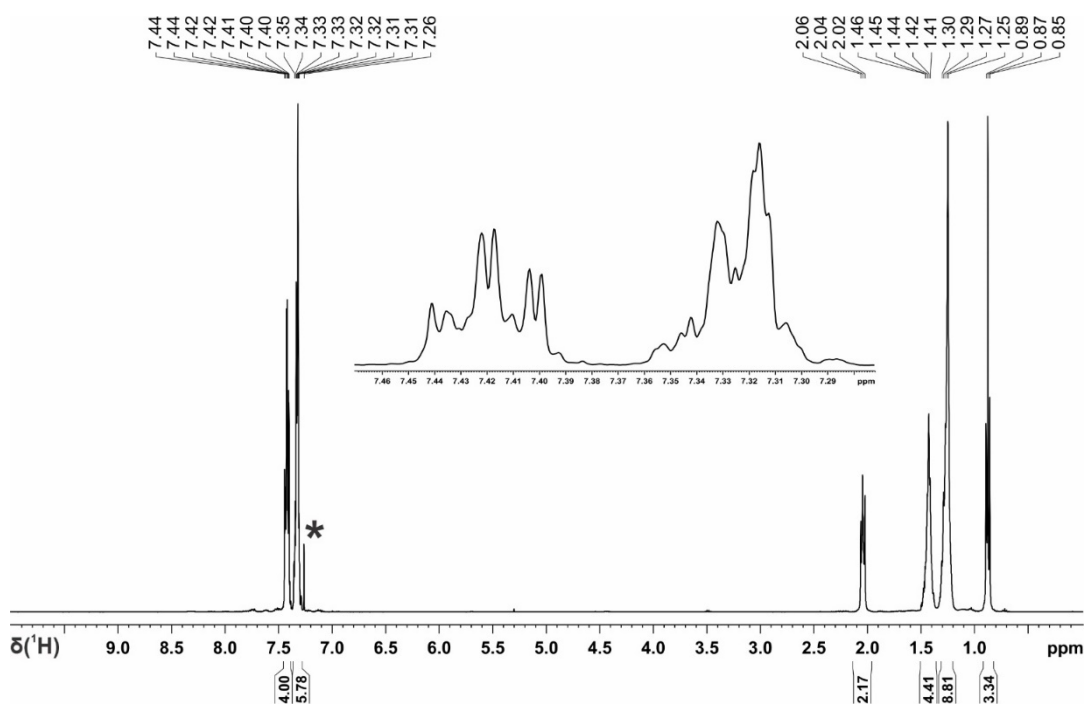
The characterization data of the product are consistent with the data found in the literature.^[S3]

^1H NMR (400 MHz, CDCl_3): δ 7.44-7.40 (m, 4H), 7.35-7.31 (m, 6H), 2.06-2.02 (m, 2H), 1.46-1.41 (m, 4H), 1.30-1.25 (m, 8H), 0.89-0.85 (m, 3H).

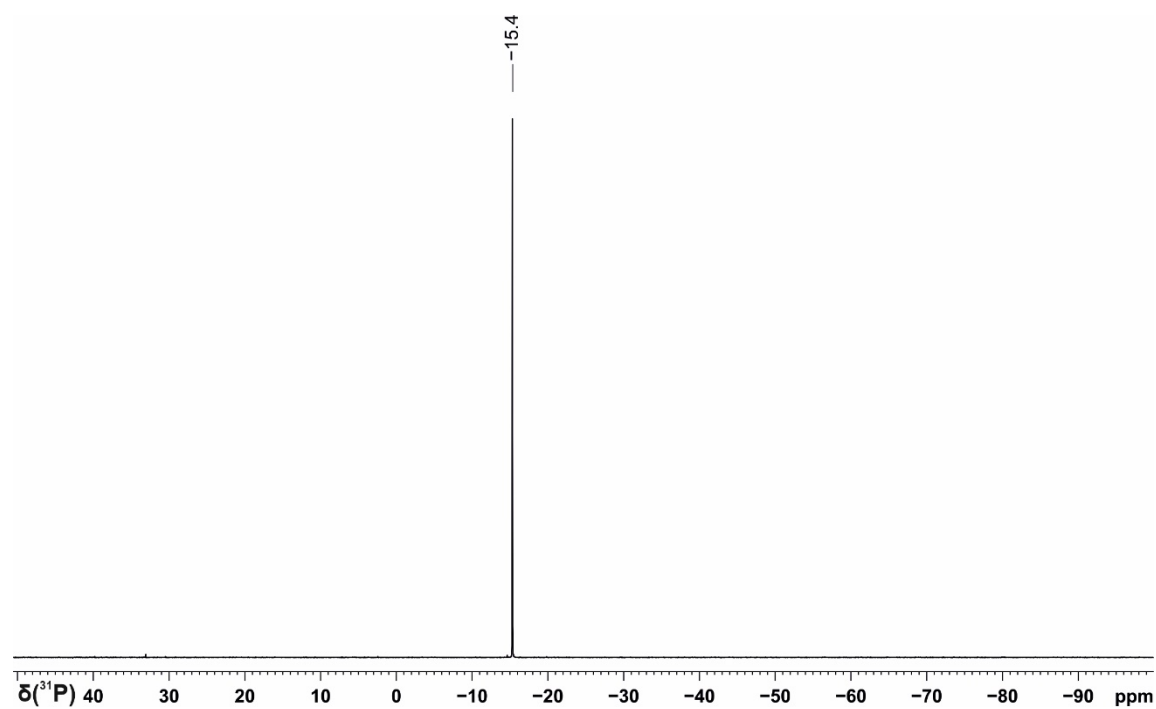
$^{13}\text{C}\{^1\text{H}\}$ NMR (100 MHz, CDCl_3): δ 139.2 (d, $J = 13.1$ Hz), 132.9 (d, $J = 18.3$ Hz), 128.6, 128.5 (d, $J = 6.6$ Hz), 32.0, 31.4 (d, $J = 12.8$ Hz), 29.3 (d, $J = 5.8$ Hz), 28.2 (d, $J = 11.1$ Hz), 26.1 (d, $J = 16.0$ Hz), 22.8, 14.2.

$^{31}\text{P}\{^1\text{H}\}$ NMR (162 MHz, CDCl_3): δ -15.4.

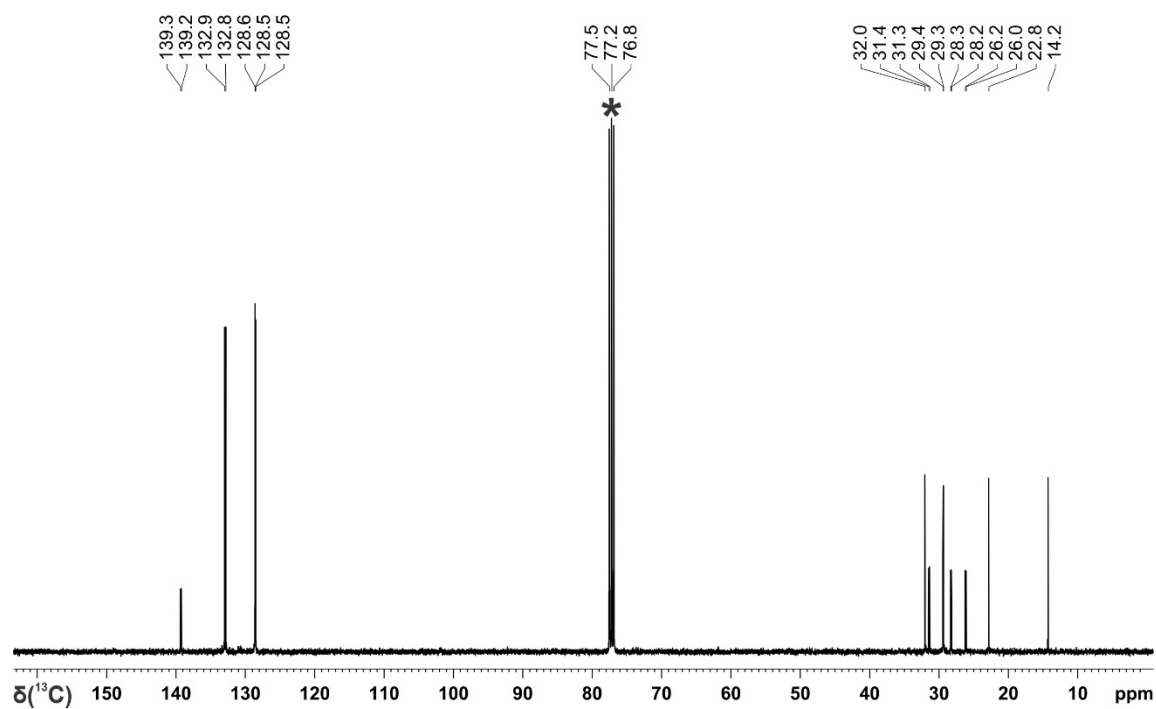
Elemental analysis: Calculated for $\text{C}_{20}\text{H}_{27}\text{P}$: C, 80.50; H, 9.12; Found: C, 80.42; H, 9.06.



Supplementary Figure 89. ^1H NMR spectrum of *n*-octyldiphenylphosphine in CDCl_3 prepared photocatalytically from HPPH_2 on a 1 mmol scale. * CDCl_3 .



Supplementary Figure 90. $^{31}\text{P}\{^1\text{H}\}$ NMR spectrum of *n*-octyldiphenylphosphine in CDCl_3 prepared photocatalytically from HPPH_2 on a 1 mmol scale.



Supplementary Figure 91. ^{13}C NMR spectrum of *n*-octyldiphenylphosphine in CDCl_3 prepared photocatalytically from HPPH_2 on a 1 mmol scale. * CDCl_3 .

Phenethyldiphenylphosphine (Table 4, V-4)

The general procedure 10 was followed using (2-iodoethyl)benzene (290 μL , 2 mmol) provided phenethyldiphenylphosphine as colourless oil in 57% yield (147.8 mg).

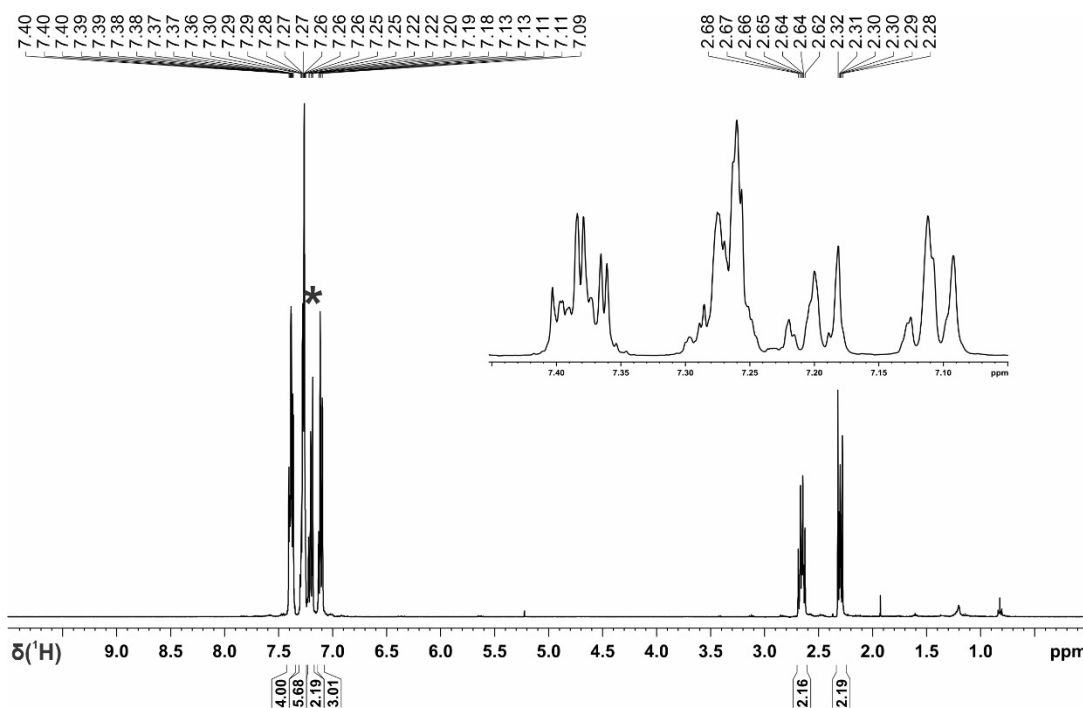
The characterization data of the product are consistent with the data found in the literature.^[S4]

$^1\text{H NMR}$ (400 MHz, CDCl_3): δ 7.40-7.36 (m, 4H), 7.30-7.26 (m, 6H), 7.28-7.18 (m, 2H), 7.13-7.09 (m, 3H), 2.68-2.62 (m, 2H), 2.32-2.28 (m, 2H).

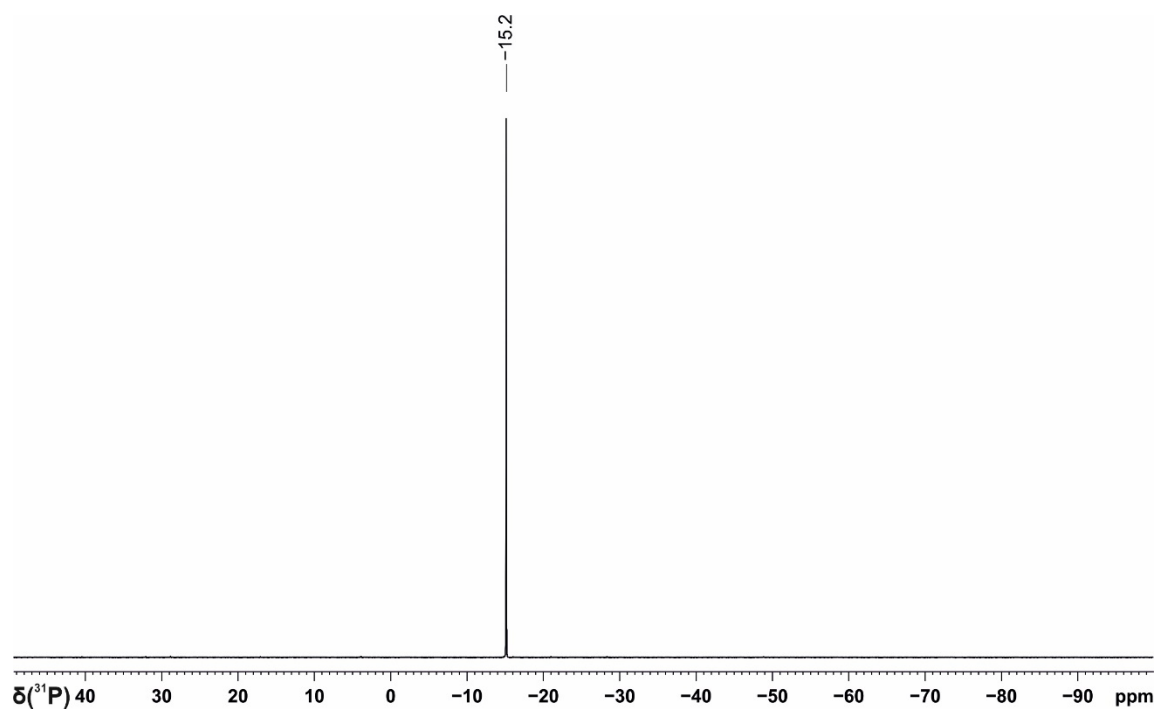
$^{13}\text{C}\{^1\text{H}\}$ NMR (100 MHz, CDCl_3): δ 142.8 (d, $J = 13.3$ Hz), 138.6 (d, $J = 13.0$ Hz), 132.9 (d, $J = 18.5$ Hz), 128.8, 128.6, 128.5, 128.3, 126.1, 32.3 (d, $J = 17.9$ Hz), 30.3 (d, $J = 12.8$ Hz).

$^{31}\text{P}\{^1\text{H}\}$ NMR (162 MHz, CDCl_3): δ -15.2.

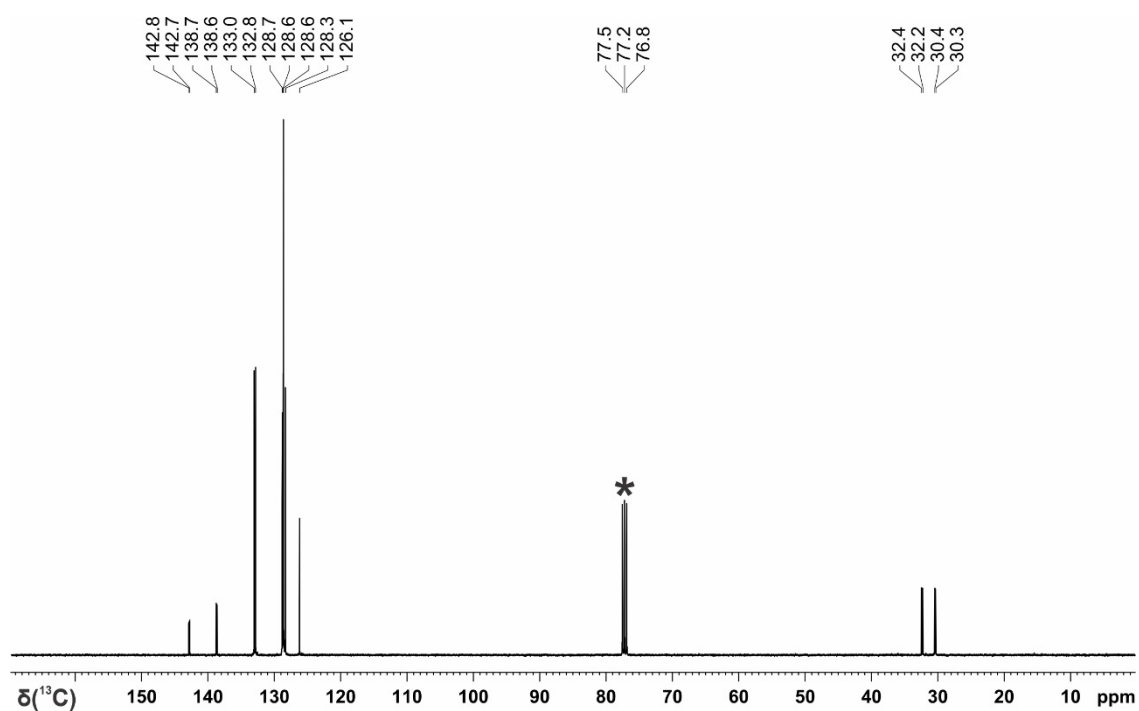
Elemental analysis: Calculated for $\text{C}_{20}\text{H}_{19}\text{P}$: C, 82.74; H, 6.60; Found: C, 82.99; H, 6.61.



Supplementary Figure 92. $^1\text{H NMR}$ spectrum of phenethyldiphenylphosphine in CDCl_3 prepared photocatalytically from HPPH_2 on a 1 mmol scale. * CDCl_3 .



Supplementary Figure 93. $^{31}\text{P}\{^1\text{H}\}$ NMR spectrum of phenethyldiphenylphosphine in CDCl₃ prepared photocatalytically from HPPH₂ on a 1 mmol scale.



Supplementary Figure 94. ^{13}C NMR spectrum of phenethyldiphenylphosphine in CDCl₃ prepared photocatalytically from HPPH₂ on a 1 mmol scale. *CDCl₃.

Benzylidiphenylphosphine (Table 4, V-5)

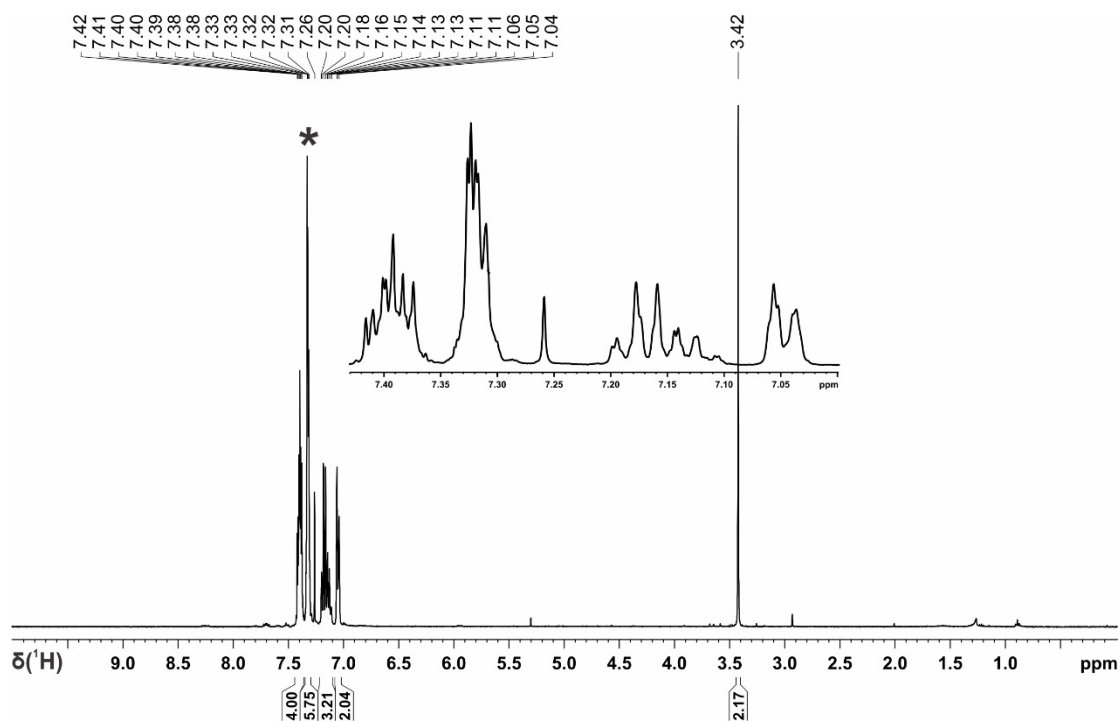
The general procedure 10 was followed using benzyl bromide (238 μL , 2 mmol) which provided benzylidiphenylphosphine as white solid in 56% yield (155.7 mg).

$^1\text{H NMR}$ (400 MHz, CDCl_3): δ 7.42-7.38 (m, 4H), 7.33-7.31 (m, 6H), 7.20-7.11 (m, 3H), 7.06-7.04 (m, 2H), 3.42 (s, 2H).

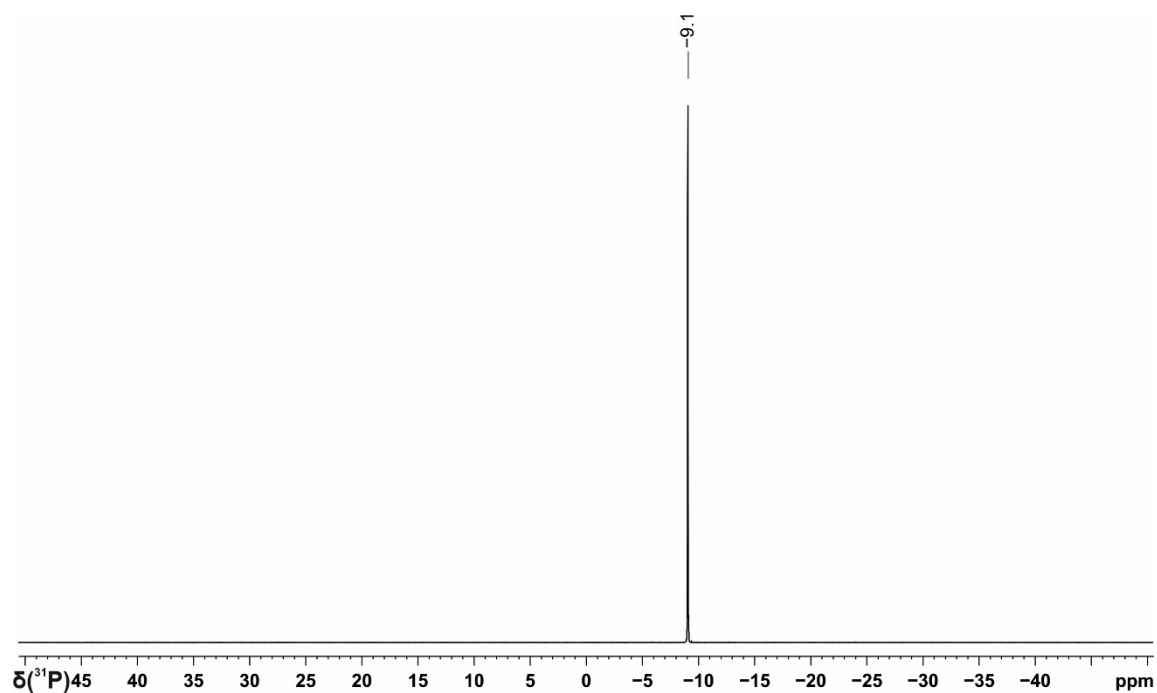
$^{13}\text{C}\{^1\text{H}\}$ NMR (100 MHz, CDCl_3): δ 138.4 (d, $J = 15.1$ Hz), 137.5 (d, $J = 8.1$ Hz), 133.0 (d, $J = 18.5$ Hz), 129.5 (d, $J = 6.7$ Hz), 128.8, 128.5 (d, $J = 6.5$ Hz), 128.4 (d, $J = 1.6$ Hz), 126.0 (d, $J = 2.7$ Hz), 36.1 (d, $J = 15.6$ Hz).

$^{31}\text{P}\{^1\text{H}\}$ NMR (162 MHz, CDCl_3): δ -9.1.

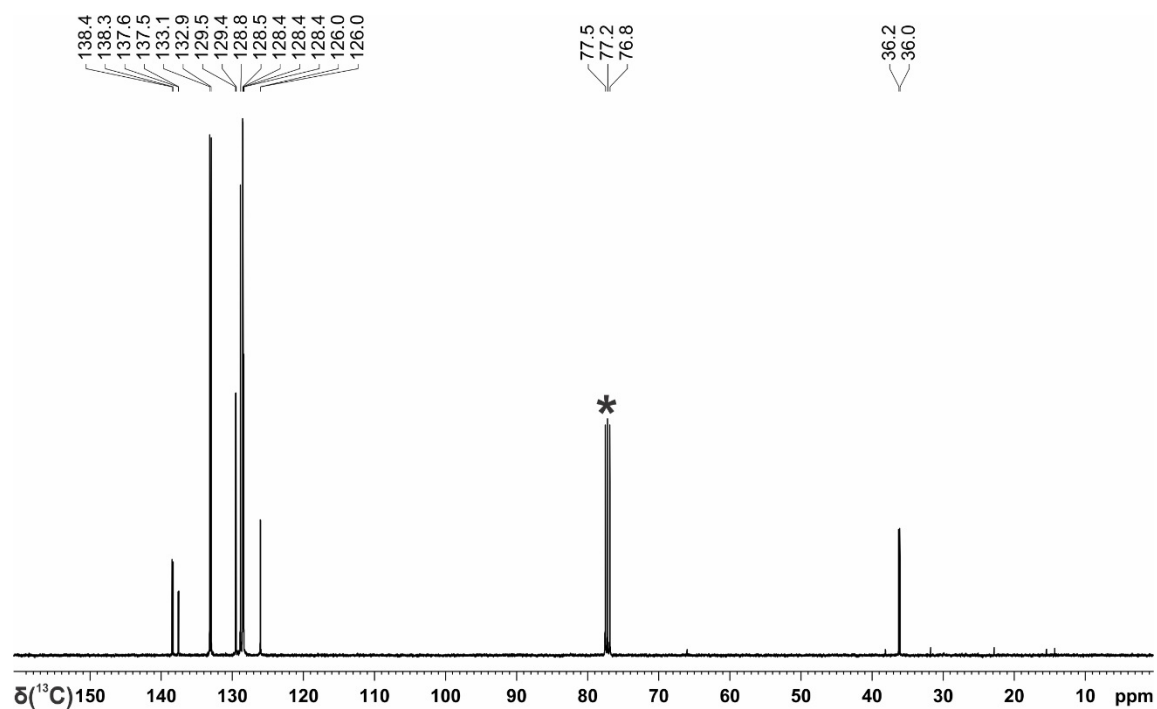
Elemental analysis: Calculated for $\text{C}_{19}\text{H}_{17}\text{P}$: C, 82.59; H, 6.20; Found: C, 82.49; H, 6.23.



Supplementary Figure 95. $^1\text{H NMR}$ spectrum of benzylidiphenylphosphine in CDCl_3 prepared photocatalytically from HPPH_2 on a 1 mmol scale. $^*\text{CDCl}_3$.



Supplementary Figure 96. $^{31}\text{P}\{^1\text{H}\}$ NMR spectrum of benzyldiphenylphosphine in CDCl_3 prepared photocatalytically from HPPH_2 on a 1 mmol scale.



Supplementary Figure 97. ^{13}C NMR spectrum of benzyldiphenylphosphine in CDCl_3 prepared photocatalytically from HPPH_2 on a 1 mmol scale. * CDCl_3 .

(4-Fluorobenzyl)diphenylphosphine (Table 4, V-6)

The general procedure 10 was followed using 4-fluorobenzyl bromide (249 μL , 2 mmol) which provided (4-fluorobenzyl)diphenylphosphine as white solid in 60% yield (175.9 mg).

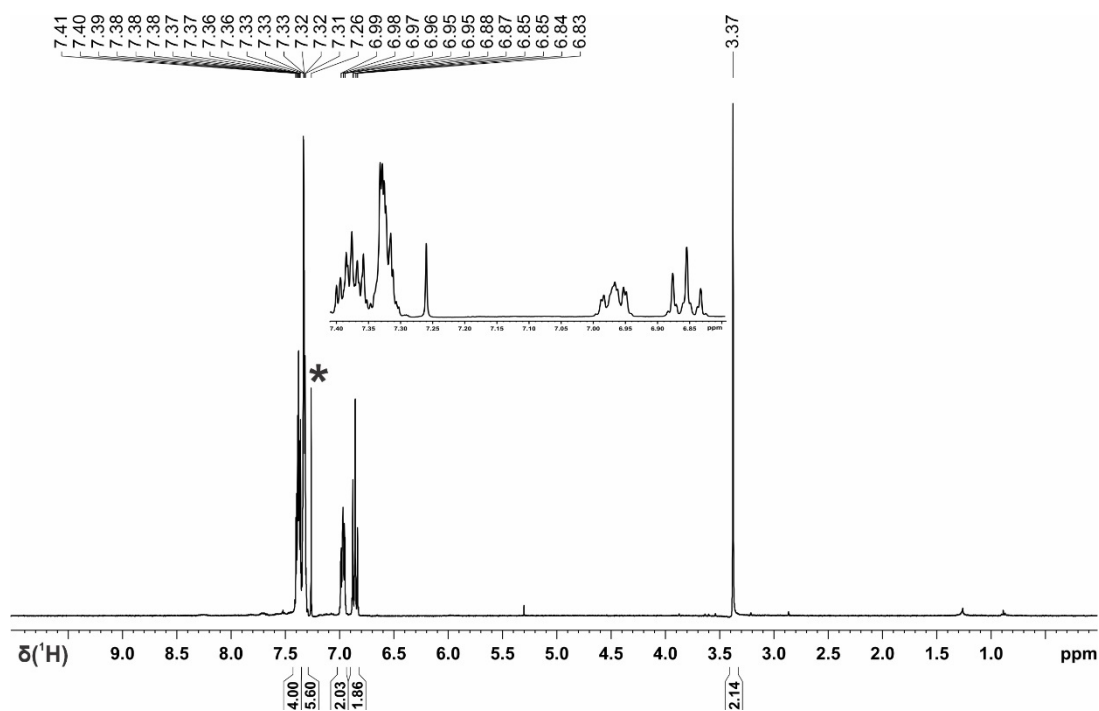
$^1\text{H NMR}$ (400 MHz, CDCl_3): δ 7.41-7.36 (m, 4H), 7.33-7.31 (m, 6H), 6.99-6.95 (m, 2H), 6.88- 6.83 (m, 2H), 3.37 (s, 2H).

$^{13}\text{C}\{^1\text{H}\}$ NMR (100 MHz, CDCl_3): δ 161.5 (dd, $J_{\text{C-F}} = 244.0$ Hz, $J_{\text{C-P}} = 3.2$ Hz), 138.1 (d, $J = 14.9$ Hz), 133.0 (d, $J = 18.4$ Hz), 130.8 (d, $J = 6.7$ Hz), 130.7 (d, $J = 6.7$ Hz), 128.9, 128.5 (d, $J = 6.6$ Hz), 115.2 (dd, $J_{\text{C-F}} = 21.2$ Hz, $J_{\text{C-P}} = 1.6$ Hz), 35.2 (d, $J = 15.6$ Hz).

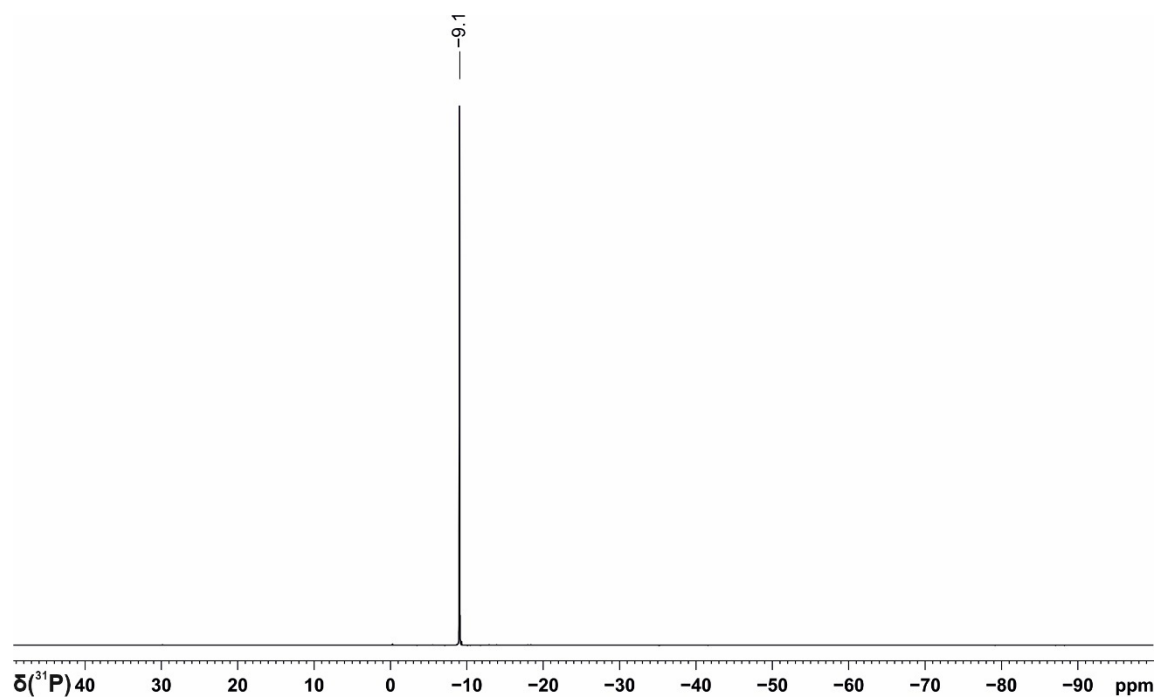
$^{31}\text{P}\{^1\text{H}\}$ NMR (162 MHz, CDCl_3): δ -9.1.

$^{19}\text{F}\{^1\text{H}\}$ NMR (366 MHz, CDCl_3): δ -117.8 (d, $^5J_{\text{P-F}} = 3.9$ Hz).

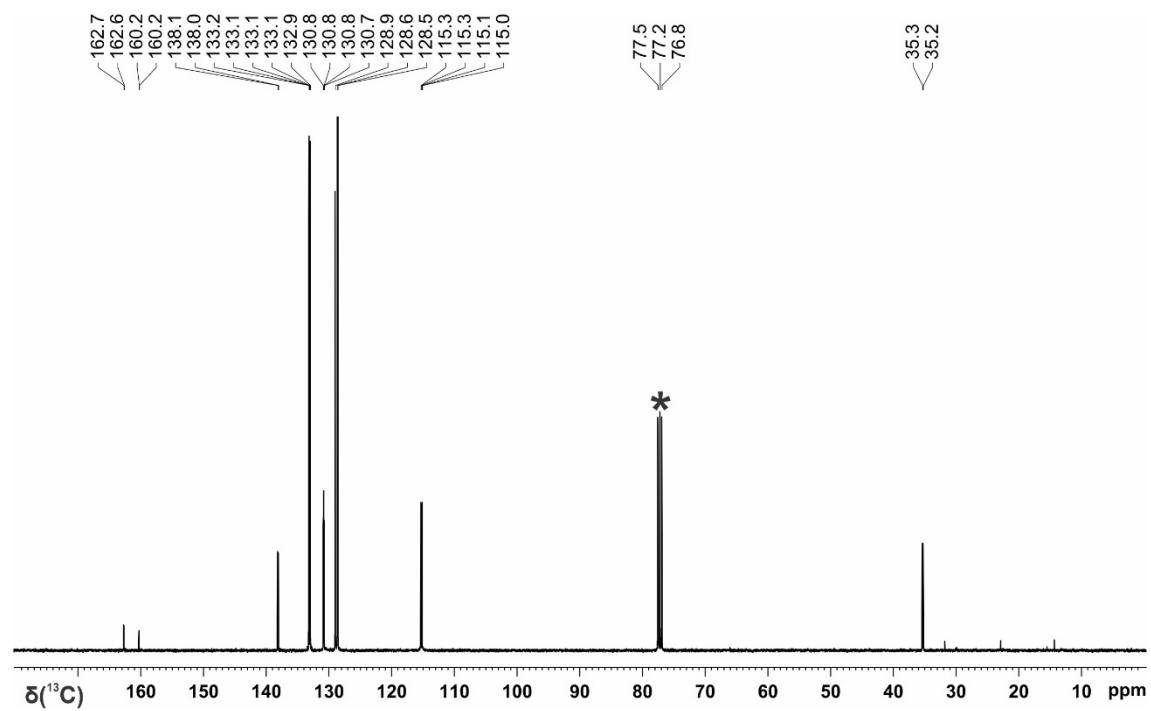
Elemental analysis: Calculated for $\text{C}_{19}\text{H}_{16}\text{P}$: C, 77.54; H, 5.48; Found: C, 77.40; H, 5.58.



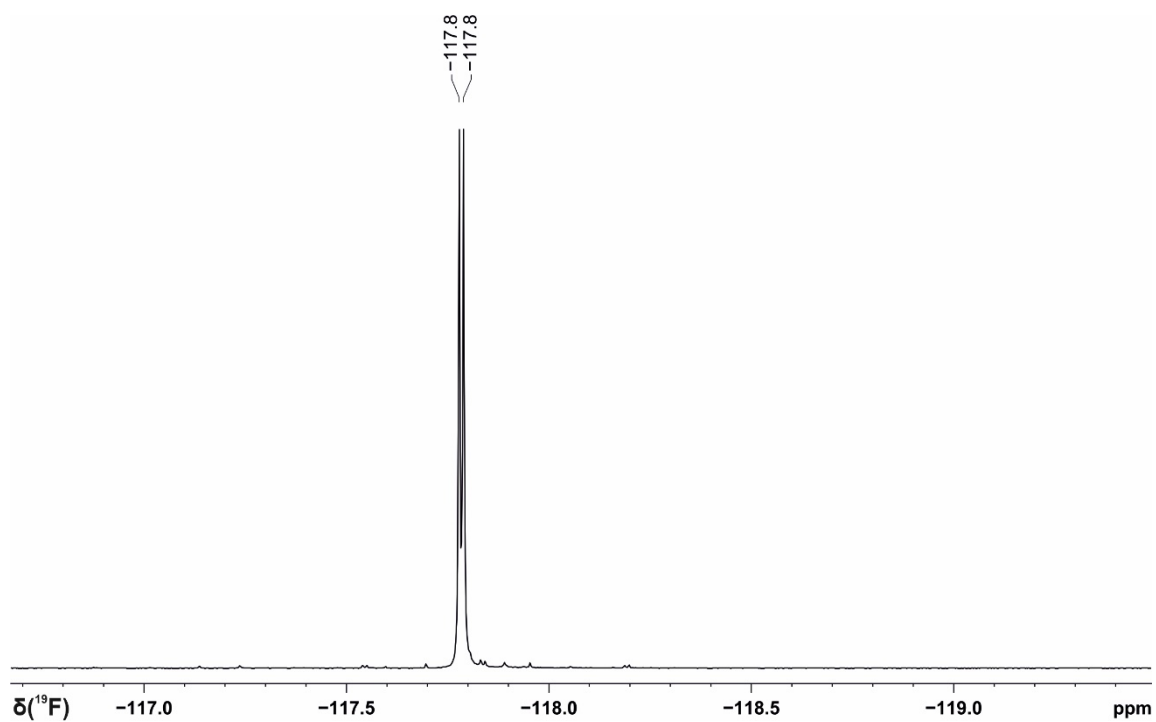
Supplementary Figure 98. $^1\text{H NMR}$ spectrum of (4-fluorobenzyl)diphenylphosphine in CDCl_3 prepared photocatalytically from HPPH_2 on a 1 mmol scale. * CDCl_3 .



Supplementary Figure 99. $^{31}\text{P}\{^1\text{H}\}$ NMR spectrum of (4-fluorobenzyl)diphenylphosphine in CDCl_3 prepared photocatalytically from HPPH_2 on a 1 mmol scale.



Supplementary Figure 100. ^{13}C NMR spectrum of (4-fluorobenzyl)diphenylphosphine in CDCl_3 prepared photocatalytically from HPPH_2 on a 1 mmol scale. * CDCl_3 .



Supplementary Figure 101. ^{19}F NMR spectrum of (4-fluorobenzyl)diphenylphosphine in CDCl_3 prepared photocatalytically from HPPH_2 on a 1 mmol scale.

(4-Trifluoromethyl)benzylidiphenylphosphine (Table 4, V-8)

The general procedure 10 was followed using 4-(trifluoromethyl)benzyl bromide (478 mg, 2 mmol) which provided (4-trifluoromethyl)benzylidiphenylphosphine as white solid in 73% yield (252.2 mg).

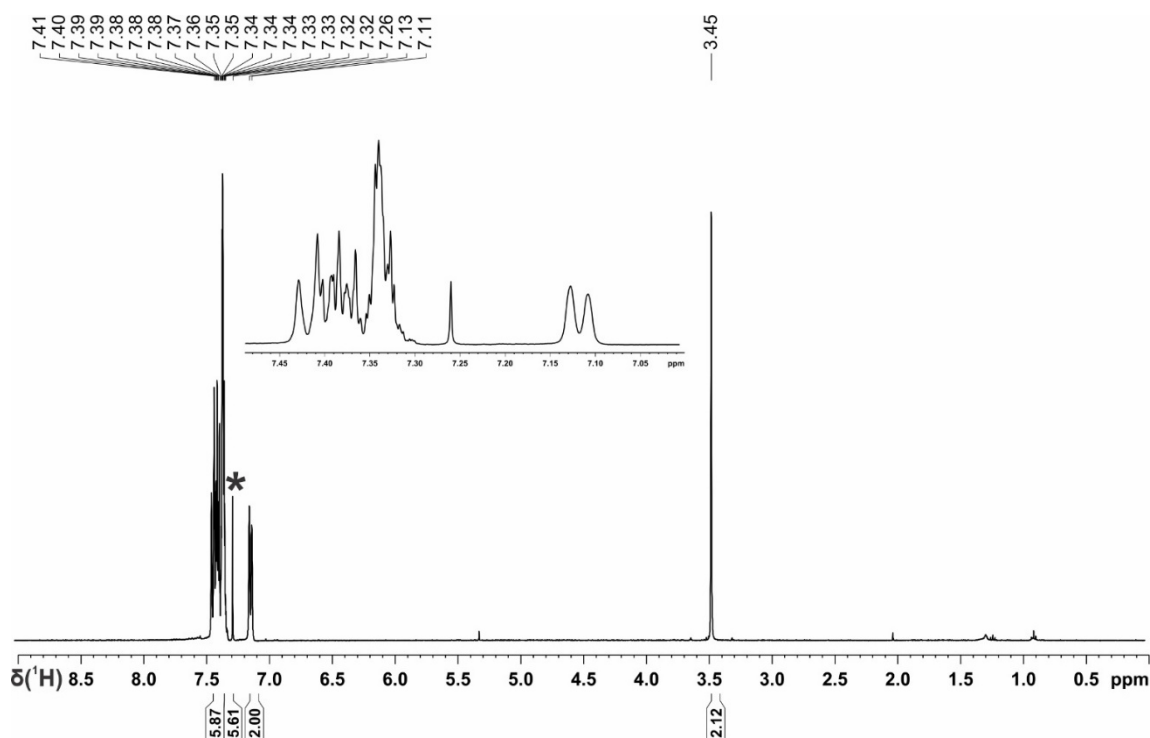
$^1\text{H NMR}$ (400 MHz, CDCl_3): δ 7.41-7.35 (m, 6H), 7.34-7.32 (m, 6H), 7.12 (d, $J = 7.8$ Hz, 2H), 3.45 (s, 2H).

$^{13}\text{C}\{^1\text{H}\}$ NMR (100 MHz, CDCl_3): δ 141.9 (d, $J = 8.2$ Hz), 137.7 (d, $J = 15.0$ Hz), 133.0 (d, $J = 18.7$ Hz), 129.7 (d, $J = 6.5$ Hz), 129.1, 128.6 (d, $J = 6.5$ Hz), 128.2 (dd, $J_{\text{C-F}} = 32.4$ Hz, $J_{\text{C-P}} = 2.7$ Hz), 125.3 (m), 124.3 (q, $J_{\text{C-F}} = 271.7$ Hz), 36.2 (d, $J = 16.9$ Hz).

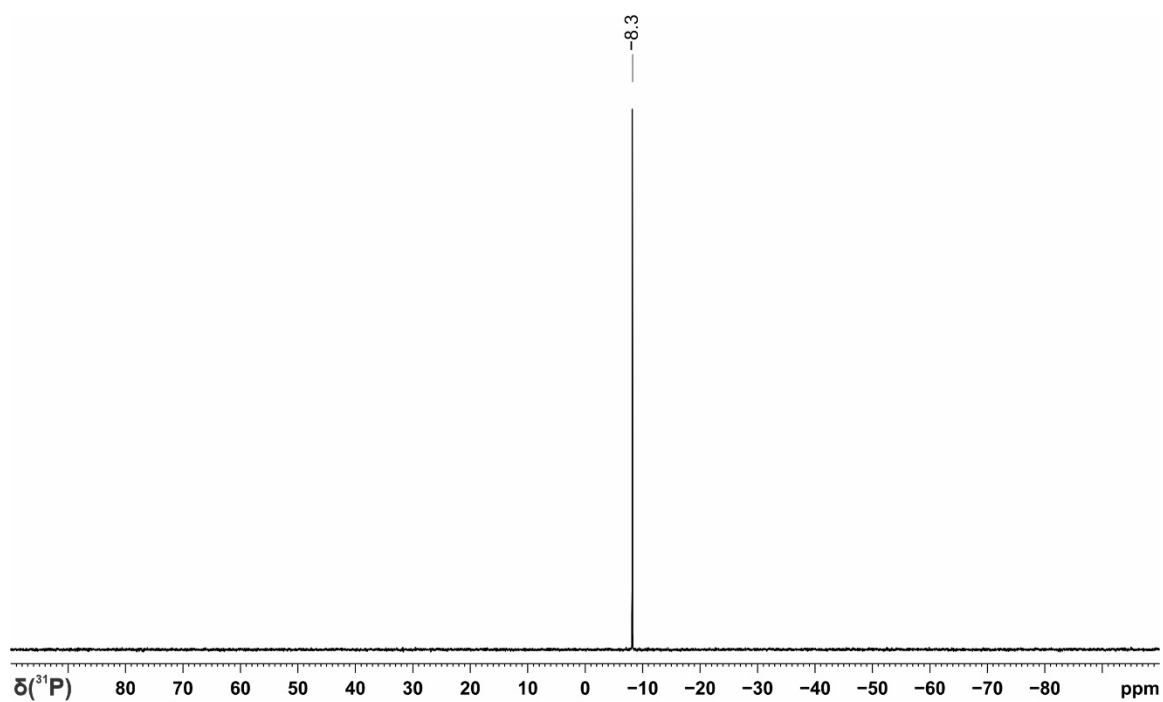
$^{31}\text{P}\{^1\text{H}\}$ NMR (162 MHz, CDCl_3): δ -8.3.

$^{19}\text{F}\{^1\text{H}\}$ NMR (366 MHz, CDCl_3): δ -62.9 (d, $^6J_{\text{P-F}} = 2.4$ Hz).

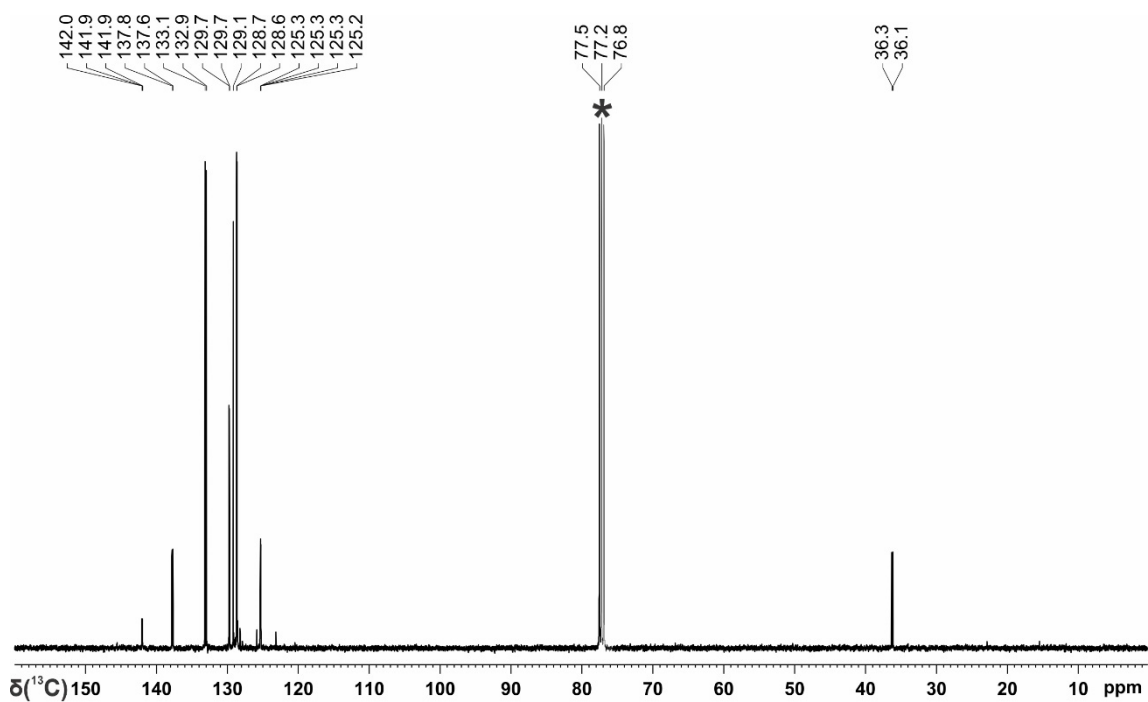
Elemental analysis: Calculated for $\text{C}_{20}\text{H}_{16}\text{F}_3\text{P}$: C, 69.77; H, 4.68; Found: C, 69.89; H, 4.32.



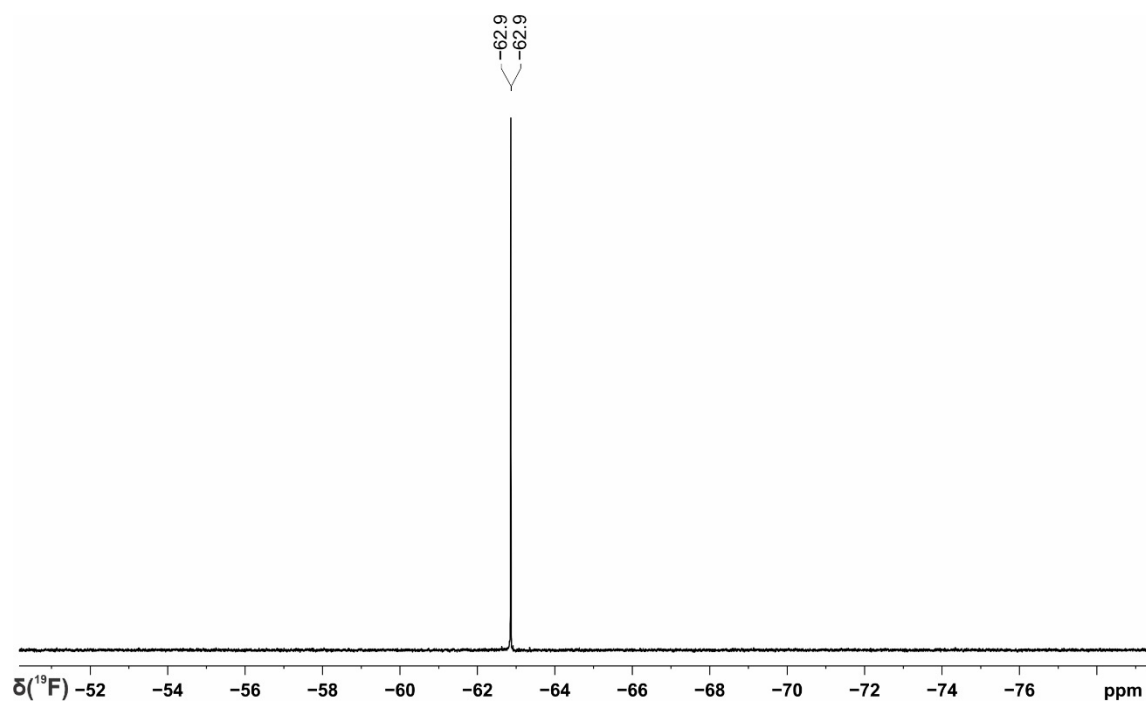
Supplementary Figure 102. $^1\text{H NMR}$ spectrum of (4-(trifluoromethyl)benzylidiphenylphosphine) in CDCl_3 prepared photocatalytically from HPPH_2 on a 1 mmol scale. * CDCl_3 .



Supplementary Figure 103. $^{31}\text{P}\{^1\text{H}\}$ NMR spectrum of (4-(trifluoromethyl)benzyl)diphenylphosphine in CDCl_3 prepared photocatalytically from HPPH_2 on a 1 mmol scale.



Supplementary Figure 104. ^{13}C NMR spectrum of (4-(trifluoromethyl)benzyl)diphenylphosphine in CDCl_3 prepared photocatalytically from HPPH_2 on a 1 mmol scale. * CDCl_3 .



Supplementary Figure 105. ^{19}F NMR spectrum of (4-(trifluoromethyl)benzyl)diphenylphosphine in CDCl_3 prepared photocatalytically from HPPH_2 on a 1 mmol scale.

Cyclohexyldiphenylphosphine (Table 4, V-10)

The general procedure 10 was followed using iodocyclohexane (259 μL , 2 mmol) which provided cyclohexyldiphenylphosphine as colourless oil in 73% yield (195.5 mg).

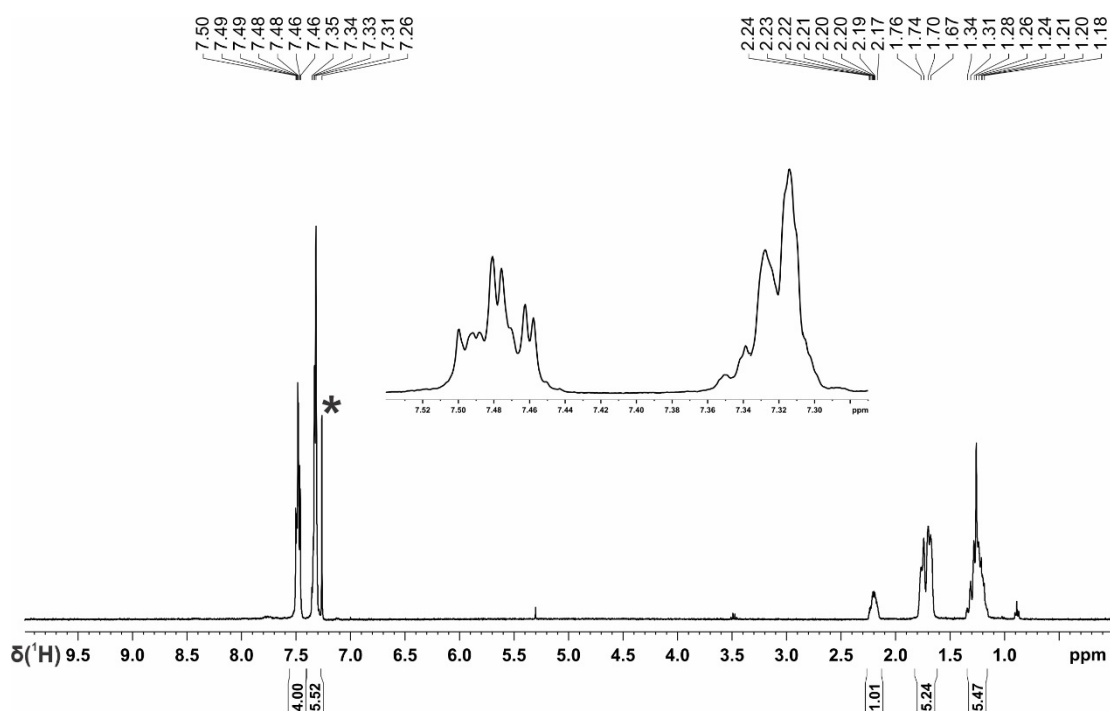
The characterization data of the product are consistent with the data found in the literature.^[S5]

$^1\text{H NMR}$ (400 MHz, CDCl_3): δ 7.50-7.46 (m, 4H), 7.35-7.31 (m, 6H), 2.24-2.17 (m, 1H), 1.76-1.67 (m, 5H), 1.34-1.18 (m, 5H).

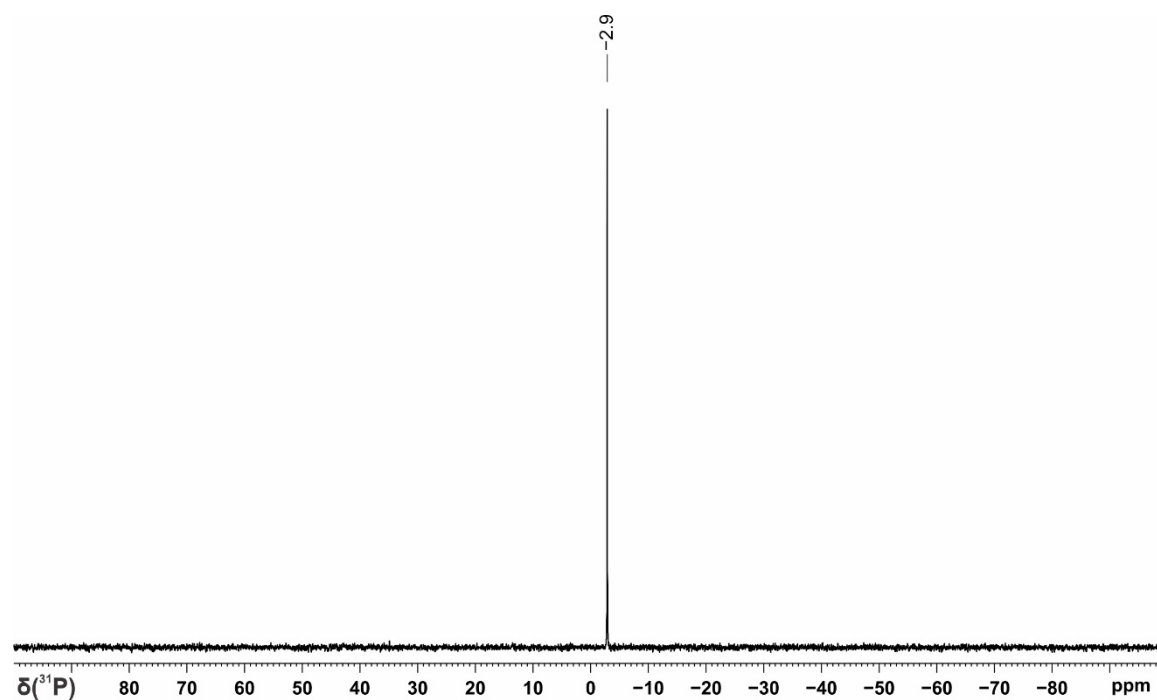
$^{13}\text{C}\{^1\text{H}\}$ NMR (100 MHz, CDCl_3): δ 137.3 (d, $J = 14.0$ Hz), 133.8 (d, $J = 19.1$ Hz), 128.7, 128.4 (d, $J = 7.0$ Hz), 35.5 (d, $J = 8.8$ Hz), 29.7 (d, $J = 15.3$ Hz), 26.9 (d, $J = 11.3$ Hz), 26.5 (d, $J = 1.1$ Hz).

$^{31}\text{P}\{^1\text{H}\}$ NMR (162 MHz, CDCl_3): δ -2.9.

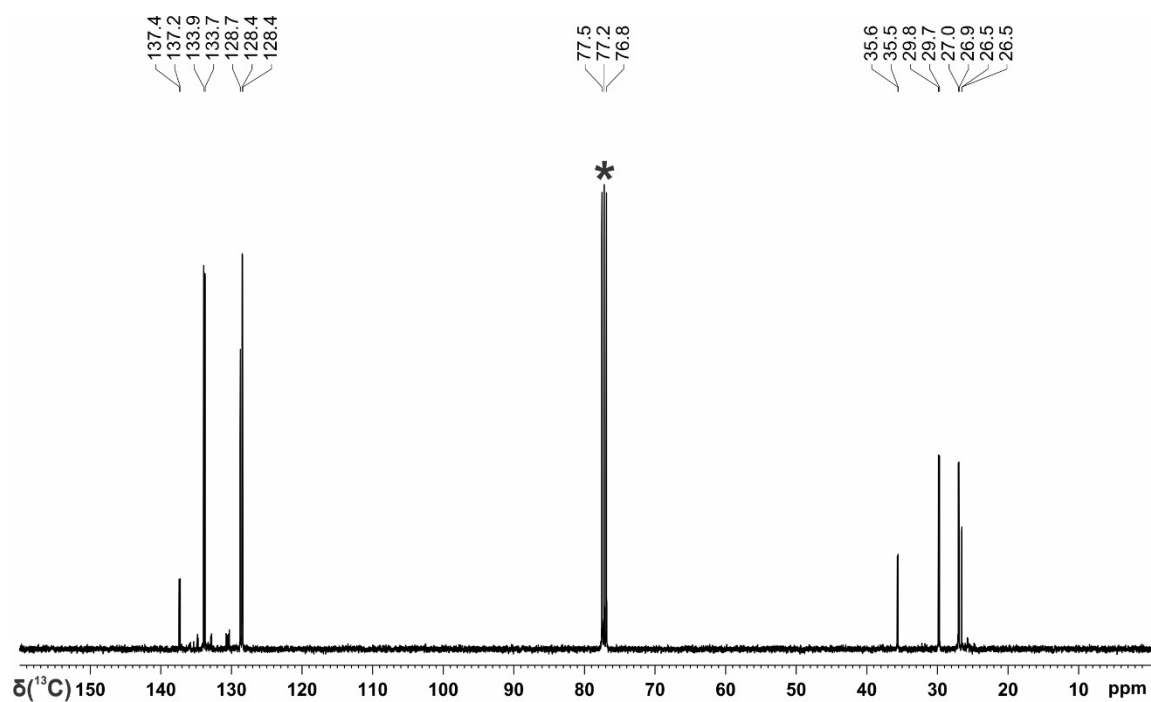
Elemental analysis: Calculated for $\text{C}_{18}\text{H}_{21}\text{P}$: C, 80.57; H, 7.89; Found: C, 80.81; H, 7.87.



Supplementary Figure 106. $^1\text{H NMR}$ spectrum of cyclohexyldiphenylphosphine in CDCl_3 prepared photocatalytically from HPPH_2 on a 1 mmol scale. * CDCl_3 .



Supplementary Figure 107. $^{31}\text{P}\{^1\text{H}\}$ NMR spectrum of cyclohexyldiphenylphosphine in CDCl_3 prepared photocatalytically from HPPH_2 on a 1 mmol scale.



Supplementary Figure 108. ^{13}C NMR spectrum of cyclohexyldiphenylphosphine in CDCl_3 prepared photocatalytically from HPPH_2 on a 1 mmol scale. * CDCl_3 .

Cyclopentyldiphenylphosphine (Table 4, V-11)

The general procedure 9 was followed using iodocyclopentane (231 μL , 2 mmol) which provided cyclopentyldiphenylphosphine as colourless oil in 71% yield (180.9 mg).

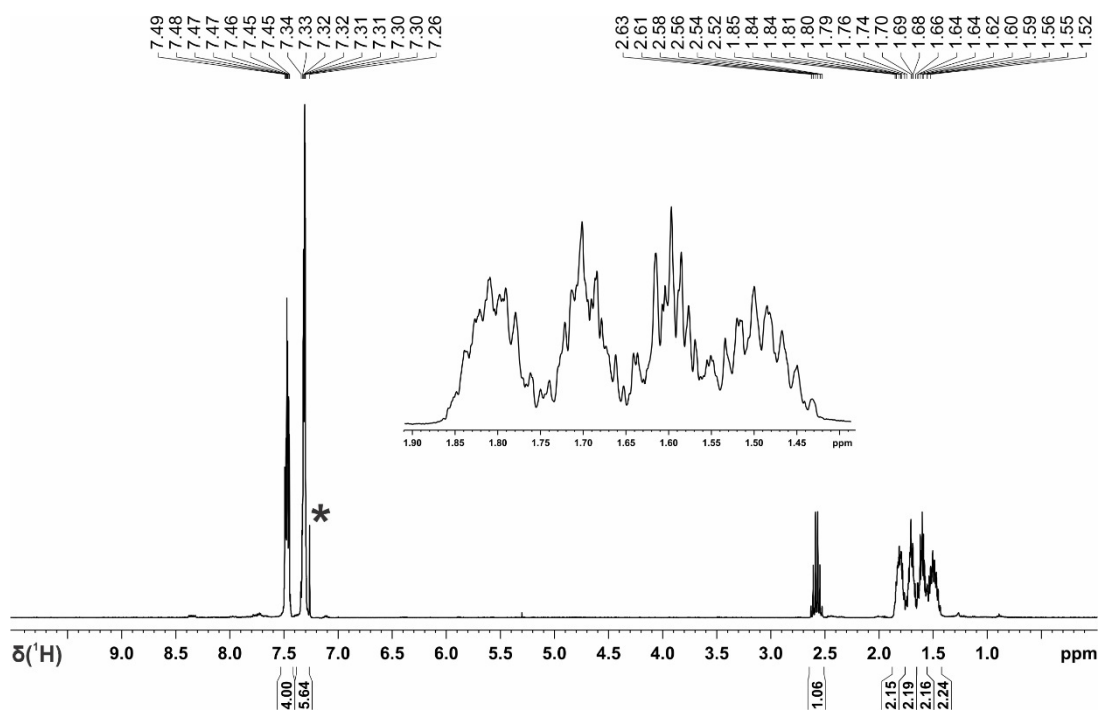
The characterization data of the product are consistent with the data found in the literature.^[S6]

^1H NMR (400 MHz, CDCl_3): δ 7.49-7.45 (m, 4H), 7.34-7.30 (m, 6H), 2.57 (dq, $J = 16.3$, 8.2 Hz, 1H), 1.85-1.79 (m, 2H), 1.76-1.66 (m, 2H), 1.64-1.59 (m, 2H), 1.52-1.43 (m, 2H).

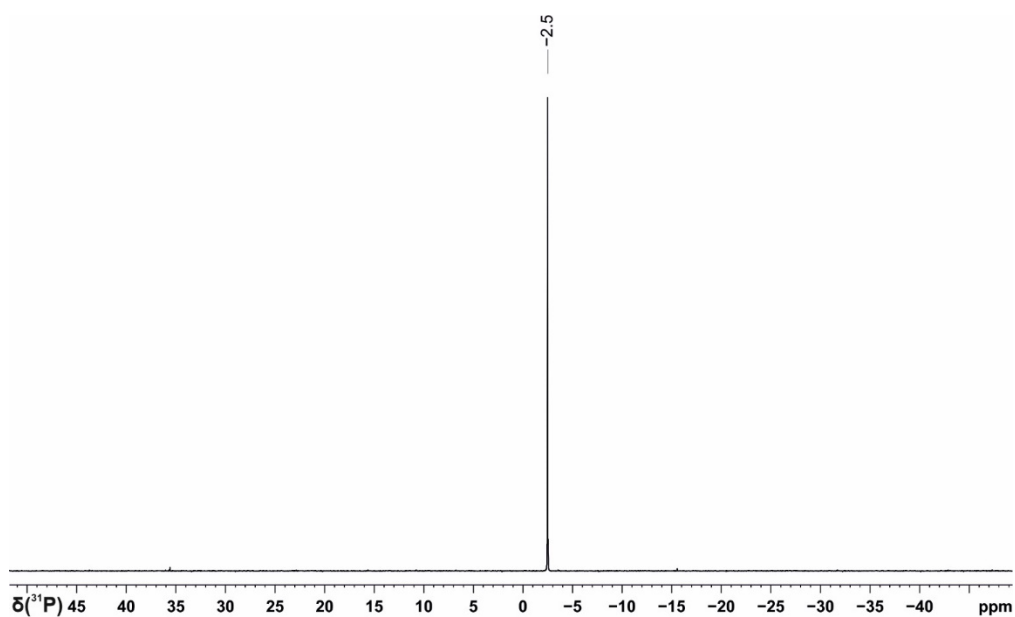
$^{13}\text{C}\{^1\text{H}\}$ NMR (100 MHz, CDCl_3): δ 139.2 (d, $J = 13.4$ Hz), 133.4 (d, $J = 18.4$ Hz), 128.6, 128.4 (d, $J = 6.7$ Hz), 36.0 (d, $J = 8.0$ Hz), 31.2 (d, $J = 19.9$ Hz), 26.7 (d, $J = 7.5$ Hz).

$^{31}\text{P}\{^1\text{H}\}$ NMR (162 MHz, CDCl_3): δ -2.5.

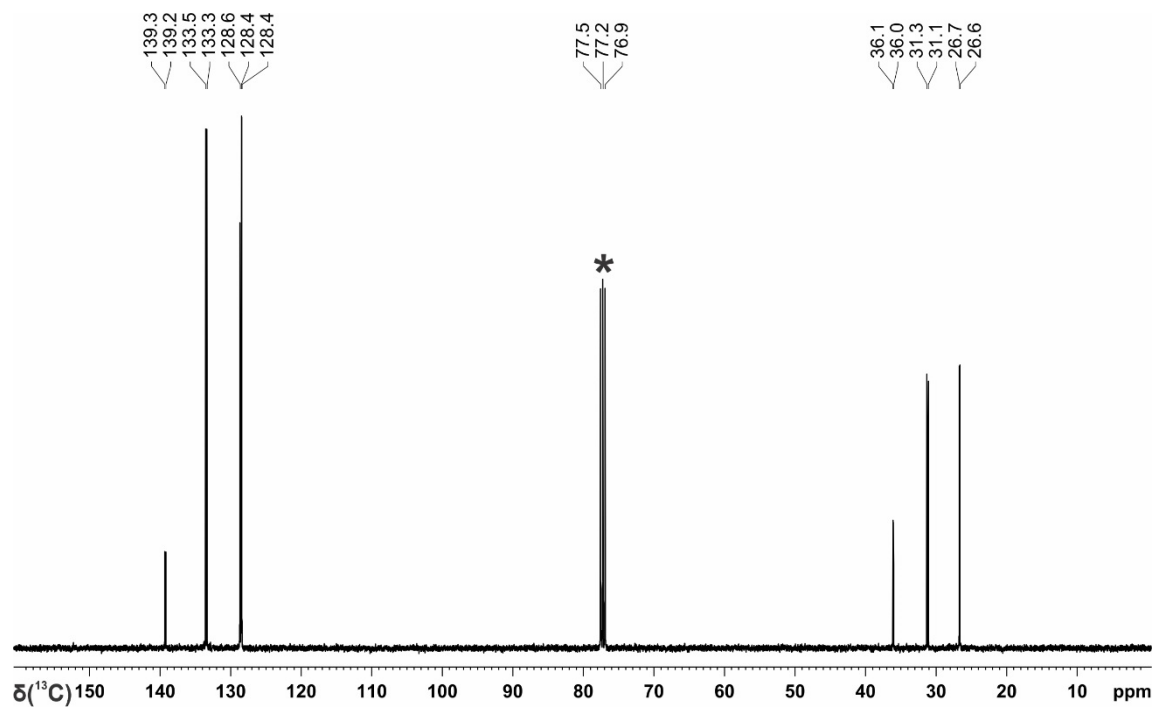
Elemental analysis: Calculated for $\text{C}_{17}\text{H}_{19}\text{P}$: C, 80.29; H, 7.53; Found: C, 80.05; H, 7.22.



Supplementary Figure 109. ^1H NMR spectrum of cyclopentyldiphenylphosphine in CDCl_3 prepared photocatalytically from HPPH_2 on a 1 mmol scale. * CDCl_3 .



Supplementary Figure 110. $^{31}\text{P}\{^1\text{H}\}$ NMR spectrum of cyclopentylidiphenylphosphine in CDCl_3 prepared photocatalytically from HPPH_2 on a 1 mmol scale.



Supplementary Figure 111. ^{13}C NMR spectrum of cyclopentylidiphenylphosphine in CDCl_3 prepared photocatalytically from HPPH_2 on a 1 mmol scale. * CDCl_3 .

Isopropyldiphenylphosphine (Table 4, V-12)

The general procedure 10 was followed using 2-iodopropane (200 μ L, 2 mmol) which provided *isopropyldiphenylphosphine* as colourless oil in 81% yield (184.6 mg).

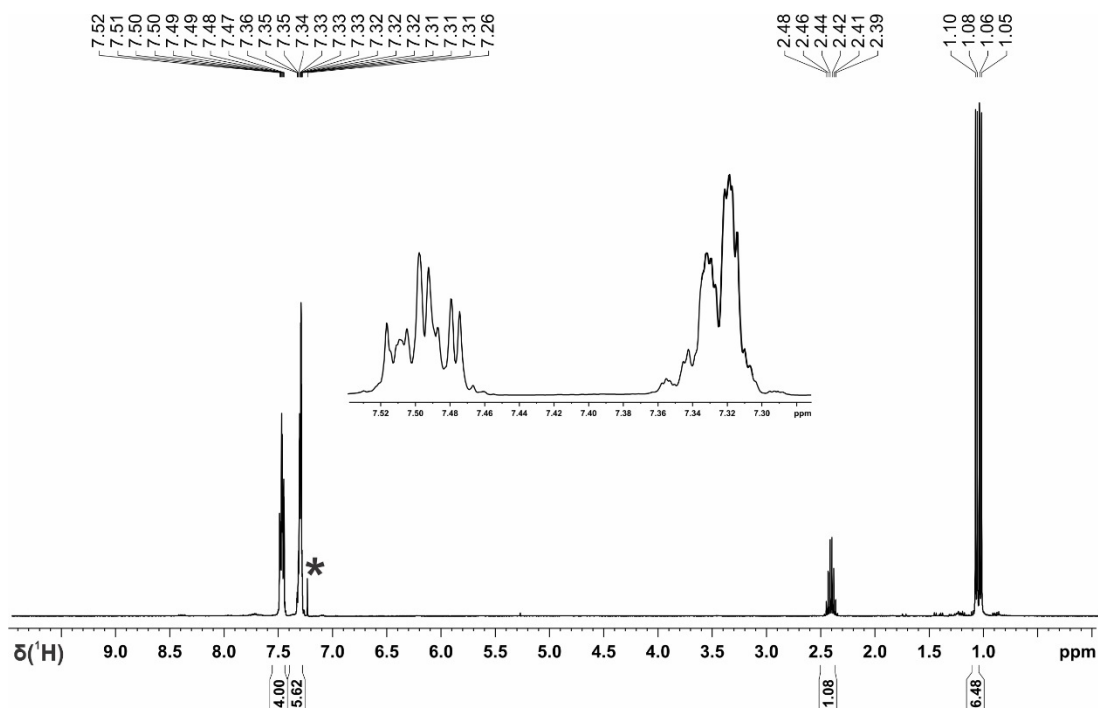
The characterization data of the product are consistent with the data found in the literature.^[S5]

$^1\text{H NMR}$ (400 MHz, CDCl_3): δ 7.52-7.47 (m, 4H), 7.36-7.31 (m, 6H), 2.42 (dq, $J = 13.7$, 6.8 Hz, 1H), 1.09 (d, $J = 6.8$ Hz, 3H), 1.06 (d, $J = 6.8$ Hz, 3H).

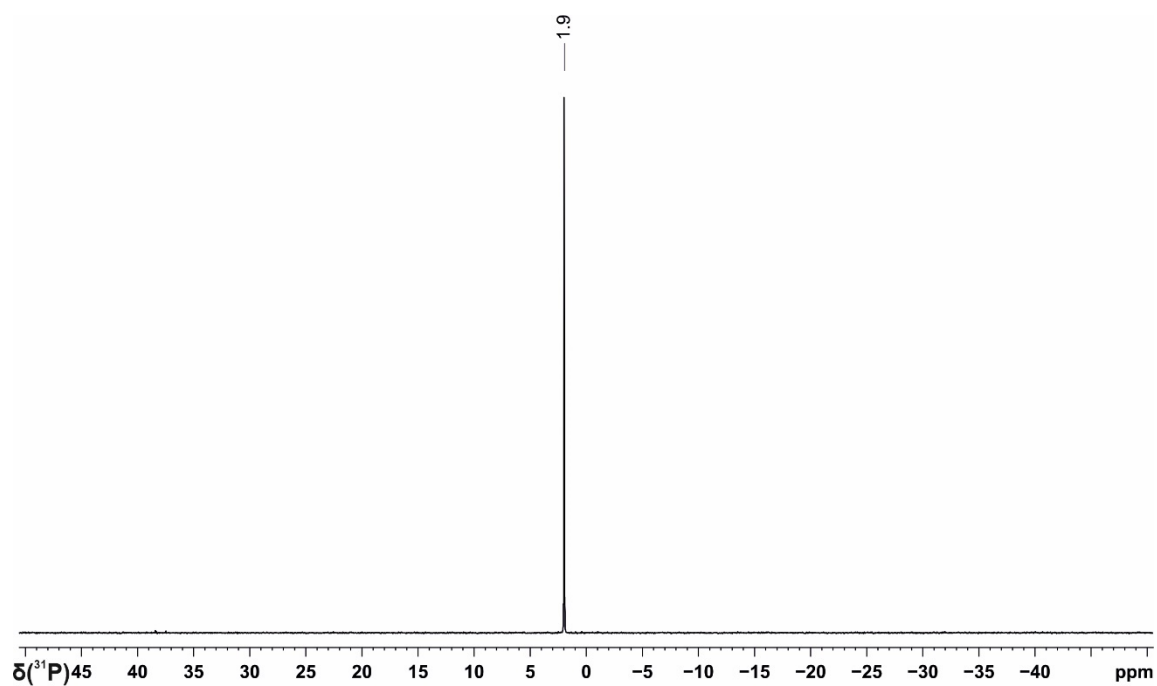
$^{13}\text{C}\{^1\text{H}\}$ NMR (100 MHz, CDCl_3): δ 137.8 (d, $J = 14.0$ Hz), 133.7 (d, $J = 18.9$ Hz), 128.8, 128.4 (d, $J = 7.0$ Hz), 25.2 (d, $J = 8.2$ Hz), 19.8 (d, $J = 18.0$ Hz).

$^{31}\text{P}\{^1\text{H}\}$ NMR (162 MHz, CDCl_3): δ 1.9.

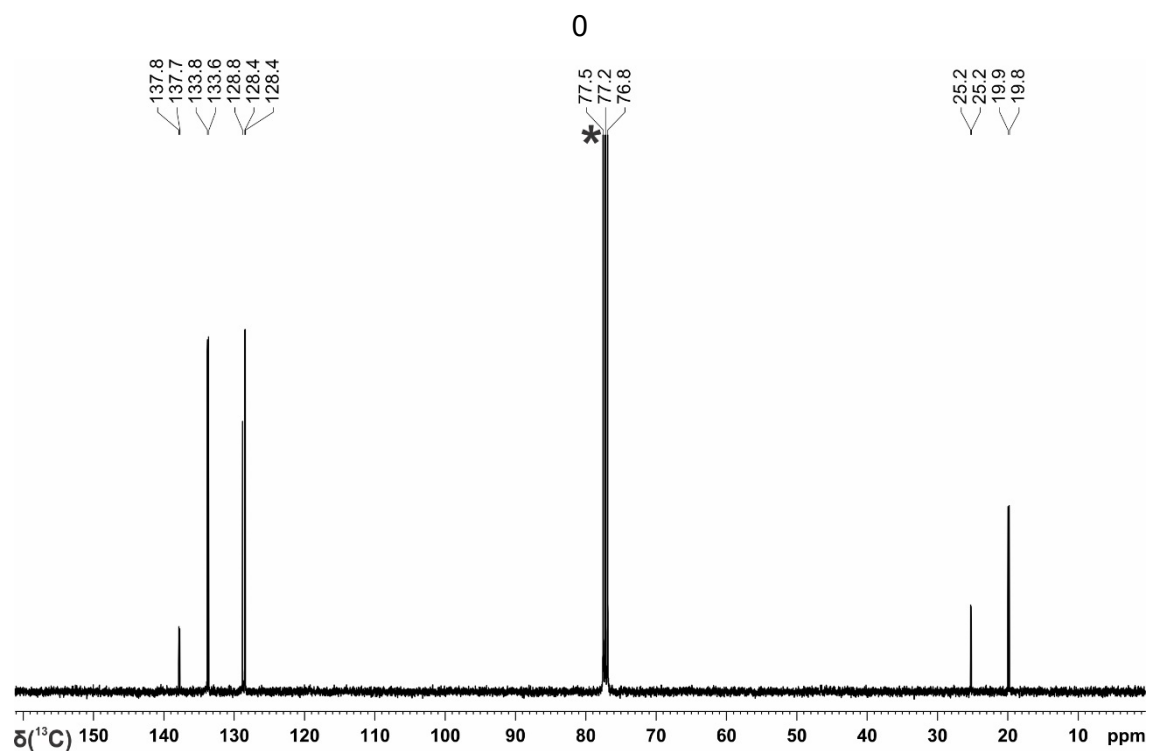
Elemental analysis: Calculated for $\text{C}_{15}\text{H}_{17}\text{P}$: C, 78.92; H, 7.51; Found: C, 78.63; H, 7.29.



Supplementary Figure 112. $^1\text{H NMR}$ spectrum of *isopropyldiphenylphosphine* in CDCl_3 prepared photocatalytically from HPPH_2 on a 1 mmol scale. * CDCl_3 .



Supplementary Figure 113. $^{31}\text{P}\{^1\text{H}\}$ NMR spectrum of *isopropylidiphenylphosphine* in CDCl_3 prepared photocatalytically from HPPH_2 on a 1 mmol scale.



Supplementary Figure 114. ^{13}C NMR spectrum of *isopropylidiphenylphosphine* in CDCl_3 prepared photocatalytically from HPPH_2 on a 1 mmol scale. * CDCl_3 .

***tert*-Butyldiphenylphosphine (Table 4, V-13)**

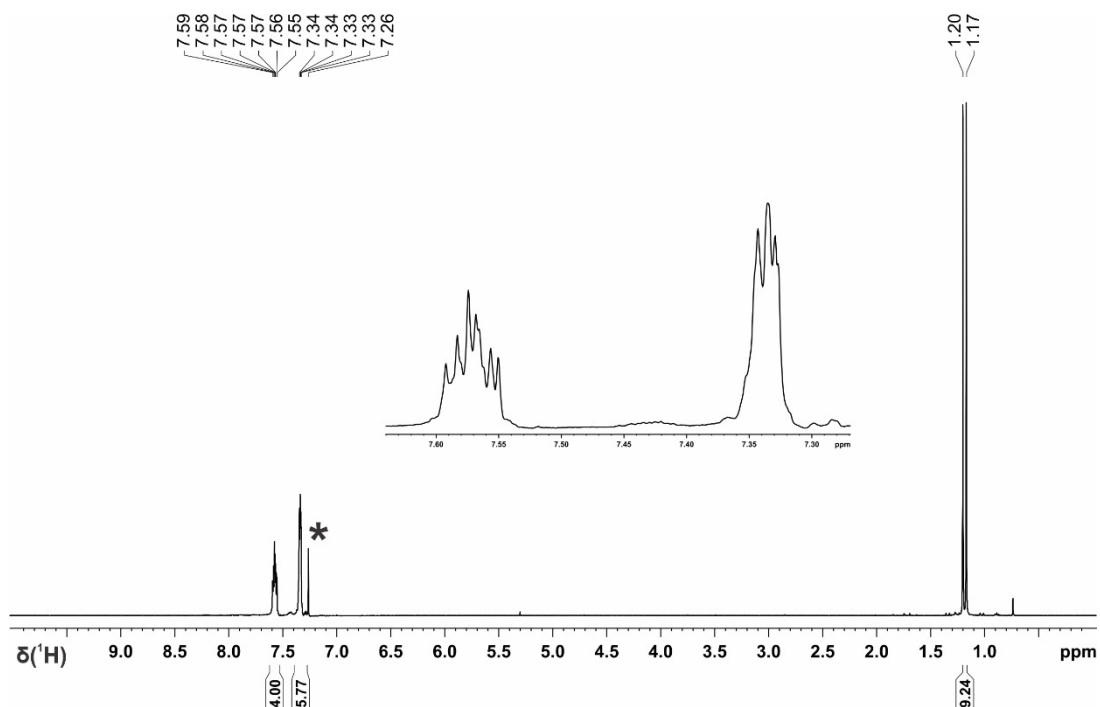
The general procedure 10 was followed using 2-iodo-2-methylpropane (238 μ L, 2 mmol) which provided *tert*-butyldiphenylphosphine as colourless oil in 61% yield (148.7 mg).

$^1\text{H NMR}$ (400 MHz, CDCl_3): δ 7.59-7.55 (m, 4H), 7.34-7.33 (m, 6H), 1.18 (d, $J = 12.5$ Hz, 9H).

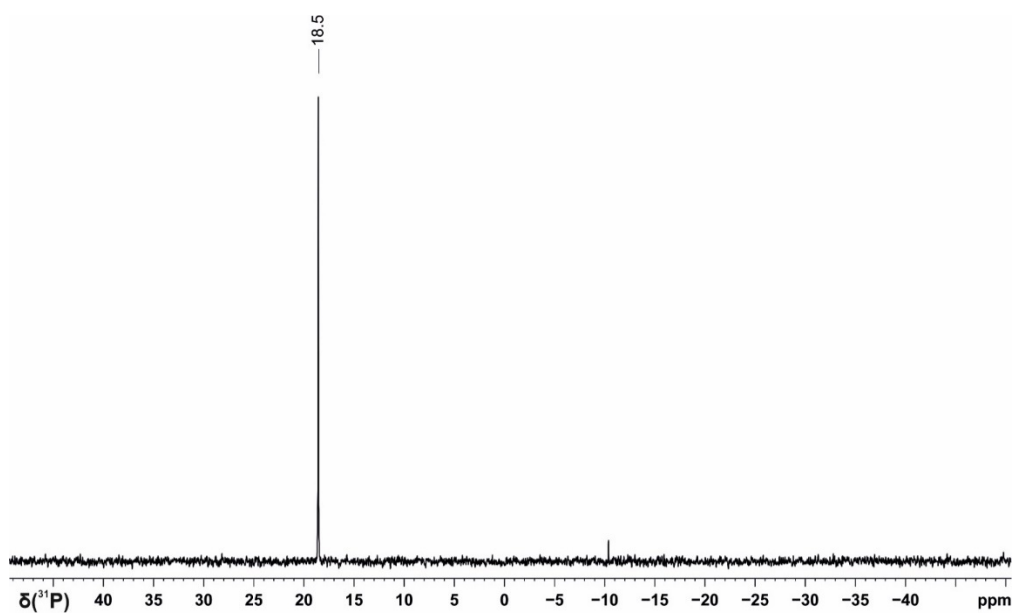
$^{13}\text{C}\{^1\text{H}\}$ NMR (100 MHz, CDCl_3): δ 137.2 (d, $J = 17.8$ Hz), 134.8 (d, $J = 19.5$ Hz), 128.6, 128.2 (d, $J = 6.9$ Hz), 31.0 (d, $J = 14.4$ Hz), 28.9 (d, $J = 14.4$ Hz).

$^{31}\text{P}\{^1\text{H}\}$ NMR (162 MHz, CDCl_3): δ 18.5.

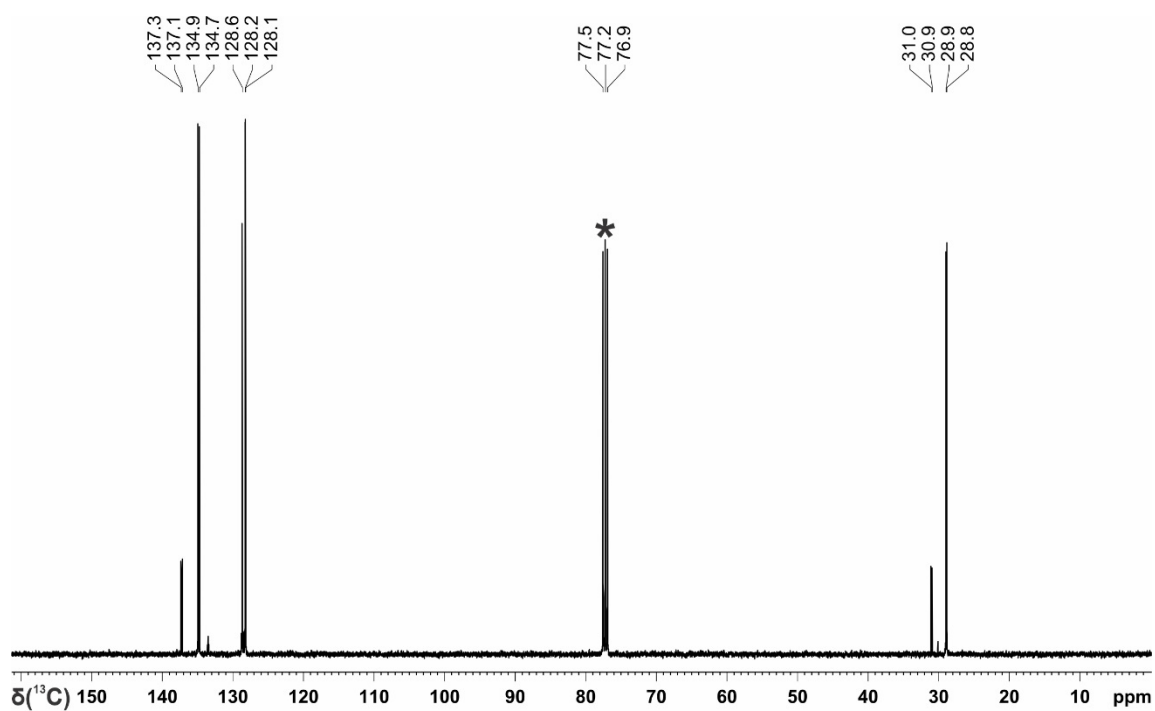
Elemental analysis: Calculated for $\text{C}_{16}\text{H}_{19}\text{P}$: C, 79.31; H, 7.90; Found: C, 79.13; H, 7.63.



Supplementary Figure 115. $^1\text{H NMR}$ spectrum of *tert*-butyldiphenylphosphine in CDCl_3 prepared photocatalytically from HPPH_2 on a 1 mmol scale. * CDCl_3 .



Supplementary Figure 116. $^{31}\text{P}\{^1\text{H}\}$ NMR spectrum of *tert*-butylidiphenylphosphine in CDCl_3 prepared photocatalytically from HPPH_2 on a 1 mmol scale.



Supplementary Figure 117. ^{13}C NMR spectrum of *tert*-butylidiphenylphosphine in CDCl_3 prepared photocatalytically from HPPH_2 on a 1 mmol scale. * CDCl_3 .

Adamantylidiphenylphosphine (Table 4, V-14)

The general procedure 10 was followed using 1-iodoadamantane (524 mg, 2 mmol) which provided adamantylidiphenylphosphine as white solid in 50% yield (159.5 mg).

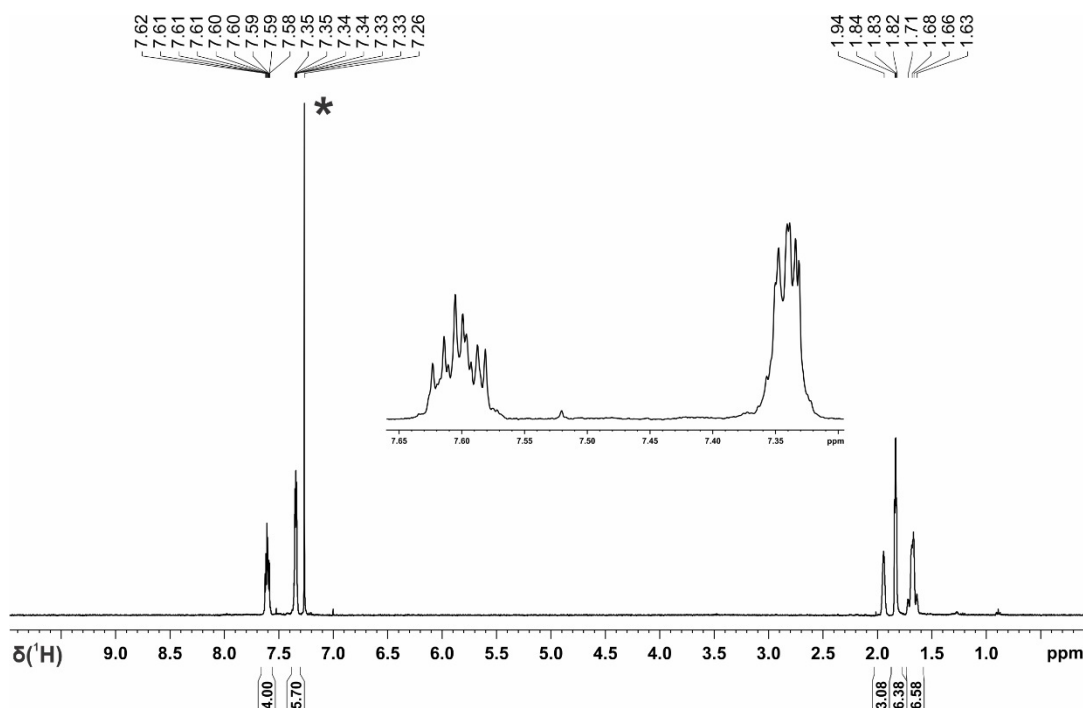
The characterization data of the product are consistent with the data found in the literature.^[S7]

¹H NMR (400 MHz, CDCl₃): δ 7.62-7.58 (m, 4H), 7.35-7.33 (m, 6H), 1.94 (bs, 3H), 1.84-1.82 (m, 6H), 1.71-1.63 (m, 6H).

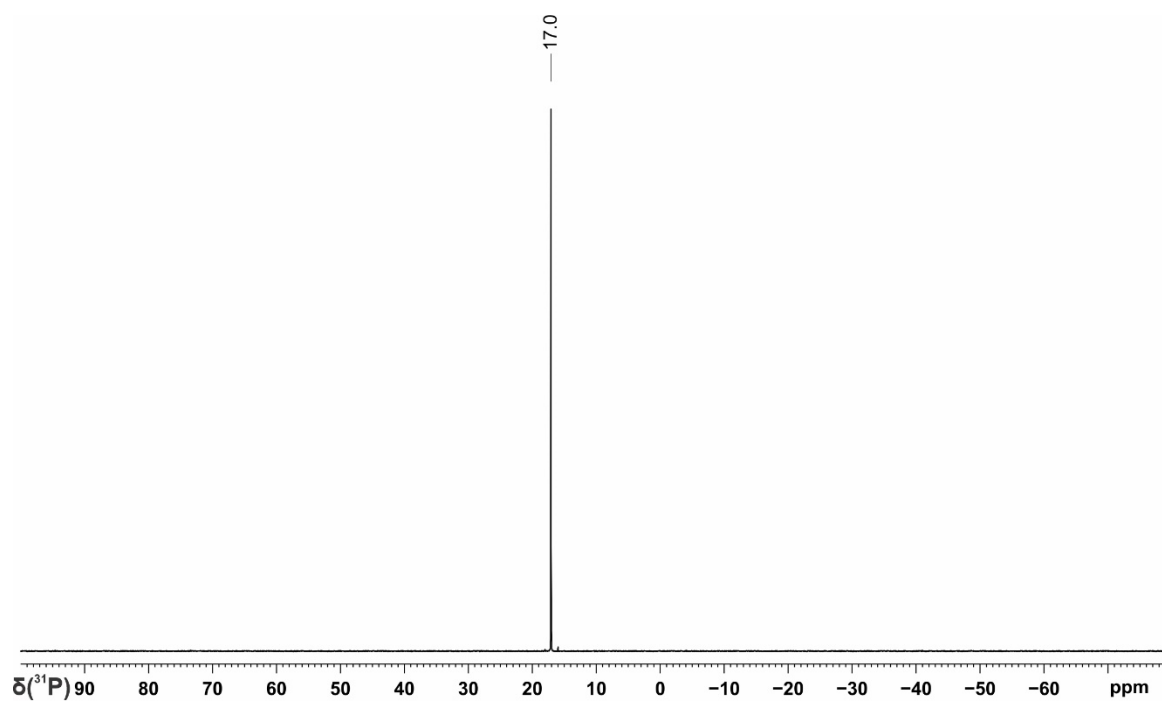
¹³C{¹H} NMR (100 MHz, CDCl₃): δ 135.8 (d, *J* = 17.4 Hz), 135.2 (d, *J* = 19.9 Hz), 128.6, 128.1 (d, *J* = 7.2 Hz), 40.0 (d, *J* = 11.4 Hz), 37.0, 34.6 (d, *J* = 14.4 Hz), 28.8 (d, *J* = 8.9 Hz).

³¹P{¹H} NMR (162 MHz, CDCl₃): δ 17.0.

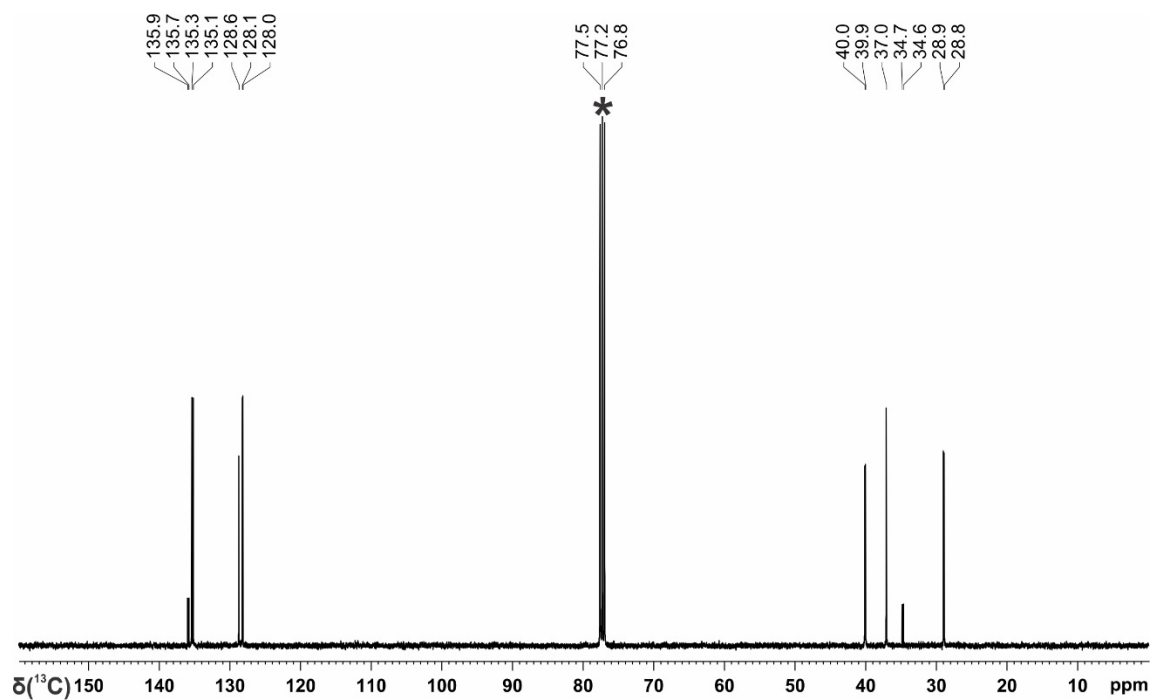
Elemental analysis: Calculated for C₂₂H₂₅P: C, 82.47; H, 7.86; Found: C, 82.77; H, 7.65.



Supplementary Figure 118. ¹H NMR spectrum of adamantylidiphenylphosphine in CDCl₃ prepared photocatalytically from HPPH₂ on a 1 mmol scale. *CDCl₃.



Supplementary Figure 119. $^{31}\text{P}\{^1\text{H}\}$ NMR spectrum of adamantyldiphenylphosphine in CDCl_3 prepared photocatalytically from HPPH_2 on a 1 mmol scale.



Supplementary Figure 120. ^{13}C NMR spectrum of adamantyldiphenylphosphine in CDCl_3 prepared photocatalytically from HPPH_2 on a 1 mmol scale. * CDCl_3 .

Dicyclohexylphenylphosphine (Table 5, VI-11)

The general procedure 11 was followed using iodocyclopentane (463 μL , 4 mmol) which provided dicyclohexylphenylphosphine as colourless oil in 45% yield (109.7 mg).

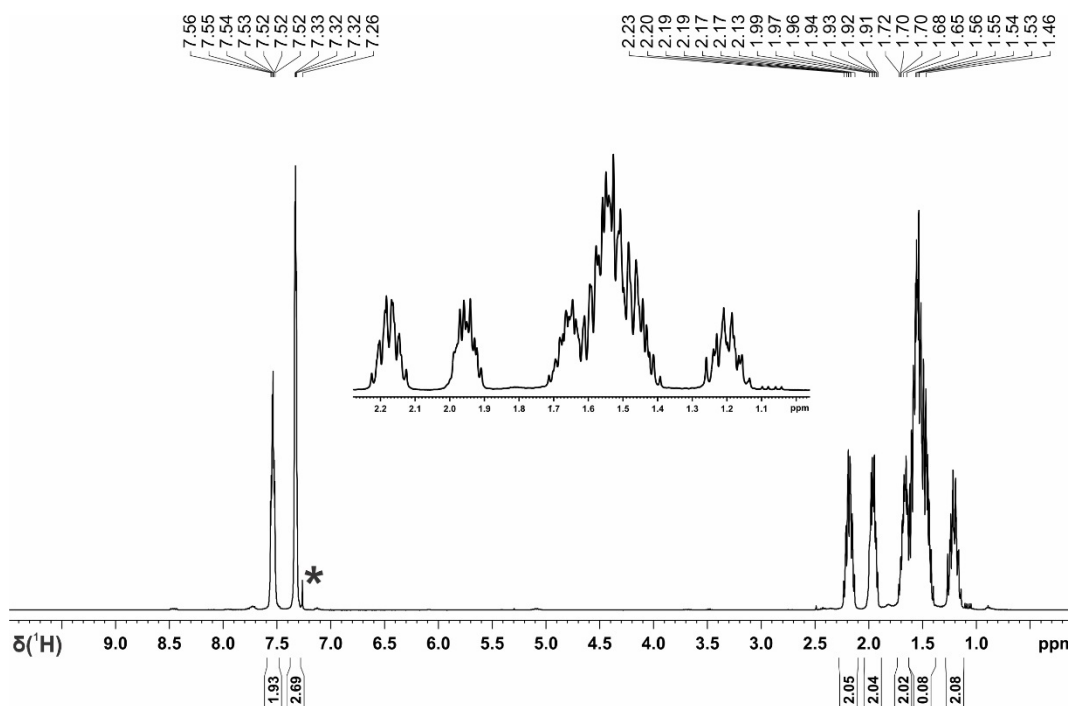
The characterization data of the product are consistent with the data found in the literature.^[S6]

$^1\text{H NMR}$ (400 MHz, CDCl_3): δ 7.56-7.52 (m, 2H), 7.33-7.32 (m, 3H), 2.23-2.13 (m, 2H), 1.99-1.91 (m, 2H), 1.72-1.65 (m, 2H), 1.54-1.39 (m, 10H), 1.26-1.46 (m, 2H).

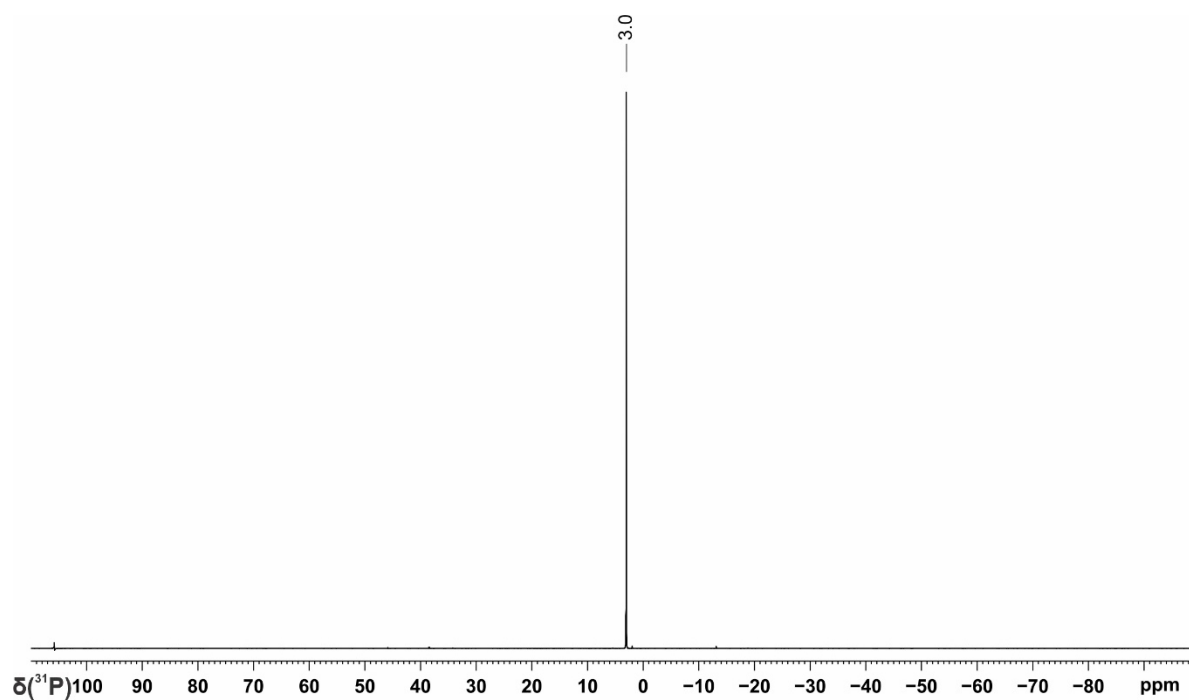
$^{13}\text{C}\{^1\text{H}\}$ NMR (100 MHz, CDCl_3): δ 138.5 (d, $J = 14.6$ Hz), 134.0 (d, $J = 18.6$ Hz), 128.8, 128.0 (d, $J = 7.2$ Hz), 37.2 (d, $J = 9.4$ Hz), 31.2 (d, $J = 20.5$ Hz), 30.9 (d, $J = 12.8$ Hz), 26.7 (d, $J = 7.8$ Hz), 25.9 (d, $J = 6.5$ Hz).

$^{31}\text{P}\{^1\text{H}\}$ NMR (162 MHz, CDCl_3): δ 3.0.

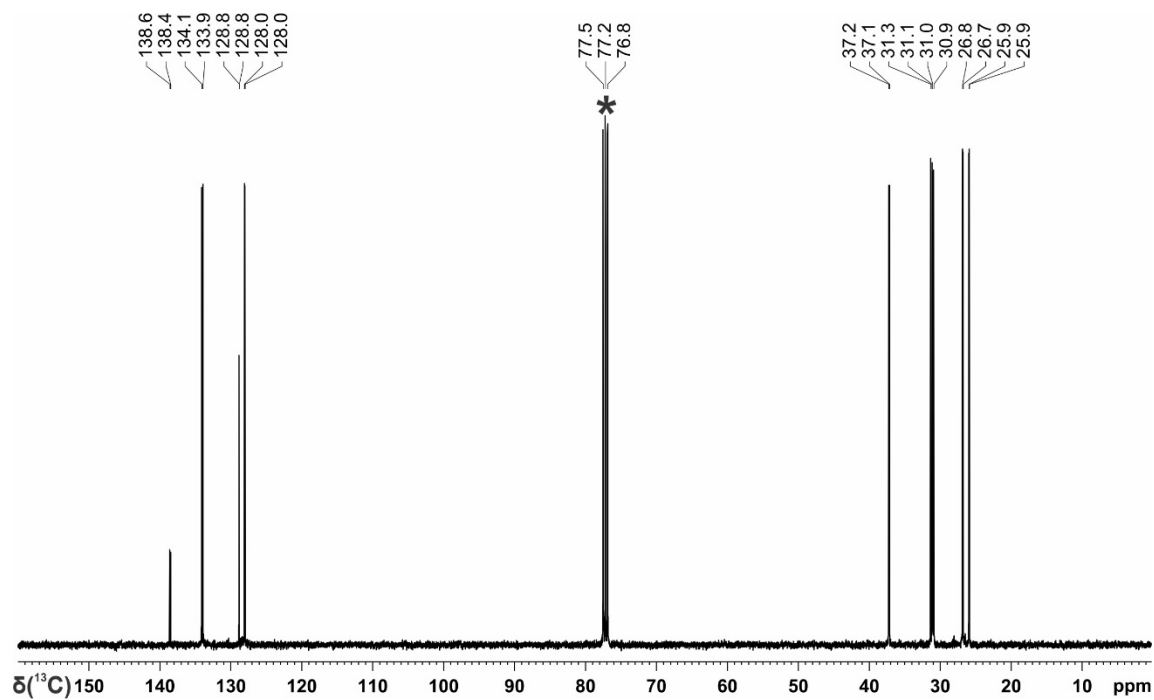
Elemental analysis: Calculated for $\text{C}_{16}\text{H}_{23}\text{P}$: C, 78.01; H, 9.41; Found: C, 77.62; H, 9.83.



Supplementary Figure 121. $^1\text{H NMR}$ spectrum of dicyclohexylphenylphosphine in CDCl_3 prepared photocatalytically from H_2PPh on a 1 mmol scale. * CDCl_3 .



Supplementary Figure 122. $^{31}\text{P}\{^1\text{H}\}$ NMR spectrum of dicyclohexylphenylphosphine in CDCl_3 prepared photocatalytically from H_2PPh on a 1 mmol scale.



Supplementary Figure 123. ^{13}C NMR spectrum of dicyclohexylphenylphosphine in CDCl_3 prepared photocatalytically from H_2PPh on a 1 mmol scale. $^*\text{CDCl}_3$.

1,3-Bis(diphenylphosphanyl)methyl benzene from P₂Ph₄ (Scheme 2, V-15)

The general procedure 13 was followed 1,3-bis(bromomethyl)benzene (0.50 mmol, 1.0 equiv) which provided 1,3-bis(diphenylphosphaneyl)methylbenzene as colourless oil in 61% yield (144.3 mg).

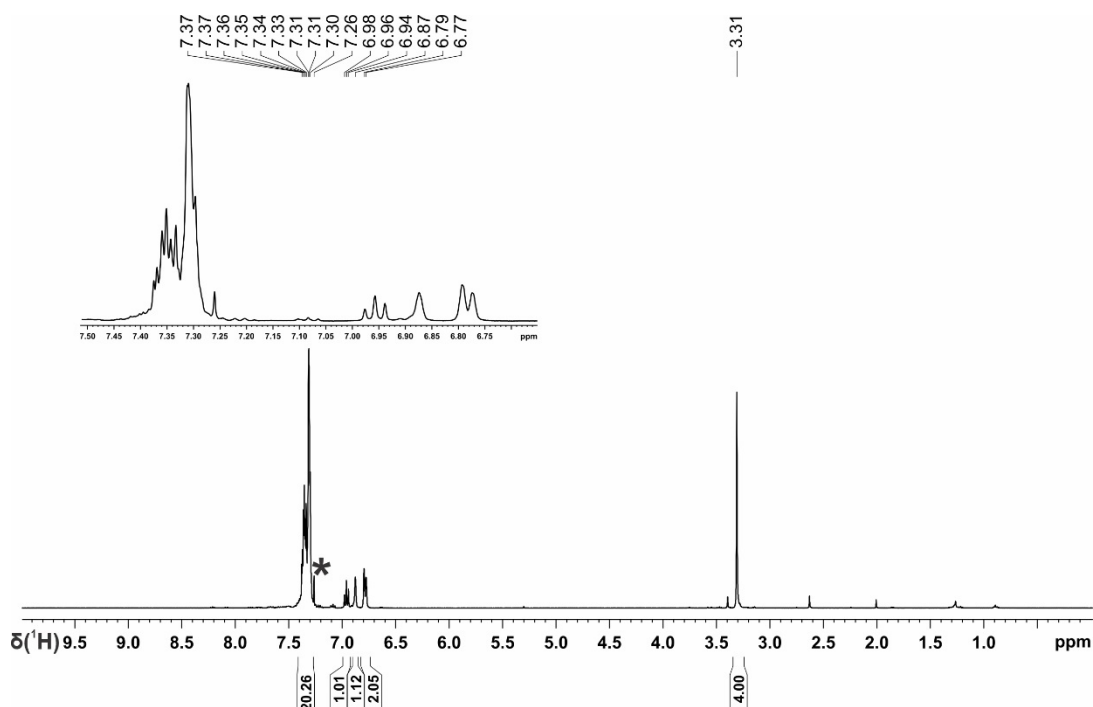
The characterization data of the product are consistent with the data found in the literature.^[S8]

¹H NMR (400 MHz, CDCl₃): δ 7.37-7.30 (m, 20H), 6.96 (t, *J* = 7.6 Hz, 1H), 6.78 (d, *J* = 7.6 Hz, 2H), 3.31 (s, 4H).

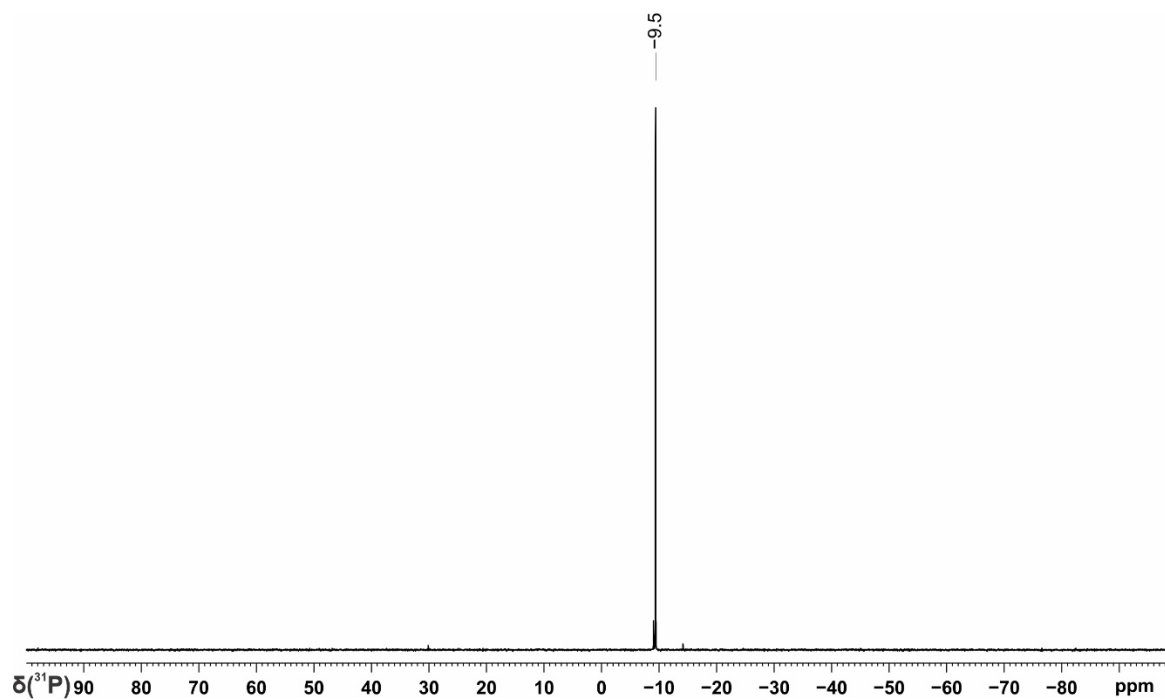
¹³C{¹H} NMR (100 MHz, CDCl₃): δ 138.5 (d, *J* = 15.4 Hz), 137.5 (dd, *J* = 8.2, 1.6 Hz), 133.0 (d, *J* = 18.5 Hz), 131.3 (d, *J* = 9.1 Hz), 130.6 (t, *J* = 6.9 Hz), 128.8, 128.4 (d, *J* = 6.6 Hz), 128.2, 127.1 (dd, *J* = 6.9, 2.4 Hz), 36.0 (d, *J* = 15.8 Hz).

³¹P{¹H} NMR (162 MHz, CDCl₃): δ -9.5.

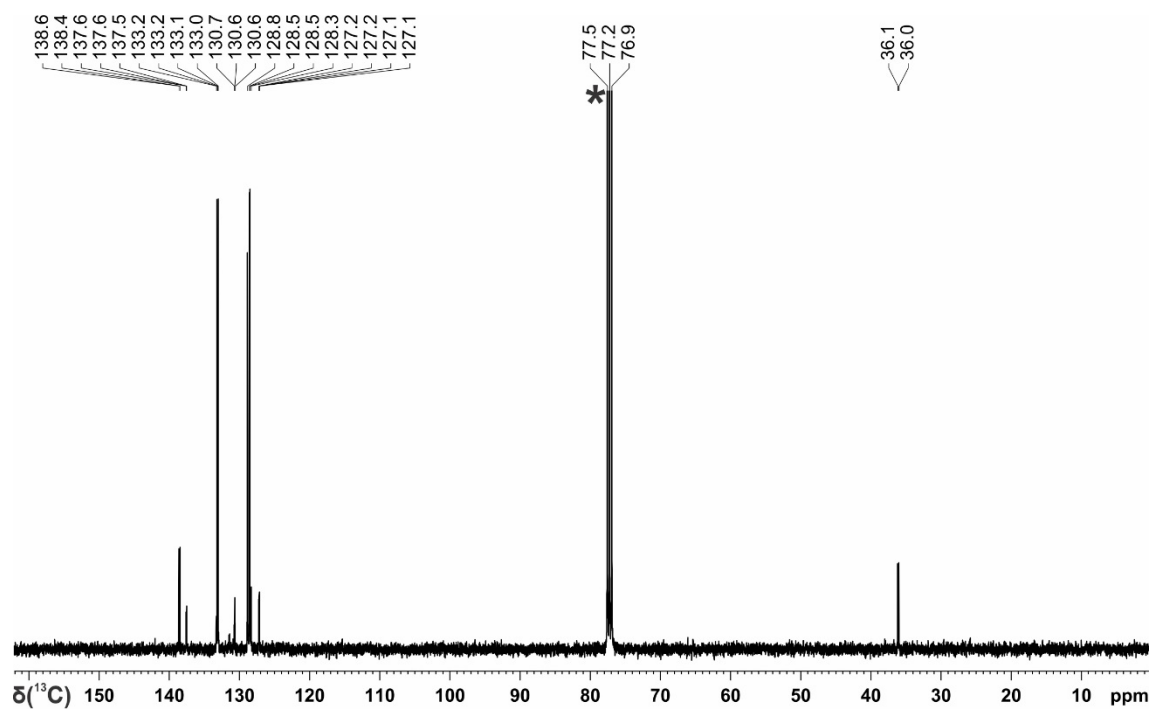
Elemental analysis: Calculated for C₃₂H₂₈P₂: C, 81.00; H, 5.95; Found: C, 80.68; H, 5.84.



Supplementary Figure 124. ¹H NMR spectrum of 1,3-bis(diphenylphosphaneyl)methylbenzene in CDCl₃ prepared photocatalytically from H₂PPh on a 1 mmol scale. *CDCl₃.



Supplementary Figure 125. $^{31}\text{P}\{^1\text{H}\}$ NMR spectrum of 1,3-bis(diphenylphosphanyl)methylbenzene in CDCl_3 prepared photocatalytically from H_2PPh on a 1 mmol scale.



Supplementary Figure 126. ^{13}C NMR spectrum of 1,3-bis(diphenylphosphanyl)methylbenzene in CDCl_3 prepared photocatalytically from H_2PPh on a 1 mmol scale. * CDCl_3 .

Tetraphenylphosphonium iodide from P₄ (1 mmol scale, Table 6, IX-1)

The general method 13 was followed using iodobenzene (1.23 mL, 11 mmol, 11 equiv. based on the phosphorus atom) which provided tetraphenylphosphoniumiodide in 24% yield (112.5 mg).

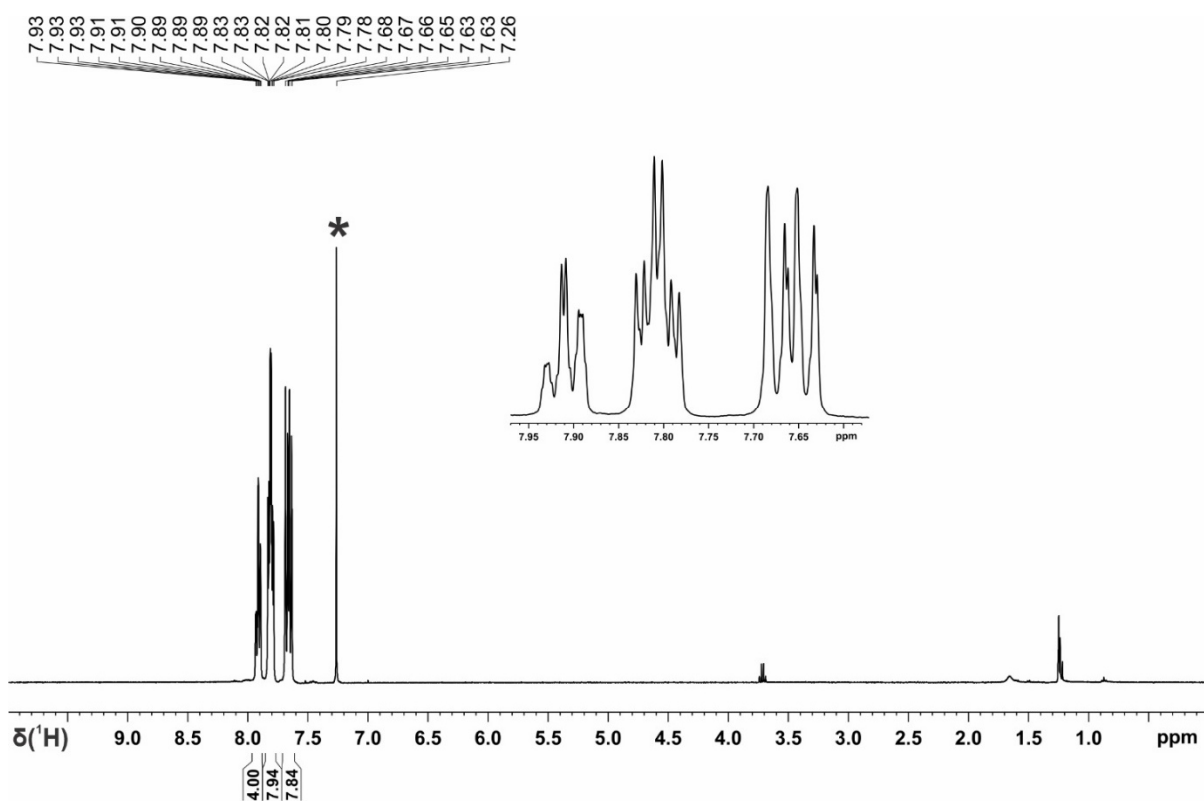
The characterization data of the product are consistent with the data found in the literature.^[S9]

¹H NMR (400 MHz, CDCl₃): δ 7.93-7.89 (m, 4H), 7.83-7.78 (m, 8H), 7.68-7.63 (m, 8H).

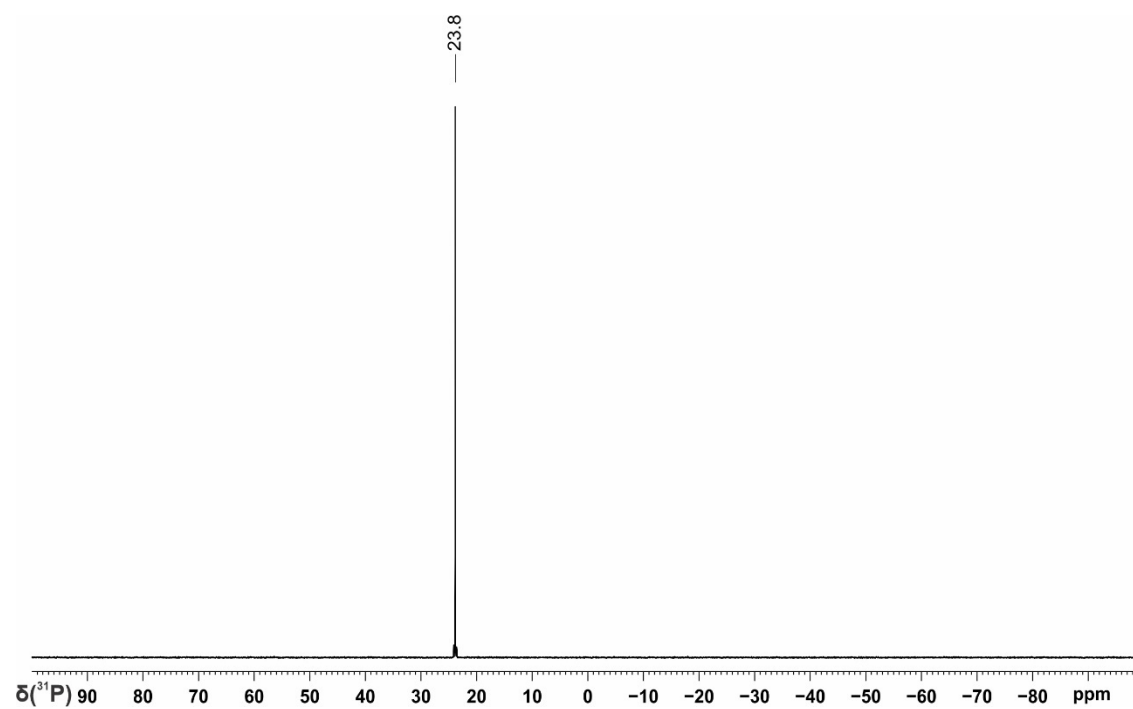
¹³C{¹H} NMR (100 MHz, CDCl₃): δ 135.9 (d, *J* = 3.0 Hz), 134.5 (d, *J* = 10.3 Hz), 133.0 (d, *J* = 12.9 Hz), 117.5 (d, *J* = 89.5 Hz).

³¹P{¹H} NMR (162 MHz, CDCl₃): δ 23.8.

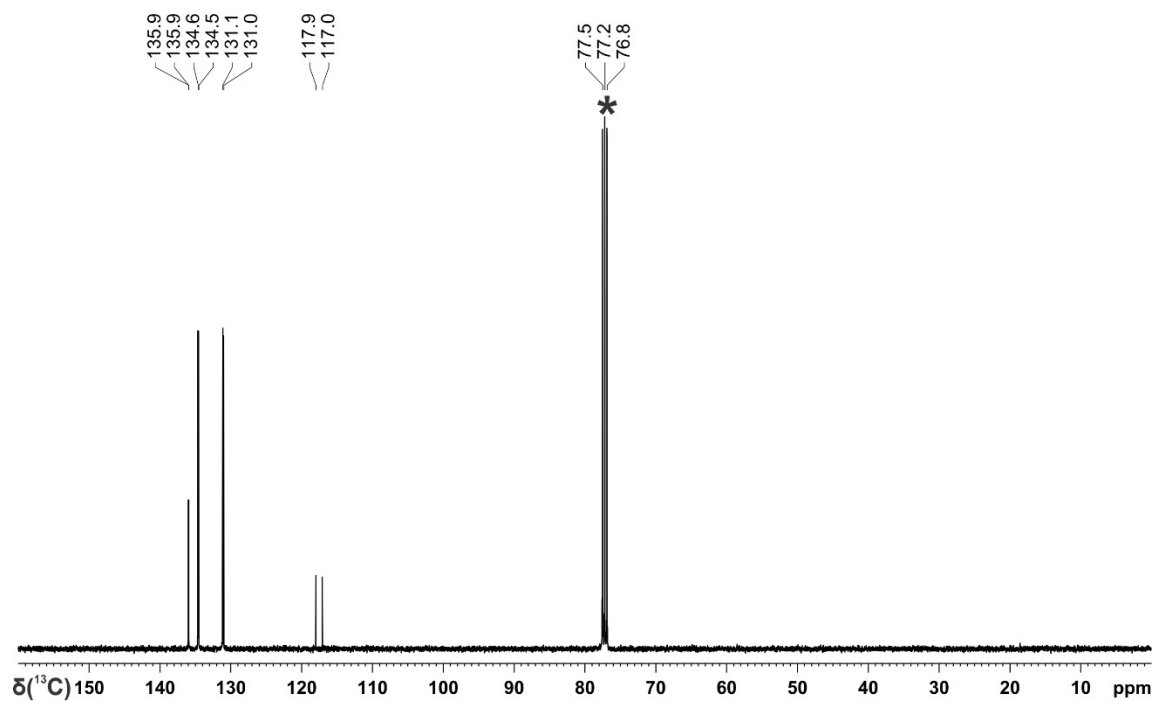
Elemental analysis: Calculated for C₂₄H₂₀I⁺P: C, 61.82; H, 4.32; Found: C, 61.57; H, 4.25.



Supplementary Figure 127. ¹H NMR spectrum of tetra(p-tolyl)phosphonium iodide in CDCl₃ prepared photocatalytically from P₄ on a 1 mmol scale. *CDCl₃.



Supplementary Figure 128. $^{31}\text{P}\{^1\text{H}\}$ NMR spectrum of tetra(p-tolyl)phosphonium iodide in CDCl_3 prepared photocatalytically from P_4 on a 1 mmol scale.



Supplementary Figure 129. ^{13}C NMR spectrum of tetra(p-tolyl)phosphonium iodide in CDCl_3 prepared photocatalytically from P_4 on a 1 mmol scale. * CDCl_3 .

Tri(*o*-tolyl)phosphine from P₄ (1 mmol scale, Table 6, VIII-2)

The general method 14 was followed using 2-iodotoluene (1492 μ L, 11.0 mmol) which provided tri(*o*-tolyl)phosphine as colorless solid (131.7 mg, 43%).

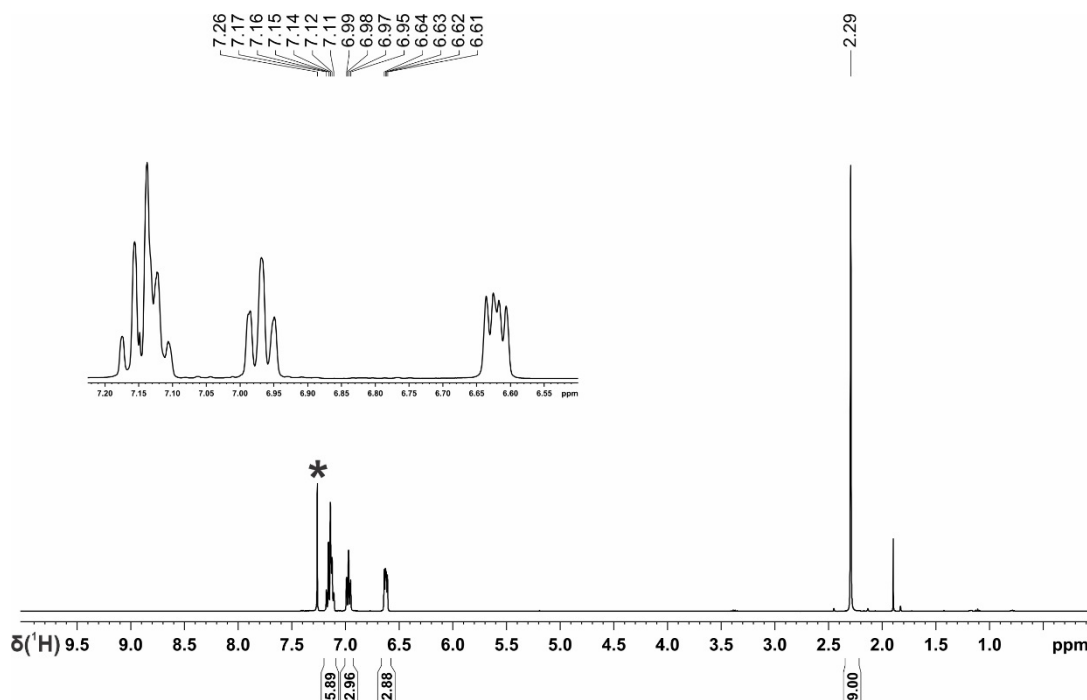
The characterization data of the product are consistent with the data found in the literature.^[S9]

¹H NMR (400 MHz, CDCl₃): δ 7.17-7.11 (m, 6H), 6.99-6.95 (m, 3H), 6.64-6.61 (m, 3H), 2.29 (s, 9H).

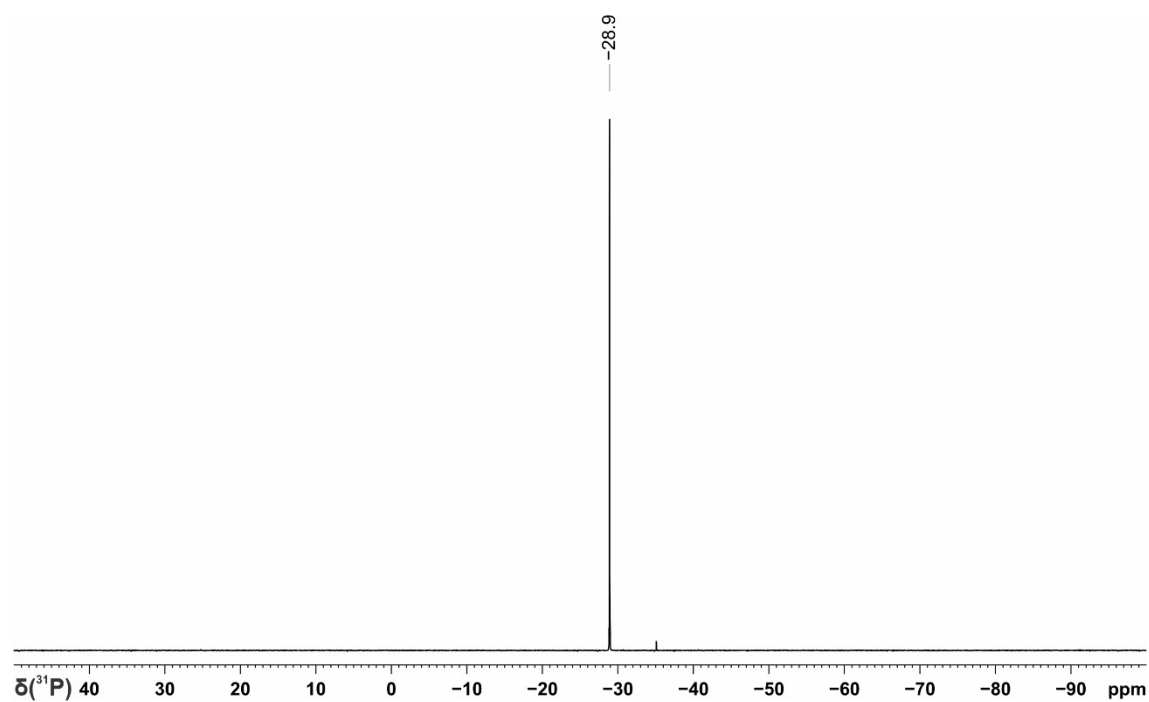
¹³C{¹H} NMR (100 MHz, CDCl₃): δ 142.9 (d, J = 26.2 Hz), 134.6 (d, J = 10.8 Hz), 133.2, 130.2 (d, J = 4.8 Hz), 128.8, 128.5, 126.3, 21.3 (d, J = 21.6 Hz).

³¹P{¹H} NMR (162 MHz, CDCl₃): δ -28.9.

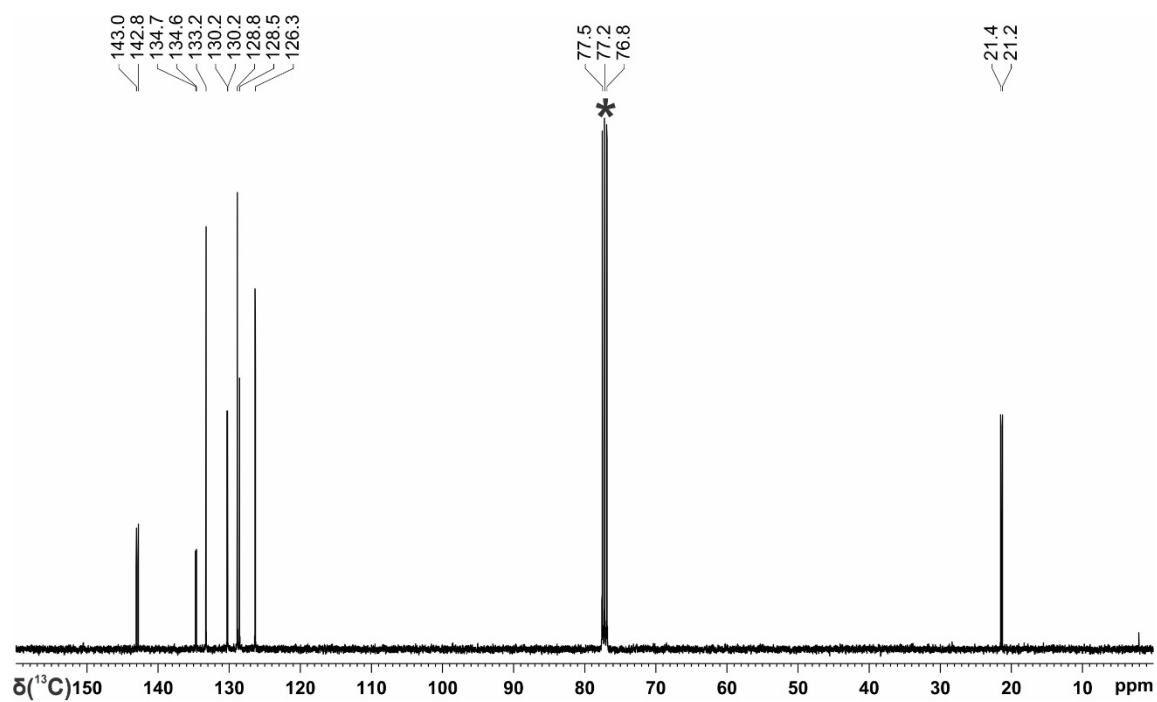
Elemental analysis: Calculated for C₂₁H₂₁P: C, 82.87; H, 6.95; Found: C, 83.11; H, 6.75.



Supplementary Figure 130. ¹H NMR spectrum of tri(*o*-tolyl)phosphine in CDCl₃ prepared photocatalytically from P₄ on a 1 mmol scale. *CDCl₃.



Supplementary Figure 131. $^{31}\text{P}\{^1\text{H}\}$ NMR spectrum of tri(*o*-tolyl)phosphine in CDCl_3 prepared photocatalytically from P_4 on a 1 mmol scale.



Supplementary Figure 132. ^{13}C NMR spectrum of tri(*o*-tolyl)phosphine in CDCl_3 prepared photocatalytically from P_4 on a 1 mmol scale. $^*\text{CDCl}_3$.

Tris(2-methoxyphenyl)phosphine from P₄ (1 mmol scale, Table 6, VIII-3)

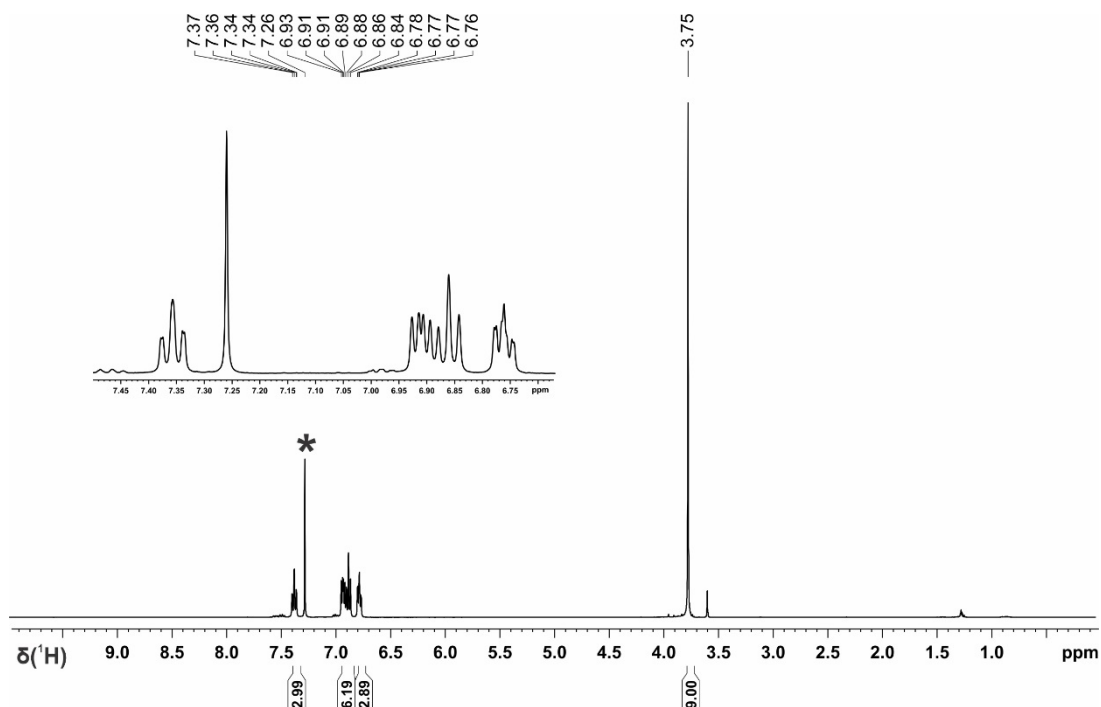
The general method 15 was followed using, 2-iodoanisole (1431 μL , 11.0 mmol, 11.0 equiv. based on the phosphorus atom) which provided tris(2-methoxyphenyl)phosphine (42.4 mg, 12%).

The characterization data of the product are consistent with the data found in the literature.^[S9]

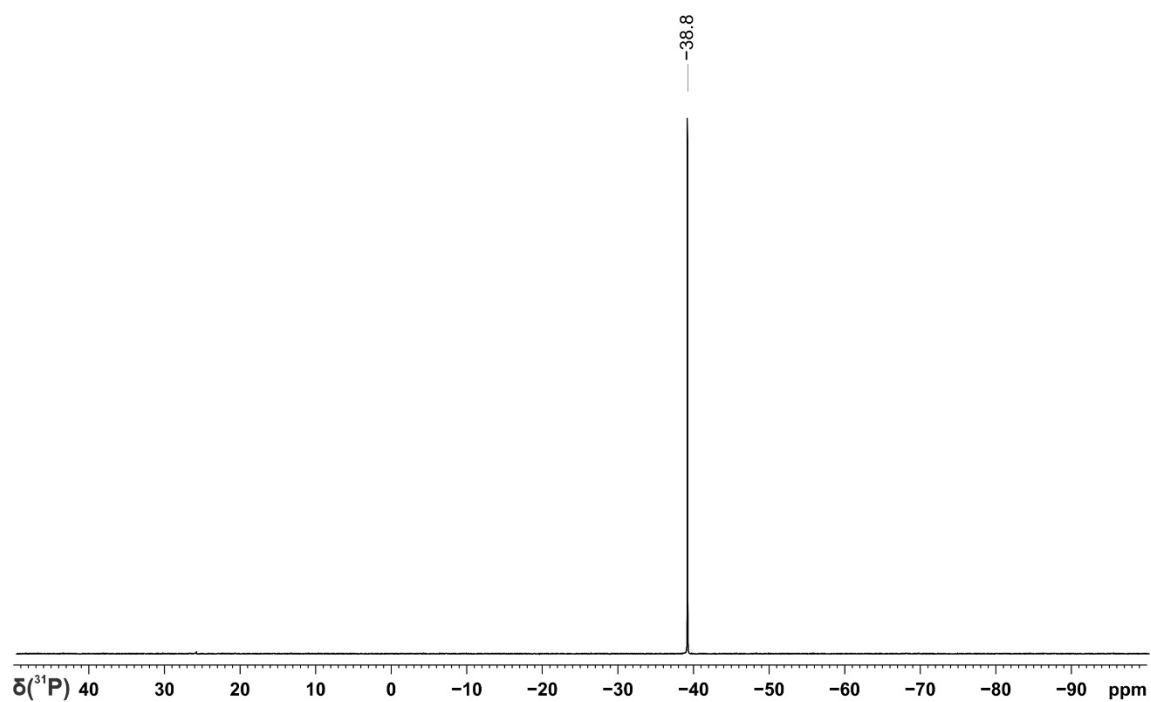
¹H NMR (400 MHz, CDCl₃): δ 7.37-7.34 (m, 3H), 6.93-6.34 (m, 6H), 6.78-6.76 (m, 3H), 3.75 (s, 9H).

¹³C{¹H} NMR (100 MHz, CDCl₃): δ 161.8 (d, J = 16.6 Hz), 134.0, 130.1, 124.8 (d, J = 12.6 Hz), 121.0, 110.4 (d, J = 1.7 Hz), 55.9.

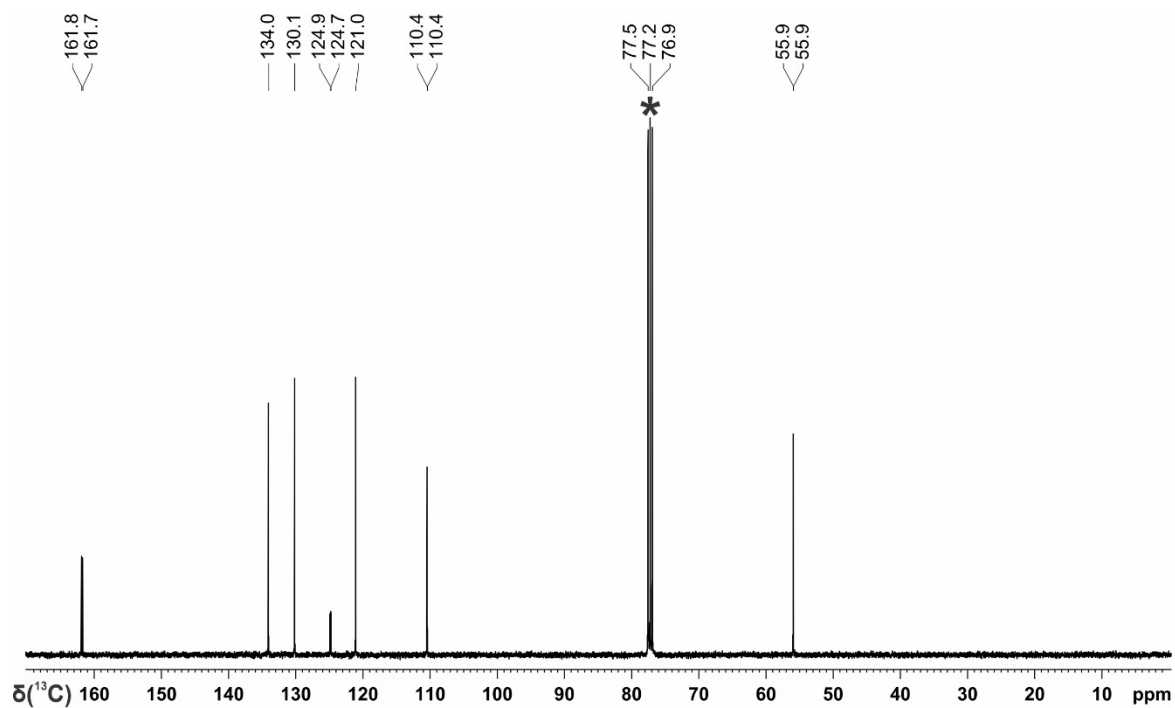
³¹P{¹H} NMR (162 MHz, CDCl₃): δ -38.8.



Supplementary Figure 133. ¹H NMR spectrum of tris(2-methoxyphenyl)phosphine in CDCl₃ prepared photocatalytically from P₄ on a 1 mmol scale. *CDCl₃.



Supplementary Figure 134. $^{31}\text{P}\{^1\text{H}\}$ NMR spectrum of tris(2-methoxyphenyl)phosphine in CDCl_3 prepared photocatalytically from P_4 on a 1 mmol scale.



Supplementary Figure 135. ^{13}C NMR spectrum of tris(2-methoxyphenyl)phosphine in CDCl_3 prepared photocatalytically from P_4 on a 1 mmol scale. * CDCl_3 .

Tris(2-(methylthio)phenyl)phosphine from P₄ (1 mmol scale, Table 6, VIII-4)

The general procedure 16 was followed using 2-iodothioanisole (1600 μL , 11.0 mmol, 11.0 equiv. based on the phosphorus atom) which provided tris(2-(methylthio)phenyl)phosphine (63.8 mg, 16%).

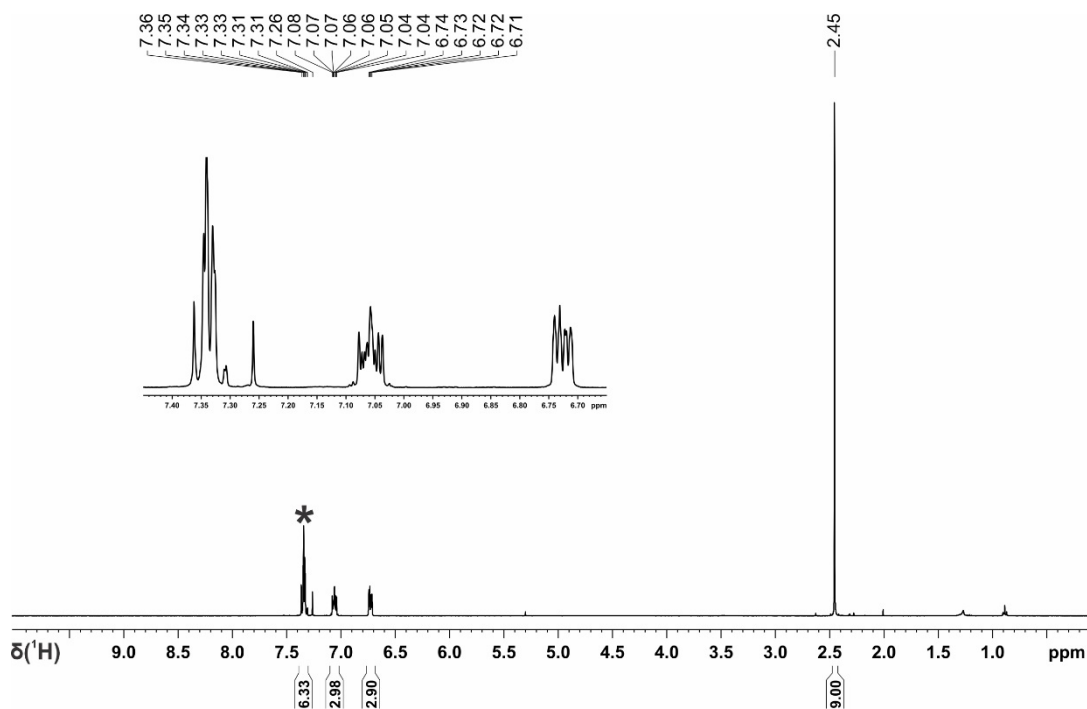
The characterization data of the product are consistent with the data found in the literature.^[S9]

¹H NMR (400 MHz, CDCl₃): δ 7.36-7.31 (m, 6H), 7.08-7.04 (m, 3H), 6.74-6.71 (m, 3H), 2.45 (s, 9H).

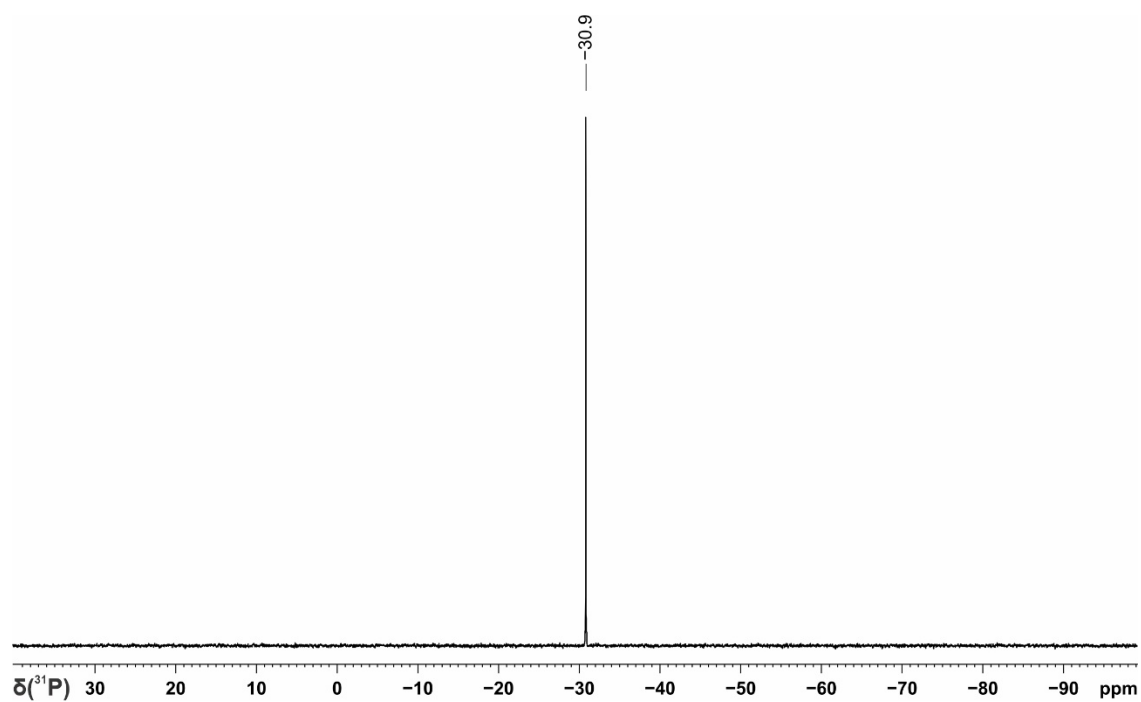
¹³C{¹H} NMR (100 MHz, CDCl₃): δ 144.3 (d, J = 29.3 Hz), 135.8 (d, J = 9.7 Hz), 133.7, 129.6, 128.5, 127.0 (d, J = 4.3 Hz), 125.6, 17.5 (d, J = 9.7 Hz).

³¹P{¹H} NMR (162 MHz, CDCl₃): δ -30.9.

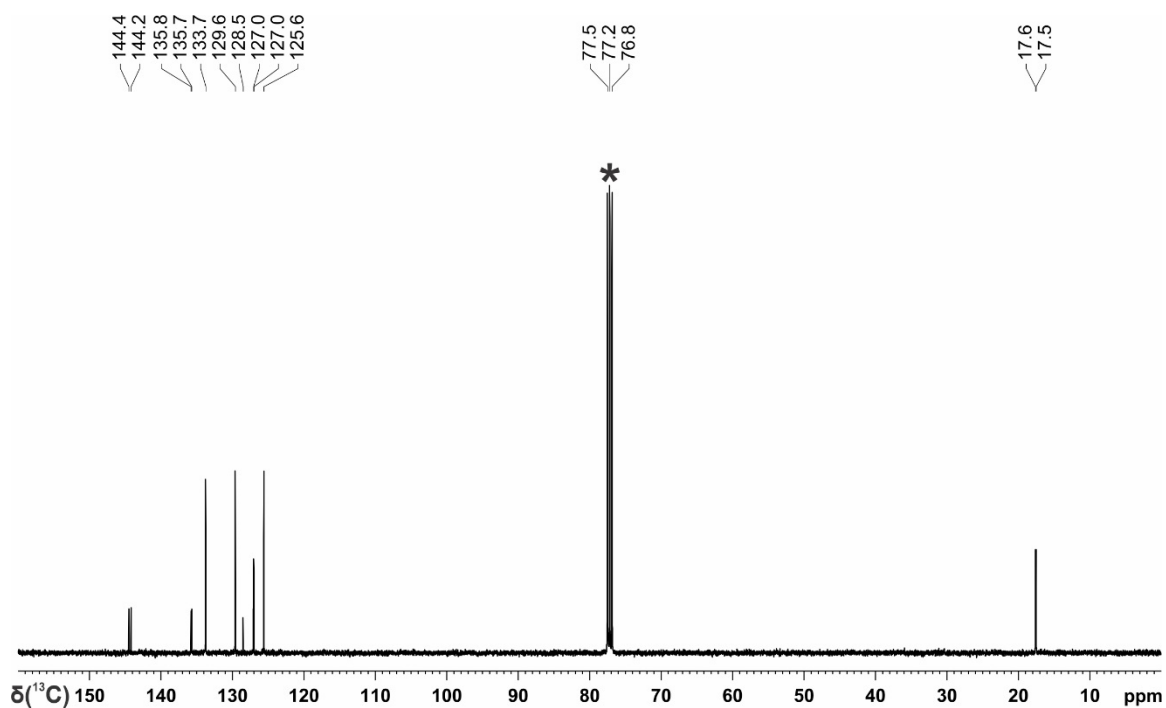
Elemental analysis: Calculated for C₂₁H₂₁S₃P: C, 62.97; H, 5.28; Found: C, 63.00; H, 5.28.



Supplementary Figure 136. ¹H NMR spectrum of tris(2-(methylthio)phenyl)phosphine in CDCl₃ prepared photocatalytically from HPPH₂ on a 1 mmol scale. *CDCl₃.



Supplementary Figure 137. $^{31}\text{P}\{^1\text{H}\}$ NMR spectrum of tris(2-(methylthio)phenyl)phosphine in CDCl_3 prepared photocatalytically from HPPH_2 on a 1 mmol scale.



Supplementary Figure 138. ^{13}C NMR spectrum of tris(2-(methylthio)phenyl)phosphine in CDCl_3 prepared photocatalytically from HPPH_2 on a 1 mmol scale. * CDCl_3 .

3.5.10 References

- S1 H. Iwahashi, Y.-i. Ishikawa, S. Sato, K. Koyano, *Bull. Chem. Soc. Jpn.* **1977**, *50*, 1278-1281.
- S2 E. Speckmeier, T. G. Fischer, K. Zeitler, *J. Am. Chem. Soc.* **2018**, *140*, 15353-15365.
- S3 L. de Quadras, J. Stahl, F. Zhuravlev, J. A. Gladysz, *J. Organomet. Chem.* **2007**, *692*, 1859-1870.
- S4 V. A. Pollard, A. Young, R. McLellan, A. R. Kennedy, T. Tuttle, R. E. Mulvey, *Angew. Chem. Int. Ed.* **2019**, *58*, 12291-12296.
- S5 S. Jin, G. C. Haug, V. T. Nguyen, C. Flores-Hansen, H. D. Arman, O. V. Larionov, *ACS Catal.* **2019**, *9*, 9764-9774.
- S6 J. M. Tukacs, D. Király, A. Strádi, G. Novodarszki, Z. Eke, G. Dibó, T. Kégl, L. T. Mika, *Green Chem.*, **2012**, *14*, 2057-2065.
- S7 O. Moncea, M. A. Gunawan, D. Poinso, H. Cattet, J. Becker, R. I. Yurchenko, E. D. Butova, H. Hausmann, M. Šekutor, A. A. Fokin, J.-C. Hierso, P. R. Schreiner, *J. Org. Chem.* **2016**, *81*, 8759-8769.
- S8 W.-C. Shih, O. V. Ozerov, *Organometallics* **2015**, *34*, 4591-4597.
- S9 U. Lennert, P. B. Arockiam, V. Streitferdt, D. J. Scott, C. Rödl, R. M. Gschwind, R. Wolf, *Nat Catal.* **2019**, *2*, 1101-1106.

4 SUMMARY

Chapter 1: DIRECT ORGANOFUNCTIONALISATION OF WHITE PHOSPHORUS TO MONOPHOSPHORUS COMPOUNDS: STATE-OF-THE-ART AND PERSPECTIVES

Chapter 1 reviews current methods to functionalise white phosphorus to P₁ compounds containing at least one P–C bond. In the first part basic methods to form P₁ compounds in KOH/water/organic solvent are described. Organic halides and unsaturated compounds react with white phosphorus to form P₁ organophosphorus compounds. Subchapter 1.3 describes reactions of white phosphorus with organolithium and -zinc compounds. Remarkably, the applicability of this method is not limited to the formation of phosphines and phosphine oxides, also phospholyl lithium compounds could be prepared by this method. The reactivity of carbenes towards P₄ is described in chapter subchapter 1.4. Only sterically nondemanding carbenes react with white phosphorus to form directly P₁ compounds. Electrochemical methods to functionalize white phosphorus are described in the following chapter. Aryl- and alkylphosphines and phosphine oxides could be prepared by this method in excellent yields. The last subchapter reviews radical methods to functionalize white phosphorus.

Chapter 2: DIRECT CATALYTIC TRANSFORMATION OF WHITE PHOSPHORUS INTO ARYL PHOSPHINES AND PHOSPHONIUM SALTS

Chapter 2 reports on the first photocatalytic method to form triarylphosphines and tetraarylphosphonium salts directly from white phosphorus in yields up to 80%. Irradiation of a solution containing the well-known photocatalyst [Ir(dtbbpy)(ppy)₂]⁺PF₆⁻ (**[1]**PF₆⁻; dtbbpy = 4,4'-bis-tertbutyl-2,2'-bipyridine, ppy = 2-(2-pyridyl)phenyl, Fig. 1), triethylamine as electron donor, iodobenzene derivatives, and white phosphorus in a MeCN/benzene (3:1) mixture as solvent with blue light yielded the corresponding triarylphosphines and phosphonium salts. The substrate scope and mechanistic details are discussed. The catalyst first oxidises Et₃N in its excited state (Fig.1, steps *i* and *ii*), and forms the reduced complex **[1]**. The latter one reduces iodobenzene derivatives to the corresponding carbon centred aryl radical (step *iii*). The *in situ* formed aryl radical attacks then P₄ (step *iv*), producing in sequence arylphosphines ArPH₂, diarylphosphine Ar₂PH, triarylphosphine Ph₃P and finally the tetraarylphosphonium salt Ar₄P⁺ (steps *v-viii*). Remarkably, every arylation step is catalytically driven. While sterically hindered iodobenzene derivatives preferentially form tertiary phosphines, less hindered aryl iodides form the corresponding quaternary phosphonium salts. This method is a first

step towards an industrial relevant catalytic procedure for a synthesis of phosphines directly from P_4 .

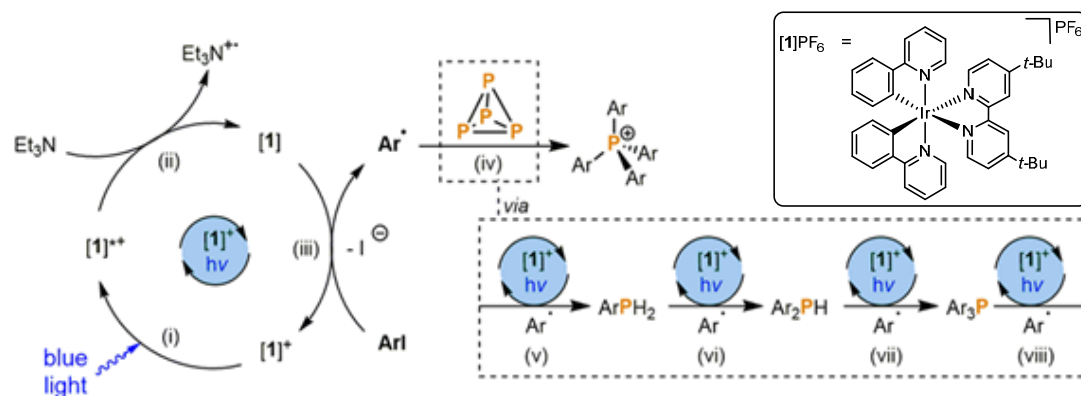


Fig. 1. Catalytic cycle. Proposed mechanism for the photocatalytic functionalisation of white phosphorus to triarylphosphines and tetraarylposphonium salts with $[1]^+$ in the presence of aryl halides

Chapter 3: VERSATILE VISIBLE-LIGHT-DRIVEN SYNTHESIS OF UNSYMMETRICAL PHOSPHINES AND PHOSPHONIUM SALTS

Chapter 3 describes a visible-light-driven organocatalytic method to prepare unsymmetrical tertiary phosphines and phosphonium salts. Based on the above-mentioned stepwise arylation of phosphines, a strategy to form mixed phosphines was developed. Primary and secondary phosphines were converted to the corresponding tertiary phosphines and phosphonium salts (Fig.2). Remarkably, the catalytic procedure works even more effectively with the organocatalyst 3DPAFIPN than with $[1]PF_6$. This shows an unprecedented example of low-temperature and organocatalyzed formation of mixed phosphines from primary and secondary phosphines. Moreover, the same organic photocatalyst can be used to replace $[1]PF_6$ in our previously reported photocatalytic functionalization of white phosphorus (*vide supra*).

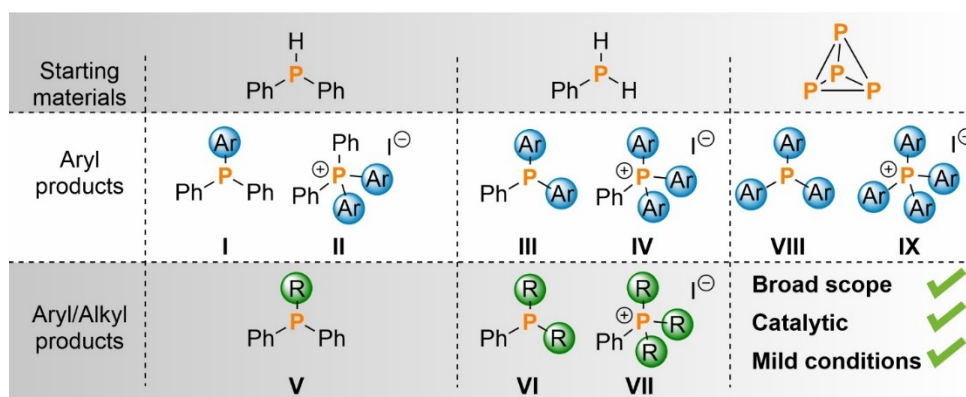


Figure 2. An overview of the broad scope of symmetrically and unsymmetrically substituted phosphines and phosphonium salts accessed in this work, and the corresponding product numbering scheme. R = alkyl, Ar = aryl

5 ACKNOWLEDGMENT

Mein besonderer Dank gilt Prof. Dr. Robert Wolf für die Aufgabenstellung und Betreuung. Obwohl er von meiner chronischen Krankheit wusste, nahm er mich in seinen Arbeitskreis auf und gab mir die Chance dieses interessante Forschungsprojekt zu bearbeiten. Vielen Dank für diese Möglichkeit!

Prof. Dr. Ruth Gschwind danke ich für das Zweitgutachten, sowie die interessanten Diskussionen hinsichtlich mechanistischer Details.

Prof. Dr. Frank-Michael Matysik (Drittprüfer) und Prof. Dr. Rainer Müller danke ich für die Bereitschaft das Prüfungskomitee zu komplettieren.

Mein herzlicher Dank gilt meinen Kooperationspartnern der letzten Jahre. Besonders hervorheben möchte ich dabei Verena Streitferdt, mit der die Zusammenarbeit immer eine Freude war. Gemeinsames Grübeln über weitere Methoden zur Aufklärung mechanistischer Fragenstellungen haben immer sehr viel Spaß gemacht.

Ich danke allen ehemaligen und aktuellen Mitgliedern des Arbeitskreises Wolf für die Zusammenarbeit.

Den Mitarbeitern der Werkstätten und analytischen Abteilungen danke ich besonders für die immer reibungslose Unterstützung, schnelle Hilfe bei Problemen und die netten Gespräche.

Besonders bedanken möchte ich mich bei Dr. med. Michael Weidenhiller, ohne den ich schon im Bachelorstudium aufgeben hätte müssen. Spontan eingeschobene Termine, Telefontermine noch freitags um 23 Uhr abends, Medikation angepasst an die jeweilige Situation, Aufklärungsbögen die samstags persönlich vorbeigebracht werden, usw. Herzlichen Dank!

Allgemein möchte ich mich bei meinen Freunden und meiner Familie bedanken, die mir immer eine Hilfe waren und sind.

Besonders möchte ich meinen Eltern danken, die mich immer finanziell, aber vor allem in allen anderen Dingen des Lebens unterstützt haben.

Als letztes möchte ich mich bei Kerstin Rothermel bedanken. Danke für alles, deine Unterstützung lässt sich nicht in Worte fassen! Ohne Dich hätte ich das Studium nie geschafft.

6 CURRICULUM VITAE

Ulrich Lennert**PERSONAL DATA**

Date of Birth	27 February 1990
Nationality	German
Place of birth	Regensburg

EDUCATION

Oct. 2016 – present	Ph.D. studies, <i>Universität Regensburg</i> supervisor: Prof. Dr. Robert Wolf.
Oct. 2014 – Sep. 2016	Master of Science in Chemistry, <i>Universität Regensburg</i> Master thesis: „ <i>Photokatalytische C-H Oxygenierungen</i> “. supervisor: Prof. Dr. Robert Wolf.
Oct. 2010 – Sep. 2014	Bachelor of Science in Chemistry, <i>Universität Regensburg</i>. Bachelor thesis: „ <i>Enzymatic Reactions in Deep Eutectic Solvents</i> “, supervisor: Prof. Dr. Werner Kunz
2009	Abitur in Parsberg.

PUBLICATIONS

- B. Mühldorf, U. Lennert, R. Wolf, “10. Coupling photoredox and biomimetic catalysis for the visible-light-driven oxygenation of organic compounds” in *Chemical Photocatalysis*. (De Gruyter: Berlin, Boston. 2000)
- U. Lennert, P. B. Arockiam, V. Streitferdt, D. Scott, C. Rödl, R. Gschwind, R. Wolf, „Direct catalytic transformation of white phosphorus into arylphosphines and phosphonium salts”, *Nat. Catal.* **2019**, 2, 1101–1106.
- P. B. Arockiam, U. Lennert, C. Graf, R. Rothfelder, D. Scott, T. G. Fischer, K. Zeitler, R. Wolf, „Versatile Visible-Light-Driven Synthesis of Unsymmetrical Phosphines and Phosphonium Salts”, accepted in *Chem. Eur. J.*

AWARDS

- Sept. 2018 **Poster prize** of the „19. Vortragstagung für Anorganische Chemie der Fachgruppen Wöhler-Vereinigung und Festkörperchemie und Materialforschung“, Regensburg.
- Apr. 2019 **Prize for best oral presentation** „16. European Workshop on Phosphorus Chemistry“, Bristol.
-

MEMBERSHIPS

- 2016-2019 **Research Training Group “Chemical Photocatalysis Graduate Speaker (2018-2019).**
-

PRESENTATIONS

- March 2016 **Oral Presentation** – 28. Seminartage des GRK 1626 “Chemical Photocatalysis,” Kloster Plankstetten.
“Redox Reactions catalysed by Riboflavin Tetraacetate”
- Aug. 2017 **Oral Presentation** – Wissenschaftliches Kolloquium von Arbeitsgruppen für Anorganische Chemie, Hirschegg.
“Licht-getriebene Oxidationen mit Riboflavin Tetraacetat”
- March 2018 **Oral Presentation** – 32. Seminartage des GRK 1626, “Chemical Photocatalysis,” Regensburg.
“Photocatalytic Activation of White Phosphorus”
- July 2018 **Poster** – 27th PhotoIUPAC, Dublin.
“Visible-Light-Driven Functionalization of White Phosphorus”
- Sept. 2018 **Poster** – 26th Lecture Conference on Photochemistry, Garching.
“Photocatalysis in the Wolf Group”
- Sept. 2018 **Poster** – 19. Vortragstagung für Anorganische Chemie der Fachgruppen Wöhler-Vereinigung und Festkörperchemie und Materialforschung, Regensburg.
“Visible-Light-Driven Functionalization of White Phosphorus”
- Apr. 2019 **Oral Presentation** – 16th European Workshop on Phosphorus Chemistry, Bristol.
“Direct Catalytic Transformation of White Phosphorus into Aryl Phosphines and Phosphonium Salts”
- July 2019 **Oral Presentation** – 29th International Conference on Photochemistry, Boulder.
“Direct Catalytic Transformation of White Phosphorus into Aryl Phosphines and Phosphonium Salts”

7 EIDESSTATTLICHE ERKLÄRUNG

Ich erkläre hiermit an Eides statt, dass ich die vorliegende Arbeit ohne unzulässige Hilfe Dritter und ohne Benutzung anderer als der angegebenen Hilfsmittel angefertigt habe; die aus anderen Quellen direkt oder indirekt übernommenen Daten und Konzepte sind unter Angabe des Literaturzitats gekennzeichnet. Die Arbeit wurde bisher weder im In- noch im Ausland in gleicher oder ähnlicher Form einer anderen Prüfungsbehörde vorgelegt.

Ulrich Lennert